Autism Counts

Stereological studies on human postmortem brains and a mouse model for autism

Imke van Kooten

The studies described in this thesis were performed at the School for Mental Health and Neurosciences, Division of Cellular Neuroscience, Maastricht University, Maastricht and the Department of Child and Adolescent Psychiatry of the University Medical Center Utrecht, Utrecht, the Netherlands.

ISBN: 978-90-393-4910-6
Cover design and type setting by Tino Stuijt, Utrecht
Printed by PrintPartners Ipskamp, Enschede
AUTISM COUNTS
Stereological studies on human postmortem brains and a mouse model for autism

Autism Counts

Stereological studies on human postmortem brains and a mouse model for autism

Autisme Telt

Stereologische studies in humane postmortem breinen en een muismodel voor autisme

(met een samenvatting in het Nederlands)

Proefschrift

ter verkrijging van de graad van doctor aan de Universiteit Utrecht,
op gezag van de rector magnificus, prof. dr. J. C. Stoof,
ingevolge het besluit van het college voor promoties
in het openbaar te verdedigen op
donderdag 6 november 2008 des ochtends te 10.30 uur

door

Im Arnoldina Joseph van Kooten
geboren op 22 oktober 1981 te Tegelen

Promotoren: Prof. dr. H. van Engeland
Prof. dr. H.W.M. Steinbusch

Co-promotor: Dr. C. Schmitz

The publication of this thesis was financially supported by the Prof. dr. L.N.J. Kamp Stichting and Bristol-Myers Squibb

The research in this dissertation thesis was funded by grants from Autism Speaks to dr. C. Schmitz and the Korczak Foundation to Prof. dr. H. Van Engeland.

Contents

Chapter 1

Introduction

Autism is a neurodevelopmental disorder characterized by the presence of pervasive impairments in social functioning, language abnormalities, and stereotyped and repetitive behaviors (American Psychiatric Association, 1994). According to the Diagnostic and Statistical Manual (DSM-IV) of the American Psychiatric Association, autism is part of a larger spectrum of pervasive developmental disorders (PDD), including Asperger's syndrome, Rett syndrome, childhood disintegrative disorder (CDD) and pervasive developmental disorder not otherwise specified (PDD-NOS) (American Psychiatric Association, 1994). All disorders of the PDD spectrum share varying degrees of the three core symptoms of autism as described earlier (Manning-Courtney et al., 2003; Volkmar and Pauls, 2003; Moretti and Zoghbi, 2006). Except for patients with Rett syndrome, all described PDDs exist more in males then in females, with ratios of 3 or 4 to 1 (Hill and Frith, 2003; Volkmar and Pauls, 2003). Various studies estimated that autism occurs at a rate of 13 per 10,000 children, whereas the prevalence for all PDDs is at least 36 per 10,000 children (Fombonne, 2006). Table 1 summarizes the core features of the PDDs as outlined by the DSM-IV criteria.

Autism can be investigated in many different ways. One of them is to focus on the neuropathology, which is in the middle of many other research areas (Fig. 1). For instance, abnormal gene expression might cause incorrectly formed proteins leading to improper protein function. Consequently, this might have a direct influence on the morphology of certain brain structures. In addition, the neuropathology of a disorder determines alterations in gross morphology of the central nervous system (CNS). In turn, structural alterations of the brain might have a neuropathological basis. Divergent cellular morphology can be the basis of enlarged brains seen in some patients with autism (Courchesne et al., 2007). Moreover, morphological and cytoarchitectural differences can affect specific brain functions and neuronal networks as well. Disconnectivity or underdeveloped connections within specific brain regions may suggest a neuropathological origin. Besides this, the vascular organization of a specific brain region can be affected by neuropathological alterations, thereby influencing the regional cerebral blood flow.

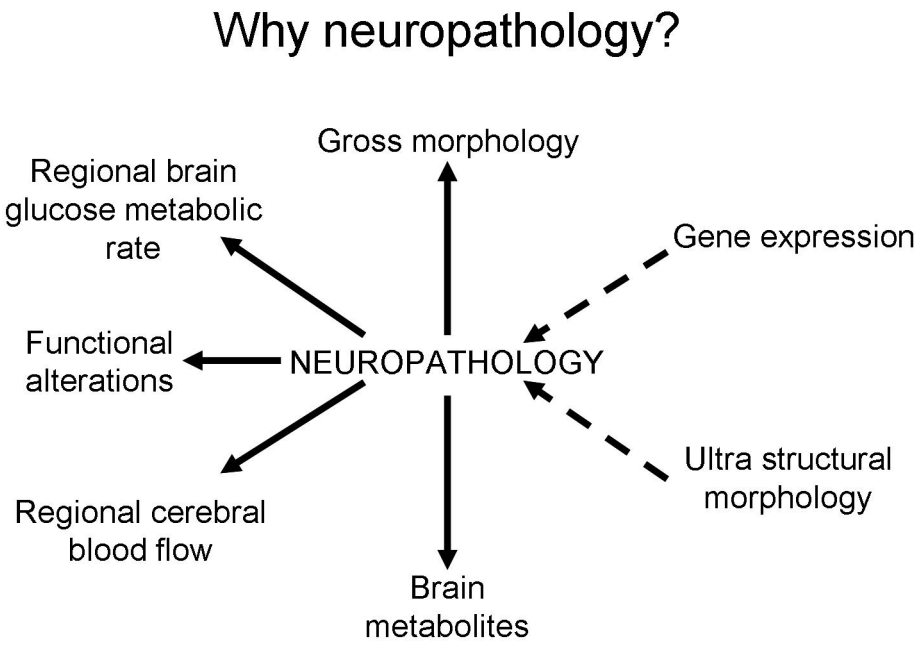

Figure 1. Scheme summarizing the importance of neuropathological studies in research on autism. Gene expression and ultrastructural morphology can affect neuropathology (dashed arrow), whereas neuropathology has an influence on the gross morphology of the CNS, regional brain glucose metabolites, functional alterations, regional cerebral blood flow and brain metabolites (arrow).

Table 1. Diagnostic criteria of autism, according to the DSM-IV

I. Childhood autism

A. A total of six (or more) items from (1), (2), and (3), with at least two from (1), and one each from (2) and (3):

1. qualitative impairment in social interaction, as manifested by at least two of the following:
    a. marked impairment in the use of multiple nonverbal behaviors, such as eye-to- eye gaze, facial expression, body postures, and gestures to regulate social interaction
    b. failure to develop peer relationships appropriate to developmental level
    c. a lack of spontaneous seeking to share enjoyment, interests, or achievements with other people (e.g., by a lack of showing, bringing, or pointing out objects of interest)
    d. lack of social or emotional reciprocity

2. qualitative impairments in communication, as manifested by at least one of the following:
    a. delay in, or total lack of, the development of spoken language (not accompanied by an attempt to compensate through alternative modes of communication such as gesture or mime)
    b. in individuals with adequate speech, marked impairment in the ability to initiate or sustain a conversation with others
    c. stereotyped and repetitive use of language or idiosyncratic language
    d. lack of varied, spontaneous make-believe play or social imitative play appropriate to developmental level

3. restricted, repetitive, and stereotyped patterns of behavior, interests, and activities as manifested by at least one of the following:
    a. encompassing preoccupation with one or more stereotyped and restricted patterns of interest that is abnormal either in intensity or focus
    b. apparently inflexible adherence to specific, nonfunctional routines or rituals
    c. stereotyped and repetitive motor mannerisms (e.g., hand or finger flapping or twisting or complex whole-body movements)
    d. persistent preoccupation with parts of objects

B. Delays or abnormal functioning in at least one of the following areas, with onset prior to age 3 years: (1) social interaction, (2) language as used in social communication, or (3) symbolic or imaginative play.

C. The disturbance is not better accounted for by Rett's disorder or childhood disintegrative disorder.

II. Asperger's Disorder

A. Qualitative impairment in social interaction, as manifested by at least two of the following:

1. marked impairment in the use of multiple nonverbal behaviors, such as eye-to-eye gaze, facial expression, body postures, and gestures to regulate social interaction
2. failure to develop peer relationships appropriate to developmental level
3. a lack of spontaneous seeking to share enjoyment, interests, or achievements with other people (e.g., by a lack of showing, bringing, or pointing out objects of interest to other people)
4. lack of social or emotional reciprocity

B. Restricted, repetitive, and stereotyped patterns of behavior, interests, and activities, as manifested by at least one of the following

1. encompassing preoccupation with one or more stereotyped and restricted patterns of interest that is abnormal either in intensity or focus
2. apparently inflexible adherence to specific, nonfunctional routines or rituals
3. stereotyped and repetitive motor mannerisms (e.g., hand or finger flapping or twisting, or complex whole-body movements)
4. persistent preoccupation with parts of objects

C. The disturbance causes clinically significant impairment in social, occupational, or other important areas of functioning

D. There is no clinically significant general delay in language (e.g., single words used by age 2 years, communicative phrases used by age 3 years).

E. There is no clinically significant delay in cognitive development or in the development of age-appropriate self-help skills, adaptive behavior (other than in social interaction), and curiosity about the environment in childhood.

F. Criteria are not met for another specific pervasive developmental disorder or schizophrenia.

III. Pervasive Developmental Disorder Not Otherwise Specified (PDD-NOS)

This category should be used when there is a severe and pervasive impairment in the development of reciprocal social interaction or verbal and nonverbal communication skills, or when stereotyped behavior, interests, and activities are present, but the criteria are not met for a specific pervasive developmental disorder, schizophrenia, schizotypal personality disorder, or avoidant personality disorder. For example, this category includes "atypical autism" -- presentations that do not meet the criteria for autistic disorder because of late age of onset, atypical symptomatology, or subthreshold symptomatology, or all of these.

Criteria for Rett disorder and childhood disintegrative disorder are not shown

Short summary of neuropathological findings in autism

After Kanner's first description of macroencephaly in patients with autism (Kanner, 1943), various imaging studies have consistently reported enlarged brains in patients with autism (Bailey et al., 1998; Kemper and Bauman, 1998; Courchesne et al., 2001; Aylward et al., 2002; Sparks et al., 2002). Nevertheless, the total brain volume of newborns who develop autism later in life is normal or even smaller compared to age-matched controls. Additionally, children with autism have been described to show abnormal brain overgrowth followed by an arrest of growth during early childhood (Courchesne et al., 2001, 2003, 2004; Courchesne, 2004). These observations could be due to increased neurogenesis, gliogenesis, or synaptogenesis, disturbed neuroblast migration, decreased apoptosis or synaptic pruning, or combinations of these effects (Palmen et al., 2004). So far, no underlying set of neurobiological mechanisms have unambiguously been defined yet. With respect to neuropathology, several research groups have consistently reported distinctive neuropathological features in the limbic system, cerebellum and cerebral cortex in the brain of patients with autism. Patients with autism were reported to show increased cell packing density and smaller neurons in the limbic system (Bauman and Kemper, 1985, 1987, 1990; Bauman, 1991; Kemper and Bauman, 1993; Raymond et al., 1996; Bailey et al., 1998). Schumann and Amaral (2006) reported a decreased number of neurons in the lateral nucleus of the amygdala in patients with autism. The cerebellar vermis and hemispheres showed loss of Purkinje cells (Williams et al., 1980; Ritvo et al., 1986; Kemper and Bauman, 1993). In addition, more than 50% of the postmortem cases studied histologically until 2004, displayed features of cortical dysgenesis (Palmen et al., 2004), alterations in neuronal migration (Levitt et al., 2004) and cell minicolumnar organization (Casanova et al., 2006; see also Chapters 3 and 4). Finally, impaired function of the cholinergic and GABAergic system have been demonstrated in patients with autism (Chapter 2).

Various lines of evidence have indicated that the cognitive alterations in autism are connected with subtle alterations in the cytoarchitecture of specific cortical regions. As outlined in detail below, these cytoarchitectural alterations would indicate that several cognitive alterations observed in patients with autism might be based on specific neuronal deficits in the related cortical regions. Specifically interesting are the minicolumnar abnormalities

in several different areas throughout the brain (Chapters 3 and 4), as well as morphological alterations in the fusiform gyrus (Chapter 5) and of the Von Economo neurons (VENs) in the anterior cingulate cortex and frontoinsular cortex (Chapter 6).

Alterations of cortical minicolumns in the brain of patients with autism

The neuropathological and structural imaging data currently available in the literature, suggest that autism is the result of a developmental lesion affecting brain growth. More specific, abnormalities in cortical microdomains, more commonly termed 'minicolumns', may be important for understanding the neurobiological deficit underlying autism (Casanova et al., 2003; Courchesne et al., 2004). Based on its modular organization, evidence exists that minicolumns are present throughout the cerebral cortex (Hutsler and Galuske, 2003). Although the functional significance of minicolumns is still unclear (Jones, 2000; Hutsler and Galuske, 2003), it has been proposed that a minicolumn is the smallest fundamental information processing unit in the cerebral cortex (Mountcastle, 1997). Additionally, they are directly related to functional activity within different cortical regions (Hutsler and Galuske, 2003). The visibility of minicolumns in thick Nissl-stained sections (defined in 2D, not in 3D) depends on the linear arrangement of pyramidal neurons and the existence of cell-free space on both sides of the column core (Buxhoeveden and Casanova, 2002b). Within a minicolumn, a number of inputs are linked to a number of outputs via overlapping internal processing chains (Mountcastle, 1997). According to this hypothesis, neurons located in the middle layers of the cortex, in which thalamic afferents end, are adhered by tapered vertical connections to cells in superficial and deep layers, so that all cells in the minicolumn are excited by incoming stimuli with only small differences in latency (Jones, 2000). Recently, alterations in the minicolumns in the cerebral cortex have been reported in patients with autism (Casanova et al., 2002a). Specifically, patients with autism showed smaller minicolumns, less peripheral neuropil space and increased distance between the constituent cells (Casanova et al., 2003). As autism is a heterogeneous disorder and the available neuropathological data so far are various, it is very important to corroborate results of earlier studies in more brain regions and other well-defined samples of postmortem brains from patients with autism and related controls. To confirm the results reported earlier by Casanova et al. (2002a) in an independent sample, we investigated a subset of brains (i.e., six

brains from patients with autism and six from matched controls) for possible alterations in the modular organization of minicolumns in the prefrontal cortex (area 9), primary motor cortex (area 4), primary sensory cortex (area S1) and primary visual cortex (area 17) (Casanova et al., 2006) (for details see Chapter 3). In addition, the frontopolar cortex (area 10), orbitofrontal cortex (area 11), anterior cingulate cortex (area 24), frontoinsular cortex (area 43), and the ventrolateral cortex, the main part of Broca's speech area (area 44) were studied as well (for details see Chapter 4).

Morphological alterations in the fusiform gyrus of patients with autism

Severe autism usually involves varying degrees of social impairments (for review see Schmitz and Rezaie, 2008). A key feature of normal social functioning in humans is the processing of faces, which allows people to identify individuals and enables them with the capacity to understand the mental state of others (Baron-Cohen et al., 1994). Although not included in the current diagnostic criteria, patients with autism have marked deficits in face processing (Grelotti et al., 2002). A key brain region which is involved in normal social functioning is the fusiform gyrus (FG). Importantly, the FG plays a role during development (Schultz, 2005). Although patients with autism can perform face processing tasks (Schultz, 2005), evidence suggest that the FG, as well as other cortical regions supporting face processing are reduced in activity in patients with autism compared to normal subjects (Kanwisher et al., 1999; Pierce et al., 2001, 2004; Bolte et al., 2006). Additionally, imaging studies reported unchanged (Pierce et al., 2001) or increased (Waiter et al., 2004) volumes of the FG in patients with autism compared to controls, or asymmetry abnormalities of the FG in autism (i.e., larger on the left side in patients with autism) (Herbert et al., 2002). However, the neurobiological basis of this phenomenon remains to be established (Palmen et al., 2004; Van Kooten et al., 2005b; DiCicco-Bloom et al., 2006). The question arises whether there could be a neuropathological correlate of the alterations in the FG as described in clinical and imaging studies. In other words, is there a neuropathological explanation for the observed hypoactivation of the FG? We hypothesized that the FG shows neuropathological alterations at the cellular level in patients with autism compared to controls. Furthermore, are the results specific for the FG or show other related brain regions, such as the primary visual cortex and the whole cortical grey matter, cytoarchitectural alterations as well? These research questions were tested in the study described in Chapter 5.

Morphological alterations of Von Economo neurons in the brain of patients with autism

Von Economo neurons (VENs) are large, bipolar neurons located in layers III and V of the frontoinsular (FI) and anterior cingulate cortex (ACC) in great apes and humans, but not in other primates (Nimchinsky et al., 1999; Allman et al., 2005). VENs have a radial orientation and show very sparsely branching dendritic trees with symmetric apical and basal projections and rare dendritic spines. The bipolar dendrites of VENs are shaped and positioned to integrate information from an entire cortical minicolumn and rapidly relay the output to other brain structures (Watson et al., 2006). Because of their hypothesized wide connectivity to several regions throughout the brain, substantial evidence has suggested the role of VENs in the coordination of distributed neuronal activity involving social cognition and emotion (Nimchinsky et al., 1995, 1999; Allman et al., 2001, 2002, 2005; Hof and Van der Gucht, 2007). The existence of VENs exclusively in mammalian species with elaborate social structures strengthens these ideas (Sanders et al., 2002; Allman et al., 2005; Hof and Van der Gucht, 2007). Both ACC and FI are involved in functions related to social cognition, and both have been proposed to be implicated in neuropsychiatric disorders, including schizophrenia and autism (Allman et al., 2005). In addition, reduced volume, decreased metabolism and blood flow, and an abnormal lamination pattern were found in the ACC of patients with autism (Kemper and Bauman, 1993; Haznedar et al., 2000; Ohnishi et al., 2000) and schizophrenia (Tamminga et al., 1992; Noga et al., 1995; Benes et al., 2001). Furthermore, imaging studies did not show FI activation when patients with autism were asked to discriminate the mental states of individuals depicted on photographs (Baron-Cohen et al., 1999). Patients with schizophrenia demonstrated reduced gray matter volume in either the left (Crespo-Facorro et al., 2000; Sigmundsson et al., 2001), right (Duggal et al., 2005) or bilateral FI (Hulshoff Pol et al., 2001; Makris et al., 2006). They also failed to activate the FI during a verbal memory test (Crespo-Facorro et al., 2000), a verbal fluency test (Curtis et al., 1998) and an experiment to modulate the subject's degree of movement control (Farrer et al., 2004). Therefore, it is reasonable to suggest that VENs may be specifically altered in the ACC and FI of patients with schizophrenia and autism (Sanders et al., 2002; Allman et al., 2005). Allman et al. (2005) recently hypothesized that abnormalities in the VENs may - at least in part - be responsible for the defects in social cognition in autism. As schizophrenia and autism are both

neurodevelopmental disorders, it is important to elucidate the role of VENs during development. VENs are first distinguishable during the 35th gestational week and increase rapidly in number during the first year of postnatal life, which is the period in which infants begin to develop social awareness and affiliation and just before the time that the first symptoms of autism typically begin to manifest (Allman et al., 2005). At birth, VENs are about equally numerous in both hemispheres, but during the first few postnatal months the number of VENs on the right side in the FI exceeds the left so that in adulthood there are consistently about 30% more VENs on the right side in humans and apes (J. Allman, California Institute of Technology, Pasadena, CA, USA; personal communication). There is also a rightward predominance in the VEN population in the ACC (J. Allman, California Institute of Technology, Pasadena, CA, USA; personal communication), which is consistent with the right hemisphere's superior capacity to discriminate emotions in facial expression (Benowitz et al., 1983). Recently reported data from four brains of patients with autism and 7 normal controls indicated that the number of VENs in the FI range from normal to hyperabundant in some forms of autism (Kennedy et al., 2007). However, these authors did not address morphology of the VENs. Abnormal morphology of VENs may cause dysfunctional VENs in the ACC and FI which could in turn be related to cognitive deficits thought to be responsible for some of the clinical symptoms seen in schizophrenia (Sanders et al., 2002). The question whether the morphology of VENs was altered in patients with autism and schizophrenia is addressed in Chapter 6. As patients with autism and schizophrenia share many clinical and biological features we investigated the VENs in a comparative manner. In addition, we wanted to find out whether the possible alterations in the morphology of VENs are specific for patients with autism or schizophrenia.

A unique sample of postmortem brains from patients with autism and matched controls

Considering neuropathological data of autism published so far, all observations were made on different samples of postmortem tissue. In other words, it is unknown whether the reported alterations reflect different aspects of a common neuropathological defect, or represent different morphological phenotypes caused by distinct mutations or environmental insults (Veenstra-Vanderweele et al., 2004). In addition, all studies had to contend with small sample sizes and high percentages of patients

with autism suffering from comorbid epilepsy (at least 40%) and mental retardation (at least 70%) (Palmen et al., 2004). Therefore, we have set up a cohort of human postmortem brains, comprising a unique case series of 7 brains from patients with autism and 10 matched controls developed in the framework of the Autism Brain Atlas Project (ABAP) of the U.S. Autism Tissue Project (ATP) (Pickett, 2003). Together with data on subcortical cytoarchitectural alterations in the same brains generated in the lab of Dr. Jerzy Wegiel (Department of Developmental Neurobiology, NYS Institute for Basic Research in Developmental Disabilities, Staten Island, NY, USA) the results presented here will serve as comprehensive basis for a quantitative atlas of the autism brain. This atlas will be significant for many reasons, including advancing the understanding of the molecular and cellular mechanisms underlying autism neuropathology and its role it may have in helping to identify a biological marker for the diagnosis of autism (Pickett, 2003). In short, whole brain hemispheres were obtained from different brain banks in the United States and Germany. In order to investigate a variety of brain regions within the same brains, we needed a specific approach of processing these human postmortem brains as described by Heinsen et al. (2000). Briefly, whole brain hemispheres were mounted in blocks of celloidin (embedding without infiltration) and cut into thick (200-500 µm) serial sections encompassing the entire hemisphere. This technique is more advanced then gelatin embedding allowing for complete neuroanatomical and neuropathological analysis of whole human brain hemispheres (Heinsen et al., 2000). Consequently, all sections were stained with Gallocyanin, mounted and coverslipped. Because of the thickness of the sections, layer specific stereological analysis could be performed (for details see chapters 3, 4, 5 and 6). In the end, these sections allow the quantitative analysis of a wide range of brain regions, including layer-specific analyses, within the same brains, which is the very basis for testing the hypothesis that autism is the result of abnormal development of a distributed neural network involving a number of brain regions (Piven, 1997).

High precision design-based stereology

Frequent questions in neuroscience are how to obtain precise and reliable morphological information on specific neuronal populations and how this can be related to data on brain function. For instance, a researcher may want to know the volume of a specific brain region of interest or the total

number and cell size of a population of neurons. The methods of choice for obtaining these morphometric data from tissue sections are those of high precision design-based stereology (Hof and Schmitz, 2000). Nowadays, this technique can be viewed as a well established state-of-the-art technology for quantitative histology (Schmitz and Hof, 2005). Within neuropathology research, design-based stereology is becoming a key methodology, as it can provide information about the degree of maturation or health of brain cells and overall brain development (Palmen et al., 2004). With respect to autism research, an important confounding factor in most of the discussed studies is that quantification of neuron density, neuron number and size was carried out with conventional quantitative methods which are subjected to considerable bias and therefore do not answer the research questions accurately. Accordingly, it is reasonable to hypothesize that a comprehensive, high-precision design-based stereologic analysis of subtle cytoarchitectural abnormalities in a variety of brain regions will contribute substantially to deciphering the neuropathology underlying autism. This would then contribute not only to a better understanding of the links between the clinical phenotype of autism on one hand and the results of functional imaging studies in autism on the other hand, but also to the development of appropriate animal models that might explain the developmental origin of these neuropathologic alterations.

Mouse models for autism

Although the neuropathological results in patients with autism are revealing, animal models are essential for better understanding of the pathophysiology, cause and treatment of autism. However, is it possible to create an animal model of autism? Various animal models of autism have been developed, based on genetic, neurochemical, neurophysiological or behavioral manipulations (Andres, 2002; Belmonte et al., 2004; Patterson, 2005b; see also Chapter 2). Given the heterogeneity of autism it is not surprising that no animal model has been created that perfectly mimics all aspects of the disorder (DiCicco-Bloom et al., 2006). Nevertheless, striking parallels between autism and animal models have already been reported. For example, genetic manipulation of neuroligin (NLGN) 3 and 4, genes that map to three loci associated with predisposition to autism (Jamain et al., 2003; Laumonnier et al., 2004), lead to loss of protein processing and loss of capacity to stimulate synapse formation (Chih et al., 2004; Comoletti et al., 2004). The Engrailed

2 (En2) knockout (KO) mice, in which the cerebellar patterning gene En2 is lacking, show a loss of Purkinje cells in the cerebellum (Liu and Joyner, 2001; Gharani et al., 2004). Interestingly, the human En2 gene is located on chromosome 7q36, which has been linked to autism (IMGSAC, 2001). Stuhmer et al. (2002) reported that DLX mutations alter the development of GABAergic neurons in the forebrain. Although twin and family studies have indicated a heritability for autism of more than 90%, it should be noted that the remaining 10% might be caused by gene-environment interaction effects (Steyaert and De La Marche, 2008). In other words, non-genetic etiologies, such as viral infections, might play a role as well (Ciaranello and Ciaranello, 1995). Infection during human pregnancy is common, and more than 10% of pregnant women experience an influenza infection during the second or third trimester (Irving et al., 2000). In addition, prenatal viral infections during the first or second trimester of pregnancy have been associated with autism (Desmond et al., 1967; Rutter and Bartak, 1971; Chess, 1977; Stubbs et al., 1984; Singh et al., 1997; Barak et al., 1998). In this respect, the maternal influenza infection model is of particularly interest because the offspring display behaviors consistent with those found in patients with autism, including deficits in exploratory and social behavior, sensorimotor gating and pup-mother attachment (Shi et al., 2003; Patterson, 2005b). With respect to neuropathology, most relevant to autism is the finding that the offspring of infected dams display a regionally-restricted deficit in Purkinje cells (Shi et al., 2008). These offspring have also been reported to display macrocephaly, gliosis and increased pyramidal cell density and atrophy, decreased neurogenesis, reduced reelin immunoreactivity and reduced thickness of the neocortex (Fatemi et al., 1999, 2002a, 2005a; Fatemi, 2004). However, the latter observations have not been confirmed applying rigorous, quantitative histologic techniques. In the study described in Chapter 7 we have therefore examined the brains of mice born to dams infected with human influenza virus on embryonic day (E) 9.5 using a high-precision design-based stereology approach. According to the aforementioned alterations (i.e., precocious enlargement followed by growth arrest of the entire brain and specifically the amygdala) we focused our analysis on alterations of the volume of the entire hemisphere, the cortical gray matter, the entire amygdala, the lateral and basolateral nuclei of the amygdala, as well as alterations in the total number and density of neurons in the lateral and the basolateral nuclei of the amygdala. We hypothesized that subjecting pregnant mice to

human influenza virus on E9.5 results in morphological alterations in the offspring's whole hemisphere (HEMI), cortical grey matter (CGM), total amygdala (AMG), lateral (LN) and basolateral nucleus (BLN) of the amygdala, resembling alterations found in the patients with autism. To cover the entire period of postnatal development we investigated offspring immediately after birth (P0), at 25 days after birth (P25) and at 3 months of age (M3). These results might contribute, as an animal model, to our understanding of the biological basis for interindividual differences in morphological alterations found in the brains of patients with autism.

After setting out a comprehensive review on autism neuropathology in Chapter 2, Chapters 3 and 4 enlighten the minicolumnar abnormalities in autism. The possible neurobiological basis for the reported hypoactivation of the fusiform gyrus (FG) when patients with autism view faces is explained in Chapter 5, whereas Chapter 6 describes the alterations of Von Economo neurons (VENs) in the anterior cingulate cortex (ACC) and frontoinsular cortex (FI) in schizophrenia and autism. Chapter 7 concentrates on the maternal influenza exposure mouse model. Finally, the main results of the thesis and possible future implications are discussed in Chapter 8.

Chapter 2

Autism: neuropathology, alterations in the GABAergic system, and animal models

Van Kooten IAJ, Hof PR, Van Engeland H, Patterson PH, Steinbusch HWM, Schmitz C.
International Review of Neurobiology 2005; 71: 1-26.

Abstract

Autism is a neurodevelopmental disorder with a strong genetic component and several known environmental risk factors. Neuropathological studies have shown consistent abnormalities in the limbic system, cerebellum and cerebral cortex. Several findings suggest a role for the GABAergic system in autism neuropathology. There are reports of elevated plasma GABA levels, reduction of the GABAergic system enzymes and decreased availability of GABA in autistic patients. Autism has a reported heritability of 60-90%. Abnormalities in the 15q11-13 region have been found in autistic people, and the $GABA_A$ receptor genes are located in this region. In addition, GABA dysfunction may occur in conjunction with Reelin. Abnormalities in the gene encoding for Reelin have been implicated in autism, and Reelin and GABA play an important role in the development of minicolumns. Compared to controls, minicolumns are more numerous, smaller and less compact in autistic patients. Several studies provided evidence for the role of GABA receptors in tangential migration of neurons. Furthermore, GABA regulates cell proliferation in some brain regions. Because the underlying causes of the reduced GABA system function in autism are not well understood, it is important to develop animal models of autism, which can give more insights into the neuropathology and behavioral aspects of the disease. Animal models of autism include misregulation of genes implicated in the disorder, as well as the use of known environmental risk factors. In the future, investigation of human autism tissues and animal models, in combination with implementation of new techniques such as design-based stereology and gene expression, may result in the elucidation of the etiology of autism.

Introduction

Autism is currently viewed as a genetically determined neurodevelopmental disorder (Bailey et al., 1996), defined by the presence of marked social deficits, specific language abnormalities and stereotyped, repetitive behaviors (American Psychiatric Association, 1994). Approximately 20% of the autistic subjects show macroencephaly, defined as head circumference above the 97th percentile (Bailey et al., 1996; Davidovitch et al., 1996; Aylward et al., 2002; van Karnebeek et al., 2002; Courchesne et al., 2003). However, this macroencephaly is not present until after the first year of life (Courchesne et al., 2003). Although evidence of increased head circumference (Bailey et al., 1993; Davidovitch et al., 1996; Fombonne, 2000; Aylward et al., 2002; van Karnebeek et al., 2002; Courchesne et al., 2003), brain weight (Bailey et al., 1998; Kemper and Bauman, 1998; Courchesne et al., 1999; Casanova et al., 2002b) and brain volume (Courchesne et al., 2001; Aylward et al., 2002; Sparks et al., 2002) has been described in autism, the underlying biological mechanisms remain to be determined. These observations could be due to increased neurogenesis, gliogenesis or synaptogenesis, disturbed neuroblast migration, decreased apoptosis or synaptic pruning, or combinations of these effects (Palmen et al., 2004). In addition, the detection of abnormalities in neurotransmitter systems, such as γ-aminobutyric acid (GABA) in autistic patients, suggests that it could be worthwhile to concentrate research on these systems. A good approach is the use of animal models that mimic features of autism.

In this chapter we examined the literature on autism neuropathology, the role of the GABAergic system in this disorder and the relevance of rodent models with autistic features.

Neuropathologic alterations in specific brain regions in autism

Limbic system

Bauman and Kemper were the first to report neuropathological findings in autism. They demonstrated increased cell packing density and smaller neurons in several regions of the limbic system, including the hippocampus, subiculum, amygdala, enthorhinal cortex, mammillary bodies and septal nuclei (Bauman and Kemper, 1985, 1987, 1990; Bauman, 1991; Kemper and Bauman, 1993; Raymond et al., 1996; Bailey et al., 1998). This pattern of small, closely packed neurons with reduced dendritic arbors could reflect features of an immature brain (Jacobsen, 1991). Bailey et al. (1998) demonstrated

increased cell packing density in all CA regions of the hippocampus in one out of five autistic cases. Raymond et al. (1996) investigated the dendritic morphology of hippocampal neurons in two well-documented autistic patients and one age-matched control. Using the Golgi stain, this group found smaller neurons and less dendritic branching of both CA1 and CA4 hippocampal neurons in autistic subjects compared to controls. These findings further suggest a curtailment of maturation, a feature previously highlighted by Kemper and Bauman (1993).

Neuropathologic findings are rather consistent with respect to the limbic system, whereas MRI studies are mostly conflicting. For example, compared to controls, volumes of the limbic system of autistic subjects are reported to be increased (Howard et al., 2000; Sparks et al., 2002), decreased (Aylward et al., 1999) or unchanged (Piven et al., 1998; Howard et al., 2000).

Cerebellum and brainstem

Williams et al. (1980) were the first to examine neuropathological alterations in the cerebellum in autism. In one out of four brains from autistic patients they found reduced Purkinje cell density. In a study by Ritvo et al. (1986), all autistic cases showed a decreased number of Purkinje cells in the cerebellar vermis and hemisphere. Kemper and Bauman (1993) replicated this finding. In another study, five adult autistic cases had a low number of cerebellar Purkinje cells, although this feature was not found in a 4-year-old autistic male (Bailey et al., 1998). In contrast, no abnormalities were found in the cerebellum of a 16-year-old female with autism and severe mental retardation (Guerin et al., 1996). Because of the consistent findings of decreased numbers of Purkinje cells in the cerebellum, (Fatemi et al., 2002b) examined the size of these cells. They showed a 24% decrease in mean Purkinje cell size in autistic brains. It should be mentioned that cerebellar Purkinje cells are the final targets of projections from the inferior olivary nucleus. A decrease in Purkinje cells may result in an abnormal development of the olivary projections to the cerebellar nuclei (Palmen et al., 2004). Many research groups have found a decrease in the number of cerebellar Purkinje cells without significant gliosis in the cerebellum (Kemper and Bauman, 1993; Bailey et al., 1998; Fatemi et al., 2002b). Most MRI studies have shown smaller cerebellar hemispheres (Murakami et al., 1989; Courchesne, 2004) or vermis (Hashimoto et al., 1995; Courchesne, 2004); but see Nowell et al., 1990; Piven et al., 1997).

Furthermore, two out of six brains from autistic patients in the study

of Kemper and Bauman (1993) demonstrated enlarged neurons in deep cerebellar nuclei and inferior olivary nucleus, whereas in the older subjects (>22 years) these neurons were small and pale, with normal numbers. In all brains, the inferior olivary nucleus did not show retrograde loss of neurons. Moreover, age-related abnormalities in the cerebellar nuclei and the inferior olive have been reported (Bauman, 1991). Apart from reports on limbic alterations, Bailey et al. (1998) demonstrated olivary dysplasia in three of five autistic cases. In another two autistic subjects they found ectopic neurons related to the olivary complex (Bailey et al., 1998). Finally, Rodier et al. (1996) reported that the brain of a 21-year-old autistic woman with mental retardation and comorbid epilepsy, exhibited near-complete absence of the facial nucleus and superior olive along with shortening of the brainstem between the trapezoid body and the inferior olive.

Migration abnormalities and cortical dysgenesis

Reelin is a signaling molecule that plays a role in migration and lamination of neurons during embryogenesis. In adult life, Reelin is involved in synaptic plasticity (Fatemi et al., 2000b; Fatemi, 2002, 2004). In the cerebellar cortex, Fatemi and Halt (2001) found a >40% reduction in Reelin and a 34%-51% reduction in Bcl-2 levels in autistic subjects. Very recently, Fatemi et al. (2005b) observed reduced Reelin signaling in the frontal cortex in autism. There is an association of decreased Reelin levels with disturbed neuronal migration and lamination of the cerebral and cerebellar cortex in mice (Gonzalez et al., 1997) and humans (Piven et al., 1990; Persico et al., 2001). Furthermore, decreased Reelin levels in the blood have been related to severe mental retardation and hypoplastic cerebellum, both of which have been reported in autism. The decreased Bcl-2 levels might inhibit apoptosis. Both decreased of Bcl-2 and increased P53 levels were correlated to mental retardation and have been suggested to result in a greater propensity for cell death (Fatemi and Halt, 2001). Cortical dysgenesis was identified in four of six (all mentally handicapped) autistic cases (Bailey et al., 1998). These brains showed thickened cortices, high neuronal density, presence of neurons in the molecular layer, irregular laminar patterns and poor gray-white matter boundaries.

Given the importance of cortical cellular organization during development, Casanova et al. (2002a) investigated the morphology of cell minicolumns. Compared to controls, there were more numerous, smaller and less compact

minicolumns in autistic subjects (Casanova et al., 2002a, 2002b). However, the functional significance of these changes in minicolumns is still unclear (Hutsler and Galuske, 2003).

Cholinergic system

Hohmann and Berger-Sweeney (1998) emphasized the importance of the cholinergic system during brain development. They reported a delay in cortical development, permanent changes in cortical architecture and cognitive function when cholinergic innervation is disrupted during early postnatal development. Furthermore, Bauman and Kemper (1994) demonstrated larger cholinergic neurons in young autistic cases compared to smaller cholinergic neurons at an older age. Perry et al. (2001) investigated levels of cholinergic enzyme and receptor activities in the frontal and parietal cerebral cortex. Compared to non-autistic mentally retarded cases, the autistic cases display 30% lower muscarinic M1 receptor binding in the parietal cortex. In addition, a reduction in α4 nicotinic receptor binding was found in all groups as compared to controls. In the cerebellum, the nicotinic receptor (α3 and α4 subunit) was reduced by 40%-50%, whereas the α7 subunit was increased in autism (Lee et al., 2002).

GABAergic abnormalities in autism

The GABAergic system has also been suggested to be involved in autism (Cook et al., 1998; Schroer et al., 1998; Blatt et al., 2001). GABA is implicated in various psychiatric disorders, including schizophrenia (Guidotti et al., 2000; Caruncho et al., 2004), mood disorders (Sanacora et al., 1999), anxiety disorders (Goddard et al., 2001) and autism (Cook et al., 1998; Schroer et al., 1998). Changes in GABA levels have been found in platelets of 18 of 18 autistic children (Rolf et al., 1993) and in the plasma and urine of one male (case study) autistic child (Cohen, 1999; 2000). Dhossche et al. (2002) hypothesized that the elevated plasma levels of GABA could reflect a compensatory increase in presynaptic GABA release in response to hyposensitivity of a subset of GABA receptors. In turn, this could produce increased postsynaptic activation of other, normal GABA receptors subtypes, resulting in complex alterations of GABAergic function throughout the brain in autistic people. The GABA plasma levels can be lowered by introducing a GABA-transaminase agonist (Cohen, 2002). During normal GABA catabolism, GABA-transaminase is responsible for the conversion of GABA into succinic semialdehyde (SSA)

(Tillakaratne et al., 1995). Such a GABA-transaminase agonist can activate GABA-transaminase enzyme activity by causing a reduction of plasma GABA levels in the brain. They proposed that this could result in an elevated signaling between axons and oligodendrocytes in the corpus callosum, which might result in a decrease of autistic features due to abnormal development of axons in the corpus callosum (Cohen, 2002). Cohen (2000) also reported increased levels of ammonia in the liver of the same autistic child, illustrating a possible link between the liver and infantile autism.

Blatt et al. (2001) investigated the hippocampal density and distribution of neurotransmitter receptors from the GABAergic, serotonergic (5-HT), cholinergic and glutamatergic systems in autistic patients and controls (age range 16-24 years). They reported that only the GABAergic receptor system was significantly reduced in autism. It has been suggested that some autistic patients respond abnormally to benzodiazepines, possibly due to pre-existing GABAergic dysfunction or abnormalities in the GABA benzodiazepine receptor complex (Garreau et al., 1993). Furthermore, ^{3}[H]-flunitrazepam-labeled benzodiazepine binding sites and ^{3}[H]-muscimol labeled $GABA_A$ receptors were reduced in the hippocampus of autistic people (Blatt et al., 2001), which provides evidence for abnormal benzodiazepine receptor complexes in the hippocampus of these people. Fatemi et al. (2002c) found reduced levels of both of glutamic acid decarboxylases (GAD)65 and GAD67 in autistic parietal and cerebellar cortex, implying a deficit in GABA. Lower GABA levels could reduce the threshold for developing seizures, which are often associated with autism (Bailey et al., 1998; Blatt et al., 2001).

The heritability of autism is 60-90% (Andres, 2002; Bespalova and Buxbaum, 2003). Abnormalities on the long arm (15q11-13) of the maternally derived chromosome 15 have been found in a small proportion of autistic people (Schroer et al., 1998; Dhossche et al., 2002). These aberrations include duplications and deletions involving the proximal long arm of this chromosome (Schroer et al., 1998). Three $GABA_A$ receptor subunit genes, GABRB3, GABRA5 and GABRG3, are located in the proximal arm of the 15q region (Schroer et al., 1998). In addition, using fluorescence *in situ* hybridization, Silva et al. (2002) showed tetrasomy in the 15q11-13 chromosomal region in a female child with autism. This tetrasomy could result in an excess of GABA receptors, leading to behavioral problems, including hyperactivity and epilepsy, a frequent comorbidity of autism. Linkage studies for this chromosomal region have produced contradictory

results (Cook et al., 1998; Schroer et al., 1998; Maestrini et al., 1999; Bass et al., 2000; Martin et al., 2000; Menold et al., 2001; Buxbaum et al., 2002; Muhle et al., 2004). As mentioned above, Casanova et al. (2002a, 2003) found narrower cell minicolumns in brains from autistics. In this regard it might be of interest that abnormalities in GABAergic interneurons have been suggested to be associated with narrowing of cell minicolumns (Nishikawa et al., 2002). Furthermore, Reelin appears to play a role in the development of minicolumns (Nishikawa et al., 2002), which may imply a relationship between the GABAergic system, minicolumns, Reelin and autism.

GABA and brain development

Early development

Several studies have pointed out that GABAergic synapses and receptors are generated and active before glutamatergic synapses in all brain regions (Koller et al., 1990; Walton et al., 1993; Chen et al., 1995; Ben-Ari et al., 2004; Bacci and Huguenard, 2006). However, GABAergic interneurons have a longer migration journey before they reach their final destination (Ben-Ari et al., 2004). Furthermore, Tyzio et al. (1999) have suggested that the first GABAergic synapses are probably located on the apical dendrites of pyramidal neurons and not on the soma.

Many different GABAergic receptor subunits are expressed in the embryonic and/or adult brain. The change in subunit composition is essential for normal development in specific brain regions (Lujan et al., 2005). Each subunit of the $GABA_A$ receptor exhibits a unique regional and temporal expression profile during brain development (Laurie et al., 1992). The α2, α3 and α5 subunits are dominantly expressed during embryonic development whereas others dominate postnatal or adult brain (Laurie et al., 1992; Fritschy et al., 1994). For example, α1 subunit expression is low at birth and increases during the first postnatal week, while the α2 subunit decreases progressively (Fritschy et al., 1994).

During early development, GABA causes depolarization (i.e. excitation) due to a relatively high concentration of intracellular Cl^- (Owens et al., 1996; Miles, 1999). Depolarization occurs via the opening of GABA-gated Cl^- channels, which also increases the intracellular Ca^+ concentration (Owens et al., 1996; Miles, 1999; Jelitai et al., 2004). Both GABA excitation and Ca^+ influx may be important for plasticity, synaptic connections and for establishing neural networks (Kriegstein and Owens, 2001). Consistent with this observation,

in primary cultures of several embryonic and neonatal brain tissues, GABA exerts a variety of neurotrophic actions such as promotion of neurite extension, synaptogenesis, and the synthesis of its own receptors (Hansen et al., 1987). Moreover, excitatory GABAergic interneurons can generate giant depolarizing potentials (GDPs), which in turn cause primitive network-driven patterns of electrical activity in all developing circuits (Ben-Ari, 2002). GDPs are hallmarks of developing neural networks and constitute the first synaptic pattern observed in the developing rat hippocampus (between P0 and P10) (Ben-Ari et al., 1989; Ben-Ari, 2001).

During maturation, GABA induces the opposite effect; Cl^- ions are pumped out and the cell becomes hyperpolarized. Thus, GABA switches from an excitatory to an inhibitory neurotransmitter during development (Miles, 1999). In the rat, this switch occurs around birth and is due to the expression of the K^+/Cl^- cotransporter 2 (KCC2) (Miles, 1999; Rivera et al., 1999; Herlenius and Lagercrantz, 2004). KCC2 expression increases progressively from embryonic stages to postnatal day 15 (P15) (Stein et al., 2004). This elevation occurs simultaneously with the GABA switch from excitatory to inhibitory (Stein et al., 2004). When the GABA switch occurs in humans is not known (Herlenius and Lagercrantz, 2001).

Migration

Migration is a process of neuronal movement essential for the establishment of normal brain architecture. Most cortical neurons migrate from their original site to their final destination in the cerebral cortex using the radial pathway from cortical ventricular zones (VZs) into the neuronal layers. In contrast, a subpopulation of cells including GABAergic neurons move tangentially within the intermediate zone (Rapp and Bachevalier, 1993; Rakic, 1995a; O'Rourke et al., 1997; Hatten, 1999). GABAergic neurons arise in the medial and lateral ganglionic eminences and migrate dorsally into the developing cortex (Rapp and Bachevalier, 1993). As early as embryonic day 10 (E10), GABA is located near the target destinations of migratory neurons and in the migrating neurons themselves in the developing mouse brain *in vivo* (Del Rio et al., 2000). Different GABA concentrations promote migration of GABAergic and non-GABAergic neuronal cortical subpopulations (Behar et al., 1996). For example, in cortical regions, femtomolar concentrations of GABA stimulate directed migration (chemotaxis), whereas micromolar levels stimulate chemokinesis (random motility) of more mature neurons (Behar et

al., 1996, 1998). Lopez-Bendito et al. (2003) showed a modified distribution of tangential migration neurons within the cortex upon blockade of $GABA_B$ receptors with a specific antagonist (CGP52432) in embryonic rat organic cultures. Furthermore, blocking of GABA receptors with saclofen or picrotoxin resulted only in a delay of cell movements, but not a complete arrest of migration. These findings could indicate that GABA receptor activation in the developing cortex modulates the rate of cell migration rather than initiating it (Behar et al., 2000). Furthermore, it has been suggested that migration, mediated by the GABAergic system, can act through Ca^{2+} ions, which alter cell movements by changing the dynamics of the cytoskeletal remodeling (Gomez and Spitzer, 1999).

Other factors regulate tangential migration as well (Marin and Rubenstein, 2001). Mitogenic factors that stimulate the movement of cells, such as hepatocyte growth factor/scattered factor (HGF/SF) and neurotrophic factors. In slice cultures, for example, exogenous HGF/SF increases the number of cells that migrate away from the subpallial telencephalon, while anti-HGF/SF antibodies inhibit cell movement (Powell et al., 2001). Little is known about the substrates that are used by migrating neurons. As described by Parnavelas (2000), it is possible that migrating interneurons use axons as a substrate in the cortex. Nevertheless, it is still unclear whether migrating interneurons interact with fiber tracts *in vivo* (Wichterle et al., 2001). Finally, the factors that guide different migratory streams through appropriate pathways towards their targets (Marin and Rubenstein, 2001), include the netrin/Dcc (Livesey and Hunt, 1997; Parnavelas, 2000), Slit/Robo (Yuan et al., 1999; Parnavelas, 2000) and semaphorin/neuropilin systems (Skaliora et al., 1998).

Proliferation

The process of proliferation is responsible for generating the correct number of specific cell types in the correct sequence in the brain (Lujan et al., 2005). Growth factors, neurotransmitters and their receptors have been implicated in the extrinsic regulation of cell proliferation in the developing telencephalon (Nguyen et al., 2001). In contrast to microglia and astrocytes, neurons exhibit very low rates of proliferation in culture (Eliason et al., 2002). Several studies have demonstrated a positive effect of GABA on cell proliferation. Ben-Yaakov and Golan (2003) demonstrated GABA-dependent cell proliferation in the hippocampus. GABA also promotes cell proliferation in cultures of cerebellar progenitors, with no effect on cell survival (Fiszman et al., 1999).

Furthermore, Haydar et al. (2000) showed that exogenous GABA increases proliferation by shortening the cell cycle in the neocortical ventricular zone (VZ) of the embryonic cerebrum in organotypic cultures. The reverse effect was found in the subventricular zone (SVZ) (Haydar et al., 2000). The same group demonstrated that the effect seen in the VZ was mediated by $GABA_A$ receptors (Haydar et al., 2000). Activation of $GABA_A$ receptors also influences DNA synthesis (Haydar et al., 2000). However, an *in situ* study demonstrated that $GABA_A$ receptors, triggered by GABA or muscimol (a $GABA_A$ receptor agonist) negatively regulate DNA synthesis in neural progenitors in the rat embryonic neocortical VZ between E16 and E19 (LoTurco et al., 1995).

In contrast, GABA (and glutamate) has been implicated in the reduction of the number of proliferating cells in dissociated or organotypic cultures of the neocortex (LoTurco et al., 1995). Moreover, Luk and Sadikot (2001) found no GABAergic effect on cell proliferation in the rodent neostriatum. In their study of parvalbumin-immunoreactive progenitors, they only revealed an effect of GABA on cell survival. However, Fiszman et al. (1999) demonstrated that GABA and $GABA_A$ receptor agonists do not influence survival in cerebellar granule cells *in vitro*. This finding could be due to a calcium influx via voltage gated calcium channel activation which subsequently activates the MAPK cascade (Fiszman et al., 1999).

Differentiation

Neuronal differentiation is another step in brain development that seems to be regulated by early glutamate- and GABA-mediated signaling. During early cortical neuronal differentiation, Cajal-Retzius (CR) cells play a key role in regulating cortical lamination (Lujan et al., 2005), and they produce Reelin (Nishikawa et al., 2002). Reeler (Reelin mutant) mice display severe cortical laminar disruption (Nishikawa et al., 2002). In addition, CR cells express diverse neurotransmitters and $GABA_A$ receptors, indicating that they can respond to GABA produced by nearby neurons (Mienville and Pesold, 1999). In cultured embryonic hippocampal neurons, $GABA_A$ receptor activation increases neurite outgrowth and maturation of GABAergic interneurons (Barbin et al., 1993). Such activation also plays a role in the morphological development of cortical neurons via membrane depolarization (Maric et al., 2001). In addition, switches in $GABA_A$ receptor unit composition (Owens et al., 1999) and changes in expression of components involved in GABA synthesis, storage and release may mediate the transition from embryonic

to adult GABAergic signalling (Somogyi et al., 1995).

Several factors regulate the differentiation of tangentially migrating neurons, such as Dlx1, Dlx2 and Mash1. These genes may control the timing of neuronal differentiation and induce the GABAergic phenotype. Dlx1 and Dlx2 are linked homeobox genes, whereas Mash1 is a basic helix-loop-helix gene that can induce Dlx1 (Fode et al., 2000). Normally, these three transcription factors are expressed in the VZ and SVZ progenitor cells in the anterior peduncular area (AEP), lateral (LGE) and medial ganglionic eminence (MGE) (Bulfone et al., 1993; Guillemot and Joyner, 1993; Porteus et al., 1994; Eisenstat et al., 1999). Studies with mice lacking Dlx1, Dlx2 or Mash1 have revealed insights in the role of these transcription factors during differentiation. Anderson et al. (1997) have shown that the functional loss of Dlx1 and Dlx2 blocks the differentiation of late-born subpallial telencephalic neurons. Interestingly, double mutations of Dlx1/Dlx2 have a four-fold reduction in GABAergic interneurons (Anderson et al., 2001). Functional loss of Mash1 leads to premature differentiation of several early-born cell populations (Casarosa et al., 1999). In Mash1 mutants, more GABAergic interneurons are lost in the marginal zone of the cortex as compared to the intermediate zone (Marin et al., 2000). Additionally, gain-of-function studies revealed that Dlx and Mash genes both can induce aspects of the GABAergic phenotype (Fode et al., 2000).

Animal models of autism

Animal models are very useful for determining the role of genes and environment, understanding the pathogenesis and for testing potential therapeutic approaches. Moreover, animal models need not to be perfect mimics of human diseases in order to be valuable. Autism is a heterogeneous disorder in which most of the susceptibility genes have not yet been identified. Nonetheless, there are several genetic changes that do entail a high risk for autism, and mouse models of these changes share some features of the human disorder. Furthermore, models based on environmental risk factors are valuable. Finally, brain lesion models are of interest. The following section describes a variety of animal models that show features of autism.

Genetic manipulation

- X-chromosome loci

Four loci on the X-chromosome have been identified in autism thus far. These genes are the Fragile X mental retardation protein (Fmr1), methyl-

CpG-binding protein type 2 (MECP2) and neuroligin (NLGN) 3 and 4. Fmr1 is silenced in Fragile X syndrome (FXS), a condition that often includes autism symptoms (Wassink et al., 2001). The fmr1 knockout (KO) mouse displays increased dendritic spine density in the visual and somatosensory cortices, with a greater number of spines with an immature appearance (Comery et al., 1997; Nimchinsky et al., 2001; Galvez et al., 2003). These features have also been found in several cortical areas in FXS humans (Irwin et al., 2001). However, there appears to be a decrease in dendritic branching in the human hippocampus (Raymond et al., 1996). Clearly, more neuropathologic studies are needed to relate this animal model to autism. The NLGN1, 3 and 4 genes map to three loci associated with predisposition to autism, 3q26, Xp22.3 and Xq13, respectively. Mutations in NLGN3 and 4 are associated with autism and, in some cases, with mental retardation, a feature often associated with autism (Jamain et al., 2003; Laumonnier et al., 2004). Chih et al. (2004) and Comoletti et al. (2004) found that these NLGN3 and 4 mutations lead to loss of protein processing and loss of the capacity for stimulation of synapse formation. Detailed neuropathology and behavioral analysis of the MECP2 KO remains to be reported.

- 15q11-q13 locus

As mentioned above, the 15q11-q13 locus is relatively small and has been linked to autism in several studies (Cook et al., 1998; Schroer et al., 1998; Menold et al., 2001; Buxbaum et al., 2002; Dhossche et al., 2002; Muhle et al., 2004). Jiang and Beaudet (2004) have identified Ube3a, a genetic locus for Angelman syndrome (AS), which is located in this region and shares some clinical features with autism. The same group investigated a mouse model with a maternal null mutation, which shows a lack of Ube3a expression in cerebellar Purkinje cells and in the hippocampus. Both features have been implicated in autism (Jiang et al., 1998). The relationship of the 15q11-q13 locus and the GABAergic system was described above. However, more neuropathology is required to establish the relationship between $GABA_A$ receptor KO mice and autism.

- Serotonin

It is generally agreed that there are serotonin (5-HT) abnormalities in autism. 5-HT levels in platelets are increased (Cook and Leventhal, 1996; Anderson et al., 2002), however, the underlying mechanism of this elevation is unclear.

Therefore, the relevance of these changes for the brain is not well understood. Some studies have emphasized the importance of 5-HT during fetal brain development (Whitaker-Azmitia, 2001; Gaspar et al., 2003), where this transmitter plays a role in neurogenesis, neuronal differentiation, neuropil formation, axon myelination and synaptogenesis *in vivo* (Whitaker-Azmitia, 2001). Thus, altering 5-HT levels during development could lead to relevant models for autism. Whitaker-Azmitia and colleagues (2001) have investigated 5-HT depleted neonatal rat pups and found decreased dendritic length and spine density in the hippocampus, the same features Raymond et al. (1996) observed in autism. Furthermore, neonatal disruption of 5-HT tracts causes alterations in cortical morphogenesis in rodents (Connell et al., 2004).

Studies on KO mice have revealed insights into the role of 5-HT in both early embryonic and postnatal development (Gaspar et al., 2003; Gingrich et al., 2003). For example, KO experiments showed that the 5-HT_{2B} receptor is involved in the regulation of neurogenesis, cell specification and cell survival during early development. At later developmental stages, depending on the brain region, such control can be mediated by the 5-HT_{1A} (regulation of dendrite growth) and $5\text{-HT}_{2A/2C}$ (regulation of axonal growth) receptors. Unfortunately, detailed neuropathology in these mice, particularly with relevance to known changes in the autistic brain, is missing.

- DLX

DLX genes regulate the development of a subset of cortical and striatal neurons. Two of the linkage loci for autism, 2q31.1 and 7q21.3, contain the DLX1/2 and DLX5/6 complexes, respectively. Stuhmer et al. (2002) reported that mutations in DLX2 and 5 genes alter the development of GABA neurons in the forebrain. As stated earlier, the GABAergic system is involved in the pathology of autism. Thus, DLX mutant mice will be of interest.

- Engrailed

The gene Engrailed *2* (En2) is located on chromosome 7, which has been linked to autism (Gharani et al., 2004). Mouse mutants of En2 and autistic individuals display similar cerebellar morphological abnormalities. En2 KO mice show a loss of Purkinje cells (Liu and Joyner, 2001; Gharani et al., 2004), as do autistic brains, where the loss appears in stripes or patches (Bailey et al., 1998). Other features shared between the En2 KO mice and human autistic cases are deficiencies in the number of deep nuclear, granule

and inferior olive neurons. Recently, increased neuronal packing, a smaller hippocampus and ectopic location of neuronal subgroups in the amygdala in En2 KO mice have been linked to autism (Kuemerle et al., 1997). There is now a need for detailed behavioral studies of these mice.

- Reelin

The Reelin gene, located on chromosome 7, has been linked to autism. Conflicting reports exist about the association of its polymorphisms with autism (Persico et al., 2001; Krebs et al., 2002; Bonora et al., 2003). In the adult brain, Reelin is normally expressed by GABAergic neurons. In patients, Guidotti et al. (2000) suggested that there might be a correlation between Reelin and GAD67, one of the two molecular forms of GAD. This interaction is clearly expressed in the cerebellum, where Reelin regulates dendritic sprouting in GABAergic Purkinje cells (Curran and D'Arcangelo, 1998). These features were also reported in the heterozygous Reeler mouse (Tueting et al., 1999). Interestingly, in the male heterozygous Reeler mouse (rl+/-), loss of Purkinje cells have been reported between 3 and 16 months of age. Furthermore, mutant Reeler mice, in which Reelin is absent, display severe cortical laminar disruption (Nishikawa et al., 2002).

Environmental factors

- Thalidomide and valproic acid

Thalidomide has been associated with a marked increase in the incidence of autism. (Stromland et al., 1994). In rats, thalidomide exposure on E9 causes increased plasma, hippocampal and frontal cortex 5-HT as well as an altered distribution of 5-HT in neurons in the raphe nuclei (Narita et al., 2002). The offspring of women taking valproic acid (VPA) during early pregnancy have an increased risk for autism (Costa et al., 2004). The offspring of pregnant rats given VPA show a reduced number of Purkinje cells, decreased cerebellar volume and a decreased cell number in the cranial nerve motor nuclei (Ingram et al., 2000). In addition, neurons in the inferior olive that innervate Purkinje cells are also reduced in number, as are those in the deep nuclei targets of Purkinje cells in the nucleus interpositus (Rodier et al., 1996). As with thalidomide, VPA exposure on E9 causes hyperserotonemia in the mouse hippocampus, frontal cortex and cerebellum (Narita et al., 2002). These observations all parallel human autistic pathologic findings. The use of thalidomide and VPA has provided important insights into autism and has led to useful animal models as well.

- Maternal infection

Maternal infection increases the risk of autism in the offspring. For example, prenatal exposure to rubella virus increases incidence of autism (Chess, 1977). Furthermore, pregnant mice infected with influenza virus at E9.5 yield adult offspring that display histological and behavioral abnormalities found in autism and schizophrenia (Shi et al., 2003). These mice have smaller brain sizes at birth, but macroencephaly in adulthood (Fatemi et al., 2002a; Shi et al., 2003). This neonatal undergrowth followed by overgrowth mirrors the pattern seen in autism. With respect to brain pathology, the offspring of maternally infected mice display a selective loss of Purkinje cells in lobule VII, as well as thinning of the neocortex and hippocampus, pyramidal cell atrophy, reduced levels of Reelin immunoreactivity, and changes in neuronal nitric oxide synthase expression and synaptosome associated protein of 25kDa (SNAP-25) (Fatemi et al., 1998, 2000a, 2002a; Shi et al., 2003). Some of these features mimic autism pathology.

- Postnatal viral infection

The most extensively studied rodent model involving postnatal viral infection utilizes intracerebral injection of Borna disease virus (BDV) within 12 hrs of birth (Pletnikov et al., 2002; Hornig et al., 2003). Several aspects of this model are relevant to autism, including alterations in 5-HT levels in various brain regions, loss of Purkinje cells in the cerebellum and granule cells in the dentate gyrus (Dietz et al., 2004). Postnatal infection with lymphocytic choriomeningitis virus (LCMV) also leads to acute loss of neurons in the cerebellum and delayed loss of neurons in the hippocampus (Pearce, 2003). There is also an association between cytomegalovirus (CMV) infection and autism, which could be followed up in animals (Yamashita et al., 2003).

Lesions

- Cerebellum

Neuropathologic observations in autism are rather consistent in respect to the cerebellum. Therefore, it is of particular interest to study genetic, surgical and toxin lesions of the cerebellum. Recently, numerous mutations and toxic insults were associated with diverse patterns of Purkinje cell loss (Sarna and Hawkes, 2003). Subpopulations of Purkinje cells are less vulnerable to death, probably because they express the neuroprotective protein HSP25/27. The same feature is seen in mouse models of Niemann-Pick disease type A/B

and C (Sarna and Hawkes, 2003). Accordingly, the pattern of cell loss in each case is specific to the type of insult. Thus, the selective loss of Purkinje cells in lobule VII in the influenza model is an important parallel with autism.

The various models discussed here are the primary ones showing neuropathologies that mimic some of the features found in autism. However, striking behavioral features of autism can be assayed in animals, such as stereotypic and repetitive behaviors, enhanced anxiety, abnormal pain sensitivity, disturbed sleep patterns, deficient maternal bonding/affiliation and deficits in sensorimotor gating (prepulse inhibition [PPI]). While the maternal infection, thalidomide and VPA models have been studied behaviorally, much remains to be done in this respect with the other models.

Discussion

In this chapter we have examined the literature on autism neuropathology, the role of the GABAergic system in this disorder and the relevance of mouse models showing features of autism. With respect to the neuropathology of autism, consistent findings have emerged for the limbic system, cerebellum and cerebral cortex. Neuropathologic data of the limbic system show increased cell packing density and smaller neurons. These observations might be explained by an arrest of normal development (Kemper and Bauman, 1998). A decreased number of cerebellar Purkinje cells without significant gliosis and features of cortical dysgenesis have been reported by several different research groups. These findings suggest a largely prenatal origin of autism, which is supported by the epidemiological findings with thalidomide, VPA and maternal infection. Furthermore, age-related abnormalities in the inferior olive and cerebellar nuclei have been found in autism. As the inferior olive project to the cerebellar Purkinje cells, a decrease in Purkinje cell number can be caused by a very early, abnormal development of these projections (Palmen et al., 2004). Cortical dysgenesis might affect correct lamination of the cortex and can cause abnormalities in the process of cell death. In line with this are findings of reduced Reelin levels and Bcl-2. Reelin also plays a role in the development of minicolumns, a feature that has been reported in autism. Furthermore, abnormalities in GABAergic neurons are associated with narrowing of the cell minicolumns. However, those studies involve small sample sizes, the use of quantification techniques not free from bias, and high percentages of autistic subjects with comorbid mental retardation or epilepsy.

As with the cholinergic system, several studies have reported a reduction in GABA function, availability and activity in autism. Furthermore, a decrease in GABA receptor binding has been shown in autism. An imbalance in the availability of GABA receptors subunits may alter receptor activity and hence change the activity of the brain's major inhibitory neurotransmitter (Schroer et al., 1998). As a consequence, the threshold for developing seizures, a frequent comorbidity of autism, might be reduced. From a genetic point of view, three $GABA_A$ receptor subunit genes have been located in the proximal arm of chromosome 15. Abnormalities in this chromosomal region have been found in a small proportion of autistic people.

As autism is a neurodevelopmental disorder, it is important to elucidate the role of GABA during development. Evidence indicates that GABA plays a role in several developmental processes including cell migration, proliferation and differentiation. As these processes might be affected in autism, GABA dysfunction could account for some neuropathology seen in autism. For example, GABA dysfunction may occur in conjunction with Reelin and therefore affect neuronal migration and the arrangement of cortical minicolumns in autism. The results reported on the influence of GABA on proliferation are somewhat controversial. A positive influence on GABA cell survival could reflect a GABA mediated decrease in apoptosis during development and in turn might explain the increased head circumference, brain weight and brain volume reported in autism. However, when abundant cells are not functioning properly, they would die, resulting in normalization of, or a decrease in, brain volume later in childhood. However, in those subgroups of autistic subjects in which this brain enlargement is still be present in adulthood, this compensatory cell death may not take place (Courchesne, 2004). Instead, these autistic subjects might be able to recruit these 'extra' neurons, possibly resulting in increased dendritic growth and thus in increased brain volume, still present in adolescence.

Although the neuropathologic results in autistic subjects are revealing, animal models are essential for better understanding of the pathophysiology, cause and treatment of autism. Although no animal model has been created that perfectly mimics all aspects of a human disease, striking parallels between autism and animal models have already been reported. For example, in genetic models, mouse mutants of En2 display decreased Purkinje cell number (Gharani et al., 2004). In NLGN mouse mutants, a loss of protein processing and a loss of the capacity for synapse stimulation are found

(Chih et al., 2004). DLX mutations are associated with abnormalities in the development of GABAergic neurons (Stuhmer et al., 2002). The recent linkages of NLGN, DLX, and En2 to autism offer possibilities for animal models, particularly if introducing the relevant, specific mutations (as opposed to simple KOs) can cause interesting pathology and behavior. In addition, infection with Borna disease virus shows behavioral disturbances in sensorimotor, emotional and social activity, together with a decrease in the number of Purkinje cells (Hornig et al., 2002). Maternal infection models display selective Purkinje cell loss (Patterson, 2002; Shi et al., 2003). This model also shows macroencephaly in the offspring, atrophy of pyramidal cells, and reduced Reelin immunoreactivity. Furthermore, these mice display deficits in social behavior, social interaction, and PPI.

Chapter 3

Minicolumnar abnormalities in autism

Casanova MF, Van Kooten IAJ, Switala AE, Van Engeland H, Heinsen H, Steinbusch HWM, Hof PR, Trippe J, Stone J, Schmitz C.

Acta Neuropathol (Berl) 2006; 112: 287-303.

Abstract

Autism is characterized by qualitative abnormalities in behavior and higher order cognitive functions. Minicolumnar irregularities observed in autism provide a neurologically sound localization to observed clinical and anatomical abnormalities. This study corroborates initial reports of a minicolumnopathy in autism within an independent sample. The patient population consisted of 6 age-matched pairs of patients (DSM-IV-TR and ADI-R diagnosed) and controls. Digital micrographs were taken from cortical areas S1, 4, 9, and 17. Image analysis produced estimates of minicolumnar width (CW), mean interneuronal distance (MCS), variability in CW (VCW), cross section of Nissl-stained somata, boundary length of stained somata per unit area, and the planar convexity. On average CW was 27.2 μm in controls and 25.7 μm in autistic patients ($p = 0.0234$). Mean neuron and nucleolar cross sections were found to be smaller in autistic cases compared to controls, while neuron density in autism exceeded the comparison group by 23%. Analysis of inter- and intracluster distances of a Delaunay triangulation suggests that the increased cell density is the result of a greater number of minicolumns, otherwise the number of cells per minicolumns appears normal. A reduction in both somatic and nucleolar cross-section could reflect a bias towards shorter connecting fibers, which favors local computation at the expense of inter-areal and callosal connectivity.

Introduction

Minicolumns are basic architectonic and physiological elements identified in all regions of the neocortex (Buxhoeveden et al., 2002) and in all mammalian species thus far evaluated (Gressens and Evrard, 1993). The minicolumnar circuit is an evolutionarily and ontogenetically conserved template adapted in the various cortical areas according to their specific developmental and functional requirements. The minicolumnar core comprises radially oriented arrays of pyramidal projection neurons. At the core and periphery of the minicolumn, combinations of GABAergic interneurons provide for a diversity of signaling properties that serve to dynamically modulate pyramidal cell inputs and outputs that perform area and task-specific information processing needs (DeFelipe, 1997; Kawaguchi and Kubota, 1997; Gupta et al., 2000; Casanova et al., 2003).

Available neuropathological and structural imaging data suggest that autism is the result of a developmental lesion capable of affecting brain growth. One possible explanation for this is the recent finding of minicolumnar abnormalities in autism (i.e., minicolumns of reduced size and increased numbers) (Casanova et al., 2002a). In this initial study measures of minicolumnar morphometry were obtained relative to pyramidal cell arrays in 6 autistic cases and an equal number of controls. The feature extraction properties of the algorithms were corrected for minicolumnar fragments, curvature of the tissue section, and 3D proportions (stereological modeling) (Casanova and Switala, 2005). Later on, the same patient population was used to confirm the presence of cortical radial abnormalities in a study using the Grey Level Index (GLI), i.e., proportional area covered by Nissl-stained to unstained elements in postmortem samples (Casanova et al., 2002b). Other studies have provided evidence that the minicolumnar alterations in autism are not a nonspecific effect of mental retardation. Investigators have found that minicolumnar width in Down syndrome patients reaches adult proportions earlier than normal, possibly as a result of accelerated aging (Buxhoeveden et al., 2002; Buxhoeveden and Casanova, 2004). In these studies minicolumnar size was reported to be normal despite the small brain size of Down syndrome patients.

An increase in the number of minicolumns is thought to underlie the neocortical expansion accompanying human encephalization, i.e., the process by which the brain has increased in size to a degree greater than expected when taking body size into account (Rakic, 1995b). Empirical

evidence and theoretical models indicate that local circuit neurons increase in number, complexity, and proportion relative to projection neurons during primate encephalization (Rakic, 1975; Hofman, 1985). These trends reflect the emergence in primates of a distinct population of dorsal telencephalic-derived inhibitory interneurons (Letinic et al., 2002) modulating activity of minicolumnar pyramidal cells. Furthermore, isocortical areas such as dorsolateral prefrontal cortex, lacking direct homologs in non-primates, contain a well-defined granule cell layer of excitatory interneurons and increased numbers of supragranular local projection neurons (Petrides and Pandya, 2002). Multiple polymorphisms associated with autism may be a consequence of phylogenetically recent changes in genetic programs guiding development of species-specific cytoarchitectonic features. Morphometric analysis of such features complements genetic analysis. This study therefore investigates minicolumnopathy in an independent sample of autistic patients. It also expands on previous findings by studying cortical cell size and density as related to pyramidal cell arrays. Changes in these parameters, early during development, would provide for basic alterations in corticocortical connections and information processing.

Materials and methods

Clinical dataset

Diagnosis for each autistic patient was established postmortem by the Autism Tissue Program (ATP). A certified rater and trainer arranged for a post-mortem visit with the family to obtain, with written consent, medical and clinical information via a questionnaires that included the Autism Diagnostic Interview-Revised (ADI-R; Lord et al., 1994).

The Harvard Brain Tissue Resource Center (HBTRC) questionnaire was modified to include autism-specific questions for ATP use. The information obtained included: donor and respondent identifying information; ethnicity, handedness and known exposure to hazardous materials; diagnostic information including dates and physician; genetic tests; pre- and postnatal medical history; immunization, medication and hospitalization information; family history and additional information about donor participation in any training or research studies such as imaging, medication trials and/or genetic studies. Supporting documents such as autopsy reports, death certificates, medical, clinical and/or educational records were obtained at the time of the home visit or by sending written requests, signed by the legal next-of-kin, to named providers.

Brain specimens

Postmortem brains (one hemisphere per case) from 6 autistic cases (mean interval between death and autopsy 20.0 ± 2.9 hours) and from 6 age-matched controls (mean interval between death and autopsy 24.0 ± 11.1 hours) were analyzed (Table 1). Brains were obtained from several brain banks in the USA and Germany. All autistic patients met the DSM-IV (American Psychiatric Association, 1994) and ADI-R (Lord et al., 1994) criteria for autism. None of them exhibited any chromosomal abnormalities. In all of the cases, autopsy was performed after informed consent was obtained from a relative. The use of these autopsy cases was approved by the relevant Institutional Review Boards. Clinical records were available for all cases.

Tissue processing

After immersion-fixation in 10 % formalin for at least 3 months all hemispheres were mounted with celloidin and cut into entire series of 200 µm thick coronal sections as described in detail elsewhere (Heinsen and Heinsen, 1991). Three hemispheres were cut at 500 µm thickness. These differences did not influence the results of this study, since imaging of the tissue was done at high magnification, with a depth of field much narrower than 200 µm (see below, Image Capture). Every third section (in one hemisphere: every second) was stained with Gallocyanin.

Table 1. Clinical characteristics of the cases included in this study.

Patient	Sex	Hemisphere	Age (y)	Cause of death	Clinical history	History of seizures	Medication history	Brain weight (g)	PMI (h)	Section thickness (µm)
A1	M	L	4	Drowning	Asthma/Bronchitis	No	Daily medication (not specified) for asthma/ bronchitis	1,160	30	200
C1	M	L	4	Myocardial infarct – Takayasu arteriitis	n.h.	n.h.	n.h.	1,380	5	500
A2	F	L	5	Car accident	Ear infections	No	Antibiotics for ear infections	1,390	13	200
C2	F	R	4	Lymphocytic myocarditis	n.h.	n.h.	n.h.	1,222	21	200
A3	M	R	8	Sarcoma	Syndactyly of the fingers and feet; Colitis; High fever; Neutropenia; Metastatic alveolar rhabdomyosarcoma; Large paravertebral mass extending from chest cavity to abdomen	Abnormal EEG; Not diagnosed with seizure disorder	Depakote (one year after EEG); Chemotherapy; Peridex; Nystatin; GCSF; Benadryl; Pheergan; Dexamethasone; Morphine	1,570	22	200
C3	F	R	7	Status asthmaticus	n.h.	n.h.	n.h.	1,350	78	500
A4	M	L	13	Seizures	Severe hypotonia; Ketogenic diet for 1.5 y	Yes	Dilatin (seizures); Anticonvulsants; Trileptal (seizures); Trazadone (sleep)	1,420	26	200
C4	M	R	14	Electrocution	n.h.	n.h.	n.h.	1,600	20	200
A5	F	R	20	Obstructive pulmonary disease	ADHD; Microcephaly; Epilepsy; Schizophrenia	Yes (3 times)	Various psychotropic medications including Haldol, Ritalin, and Congentin; DepoProvera (birth control); Mellaril (sleep); Zoloft	1,108	15	200
C5	M	R	23	Ruptured spleen	n.h.	n.h.	n.h.	1,520	6	200
A6	M	R	24	Drowning	Pneumonia; Bronchitis; Behavioral problems	First seizure prior to death	Quetiapine (200 mg BID); Propanolol (400 mg BID); Thioridazine (50 mg HS)	1,610	14	200
C6	M	R	25	Cardiac tamponade	n.h.	n.h.	n.h.	1,388	14	500

A, autism; C, control; M, male; F, female; L, left; R, right; n.h., no history; BW, brain weight; PMI, postmortem interval; y, years; h, hours.

Brain regions

Gallocyanin-stained sections were used by three of us (I.A.J.v.K, H.H. and C.S.) to identify cortical areas M1, V1, frontal association cortex, and S1 (areas 4, 17, and 9 of Brodmann (Brodmann, 1909) and area 3b of Vogt and Vogt (Vogt and Vogt, 1919), respectively) according to anatomical landmarks and cytoarchitectural criteria (Fig. 1). Gross anatomical landmarks for M1 include the anterior wall of the central sulcus and adjacent portions of the precentral gyrus. Cytoarchitectonically, the region is clearly demarcated by its giant Betz cells and minimization of layer IV (Rivara et al., 2003). Area 17 (V1) is located along the walls of the calcarine sulcus in the occipital lobe and adjacent portions of the cuneus and lingual gyrus (Carpenter, 1985). It is defined histologically by a broad lamina IV divided into 3 sublayers with numerous very small pyramidal cells in layers II and III. It is noted for the dense line of Gennari in myelin stains. Area 9 lies in the superior and middle frontal gyrus. (Rajkowska and Goldman-Rakic, 1995a, 1995b) found that it was located in the middle third of the superior frontal gyrus in all the cases they examined. It covered both dorsolateral and dorsomedial surfaces of the gyrus and extended in some cases to the depth of the superior frontal gyrus and portions of the middle frontal gyrus.

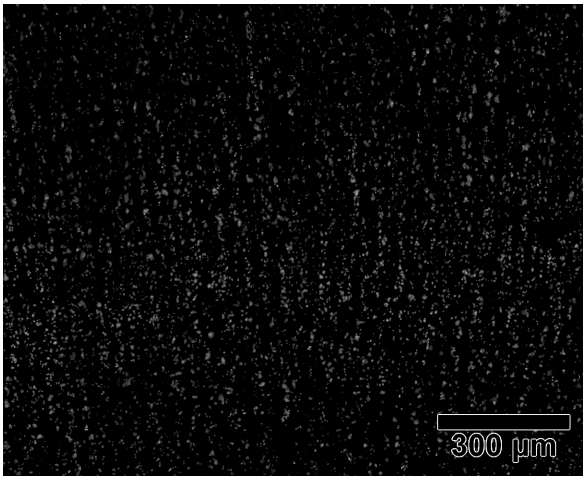

Figure 1. Primary sensory cortex of an 8 year old, autistic male. Automatic segmentation has classified pixels as background, shown in black, and neurons, in grayscale. Clumps of neurons have been further separated into individual objects using the morphological watershed transform.

Image capture

Regions of interest were delineated with a stereology workstation, consisting of a modified BX50 light microscope with UPlanApo objectives (Olympus, Tokyo, Japan), motorized specimen stage for automatic sampling (Ludl Electronics, Hawthorne, N.Y., USA), HV-C20AMP CCD colour video camera (Hitachi, Tokyo, Japan) and StereoInvestigator software (MicroBrightField, Williston, Vt., USA). Delineations were performed with a 10× objective (NA = 0.40). Digital micrographs each measuring about 200 µm by 150 µm were produced using the stereology workstation described above and a 40× oil objective (NA = 1.0). A few hundred such images were captured per region of interest to cover the entire cortical thickness. These images were assembled into one mosaic using the Virtual Slice module of the StereoInvestigator software. Only slight adjustments of contrast and brightness were made, without altering the data of the original materials.

Depth of field d_{tot} of the mosaic component images can be computed according to the formula:

$$d_{\text{tot}} = \left(\frac{\lambda}{\text{NA}} + \frac{e}{M} \right) \cdot \frac{n}{\text{NA}}$$

where λ is the wavelength of the illumination, M is the magnification, e is the resolution of the CCD (twice the distance between detectors), and n is the refractive index of the medium. These last two were e = 16.2 µm for the HV-C20AMP camera and n = 1.5 for oil. Taking λ on the order of 1 µm, d_{tot} was equal to about 2.1 µm, so images represent only a small virtual slice of the 200 µm or 500 µm thick sections, and differences in section thickness were thus not considered as a confound.

Computerized image analysis

Multiple techniques reduced the images to sets of descriptive parameters. The minicolumn fragment method (Casanova and Switala, 2005) produced estimates of the mean width (CW) of minicolumns in a region of interest, the relative deviation (V_{CW}) of minicolumnar widths about the mean, and the mean distance (MCS) between neighboring neurons within the same minicolumn fragment (the 'CW' and 'MCS' notation being used for consistency with earlier publications (Casanova et al., 2002a)). The parameters mean grain size ($\bar{A}$), mean grain perimeter ($\bar{U}$), and intensity (λ) of a Boolean spatial

model (Stoyan et al., 1995) were fit to each image. The gray level index, or GLI, method (Schleicher and Zilles, 1990; Schleicher et al., 2005) reported the mean (D) and standard deviation (sd_D) of distances between ridges of high stain intensity, mean (W) and standard deviation (sd_W) of the width of these ridges, and their average height (A) above background. Lastly the distribution of distances between neighboring neurons within each image was modeled as mixture of two distributions with means (m_{near} and m_{far}) and standard deviations (s_{near} and s_{far}, respectively) with $m_{near} < m_{far}$. Details of each of the four methods are outlined below.

Computerized image analysis of minicolumnar structure in laminae II through VI was performed with algorithms described in the literature (Casanova and Switala, 2005). The feature extraction properties of the program correct for minicolumnar fragments, curvature of the tissue section, and have been adapted to 3D proportions (stereological modeling). The resulting estimates of minicolumnar width have also been validated against physiological measurements using intrinsic optical signaling and against anatomical measurements using myelinated fiber bundles (Casanova and Switala, 2005). Color mosaics were converted to intensity images and adaptively thresholded using a scale space approach (Lega et al., 1995). Overlapping objects in the thresholded images were further separated using the watershed transformation. Each connected region in the resulting image was further classified according to size. Objects smaller than 10 μm^2, assumed to be glia, neuron fragments, or noise, were discarded altogether. Of the remaining objects, those with areas above the 15th percentile were used for minicolumn fragment detection, while the smaller objects were classified as interneurons based on the fraction of all neurons estimated to be inhibitory by Braitenberg and Schüz (Braitenberg and Schuz, 1998).

Local neuron density was computed as the sum of equal contributions from large objects above the 15th percentile in cross-section. Each large neuron produced a density hump, peaking at the object's centroid, with elliptical contours oriented so that the major axes were parallel to the local radial direction, i.e. along the axis of the minicolumn, at each point in an image. Ridges in neuronal density indicated the cores of minicolumn fragments, and objects including those classified as interneurons were parcellated into clusters according to the nearest fragment core. The average distance between neighboring fragment cores was addressed as the minicolumnar width CW (Fig. 2). Standard deviation of the logarithm of these distances

was the scale-independent measure variability in minicolumn width (V_{CW}). Interneuronal distance (MCS) was the average distance between centroids of neighboring neurons within the same fragment. Only fragments with more than ten neurons were considered when computing the means and standard deviations.

From the adaptively thresholded images computerized image analysis produced estimates of the relative amount of area occupied by Nissl-stained tissue (A_A), the total boundary length of stained tissue per unit area (L_A), and the planar convexity (N_A^+), which quantities are of no interest in themselves but suffice to compute parameters of a Boolean model with convex primary grains using the method of moments (Stoyan et al., 1995). Each realization of the Boolean model is the union of a number of convex random closed sets (grains) -independently and identically distributed with mean area $\bar{A}$ and mean perimeter $\bar{U}$- located, or centered, at the points of a Poisson process with intensity λ. These three parameters, which completely determine the model, were obtained algebraically from the following equations (Stoyan et al., 1995), substituting for A_A, L_A, and N_A^+ their respective estimates:

$$A_A = 1 - e^{-\lambda \bar{A}},$$
$$N_A^+ = \lambda (1 - A_A),$$
$$L_A = N_A^{+\bar{U}}.$$

Considering that the foreground pixels of a thresholded image correspond to locations in the original image overlapped by one or more stained cell soma, $\bar{A}$ is the average area of a neuronal cross-section and λ is their density, i.e. number of neuronal cross-sections per unit area. This technique was used to obtain these values without any need to segment individual neurons. The method of minicolumn fragments, on the other hand, does attempt to segment individual cell somata but uses the size of segmented objects only to sort them into size classes as described above.

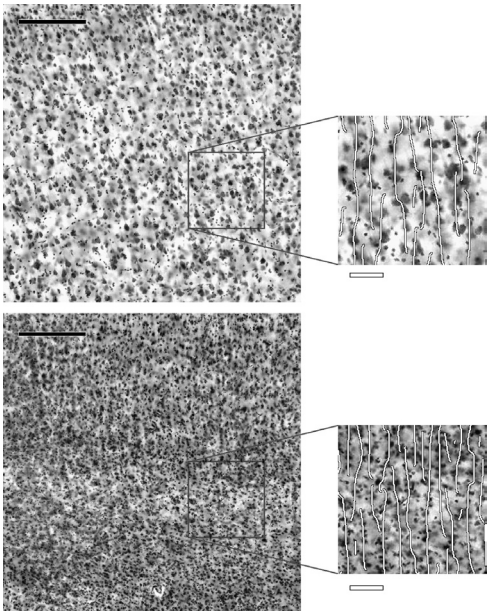

Figure 2. Minicolumns in Brodmann area 4, lamina III, in an autistic patient (bottom) and an age-matched control case (top). Insets highlight the cores of minicolumn fragments identified by our software, illustrating the reduction in minicolumnar width (CW). Scale bars measure 200 μm on left and 50 μm on right.

Thresholded images were also analyzed according to the gray level index (GLI) method (Schleicher and Zilles, 1990; Schleicher et al., 2005), slightly modified so that the GLI would vary smoothly across a region (Figs. 3 and 4). Here, the inverse thresholded image, with foreground set equal to one and background set equal to zero, was convolved with a kernel measuring 11 μm by 110 μm at half-maximum. The long axis of the kernel was parallel to the axes of the minicolumns, assumed to be the image *Y*-axis. The result was an estimate of the GLI, or staining intensity, in the neighborhood of each pixel (Fig. 3). Each GLI image so produced was measured in profiles in the *X* direction to obtain the following parameters: (i) mean (*D*) and (ii) standard deviation (sd_D) in distance between local maxima of the GLI, (iii) amplitude (*A*) of the local maxima, or difference between peak GLI and the lowest GLI between the peak in question and the next peak in the profile, and (iv) mean (*W*) and (v) standard deviation (sd_W) in the width, i.e. full width to half maximum, of the peaks (Fig. 4).

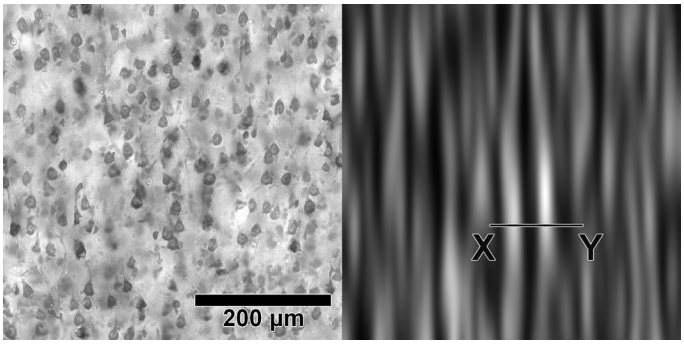

Figure 3. Left: A 0.5 mm × 0.5 mm field from normal human primary motor cortex, lamina III. Right: Local GLI in the vicinity of each point in the field. Values are shown in grayscale from 1 % (black) to 70 % (white). For the significance of points X and Y, see Fig. 4. The gray level profile in this figure differs qualitatively from the example in Schleicher and Zilles (1990) because we estimated GLI with a smooth, bell-shaped kernel and did not subsample the image. This allows for better localization of gray level peaks and troughs.

A follow-up study considered the distance between neighboring objects. Objects were those classified as large neurons for purposes of minicolumnar analysis (see above). Neurons were considered neighbors if (a) they were endpoints of an edge of the Delaunay triangulation of object centroids (Fig. 5), and (b) they were not further apart than the distance from either of them to the edge of the region of interest. Criterion (a) is equivalent to the geometric statement that three neurons are neighbors if the circle drawn through their centroids does not enclose the centroid of any other neuron. The criterion (b) is necessary to correct for a boundary effect where distant neurons are incorrectly labeled as neighbors because the true neighbors of one or more of them lie outside the region of interest. Now given that objects in a single lamina were clustered, as cells in minicolumns, an object's neighbors may include members of the same cluster or members of a nearby cluster (Fig. 6) Accordingly, the distribution of distances between neighbors (*d*) would then be a mixture of intracluster or near distances, and intercluster or far distances. This was modeled as a two component lognormal mixture distribution; that is to say, the log *d* were assumed to be drawn from either of two Gaussian distributions of near and far distances:

$$\log d \sim \alpha N(\mu_{\text{near}}, \sigma^2_{\text{near}}) + (1-\alpha) N(\mu_{\text{far}}, \sigma^2_{\text{far}}) \; ; 0 \le \alpha \le 1.$$

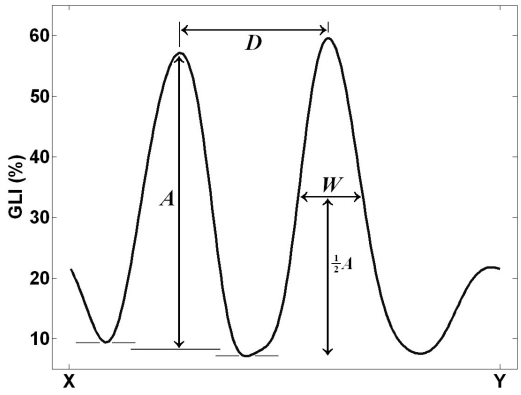

Figure 4. GLI parameters are illustrated on a profile from points X to Y in Fig. 3: amplitude *A*, the difference between peak GLI and average trough GLI, distance *D* between peaks, and full width at half amplitude *W*.

Nucleolar size

Nucleoli were identified visually in digitized images. Twelve random locations were selected, per mosaic, by computer. The user identified the nucleolus nearest to each random point, excepting those points that did not fall within laminae II through VI. Nucleoli were segmented from the surrounding cytoplasm by thresholding according to Otsu's (Otsu, 1979) method. If the thresholded nucleolus appeared to touch another object, the user manually removed pixels from that object until the nucleolus was separate. Nucleolar cross sections were measured by counting pixels in the thresholded nucleoli.

Statistical analysis

Autistic and control cases were sorted into age-matched pairs for purposes of statistical analysis. Wilcoxon signed-rank tests were used to verify the absence of pairwise differences in brain weight or postmortem interval. Both tests were insignificant with $p = 0.84$. Otherwise, statistical analysis for all measurements employed repeated measures analysis of variance. Case pair (1–6) was the random factor, and fixed factors included diagnosis, sex, cortical area, and hemisphere. Interactions of the main effects involving both sex and cerebral hemisphere were excluded from the model due to multicolinearity. For the minicolumn fragment data only, a follow-up test was performed using a second model comprising the original model plus a factor for cortical lamina: III or V/VI. The model fitting and inferential statistics were performed with Matlab (The MathWorks, Natick, Mass., USA).

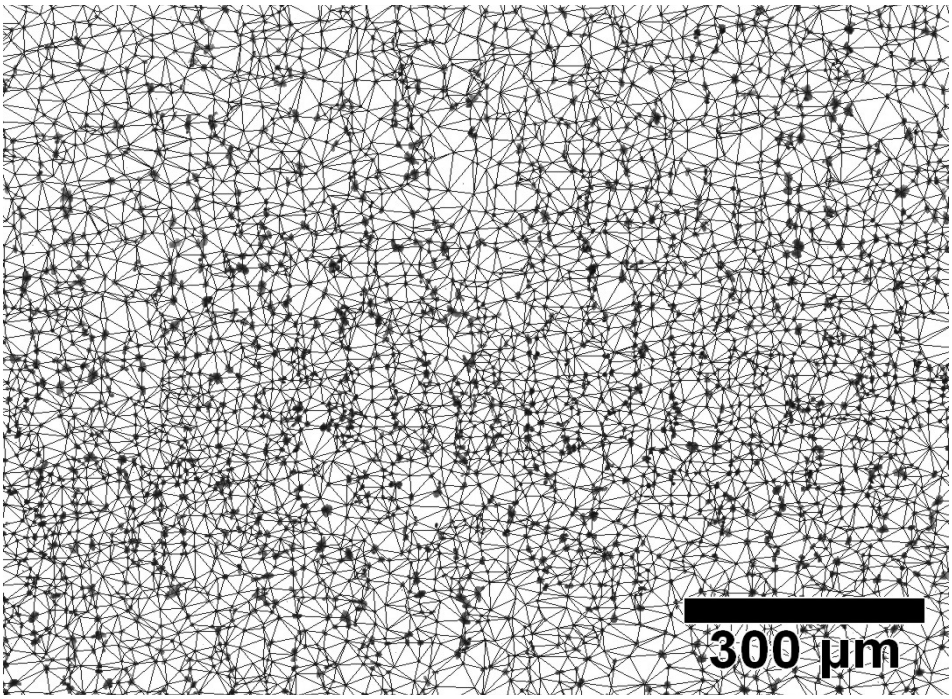

Figure 5. Delaunay triangulation of larger neurons (grayscale) in the primary sensory cortex of an 8 year old, autistic male. Given a point set in the plane, neuron centroids in this case, the Delaunay triangulation is defined such that three points form the vertices of a triangle if and only if the circle through those points has no point from the set in its interior.

Results

Minicolumnar width (CW) was greater in controls than in autistic persons by 1.46 µm or 5.54 % of the mean (Student $t = 2.466$ with 19 degrees of freedom [df]; $p = 0.0234$). CW also varied with cortical area ($F = 17.50$ with 3 numerator df and 19 denominator df; $p < 0.0001$), but no other effects were statistically significant. MCS exhibited a sex dependence in that the difference between control and autistic cases was greater in females than in males ($t = 2.227$ with 19 df; $p = 0.0382$); mean MCS was 18.3 µm and 18.9 µm in autistic females and males, respectively, and 19.7 µm and 18.6 µm in normal females and males, respectively. Again the only other significant effect was cortical area ($F = 16.09$ with 3 numerator df and 19 denominator df; $p < 0.0001$) (Table 2). There were no significant findings in V_{CW}. The follow-up analysis on those minicolumn fragments lying outside of lamina IV, using the supplemental model with lamina included

as a factor, found no significant dependence of any measurement on lamina or lamina by diagnosis interaction.

Simultaneous multivariate analysis of neuron density and neuron profile area and perimeter (Table 3) revealed significant diagnosis dependence (F = 5.47 with 3 numerator df and 17 denominator df; p = 0.0081) and diagnosis by cortical area interaction (F = 3.65 with 9 numerator df and 41.5 denominator df; p = 0.0020). Mean particle cross section was 30.5 μm2 less in autistic cases compared to controls (t = 3.804 with 19 df, p = 0.0012), while particle density was greater in autism: 5.15×103 mm^{-2}, versus 4.19×103 mm^{-2} in controls (t = –2.723 with 19 df; p = 0.0135).

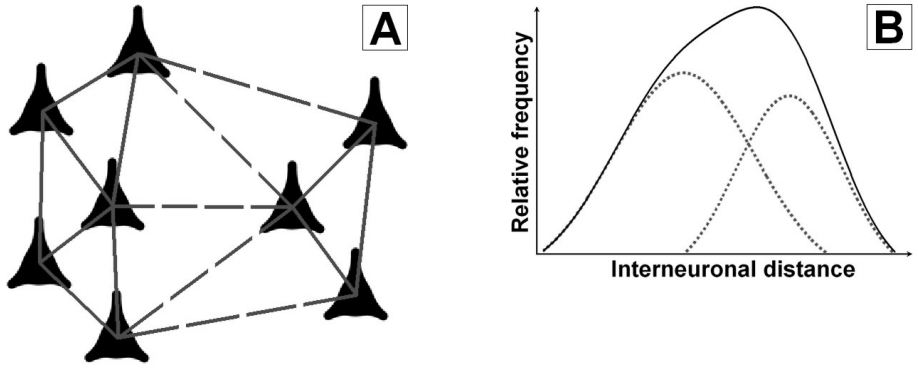

Figure 6. (A) Due to the clustering of neurons within minicolumns, the triangulation will include edges between objects in the same cluster (solid lines) and edges between objects in other clusters (dotted lines). The distribution of edge lengths over the whole graph will be a mixture of these two subgraphs' distributions. (B) We have estimated the locations and scales of distances within and between clusters by modeling the logarithm of edge lengths as a two component Gaussian mixture (see text for details).

Table 2. Average minicolumnar morphometry, broken down by diagnosis and cortical area.

Area	CW (µm)		MCS (µm)		V_{cw} (%)	
	Autistic	Control	Autistic	Control	Autistic	Control
3	25.8	27.0	18.4	18.7	15.1	14.8
4	27.5	28.2	19.9	20.0	14.2	14.6
9	26.5	29.4	19.1	20.7	15.0	14.9
17	23.0	24.1	17.0	17.3	14.4	14.7
s.d.	1.2		0.8		0.9	

Scale-independent variation in minicolumnar width V_{CW} is expressed as percentage of the mean. CW, minicolumnar width; MCS, mean cell spacing (interneuronal distance); V_{CW}, variability in minicolumnar distance; s.d., within-group standard deviation.

Table 3. Estimated Boolean spatial model parameters of the texture of Nissl-stained material from each cortical area examined, in autistic and control individuals.

	Area	Ā (µm2)	Ū (µm)	λ (µm–2)
Autistic	3	128.0	44.2	0.0047
	4	144.9	45.7	0.0047
	9	131.9	44.5	0.0051
	17	114.8	44.8	0.0062
Control	3	151.1	49.4	0.0042
	4	154.7	48.3	0.0043
	9	182.3	51.8	0.0038
	17	153.4	53.3	0.0045
s.d.		13.0	2.8	0.0008

Ā, mean soma cross-section; Ū, mean soma perimeter; λ, neuronal density; s.d. within-group standard deviation.

Each GLI parameter (Table 4) was reduced in autism: D by 1.93 μm (t = 2.8465 with 19 df; p = 0.0103), sd_D by 0.96 μm (t = 2.1402 with 19 df; p = 0.0455), A by 2.2 % (t = 2.226 with 19 df; p = 0.0383), W by 0.86 μm (t = 2.6936 with 19 df; p = 0.0144), and sd_W by 0.59 μm (t = 2.2643 with 19 df; p = 0.0354).

Table 4. Inhomogeneities in the Grey Level Index, broken down by diagnosis and cortical area.

	Area	A (%)	D (μm)	W (μm)	sd_D (μm)	sd_W (μm)
Autistic	3	16.0	32.1	15.2	13.1	6.1
	4	18.2	33.7	16.2	13.5	6.5
	9	16.9	32.3	15.4	12.8	5.9
	17	13.4	29.0	14.1	10.9	5.0
Control	3	17.4	33.3	15.8	13.5	6.3
	4	19.1	35.2	16.7	14.3	7.0
	9	19.2	35.0	16.7	14.0	6.8
	17	17.7	31.3	15.1	12.4	5.8
s.d.		1.9	1.3	0.6	0.9	0.5

A, peak GLI above background; D, mean distance between peaks; W, mean peak width; sd_D, standard deviation of distance between peaks; sd_W, standard deviation of peak width; s.d. within-groups standard deviation.

Multivariate ANOVA, with dependent variable the estimated mean logarithmic neighbor distances μ_{near} and μ_{far} (Table 5), found the diagnosis effect significant (F = 3.72 with 2 numerator df and 18 denominator df; p = 0.044). Near distances in autistic cases, averaged across all four areas, were 98.0% those of controls (confidence interval [94.8%, 101.0%]), and far distances were 94.8% those of the normal comparison group (confidence interval [93.0%,96.7%]). Diagnosis by cortical area interaction was statistically insignificant.

Table 5. Average modes $m_{near} = \exp(\mu_{near})$ and $m_{far} = \exp(\mu_{far})$ of the two components of the neighbourhood distance distribution, broken down by cortical area and diagnosis.

Area	m_{near} (µm)		m_{far} (µm)	
	Autistic	Control	Autistic	Control
3	15.2	15.5	25.6	26.1
4	17.3	17.1	27.6	28.9
9	18.1	17.8	27.6	30.4
17	14.9	16.2	22.9	24.1

Within-group standard deviation is 7.1 % of the mean.

Nucleolar cross sections (Table 6) were converted to radii of circles with the same area (requiv) in order to stabilize the variance for statistical analysis. Univariate ANOVA of mean (within each mosaic) requiv, again with the same model, revealed significant differences between autism and normal patients ($F = 19.52$ with 1 numerator and 17 denominator df; $p = 0.0004$). While requiv varied with cortical area ($F = 5.28$ with 3 numerator and 17 denominator df; $p = 0.0093$), there was no significant interaction with diagnostic group ($F = 0.89$ with 3 numerator and 17 denominator df; $p = 0.465$).

Table 6. Mean nucleolar equivalent radius, i.e. the radius of a circle with area equal to the nucleolar cross section, by diagnosis and cortical area.

Area	r_{equiv} (µm)	
	Autistic	Control
3	2.27	3.19
4	2.24	3.08
9	2.56	3.19
17	2.03	2.46

Within-group standard deviation is 0.31 µm.

Discussion

The results of this study indicate that, within a limited brain sample, minicolumnar morphometry varies according to cortical region. Since traditional parcellation schemes have relied on subjective appraisals, the semi automated method used in this study may offer a rapid and accurate procedure to define cytoarchitectural brain regions. Results also corroborate a reduction in the width of minicolumns in the brains of autistic patients with two different methods: one that measures pyramidal cell arrays (Casanova and Switala, 2005) and another using the Grey Level Index (Schleicher and Zilles, 1990; Schleicher et al., 2005). The Wilcoxon signed-rank test indicated essentially no (monotonic) difference between autistic patients and controls with respect to brain weight ($p = 0.84$) or postmortem interval ($p = 0.84$). The statistical design for all analyses included sex and cerebral hemisphere as fixed factors. Statistically significant, diagnosis-dependent differences between groups correspond, therefore, to the effect of diagnostic category independent of those other factors.

Given the lack of significant differences in brain weights between our comparison groups (Table 1), a generalized reduction in minicolumnar width in the autistic patients suggests their increase in total numbers. Although minicolumnar width was measured as distance between cell arrays in both the present and previous studies, differences in section thickness, tissue processing, and microscope objectives prevent us from making absolute comparisons. The feature extraction routines of our algorithms measure vertical clusters of neuronal profiles whose axis are parallel to the plane of tissue section. Depending on the depth of field and focus of an objective the use of thicker sections allows for a substantial overlap of neighboring minicolumns (see Image capture). The result is a relative diminution in minicolumnar width for both patients and controls when comparing the present study to previous ones (Casanova et al., 2002a).

Our initial finding, now corroborated in this study, is that the brains of autistic patients have minicolumns of reduced width and consequently of increased numbers per linear length of distance (Casanova et al., 2002a). Minicolumnar width varied with cortical area but no other effects were statistically significant. Of the four sampled areas (areas 3, 4, 9, and 17), the dorsolateral prefrontal cortex showed the greatest reduction in minicolumnar width when comparing autistics and controls (Table 2). Since the lateral or granular prefrontal cortex is apparently unique to primates (Preuss, 1995) the

finding could have important implications regarding putative animal models for autism, especially in rodents. Further topographical inferences regarding a minicolumnopathy in autism would require a larger patient population and a greater number of regions of interest.

The presence of supernumerary minicolumns is said to account for the process of cortical expansion during encephalization (Rakic, 1995b). Cortical expansion necessitates an increased number of neurons, but not proportionally (Holloway, 1968; Changizi, 2001). Although the human brain, largely the neocortex, is three times the size of the chimpanzee brain, there is only a 25% increase in the total number of neurons (Holloway, 1968). In our study evidence suggestive of an increased number of minicolumns per linear length in the brains of autistic individuals led us to examine neuronal density. A point process model indicated increased neuronal density but failed to discern the basis for the same, e.g., the presence of supernumerary minicolumns, an increase in the total number of cells per minicolumn, or both. A subsequent analysis based on a Delaunay triangulation addressed the aforementioned possibilities. The new algorithm indicated significant differences in the edges of intercluster distances but not within intracluster distances. Minicolumns appeared to be packed closer together in autism (reduction in far distances) but the total number of cells per minicolumn (near distances) appeared normal. Finally, neurons within the minicolumns of autistic patients were smaller in size and had a reduction in the size of their nucleoli. In light of the small sample size, the fact that all the various measurements revealed statistically significant differences is surprising. There is a strong possibility, then, that the true effect size associated with some of these measurements is greater than we have observed. Further studies with a larger sample may put tighter bounds on the magnitude of these differences between autistic patients and controls. The following paragraphs discuss the previously mentioned results from the perspective of both neuropathology and possible clinical correlates.

Minicolumns (development and numbers)

Cell arrays are the first radially aligned structure appreciable during development. These modules comprise layer V pyramidal cells (whose dendrites form a bundle extending through layer II), clusters of layer II and III cells, as well as associated interneurons (Peters and Sethares, 1996). They have been investigated in a number of species, including barrel field cortex

of the mouse (White and Peters, 1993), barrel field cortex of the rat (Peters and Kara, 1987), area 17 of cat (Peters and Yilmaz, 1993), visual cortex of non-human primates (Peters and Sethares, 1991, 1996, 1997; Buxhoeveden and Casanova, 2000), and various human cortical areas (Von Bonin and Mehler, 1971; Seldon, 1981a, 1981b). Pyramidal cell arrays have been the focus of investigation in studies of columnar development in series of fetal and adult postmortem tissue. Krmpotic-Nemanic et al. (1984) described development of cell arrays in human fetal and postnatal auditory cortex in a series from celloidin-embedded postmortem material with dates ranging from 9 weeks gestational to 3 months postnatal. They identified continuity in development of ontogenetic columns into pyramidal arrays with regional differences in elaboration of the basic columnar structure. Pyramidal cell arrays therefore derive from the ontogenetic cell column and provide the matrix around which growing axonal and dendritic processes are organized. In both monkeys and humans most of the founder cell divisions that account for the number of cortical columns occur before embryonic day 40 (Rakic, 1974, 1985). The genesis for an increase in the total number of minicolumns in autism would therefore transpire at an early stage of gestation.

Minicolumnar size

The possible significance of smaller minicolumns in autistic patients can be gleaned from results obtained in comparative studies of columns in cortical area 17 (V1) (Peters and Walsh, 1972; Feldman and Peters, 1974; Peters and Kara, 1987; Peters and Sethares, 1991, 1996, 1997; Peters and Yilmaz, 1993). In primates, the primary visual cortex contains small minicolumns when compared to many other mammals. This is the case even though the brain size of primates is many times greater than the comparison species. Studies using uniformed section thickness in rhesus monkeys have reported minicolumns to be about 23 μm to 31 μm on the basis of apical dendrite bundles. By contrast they range from 50 μm to 60 μm in other small-brained mammals (Buxhoeveden and Casanova, 2002a, 2005). Researchers have concluded that the narrow minicolumns reflect the increased processing complexity of primate vision and interpreted the smaller minicolumns as being a more complex, interconnected system. In effect, reduced minicolumnar spacing may provide for an increased overlap of their dendritic trees making the function of neighboring minicolumns more interdependent (Seldon, 1982, 1985).

Cell size and number

Studies estimating cell counts and/or describing cytoarchitectural features in autism have been few in number and have revealed no consistent findings. Aarkrog (1968) described "some cell increase" in a frontal lobe biopsy. Coleman et al. (1985) found significant differences in six out of 42 comparisons when studying the brain of a 21 year old autistic female and two controls. Kemper and Bauman (1993) used qualitative means to describe disturbed lamination in the anterior cingulate gyrus in five out of six autistic patients. No abnormalities in cell counts were reported by Bailey et al. (1998) in their six autistic cases. Previous results by Casanova et al. (2002a) indicate that the brains of autistic patients have smaller and more abundant minicolumns. The tighter packing of cortical modules suggested increased cellular density. A more recent case study examined three cortical areas in nine autistic patients and 11 controls (Casanova et al., 2002b). The overall mean GLI in this series was 19.4% for the control group and 18.7% for the autistic group ($p = 0.724$) with diagnosis dependent effects in *D*. The latter authors concluded that in autism a normal GLI and an increased number of modules indicate a reduction in the total number of cells per minicolumn.

In the present study the overall GLI did not differ significantly between autistic patients and controls. Differences in gray level in homogeneity as described by *D* and *W* (Fig. 4) corroborate previous findings that minicolumnar width is reduced in autism (Casanova et al., 2002b, 2002a). Significant differences in sd_D and sd_W, together with the lack of significant differences in scale-independent variability in minicolumnar width imply a direct proportionality between the mean and standard deviation of minicolumnar widths within a cortical area.

Instead of cell loss the present study proposes an alternate explanation to the preservation of GLI and increased number of minicolumns: a reduction in neuronal size. Our results indicate the presence of diminished neuronal cell size and increased density in the brains of autistic patients. These findings varied according to brain region (diagnosis by cortical area interaction). The results counter the general notion that, with the exception of striate cortex, cell density is similar across different cortical areas and even among species (Rockel et al., 1980). The impression of cellular uniformity in cortical columns has been refuted with use of modern unbiased techniques (Beaulieu and Colonnier, 1989; Beaulieu, 1993).

The neurons in our study sample had well defined nucleoli that were easily

distinguishable from other components of the karyoplasm. Histological studies have characterized the nucleolus as an RNA organelle whose function is to regulate protein synthesis. As such the volume of the nucleolus is a constitutional factor adjusted to match the basal metabolic requirements of a cell (Mann, 1982). The exception to this rule appears to be fast spiking neurons where increased metabolism appears coupled to smaller neuronal size and nucleoli (Bacci and Huguenard, 2006). Pathological conditions causing either increased or decreased cellular activity have an impact on pyramidal cells' nucleolar size in accordance with their protein synthesis requirements (Mann, 1982). Studies of this and similar morphometric indices have illustrated their utility in conditions such as Alzheimer's disease (Mann et al., 1977; Mann and Sinclair, 1978; Mann, 1982) and schizophrenia (Colon, 1972; Lohr and Jeste, 1986). In autism a significant diminution in nucleolar size, after thresholding interneurons, suggests a corresponding reduction in neuronal metabolic activity/efficiency.

Clinical correlates

Brain growth causes the isolation of non-adjacent neurons by expanding their intervening distance. With longer distances the presence of smaller neurons imposes a metabolic constraint on connectivity. Longer connections necessitate larger and more active neurons, where each cell is networked into a dynamically controlled energy system (Laughlin and Sejnowski, 2003; Chklovskii and Koulakov, 2004). A cortex biased towards smaller neurons would facilitate signal delays and metabolic inefficiencies when linking disparate brain areas. The result would be reduced or impaired functional connectivity between distant cortical regions (Horwitz et al., 1988; Belmonte et al., 2004; Just et al., 2004). In such a system both sensory coding and motor output, the endpoints of networked chain translating sensory information into behavioral actions, are normal. It is the intervening steps of information analysis that are abnormal.

The presence of smaller neurons in autism may help explain the fact that autism spectrum disorder (ASD) patients normally activate the fusiform gyrus when viewing faces as compared to non-face stimuli (Hadjikhani et al., 2004). The data indicates that the face-processing deficits encountered in ASD are not due to dysfunction of an individual area, in this case the fusiform gyrus, but to more complex anomalies in the distributed network of interconnected brain regions (Boddaert and Zilbovicius, 2002; Hadjikhani et al., 2004; Pierce

et al., 2004). In effect, the level of synchronization during activation tasks involving distant brain regions suggests impaired connectivity in autism (Horwitz et al., 1988; Zilbovicius et al., 1995; Castelli et al., 2002; Just et al., 2004; Koshino et al., 2005). It may be, as Minshew et al. (1989) have suggested, that autism is manifested as abnormalities in high level tasks whenever an elevated demand is placed on information processing (Mundy and Neal, 2001; Frith, 2004).

Just et al. (2004) have subsumed the evidence for a lower degree of information integration in autism under the rubric of the "underconnectivity theory." However, the term may prove to be a misnomer when applied to shorter intra areal connections (arcuate or u-fibers). In autism, an increase in the total number of minicolumns requires a scale increase (roughly a 3/2 power law) in white mater to maintain modular interconnectivity (Hofman, 2001). This additional white matter takes the form of short range connections which makes up the bulk of intracortical connections (Casanova, 2004). Recent structural imaging studies suggest that short association fibers are overrepresented in autism (Herbert et al., 2004). This fact may help explain the superior abilities of autistic patients when performing tasks that require local information processing (Happe, 1999). A diminution in neuronal cell size and a concomitant increase in the total number of minicolumns biases cortical connectivity in favor of local rather than global information processing (Baron-Cohen, 2004). The result is a "hyper-specific brain" (Grandin, 2005), where segments of perception are retained at the expense of losing the "big picture" (Shakow, 1946). In autism, a computational perspective validates this framework and sees hyperspecificty as a possible framework of neural codes in charge of elaborating concepts (McClelland, 2000).

It is noteworthy that an adaptive strategy for increasing the metabolic efficiency of a system driven by smaller neurons is to increase their total cell numbers while reducing the activity of each neuron (Levy and Baxter, 1996). This approach, called sparse distributed coding, achieves high representational capacity by distributing small amounts of activity over a large population of neurons (Laughlin, 2004). In sparse coding, neurons have the potential to respond strongly to focal features of sensory inputs (Field, 1994; Hahnloser et al., 2002). Since neurons rarely encounter their feature, they will fire in short bursts, sparingly distributed in time (Laughlin, 2004). Sparse distributed coding is characteristic of the visual system (Vinje and Gallant, 2000; Weliky et al., 2003). A brain whose neuronal population

is biased towards small neurons and corresponding metabolic exigencies would therefore create and execute strategies that emphasize selective convergence of information among closely adjacent modules, as e.g. in the visual system.

Large system operations can be subdivided into task-specific modules where information processing proceeds along hierarchical stages (Hubel and Wiesel, 1962). Metabolic constraints facilitate the connectivity of closely adjacent cortical areas (Miller, 1994; Goodhill, 1997) which represent similar features of perception (Schwartz, 1980). The analogy is to an operon where related genes (e.g., coding for enzymes in the same metabolic pathway) cluster together so that outside influences can provide for simultaneous negative or positive control to all of its units. This type of assembly is efficient because perceptions commonly "overlap with one another, sharing parts which continue unchanged from one moment to another" (Barlow, 1972). By way of contrast information at higher echelons emphasizes complex conjunctions of perceptual attributes.

When comparing the hierarchy of perceptual networks, primary association cortices, modules become larger and representation more categorical (Fuster, 2003; Hawkins, 2004). As a consequence, information at lower echelons of the perceptual hierarchy is more localized and lesions result in concrete deficits. At higher levels, information is more dependent on distributed networks. One good example of a physiological characteristic dependant on a distributed network is face recognition, i.e., nodes in temporal, fusiform and prepiriform cortex (Fuster, 2003). Another example of greater relevance to autism is joint attention. More so than face processing, multiple studies relate joint attention to diagnosis and outcome in autism (Mundy and Burnett, 2005). Development of joint attention involves the prefrontal cortical areas 8 and 9 and anterior cingulate area 24. These areas serve to integrate self-monitored information about social intentions with information processed in the parietal and temporal lobe about goal related behavior in other people (Lau et al., 2004). This so-called "social executive process" (Mundy, 2003) may be especially prone to disturbance wherever an increase in number and proportion of small neurons facilitate the integration of information within a given region while attenuating distal connectivity and coherence.

Appendix

Cognitive/functional level of the autistic patients in this study

A1

- Regression at 24 months of age
- Normal or early attainment of all developmental milestones before 2 years of age
- Articulation of 2-3 words sentences with difficulty, echoing
- No spontaneous use of pointing
- Inconsistency in responding to his own name
- Inability to socially greet someone
- No sensitivity to noise
- Stereotypic rather then creative/imaginative play
- Poor eye contact
- No unusual preoccupations or rituals, other than spinning wheels on transportation toys
- No aggression to others or himself
- Tantrums
- Sometimes toe walking; no spinal problems; very agile
- Age-appropriate growth profile
- No idiosyncratic hand or finger mannerisms
- No neurocutaneous stigmata or musculoskeletal abnormalities
- Immature pencil grip when attempting graphomotor tasks

A2

- Motor milestones met within normal limits; never toilet trained
- Somewhat delayed fine and gross motor skills
- Isolated and withdrawn, in addition to engaging in repetitive behaviours, at 18 months of ahe
- Language delays
- Lack of speech and low frustration tolerance
- Speech therapy, physical therapy, and occupational therapy
- No consistent use of any words at the age of 5 years

- No imitation of others' actions or direction of others' attention to things of interest to her
- Qualitative impairments in reciprocal social interaction
- Reduced eye contact and difficulty regulating eye contact in social situations
- Inappropriate facial expressions, such as laughing and crying for no apparent reason
- Occasional engagement in imaginative play by herself; no engagement in imaginative play with others
- Very little interest in other children
- Repetitive play
- Repetitive body movements, such as finger flicking and hand flapping

A3

- Motor milestones were met within normal limits; fully toilet trained
- Use of single words at 18 months of age
- No development of phrase speech by 3 or 4 years of age
- Echoing at the age of 3, occurring only occasionally by the age of 8
- Poor eye contact between 4 and 5 years of age, with improvement during development
- Speech therapy, physical therapy, and occupational therapy
- Ability to speak in simple sentences, using verbs and other grammatical markings, by 8 years of age
- Difficulty engaging in reciprocal conversation on topics the patient himself introduced
- Difficulty answering direct questions
- Difficulty pronouncing certain words
- Regular use of stereotyped words and phrases
- Difficulty spontaneously imitating the action of others
- Pointing to make requests
- Inattentive to those talking to him
- Well-developed receptive language skills
- Qualitative impairments in reciprocal social interaction
- Inability to express or explain his own pain
- Typical range of facial expressions, but occasionally inappropriate, such as laughing for no apparent reason
- Engagement in some pretend play on his own at the age of 8 years

- Difficulty engaging in reciprocal social play
- Repetitive play
- Stereotyped whole body movements, such as jumping up and down on his tiptoes
- Extremely affectionate, loving, and kind-hearted
- Well-developed visual-spatial skills,
- Excellent memory

A4

- Severe hypotonia at 6 months of age
- Ability to sit up sit up without support at 7 months of age
- No walking without support until 4 years of age
- Never toilet trained
- Developmental delays at 29 months of age
- Delays in both fine and gross motor skills
- Physical therapy, occupational therapy, and intensive speech therapy
- Qualitative impairments in communication
- Language delays evident at 15 months of age, using a few single words inconsistently
- Ability to sign a few words learned at about 18 months of age but lost by the age of 4
- Rare spontaneous use of conventional or instrumental gestures between 4 and 5 years of age, only occasional looking up when someone would enter the room without calling patient's name
- Vocalization in the form of jargon and consonant-vowel sounds that were not consistently directed at anyone at the age of 13
- Ability to follow simple directions at 13 years of age
- Rare spontaneous imitation of another person's actions
- Frequent screaming
- Hypersensitivity to certain noises
- Qualitative impairments in reciprocal social interaction
- Ability to make brief eye contact with familiar adults
- Vocalizing, jumping up and down, and flapping his arms and hands to express excitement
- Struggle to understand emotional experience of others
- Limited range of facial expressions between 4 and 5 years of age, but

sufficient by the age of 13 for the patients to understand the major emotions that he experienced, such as happiness, anger, and frustration
- Inappropriate facial expressions, such as laughing for no apparent reason, worsening with age
- No engagement in imaginative play by himself or with others between the ages of 4 and 5, playing next to other children
- Rare interaction with siblings and unresponsiveness to their social approaches or the approaches of less familiar children
- Repetitive play
- Anxiety caused by minor changes in his routine and changes to his immediate environment
- Difficulty processing new environments
- Many unusual sensory interests
- History of aggression towards family members, especially between the ages of 10 and 11, sometimes at school
- Affectionate, good natured, and sweet

A5

- Delayed motor milestones
- Delayed language development
- Use of single words, such as “dog,” and “hi” at approximately 3 years of age
- Ability to speak in short phrases at age 5; no progress beyond spontaneous use of two word combinations; no ability to speak 3 word phrases spontaneously
- Language regression at age 5 following a grand mal seizure
- Occupational and physical therapy, music and art therapy as well as speech and language, social and life skills training
- No interest in her peers between the ages of 4 and 5
- Qualitative impairments in communication
- Some difficulty coordinating her gaze
- Occasional imitation of noises she had heard; no spontaneous imitation of the actions of others
- No engagement in any form of pretend play
- Qualitative impairments in social interaction
- Difficulty making and maintaining eye contact
- Exceptional visuospatial skill

- Greater interest in certain parts of toys rather than using the toy as it was intended
- No unusual hand or finger mannerisms
- Bouncing up and down while bent over at the waist with arms pulled in tightly to chest to express excitement
- No unusual sensory interests
- Sensitivity to bright lights and excessive noise
- Tactile defensiveness, responding negatively to being touched by others

A6

- Speech delay, rocking, hyperactivity to the point of breaking several playpens, and periodic crying spells at 26 months of age
- Poor eye contact, failure to attend to the breast while feeding, and crying spells as early as 7 months of age (noted retrospectively)
- Independent walking not delayed, noted at 14 moths of age
- No word use until 9 years of age; no phrases use
- Gradual loss of interest of toileting self-care skills
- Disrupted sleeping habits
- Poor eye contact
- Absence of social smiling and limited facial expression
- No imaginative play with others, nor interest in other children
- Absence of shared attention skills
- Lack of empathy
- Use of another's body to communicate
- Laughing for no apparent reason at 4-5 years of age
- No use of any form of gesture to communicate, including pointing and head shaking, and no imitation of others
- Repetitive behaviours including circumscribed interest in listening to music all day, repetitive toy play, insistence on carrying out certain rituals, smelling everything (including non-food items), hand and finger mannerisms, and rocking
- Extreme anxiety with any change in his routine (leading to self-hitting)
- Sound sensitivity, hyperactivity, and aggression toward others (punching)

Chapter 4

Abnormalities of cortical minicolumnar organization in the prefrontal lobes of autistic patients

Casanova MF, Van Kooten IAJ, Switala AE, Van Engeland H, Heinsen H, Steinbusch HWM, Hof PR, Schmitz C.

Clinical Neuroscience Research 2006; 6: 127-133.

Abstract

Recent functional imaging studies suggest deficits in connectivity between disparate and distant regions in the brains of autistic individuals. One possible explanation to these findings is the presence of modular abnormalities in the neocortex of autistic patients: a change in neuronal specialization within minicolumns that emphasizes short connecting fibers. In this study we expand on previous findings by exploring the topography of minicolumnar abnormalities in autism. Our postmortem study included six patients with autism (DSM-IV-TR and ADI-R diagnosed) and six age-matched controls. Entire brain hemispheres were celloidin embedded, serially sectioned, and stained with Gallocyanin. Digital photomicrographs of n = 9 cortical areas (including paralimbic, heteromodal association, unimodal association, and primary areas) obtained at high magnification were assembled into montages covering the entire cortical thickness. Stained cell somata were segmented from neuropil by thresholding. Computer image analysis clustered neurons into minicolumnar fragments. The full width of the image region nearest each fragment and the width of the cell-dense core of the fragment were estimated. The difference between these two quantities can be used as a measure of the peripheral neuropil space of minicolumns. We found an interaction of diagnosis and region for peripheral neuropil space ($p = 0.041$). Post-hoc analysis revealed significant differences ($p < 0.05$) for the frontopolar region (area 10) and the anterior cingulate gyrus (area 24). The frontopolar cortex is involved in executive functions by implementing control over internally generated thoughts and relational integration (combination of multiple cognitive rules). The anterior cingulate gyrus is involved in the analysis of socially salient information, including the processing of familiar faces. Pathological findings in these areas may provide a correlate to some of the more salient manifestations of autism.

Introduction

"Indeed, frontal lobe dysfunction may account for much of what makes a person with a mental disorder into a "mental patient"- that is, someone with manifestly abnormal behavior or beliefs." Fogel, pages 8-9, 2001.

Informed clinical consensus defines autism as a behavioral syndrome characterized by pervasive impairment in several areas of development: social interaction, communication skills, and repertoire of interests and activities. Thus far there have been no neuropathological findings nor laboratory/performance based measures providing construct validity to the diagnosis. It is not surprising that given the complexity of the clinical symptoms researchers have claimed abnormalities in widely divergent areas of the brain (Palmen et al., 2004; Bauman and Kemper, 2005; Van Kooten et al., 2005b). Generalized deficits have been inferred from recent neuropathological studies suggesting disturbances of brain size, cortical lamination and columnarity (Bailey et al., 1998; Casanova et al., 2002b; Casanova et al., 2002a; Lainhart et al., 2005).

In the absence of pathognomonic abnormalities research in autism has been guided by a variety of ideologies and epistemological assumptions each contributing to the development of explanatory models or "theories": executive function (Ozonoff et al., 1991), complex information processing (Minshew et al., 1997), theory of mind (Baron-Cohen et al., 1985), and empathy (Baron-Cohen, 2002). By themselves these theories are incapable of accounting for all of the developmental, social, cognitive and affective variables which define autistic psychopathology. Autism is thought to be influenced by multiple genes as well as environmental factors thus providing for multifactorial inheritance (Muhle et al., 2004). Accordingly, there is no singular causal pathway to autism. Therefore an integrative framework capable of relating available theoretical constructs based on their reciprocally related variables appears justified. Recent attempts at deriving such an overarching metatheory have focused on a basic abnormality of neural connectivity (Belmonte et al., 2004). This model is empirically based on lack of coordinated brain activity (functional imaging) and abnormal "binding" (EEG tracings) in the brains of autistic patients (Brock et al., 2002; Just et al., 2004; Brown, 2005; Koshino et al., 2005).

In autism one possible explanation for abnormalities in brain growth, cortical cytoarchitecture, and neural connectivity is the recent finding of a

minicolumnopathy (Casanova et al., 2002a, 2002b). Minicolumns appear to be a basic anatomical and physiological unit of the cortex (Mountcastle, 2003). The functional significance of minicolumns is still unclear (Jones, 2000; Hutsler and Galuske, 2003) but several attempts have been made to identify them as the anatomical correlate to the smallest processing unit in the cerebral cortex (Mountcastle, 2003). Minicolumns have been identified in all regions of the neocortex (Buxhoeveden and Casanova, 2002b) and in all mammalian species thus far evaluated (Gressens and Evrard, 1993; Buxhoeveden and Casanova, 2005). An increase in the total number of minicolumns is thought to underlie the process of neocortical expansion that accompanies encephalization, i.e., a measure of brain size taking into account body mass.

It has been noted that minicolumns in autism are of reduced size and might be increased in numbers (Casanova et al., 2002a, 2002b). Furthermore within each minicolumn a reduction in both cell and nucleolar size suggests a change in axonal projections that facilitates the integration of information within a given area at the expense of interareal and interhemispheric connectivity (Van Kooten et al., 2005a; Casanova et al., 2006). In this study we expand on previous findings by examining the topographical distribution of the putative autistic minicolumnopathy.

Methods

Brain Specimens

Postmortem brains (one hemisphere per case) from 6 autistic cases (mean interval between death and autopsy 20.0 ± 2.9 hours: mean ± S.E.M.) and from 6 age-matched controls (mean interval between death and autopsy 24.0 ± 11.1 hours) were analyzed (Table 1). Brains were obtained from several brain banks in the USA and Germany. All autistic patients met the Diagnostic Statistical Manual, 4th revision (DSM-IV-TR) and Autism Diagnostic Interview-Revised criteria for autism (Lord et al., 1994). In all of the cases, autopsy was performed after informed consent was obtained from a relative. The use of these autopsy cases was approved by the relevant Institutional Review Boards. Clinical records were available for all cases.

Tissue Processing

After immersion-fixation in 10% formalin for at least 3 months all hemispheres were mounted with celloidin and cut into entire series of 200 µm thick coronal

sections as described in detail elsewhere (Heinsen and Heinsen, 1991). Three hemispheres were cut at 500 µm thickness. Every third section (in one hemisphere: every second) was stained with Gallocyanin. These differences did not influence the results of the present study. Imaging of the tissue was done at high magnification, with a depth of field much narrower than 200 µm.

Table 1. Clinical characteristics of the cases included in this study

No	Sex	Site	Age (y)	Cause of death	BW (g)	PMI (h)
A1	M	L	4	Drowning	1,160	30
C1	M	L	4	Myocardial infarct – Takayasu arteriitis	1,380	5
A2	F	L	5	Car accident	1,390	13
C2	F	R	4	Lymphocytic myocarditis	1,222	21
A3	M	R	8	Sarcoma	1,570	22
C3	F	R	7	Status asthmaticus	1,350	78
A4	M	L	13	Seizures	1,420	26
C4	M	R	14	Electrocution	1,600	20
A5	F	R	20	Obstructive pulmonary disease	1,108	15
C5	M	R	23	Ruptured spleen	1,520	6
A6	M	R	24	Drowning	1,610	14
C6	M	R	25	Cardiac tamponade	1,388	14

BW, brain weight; g, gram; PMI, postmortem interval; h, hours; A, autism; C, control; M, male; F, female; L, left; R, right; y, years.

Brain Regions

Gallocyanin-stained sections were used by I.A.J.v.K., H.H., P.R.H. and C.S. to identify the following areas according to anatomical landmarks and cytoarchitectural criteria as explained in detail in Braak (1980) and Paxinos and Mai (2004): 10 (frontopolar cortex), 11 (orbitofrontal cortex), 9 (dorsolateral prefrontal cortex), 4 (primary motor cortex; M1), 3b (primary sensory cortex; S1), 43 (frontoinsular cortex), 44 (ventrolateral cortex, the

main part of Broca's speech area), 24 (anterior cingulate cortex) and 17 (primary visual cortex; V1).

Image Capture

Regions of interest were delineated with a stereology workstation, consisting of a modified BX50 light microscope with UPlanApo objectives (Olympus, Tokyo, Japan), motorized specimen stage for automatic sampling (Ludl Electronics, Hawthorne, NY, USA), HV-C20AMP CCD colour video camera (Hitachi, Tokyo, Japan) and StereoInvestigator software (MicroBrightField, Williston, VT, USA). Delineations were performed with a 10× objective (NA = 0.40). Digital micrographs each measuring about 200 µm by 150 µm were produced using the stereology workstation described above and a 40× oil objective (NA = 1.0). Several hundred of such images were captured per region of interest to cover the entire cortical thickness. These images were assembled into one mosaic using the Virtual Slice module of the StereoInvestigator software. Only slight adjustments of contrast and brightness were made, without altering the appearance of the original materials.

Computerized Image Analysis System

Computerized image analysis of minicolumnar structure in layers II through VI (see below) was performed with algorithms described in the literature (Casanova and Switala, 2005). The feature extraction properties of the program correct for minicolumnar fragments, curvature of the tissue section, and have been adapted to 3D proportions (stereological modeling). The results have also been cross-validated against measurements of both physiological (intrinsic optical signaling) and anatomically (myelinated bundles) derived minicolumns (Casanova and Switala, 2005).

Color mosaics were converted to intensity images and adaptively thresholded using a scale space approach (Lega et al., 1995). Overlapping objects in the thresholded image were further separated using the watershed transformation. Each connected region in the resulting image was further classified according to size. Objects smaller than 10 μm^2, assumed to be glia, neuron fragments, or noise, were discarded. Of the remaining objects, those with areas above the 15^{th} percentile were used for minicolumn fragment detection, while the smaller objects were classified as interneurons, based on the fraction of all neurons estimated to be inhibitory by (Braitenberg

and Schuz, 1998). Stained cell somata were segmented from neuropil by thresholding with Otsu's method. Computerized image analysis clustered neurons into minicolumnar fragments and then estimated the full width of the image region nearest each fragment and the width of the cell-dense core of the fragment. The difference between these two quantities measures the peripheral neuropil space of minicolumns, denoted NS.

Statistical analysis

Autistic and control cases were paired for purposes of statistical analysis, which employed repeated measures analysis of variance. Case pair (1–6) was the random factor, and fixed factors included diagnosis, sex, cortical area, and hemisphere. Interactions of the main effects involving both sex and cerebral hemisphere were excluded from the model due to multicolinearity. The model fitting and inferential statistics were performed with Matlab (The MathWorks, Natick, MA, USA).

Results

Analysis of variance revealed no generalized difference between diagnostic groups ($F = 0.02$ with 1 numerator and 103 denominator degrees of freedom [df]; $p = 0.877$). The interaction of diagnosis and cortical area, however, was statistically significant ($F = 2.12$ with 8 numerator and 103 denominator df; $p = 0.0408$). Post hoc testing found significant differences in frontopolar area 10 and anterior cingulate area 24, where greater NS was found in autism (Table 2). NS was reduced in autism in areas 9 and 17, consistently with prior results (Casanova et al., 2002a), but not significantly ($p > 0.05$) in the present study. Post-hoc power analysis estimated only 14% power to detect an effect size of 0.5 standard deviations and only 41% power given an effect size of 1 standard deviation. Within-group standard deviation estimated from the residuals of the linear model used for ANOVA was 0.97 μm.

Table 2. Mean peripheral neuropil space, per cortical area, in autistic and control groups.

Brodmann area	NS (µm)	
	Autism	Normal
3	11.1	11.1
4	11.9	11.2
9	11.2	11.9
10	11.7*	11.2
11	11.5	12.0
17	9.1	9.8
24	12.4*	11.0
43	12.1	12.3
44	12.0	12.7

An asterisk (*) indicates mean NS in autism that differs significantly ($p < 0.05$) from the mean NS in the normal comparison group.

Discussion

The present study sampled four types of cortices that display varying degrees of cytoarchitectural differentiation: paralimbic, high-order (heteromodal) association, modality-specific (unimodal) association and idiotypic areas (primary sensory/motor cortices) (Mesulam, 2000). Other areas, i.e., corticoid[1] and allocortical formations, were not included in our sampling scheme due to their lack of minicolumnar organization. Significant differences in minicolumnar morphometry between autistics and controls were found in Brodmann areas 10 (frontopolar) and 24 (anterior cingulate gyrus). These two areas, paralimbic (area 24) and heteromodal (area 10), are interlinked by local connections and common

1. Areas of simplified cytoarchitecture, i.e., amygdaloid complex and substantia innominata, are referred to as “corticoid” or cortex-like in appearance (Mesulam, 2000)

terminal fields, e.g., dorsolateral prefrontal cortex (area 9) (Petrides and Pandya, 2004). In addition, both of these cortical regions are considered part of the prefrontal lobes. On the other hand, in our study not all cortical areas within the prefrontal lobes exhibited minicolumnar abnormalities. Specifically, no significant changes were evident in: area 9 (dorsolateral prefrontal cortex), area 11 (orbitofrontal cortex), and area 44 (ventrolateral prefrontal cortex, the main part of Broca's speech area).

Early work on the prefrontal lobes was based on the availability of various types of traumatic injuries. The fact that lesions were not associated with primary sensory or motor deficits suggested an executive rather than operational role for this part of the brain: "the tertiary portions of the frontal lobes are in fact a superstructure above all parts of the cerebral cortex, so that they perform a far more universal function of regulation of behavior" (Luria, 1973: page 89; see also Mesulam, 2002). The widespread corticocortical and cortico-subcortical connections of the prefrontal lobes integrate/coordinate information processing within the context of parallel and widely distributed neural networks (Goldman-Rakic, 1988; Mesulam, 1990; Goldman et al., 2004). Rather than being confined to one particular cognitive domain, the executive faculties allow navigation through the variegated challenges confronted in autonomous social behavior (Goldman-Rakic, 1993; Duffy and Campbell, 2001). A breakdown of executive functions simplifies behaviors rendering them stimulus-bound, that is, the range of self-determined behavioral options is curtailed and appears to be more reflexive or environmentally determined.

Disturbances in prefrontal cortical function provide for a brain which is less equipped to use learning as an adaptive strategy and has diminished resources (plasticity) to handle social interaction/behaviors. Social complexity in primates (e.g., group size) correlates with both relative and absolute increases in neocortical size (Dunbar, 1998; Striedter, 2005). Arguably, learned heuristics and our capacity to inhibit behaviors evolved as a cognitive competency with absolute brain size and not with encephalization quotient (Geary, 2005). It is therefore noteworthy that in humans the prefrontal cortex has increased in absolute size and gyrification over that of great apes and other primate species (Semendeferi and Damasio, 2000; Semendeferi et al., 2001; Zilles, 2004). The increased cortical folding observed in the prefrontal lobes (Zilles et al., 1989; Zilles, 2004) may allow for faster communication among closely adjacent areas thereby creating a potential for greater cortical

modularity and differentiation of function (Deacon, 1990). Cortical modularity therefore may reflect an inherited multifactorial trait as social behaviors covaried with survival and reproductive outcomes. Variability in cortical modularity is therefore an expression of evolutionary change.

During encephalization the addition of supernumerary modules (minicolumns) caused an even greater increase in connectivity. It has been suggested that in the cortex each module is connected to on the order of 10^3 other modules (Hofman, 2001). If connectivity is fixed as brain size increases then the number of connections scale as the number of modular units squared, in other words, doubling the number of minicolumns quadruples the number of fibers (Casanova, 2004). Since longer connectivity imposes penalties in conduction delays and increased metabolic demands the additional white matter takes the form of short-range association fibers (Laughlin and Sejnowski, 2003; Casanova, 2004; Chklovskii and Koulakov, 2004).

Previous studies in autism have shown a reduction in minicolumnar width (Casanova et al., 2002a, 2002b). Since most autistics have average or above average brain size their small minicolumns points to the existence of more minicolumns per unit of length. As discussed above, this increase in modularity would be accompanied by an even greater number of interconnections. A recent neuroimaging study in autism has shown a significant increase in volume within the outer radiate compartment of white matter affecting primarily the prefrontal lobes (Herbert et al., 2004). This compartment consists of late myelinating short association fibers. Longer association bundles and commissural pathways (e.g., corpus callosum) are reduced in size (Lainhart et al., 2005). Dysfunction of long association bundles translates into complex abnormalities within widely distributed networks (Boddaert and Zilbovicius, 2002; Hadjikhani et al., 2004; Pierce et al., 2004). A “dysexecutive syndrome” in autism could therefore result from the prefrontal cortex’s complex pattern of connectivity. Thus, previous studies have shown that the prefrontal cortex interconnects with every distinct functional unit of the brain (Nauta, 1972). This widely distributed network of connectivity accounts for the phenomenon of frontal lobe diaschisis, i.e., executive cognitive deficits in lesions distant to the anterior cortical region (Mesulam, 2002).

The many connections of the prefrontal cortex allow it to access multiple representations of internal and external events within working memory (Mesulam, 1998). The resultant increase in computed variables appears essential for “dissociating appearance from, significance, grasping changes

of context, shifting from one mental set to another, assuming multiple perspectives, and comparing potential outcomes of contemplated actions" (Mesulam, 2000: page 48). According to Goldman-Rakic and Selemon (1997) these variables stem, in part, from intramural connectivity as the prefrontal lobes exhibit different working domains according to anatomical region. Paralimbic aspects of the prefrontal lobes (e.g., anterior cingulate gyrus) provide a node to other working memory sites (e.g., frontopolar cortex) binding emotional states to memories and experiences. Unsurprisingly, recent studies have found abnormalities of size and metabolism in the anterior cingulate gyrus of patients with autism (Haznedar et al., 1997b; Levitt et al., 2003) that apparently relate to observed impairments in communication and social interaction (Ohnishi et al., 2000). A putative pathological correlate to these neuroimaging studies is the finding of smaller neurons and increased cell density in the anterior cingulate gyrus of autistic patients (Kemper and Bauman, 1998).

Abnormalities within the anterior cingulate gyrus of autistic patients may be mediated, in part, by defective development of Von Economo[2] (spindle cell) neurons (Allman et al., 2005). These cells are characterized by large apical and basilar dendrites that define their bipolar appearance. In hominoids, i.e., humans and apes, spindle cells diminish in abundance with increasing phylogenetic distance away from humans (Nimchinsky et al., 1999). Also in hominoids, the size of the frontopolar cortex bears a direct correlation to spindle cell density (Allman et al., 2002). Functional imaging studies have shown coactivation of areas 10 and 24 when subjects retrieve episodic memories (Lepage et al., 2000). These observations have led Allman et al. (2002) to suggest that spindle cells from the anterior cingulate gyrus project primarily to the frontopolar region. In the present study both areas 10 and 24 displayed significant minicolumnar abnormalities in our autistic patients.

Recent MRI studies have consistently found an increase in brain volume in younger children with autism but not at older ages (Lainhart et al., 2005). Difficulties in scanning and establishing diagnosis have provided for small sample size of younger age groups in neuroimaging studies. In spite of these difficulties, it appears that autism is characterized by accelerated head growth that is maximal at 2-4 years of age and then plateaus (Courchesne,

2. Von Economo (1929) was the first person to describe spindle cells. He used the term "corckscrew cells" because of their appearance.

2004). The reported overgrowth is focalized, affecting primarily the prefrontal lobes (Carper et al., 2002). A recent MRI study parcellated the prefrontal lobes and found significant enlargements of the dorsolateral and medial prefrontal cortices in autistic patients aged 2 to 5 years as compared to controls (Carper and Courchesne, 2005). Courchesne and Pierce (2005) believe that the prefrontal growth disparity is conductive to a reduction in frontal-posterior reciprocal connectivity that impairs goal-directed feedback to lower level systems.

The basis for a disparity in minicolumnar morphometry among different prefrontal regions is not known. Between-area differences may be mediated by the total number of founder cells, the duration of the cell-division cycle, the number of successive cell cycles during the period of neurogenesis, the modes of cell division, and selective cell death (Rakic and Kornack, 2001). Variability in the timing and/or mode of progenitor cell divisions may specify differences in the number of radial units within a given region of the brain (Chenn and Walsh, 2002; Piao et al., 2004). Genes may influence the generation of progenitor cells and total area of the neocortex (Zhang, 2003; Evans et al., 2004). Some genes may modulate the development of the prefrontal cortex more so than other cortical areas (Piao et al., 2004). Different growth/trophic factors affect neurogenesis and therefore minicolumnar morphometry. These growth factors influence neuronal progenitor populations at specific anatomical regions (Van Praag et al., 2004), e.g., brain-derived neurotrophic factor (BDNF) is differentially expressed within the prefrontal cortex: dorsomedial more than ventral cortex (Huntley et al., 1992). Levels of BDNF are abnormal in newborns that in later life were diagnosed as autistic (Nelson et al., 2001). Carper and Courchesne (2005) have suggested abnormalities in neurotrophic factors as a putative explanation to differences in regional frontal development in autism.

Our results suggest that in autism deficits in higher order cognitive abilities may result from minicolumnar abnormalities within the prefrontal cortex. Given the low statistical power (<50%) associated with the effect sizes that one might expect given these data (Table 2), a larger series should be used in future studies. Also, more extensive sampling is needed to differentiate pathology within analogous zones of heteromodal cortex, such as posterior parietal areas 39 and 40 and lateral temporal area 37. No significant findings were observed in idiotypic cortex. In this regard sensory input and motor output systems in autism appear normal but the observed behavior exhibits contextual peculiarities due to abnormalities of intermediary processing (Mesulam, 2000).

Chapter 5

Neurons in the fusiform gyrus are fewer and smaller in autism

Van Kooten IAJ, Palmen SJMC, Von Cappeln P, Steinbusch HWM, Korr H, Heinsen H, Hof PR, Van Engeland H, Schmitz C.

Brain 2008; 131: 987-999.

Abstract

Abnormalities in face perception are a core feature of social disabilities in autism. Recent functional magnetic resonance imaging studies showed that patients with autism can perform face perception tasks. However, the fusiform gyrus and other cortical regions supporting face processing in controls are hypoactive in patients with autism. The neurobiological basis of this phenomenon is unknown. Here, we tested the hypothesis that the fusiform gyrus shows neuropathological alterations in autism, namely alterations in neuron density, total neuron number and mean perikaryal volume. We investigated the fusiform gyrus (analyzing separately layers II, III, IV, V, and VI), in 7 postmortem brains from patients with autism and 10 controls for volume, neuron density, total neuron number and mean perikaryal volume with high-precision design-based stereology. To determine whether these results were specific for the fusiform gyrus the same analyses were also performed in the primary visual cortex and in the cortical gray matter as a whole. Compared to controls, patients with autism showed significant reductions in neuron densities in layer III, total neuron numbers in layers III, V, and VI, and mean perikaryal volumes of neurons in layers V and VI in the fusiform gyrus. None of these alterations were found in the primary visual cortex or in the whole cerebral cortex. Although based on a relatively small sample of postmortem brains from patients with autism and controls, the results of the present study may provide important insight about the cellular basis of abnormalities in face perception in autism.

Introduction

Autism is a neurodevelopmental disorder with an estimated heritability of more than 90% (DiCicco-Bloom et al., 2006). It is defined by the presence of social deficits, language abnormalities, and stereotyped and repetitive behaviors (American Psychiatric Association, 1994) which are thought to be specific to autism (Bodfish et al., 2000). A key feature of normal social functioning in humans is the processing of faces, which allows people to identify individuals and enables them with the capacity to understand the mental state of others (Baron-Cohen et al., 1994). Although not included in the current diagnostic criteria, patients with autism have marked deficits in face processing (Grelotti et al., 2002). As such, alterations of this crucial skill for social interaction may represent a central feature of social disabilities in autism (Schultz et al., 2000). Imaging studies have provided evidence for a role of temporal lobe structures in face processing. It is well recognized from functional magnetic resonance imaging (fMRI) studies that the fusiform gyrus (FG) is consistently active when normal humans view faces (Kanwisher et al., 1999). Patients with autism can perform face perception tasks (Schultz, 2005) but there is strong evidence that the FG, as well as other cortical regions supporting face processing in controls, is hypoactive in patients with autism (Kanwisher et al., 1999; Pierce et al., 2001, 2004; Bolte et al., 2006). However, the neurobiological basis of this phenomenon remains unknown (Palmen et al., 2004; Van Kooten et al., 2005b; DiCicco-Bloom et al., 2006).

It has been proposed that the failure to make direct eye contact may explain the observed hypoactivation of the FG in face perception tasks in autism (Dalton et al., 2005). Imaging studies have reported unchanged (Pierce et al., 2001), or increased (Waiter et al., 2004) volumes of the FG in patients with autism compared to controls, or asymmetry abnormalities of the FG in autism (i.e., larger on the left side in patients with autism) (Herbert et al., 2002). It has also been suggested that an innate impairment of specialized neural systems may explain the reported functional abnormalities of the FG in autism (Sasson, 2006). Based on this evidence, we hypothesized that the FG would show neuropathological alterations at the cellular level, i.e., in neuron density, total neuron number and mean perikaryal volume in autism compared to controls. We tested this hypothesis by investigating these parameters in the FG of 7 postmortem brains from patients with autism and 10 matched controls using high-precision design-based stereology. To determine whether these results were specific for the FG in autism we

performed the same analyses on the primary visual cortex and the whole cortical gray matter as well. It should be mentioned that a subset of the postmortem brains investigated here (i.e., 6 brains from patients with autism and six from controls) were recently also investigated for possible alterations in the modular organization of cellular microdomains (minicolumns) in the prefrontal cortex (area 9), primary motor cortex (area 4, primary sensory cortex (area S1) and primary visual cortex (area 17) (Casanova et al., 2006).

Materials and Methods

Brain specimens

Postmortem brains (one hemisphere per case) from 7 patients with autism (4 males, 3 females; mean age 12.1 ± 2.8 years; mean ± SEM) and 10 matched controls (8 males, 2 females; mean age 30.1 ± 7.5 years) were analyzed. Clinical data and the origin of the brains are shown in Tables 1 and S1 (in Supplementary data). The patients with autism did not differ from the controls with respect to mean age (two-tailed Student's t test; $t_{(15)} = 1.917$ [15 degrees of freedom], $p = 0.07$), mean brain weight ($t_{(15)} = 0.3913$, $p = 0.70$), mean interval between death and autopsy ($t_{(15)} = 0.0423$, $p = 0.97$) and mean fixation time ($t_{(15)} = 1.296$, $p = 0.21$). All patients with autism met the Diagnostic Statistical Manual, 4th revision (DSM-IV) (American Psychiatric Association, 1994) and Autism Diagnostic Interview (Lord et al., 1994) criteria of autism, and none of them exhibited any chromosomal abnormalities. In all of the cases, autopsy was performed after informed consent had been obtained from a relative. The use of these autopsy cases for scientific investigations was approved by the relevant Institutional Review Boards. Except for the tissue provided by the Morphologic Brain Research Unit, University of Wuerzburg, Wuerzburg, Germany (UWMBRU), allocation of tissue was officially approved by the Tissue Advisory Board (TAB) of the US-Autism Tissue Program (ATP). Clinical records were available for all cases.

Tissue processing

In all cases, the brains were divided mediosagittally. Either the left or the right hemisphere was available for each case (see Table 1). After immersion-fixation in 10% formalin for at least 3 months, the selected hemispheres were embedded in celloidin and cut into complete series of 200 µm-thick coronal sections as previously described (Heinsen et al., 2000) (all steps were performed at the New York State Institute for Basic Research in Developmental Disabilities, Staten Island, NY, USA). Every third section was shipped to UWMBRU.

The hemispheres provided by UWMBRU were cut at a thickness of 500 µm, and every other section was selected (these differences did not influence the outcome of the study). All selected sections were stained at UWMBRU with Gallocyanin, mounted, and coverslipped as previously described (Heinsen and Heinsen, 1991).

Table 1. Clinical characteristics of all cases included in this study.

No	Age [y]	G	H	PMI [h]	BW [g]	Fix [d]	Th [µm]	Cause of death
A1	4	M	l	30	1160	4560	200	Drowning
A2	5	F	l	13	1390	1568	200	Car accident
A3	8	M	r	22	1570	196	200	Sarcoma
A4	11	F	l	13	1460	311	200	Seizure prior to drowning
A5	13	M	l	8	1470	75	200	Seizures
A6	21	F	r	50	1108	136	200	Obstructive pulmonary disease
A7	23	M	r	14	1610	505	200	Drowning
C1	4	M	l	3	1380	67	500	Myocardial infarct
C2	4	F	r	21	1222	233	200	Lymphocytic myocarditis
C3	7	F	r	74	1350	1290	500	Status asthmaticus
C4	14	M	r	20	1464	1067	200	Electrocution
C5	23	M	r	6	1520	95	200	Ruptured spleen
C6	25	M	r	14	1388	89	500	Cardiac tamponade
C7	48	M	l	24	1622	215	200	Atherosclerotic heart disease
C8	52	M	r	13	1450	158	200	Atherosclerotic cardiovascular disease
C9	59	M	l	24	1412	266	200	Cardiac arrest
C10	65	M	l	19	1430	85	500	Bronchpneumonia

A, patient with autism; C, control. G, gender; M, male; F, female. H, hemisphere; l, left; r, right. PMI, postmortem interval (time between death and autopsy); h, hours. BW, brain weight; g, gram. Fix, fixation time; d, days. Th, section thickness.

Brain regions

The fusiform gyrus (FG), the primary visual cortex (Brodmann's area 17) (Brodmann, 1909) and the cortical gray matter (CGM) were identified on all sections showing these regions, according to anatomical landmarks and cytoarchitectonic criteria (Figs. 1 and 2). The fusiform face area (FFA) within the FG could not be identified separately because neither gross anatomical landmarks nor cytoarchitectonic criteria have been established in the literature to identify the FFA within the FG in human postmortem brains. However, potential cytoarchitectonic differences in volumes of cell layers, neuron densities, total neuron numbers and mean perikaryal volumes between patients with autism and controls can be assessed by measuring these variables within the FG that encompasses the possible range of the FFA within a comparable part of the FG in each brain section showing the FG. The FG is located in the temporal lobe, lateral to the parahippocampal gyrus. Its medial boundary was defined by the collateral sulcus and its lateral boundary by the temporo-occipital sulcus, which runs anterior to posterior from the temporal pole to the occipital gyrus. The superior boundary was characterized by a straight line between the cortical ribbon and the apex of each sulcus (McDonald et al., 2000; Pierce et al., 2001; see also Mai, Assheuer, and Paxinos at http://braininfo.rprc.washington.edu/) (Fig. 2). Area 17 is located in the occipital lobe along the walls of the calcarine sulcus and adjacent portions of the cuneus and lingual gyrus (Carpenter, 1985). It is defined histologically by a broad layer IV divided into three sublayers and numerous very small pyramidal cells in layers II and III. The abrupt disappearance of the stripe of Gennari allows for the precise delineation of the borders of area 17 (Braak, 1980). The CGM is characterized by its layered structure well visible with classical cellular stains, such as gallocyanin or cresyl violet (Fig. 1) (Paxinos and Mai, 2004). The boundaries of the FG and area 17 were identified using an Olympus SZX9 stereomicroscope (Olympus; Tokyo, Japan) and were marked on the back side of the glass slides with a felt-tip pen. Identification and delineation of boundaries was performed in a blind manner by I.A.J.v.K. (FG), S.J.M.C.P. (CGM), and P.v.C. (area 17) until all regions per hemisphere were analyzed, and were independently cross-evaluated (and, if necessary, slightly modified) by C.S., H.H. and P.R.H.

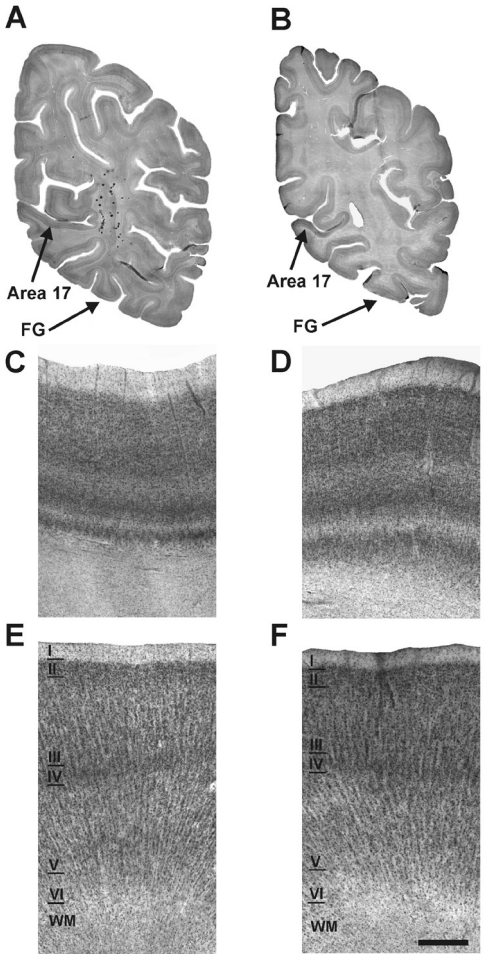

Figure 1. Representative photomicrographs of 200 µm-thick coronal sections of the brain hemispheres from a control patient (A, C, E) and a patient with autism (B, D, F), showing either the entire hemisphere (A, B) or area 17 (C, D) and the fusiform gyrus (FG) (E, F). Scale bar = 15 mm in A and B, and 400 µm in C to F.

Stereologic analysis

Stereologic analyses were performed with a computerized stereology workstation, consisting of a modified light microscope (Olympus BX50 with PlanApo objective 1.25× [numerical aperture (N.A.) = 0.04] and UPlanApo objective 20× [oil; N.A. = 0.8]; Olympus, Tokyo, Japan), motorized specimen stage for automatic sampling (Ludl Electronics; Hawthorne, NY, USA), CCD

color video camera (HV-C20AMP; Hitachi, Tokyo, Japan), and stereology software (StereoInvestigator; MBF Bioscience, Williston, VT, USA).

Volumes of brain regions were analyzed using the Cavalieri's principle (Cavalieri, 1966; Schmitz and Hof, 2005), by determining the projection area of a given brain region on each selected section showing this region, summing up the data from all sections, and multiplying this value with the interval of selecting sections for staining with Gallocyanin (2 or 3; see above) and the average actual section thickness after tissue processing (determined with the stereology workstation [in case of the 200 µm-thick sections] or a calibrated fine adjustment knob of an Olympus BH microscope and a PlanApo objective (40×; N.A. = 1.0) as described (Heinsen et al., 1994) [in the case of the 500 µm-thick sections]). The projection areas of the entire hemisphere and the cortical gray matter were determined with point counting (Gundersen and Jensen, 1987; Schmitz and Hof, 2005). In contrast, the projection areas of the FG and area 17 (combined analysis of all layers [FG and area 17], followed by separate analyses of layers II, III, IV, V and VI [FG]), were determined by tracing their boundaries on each selected section on video images displayed on the monitor of the stereology workstation (see Fig. S1 in Supplementary data). No specific descriptions of the cytoarchitecture of the cortical gray matter in the FG have been provided in the literature. We therefore used the general criteria as provided by, for example, Braak (1980) and Kandel et al. (2000) to discriminate cortical layers using the advanced differentiability of laminar boundaries in 200 µm-thick and 500 µm-thick Gallocyanin-stained sections from human postmortem brains stained with Gallocyanin; see also Heinsen et al. (2000): layers II and IV comprise mainly small spherical (granule) neurons, layer III contains mainly pyramidal-shaped neurons, and those laying deep in layer III are larger compared to those located more superficially. Layer V includes pyramidal-shaped neurons that are larger than those in layer III, and layer VI is a heterogeneous layer of neurons blending into the white matter and forming the deep limit of the cortex (see also Fig. S1 in Supplementary data).

Total neuron numbers were estimated with the Optical Fractionator (West et al., 1991; Schmitz and Hof, 2005). All neurons whose nucleus top came into focus within unbiased virtual counting spaces distributed in a systematic-random fashion throughout the delineated regions were counted, and their perikaryal volume was measured with the Nucleator (Gundersen, 1988; Schmitz and Hof, 2005) (see Supplemantary data about the use of the Nucleator to estimate mean perikaryal volumes on coronal sections). Neurons were differentiated from glial and endothelial cells by histological criteria. Neurons showed a large cytoplasm,

and a prominent nucleolus within a pale nucleus. Glial cells were identified by the absence of cytoplasmic staining, intense staining of the nucleus with dispersed chromatin and lack of a nucleolus (see also Fig. S2 in Supplementary data).

Then, total neuron numbers were calculated from the numbers of counted neurons and the corresponding sampling probability, as well as the mean perikaryal volume of all analyzed neurons. All details of the counting procedure (including information about the sampling parameters) for all investigated brain regions are summarized in Table 2. Select cases were analyzed for total neuron numbers with the same parameters by 3 independent researchers (I.A.J.v.K., S.J.M.C.P. and P.v.C.). In all cases the inter-rater variability was less than 5%, reflecting the benefits of the high-precision design-based stereology approach used here (see also Schmitz and Hof (2005). However, a comprehensive inter-rater/intra-rater analysis was not performed.

Statistical analysis

For both patients with autism and controls, mean and standard error of the mean were calculated for all investigated variables. Then, Kolmogorov-Smirnov (KS) tests were performed to assess whether the values from each investigated variable came from a Gaussian distribution (these analyses were performed separately for the patients with autism and the controls). Only in 4 out of 58 datasets (6.9%) (2 groups and 29 investigated variables per group) it was found that the data did not pass the KS normality test (patients with autism: density in the cortical gray matter [$p = 0.007$] and neuron density in layer V of the FG [$p = 0.028$]; controls: volume of area 17 [$p = 0.047$] and mean perikaryal volume of the neurons in layer III of the FG [$p = 0.045$]). All other datasets passed the KS normality test with $p > 0.1$. Furthermore, F tests were performed to compare the variances of all investigated variables between patients with autism and controls. For none of the 29 investigated variables the variances were significantly different between the two groups (i.e., $p > 0.05$). Accordingly, comparisons between patients with autism and controls could be performed with parametric statistics using generalized linear model multivariate analysis (MANOVA), with diagnosis as fixed factor and the patients' age, gender, hemisphere, postmortem interval, brain weight and fixation time as covariates (see Supplementary data for details about reasons not to consider the history of seizures of some of the patients with autism in the statistical analysis). For each investigated variable all investigated brain regions were tested simultaneously. Post-hoc tests in the analyses of covariance were

performed with linear regression analysis (patients' age and fixation time) or two-way analysis of variance (hemisphere). In all analyses an effect was considered statistically significant if its associated p value was smaller than 0.05. To test the hypothesis that the results of this study were independent of the higher mean age of the controls than the mean age of the patients with autism, the statistical analysis was repeated by disregarding the control cases (i) C10, (ii) C9 and C10, and (iii) C8 to C10. Calculations were performed using SPSS (Version 12.0.1 for Windows; SPSS, Chicago, IL, USA) and GraphPad Prism (Version 4.0 for Windows, GraphPad software, San Diego, CA, USA).

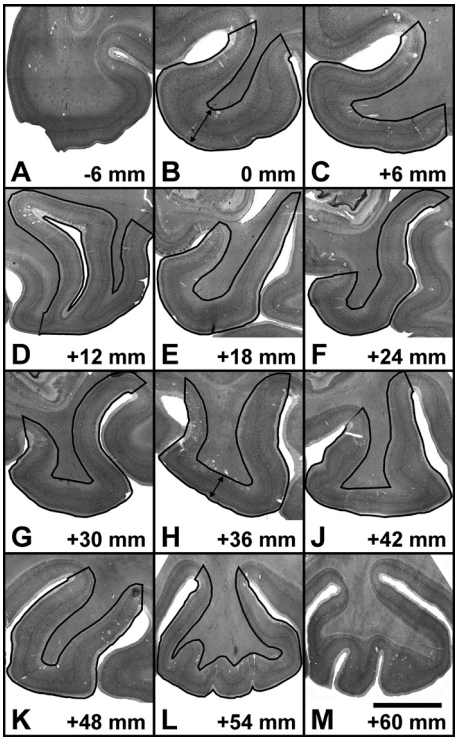

Figure 2. Representative photomicrographs of 200 µm-thick coronal sections throughout the fusiform gyrus (FG) in the postmortem brain from a patient with autism, showing the delineation procedure of the entire FG (B to L). The next sections in the series rostral to the FG (A) and caudal to the FG (M) are also shown. The arrow in E indicates the collateral sulcus and the arrowhead the temporo-occipital sulcus. Note the tangential cut of the FG in B (arrow) indicating the rostral pole of the FG compared to the center of the FG (H) in which the cortical gray matter was found to be much thinner (arrow in H). Scale bar = 15 mm.

Table 2. Details of the stereologic analysis procedures.

	Hem	CGM	Area 17	FG I-VI	FG II	FG III	FG IV	FG V	FG VI
S	20.2	20.2	10.2	10.8	10.8	10.8	10.8	10.8	10.8
Obj. 1	1.25x	1.25x	1.25x	1.25x	1.25x	1.25x	1.25x	1.25x	1.25x
sla-x, sla-y [µm]	2000	2000	-	-	-	-	-	-	-
∑P	9989	5645	-	-	-	-	-	-	-
Obj. 2	-	20x	20x	-	20x	20x	20x	20x	20x
sln-x, sln-y [µm]	-	6500	1100	-	700	900	700	900	650
a [µm^2]	-	6400	6241	-	4900	4900	4900	4900	6400
h [µm]	-	20	20	-	20	20	20	20	20
d [µm]	-	10	10	-	10	10	10	10	10
∑OD	-	506	585	-	211	289	203	281	218
∑N	-	2250	2195	-	582	634	581	696	456
t_1 [µm]	172	172	172	-	172	172	172	172	172
t_2 [µm]	472	472	472	-	472	472	472	472	472
$CE_{pred.}$[n]	-	0.021	0.021	-	0.041	0.040	0.041	0.038	0.047

Hem, entire hemisphere; CGM, cortical gray matter; FG, fusiform gyrus; I, II, III, IV, V and VI, cortex layers I, II, III, IV, V and VI. S, average number of analyzed sections; Obj. 1, objective used for delineating the regions of interest and point counting; sla-x and sla-y, distance between the points used for volume estimates in mutually orthogonal directions x and y; ∑P, average number of points counted; Obj. 2, objective used for counting neurons and estimating perikaryal volume; sln-x and sln-y, distance between the unbiased virtual counting spaces used for counting neurons in mutually orthogonal directions x and y; a and h, base and height of the unbiased virtual counting spaces; d, depth within the section at which the unbiased virtual counting spaces were placed; ∑OD, average number of unbiased virtual counting spaces used; ∑N, average number of neurons counted; t_1, measured actual average section thickness of the sections cut at 200 µm after histological processing; t_2, measured actual average section thickness of the sections cut at 500 µm after histological processing; $CE_{pred.}$[n], average predicted coefficient of error of the estimated total neuron numbers using the prediction method described by Schmitz and Hof (2000).

Photography

Photomicrographs shown in Figs. 1, 2 and S1 (in Supplementary data) were produced by digital photography using the stereology workstation described above. On average approximately 100 images were captured for the composite in each Fig. 1 A-B, 25 images for the composite in each Fig. 1 C-F, 70 images for the composite in Fig. 2 and 60 images for the composite in Fig. S1 A. These images were made into one montage using the Virtual Slice module of the StereoInvestigator software. Photomicrographs shown in Fig. 3 A-K and S2 (in Supplementary data) were produced by digital photography using an Olympus DP 70 digital camera attached to an Olympus AX 70 microscope and cellP software (version 2.3; Soft Imaging System, Münster, Germany). The final figures were constructed using Corel Photo-Paint v.11 and Corel Draw v.11 (Corel, Ottawa, Canada). Only minor adjustments of contrast and brightness were made, without altering the appearance of the original materials.

Results

The FG (and separate layers II, III, IV, V, and VI), area 17, and the CGM were identified on all sections showing these regions according to Figs. 1, 2 and S1 (Supplementary data). The mean volumes of the investigated brain regions did not significantly differ between the patients with autism and the controls (Fig. S3 and Table S2 in Supplementary data).

Compared to the controls, the patients with autism showed a significantly reduced mean neuron density in layer III of the FG (-13.1%; $F_{(1)} = 19.321$ [one degree of freedom], $p = 0.002$) (Fig. S4 in Supplementary data). Furthermore, the patients with autism had a significantly reduced mean total neuron number in layers III (-23.7%; $F_{(1)} = 6.356$, $p = 0.033$), V (-14.3%; $F_{(1)} = 6.446$, $p = 0.032$) and VI (-10.6%; $F_{(1)} = 5.518$, $p = 0.043$) of the FG compared to the controls (Figs. 3 and 4). In layer III the reduced mean total neuron

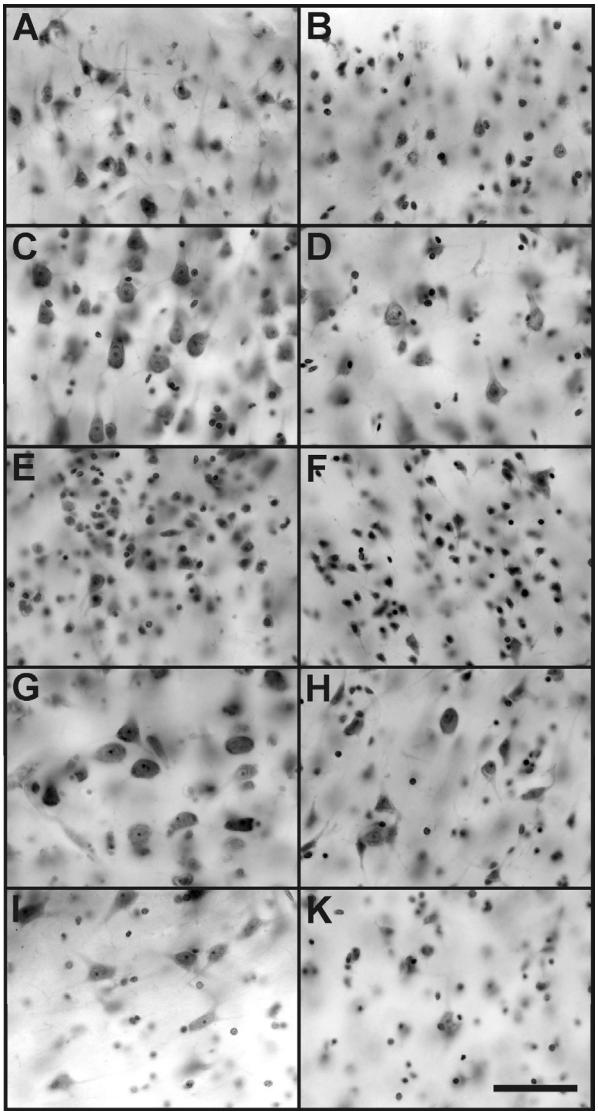

Figure 3. Representative photomicrographs of 200 µm-thick coronal sections showing layers II (A, B), III (C, D), IV (E, F), V (G, H), and VI (I, K) of the fusiform gyrus in the brains from a control patient (A, C, E, G, I) and a patient with autism (B, D, F, H, K). These photomicrographs are representative of the magnification at which the stereologic estimates were performed. Note the reduced numbers of neurons in layers III, V, and VI in the brain from the patient with autism compared to the control. Scale bar = 50 µm.

number reflected a combined reduction in the mean volume of this layer (-12.7% [patients with autism vs. controls] as well as the mean neuronal density within this layer (-13.1%). In contrast, the reduced mean total neuron number in layers V and VI reflected a reduced mean volume of these layers (-16.8% [layer V] and -17.0% [layer VI], respectively), rather than a reduced mean neuronal density within these layers (actually the mean neuronal density was slightly increased in layer V [+2.7%] and layer VI [+8.0%] in the brains from the patients with autism compared to the controls).

In addition, the patients with autism showed a significantly reduced mean perikaryal volume of the neurons in layers V (-21.1%; $F_{(1)} = 14.763$, $p = 0.004$) and VI (-13.4%; $F_{(1)} = 8.853$, $p = 0.016$) of the FG (Figs. 3 and 5) compared to the controls. There were no significant differences between the patients with autism and the controls with respect to neuron density, total neuron number and mean perikaryal volume in the whole CGM and in area 17 (Figs. 4 and 5, as well as Fig. S4 in Supplementary data).

The statistical analysis showed a number of significant effects of the covariates on the investigated variables. With respect to the variables which showed significant differences between the patients with autism and the controls, the age of the subjects under study and the fixation time had a significant effect on the perikaryal volume in layer V of the FG ($F_{(1)} = 6.910$, $p = 0.027$ [patients' age] and $F_{(1)} = 5.446$, $p = 0.044$ [fixation time], respectively). However, post-hoc linear regression analysis only revealed a positive significant correlation between the controls' age and the perikaryal volume in layer V of the FG ($r^2 = 0.444$, $F_{(1,10)} = 6.384$, $p = 0.035$). Accordingly, there was no positive correlation between the age of the patients with autism and the perikaryal volume in layer V of the FG ($r^2 = 0.053$, $F_{(1,7)} = 0.27$, $p = 0.620$). Furthermore, the hemisphere had a significant effect on the mean perikaryal volume in layer VI of the FG ($F_{(1)} = 5.147$, $p = 0.049$) (Fig. S5 in Supplementary data). Furthermore, two-way ANOVA showed a significant difference only in the mean perikaryal volume in layer VI of the FG with respect to diagnosis ($p = 0.021$) but not with respect to hemisphere ($p = 0.073$) or the interaction between diagnosis and hemisphere ($p = 0.839$).

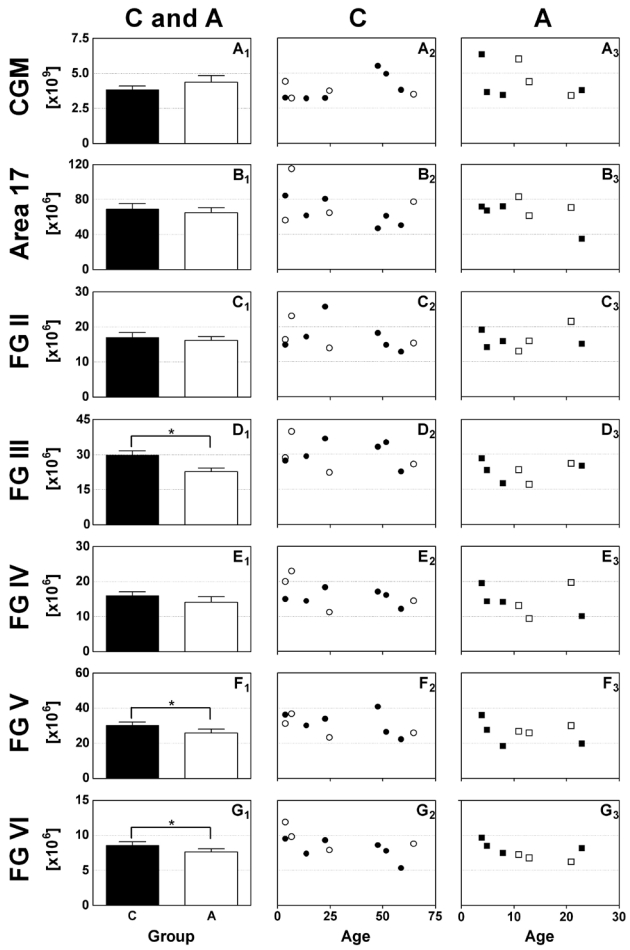

Figure 4. Total neuron numbers in the cortical gray matter (CGM) (A_1, A_2, A_3), area 17 (B_1, B_2, B_3) and layers II, III, IV, V, and VI of the fusiform gyrus (FG) (C_1, C_2, C_3 to G_1, G_2, G_3, respectively), in postmortem brains from 7 patients with autism (A; open bars in A_1 to G_1, squares in A_3 to G_3) and 10 matched controls (C; closed bars in A_1 to G_1, dots in A_2 to G_2). In A_1 to G_1, data from patients with autism and controls are shown as mean and standard error of the mean. In A_2 to G_2, individual data from controls are shown as a function of the patients' age. Black dots represent data obtained on brains cut at 200 µm and open dots data obtained on brains cut at 500 µm. In A_3 to G_3, individual data from patients with autism are shown as a function of the patients' age. Black squares represent data obtained on brains from patients without history of seizures, and open squares data obtained on brains from patients with a history of seizures. *, $p < 0.05$ for the fixed factor diagnosis in general linear model multivariate analysis of variance (MANOVA).

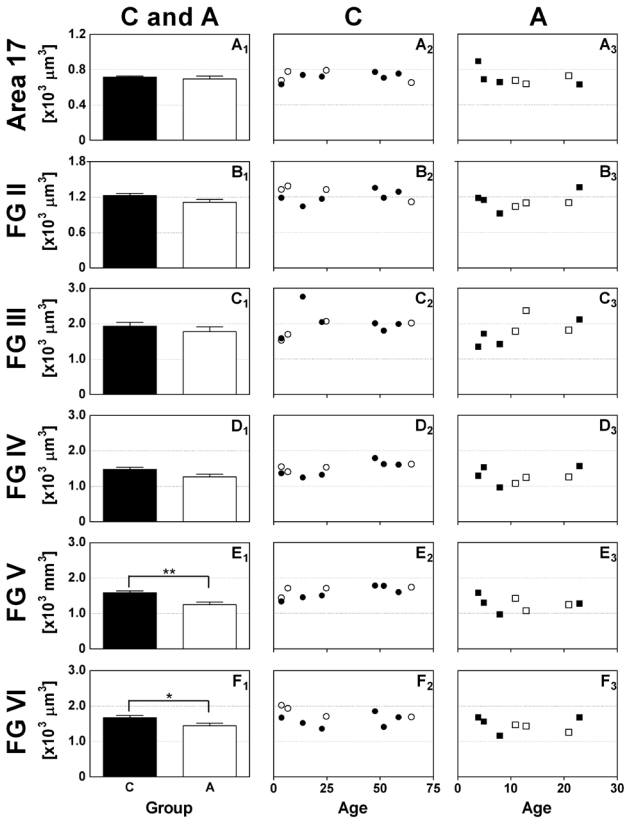

Figure 5. Mean perikaryal volume of neurons in area 17 (A_1, A_2, A_3) and layers II, III, IV, V, and VI of the fusiform gyrus (FG) (B_1, B_2, B_3 to F_1, F_2, F_3, respectively), in the postmortem brains from 7 patients with autism (A; open bars in A_1 to F_1, dots in A_3 to F_3), and 10 controls (C; black bars in A_1 to F_1, squares in A_2 to F_2). In A_1 to F_1, data from patients with autism and controls are shown as mean and standard error of the mean. In A_2 to F_2, individual data from controls are shown as a function of the patients' age. Black dots represent data obtained on brains cut at 200 µm and open dots data obtained on brains cut at 500 µm. In A_3 to F_3, individual data from patients with autism are shown as a function of the patients' age. Black squares represent data obtained on brains from patients without history of seizures, and open squares data obtained on brains from patients with a history of seizures. *, $p < 0.05$ and **, $p < 0.01$ for the fixed factor diagnosis in general linear model multivariate analysis of variance (MANOVA).

In summary, it can be concluded that the alterations in mean perikaryal volumes found in the investigated regions in the brains from the patients with autism were not caused by the patients' age and gender, the investigated hemispheres, the postmortem interval, the brain weight and the fixation time.

Finally it should be mentioned that the outcome of the present study was the same when the older control cases (i) C10, (ii) C9 and C10, or (iii) C8 to C10 were disregarded. Furthermore, the results obtained on the brains cut at 200 µm section thickness showed no systematic deviation from those cut at 500 µm (Figs. 4 and 5, as well as Figs. S3 and S4 in Supplementary data). Moreover, the results obtained on the brains from the patients with a history of seizures showed no systematic deviation from those without a history of seizures (Figs. 4 and 5, as well as Figs. S3 and S4 in Supplementary data).

Discussion

This is the first study focusing on volume, neuron density, total neuron number and mean perikaryal volume of neurons in the fusiform gyrus (FG) of patients with autism and matched controls. The main findings of the present study include a significant reduction in the mean neuron density in layer III (-13.1%), a reduced mean total neuron number in layers III, V and VI (-23.7%, -14.3% and -10.6%, respectively), and a decreased mean perikaryal volume of neurons in layers V and VI in the FG (-21.1% and -13.4%, respectively) in the brains of the patients with autism compared to the controls. These alterations did not reflect general neuropathological alterations found in all cortical regions in autism, as demonstrated by the fact that no differences in these variables were found in area 17 or in the whole cortical gray matter (CGM). In addition, the age of the patients with autism was not correlated with any of the observed neuronal alterations, suggesting that the alterations found in the FG might be of neurodevelopmental origin. The mean volumes of the FG and CGM found in the present study agree with previous reports in the literature (McDonald et al., 2000; Kreczmanski et al., 2007). Although this study consists of a relatively small sample, it is, besides the series investigated by Schumann and Amaral (2006) (9 patients with autism vs. 10 controls), larger than all other autism postmortem brain series studied in the past 20 years (Bauman and Kemper, 1985; Raymond et al., 1996; Bailey et al., 1998; Blatt et al., 2001; Fatemi and Halt, 2001; Schumann and Amaral, 2005).

Compared to the controls, we did not find alterations in the mean volumes of the whole hemispheres and the CGM in the brains from the patients with

autism. The observed lack of increase in brain volume in patients with autism at older ages is in accordance with some, but not all, related MRI studies (Piven et al., 1995; Courchesne et al., 2001; Hardan et al., 2001; Aylward et al., 2002; Palmen et al., 2004b). Although it has been suggested that abnormal brain development is a typical feature of autism regardless of IQ (Aylward et al., 2002), the differences in outcome between the present and previous studies may be explained by the influence of several factors associated with smaller brains such as mental retardation and epilepsy (Mosier et al., 1965; Theodore et al., 2003), which are the most common comorbid features of autism (Guerin et al., 1996; Canitano, 2007). Despite the fact that exact IQ data were not available in our study, all patients with autism investigated here were classified as high functioning patients in the clinical records.

Incomplete pruning during brain development, resulting in overabundant synapses and neurons, has been suggested to result in the larger brain size reported in some patients with autism (Frith, 2003; Belmonte et al., 2004). As suggested elsewhere (Courchesne et al., 2004), this could indicate improper function of overabundant synapses and neurons in patients with autism, that is eventually followed in later childhood by death of neurons and subsequent normalization or even decrease in brain volume (and total neuron number in the CGM) in autism. We found no significant difference in the mean total neuron number in the CGM between the patients with autism and the controls. However, this does not provide evidence for or against the hypothesis that the total neuron number in the CGM could change with age in brains from patients with autism. This is due to the fact that our sample encompassed a rather wide age range (i.e., from 4 to 23 years). Differences in total neuron number in the CGM could still be there at a specific age or time period of development. Further research is necessary to address this question.

A growing body of evidence suggests that patients with autism have difficulties in face perception (Schultz, 2005). Recognition of persons, especially of their individual faces, is a key part of an individual's social experience and successful functioning within a social group. Virtually all normal adults are experts in the recognition of faces (Tanaka and Guauthier, 1997), whereas patients with autism are consistently impaired in this task (Joseph and Tanaka, 2003). Most functional neuroimaging studies have reported reduced activity in the FG during face processing tasks in autism (Schultz et al., 2000; Hall et al., 2003; Hubl et al., 2003; Hadjikhani et al.,

2004; Pierce et al., 2004; Piggot et al., 2004). In addition, several studies demonstrated the involvement of a specific region located within the FG, the fusiform face area (FFA) (Schultz et al., 2003; Schultz, 2005; Hadjikhani et al., 2007). This region is more engaged by human faces than by any other object (Kanwisher et al., 1997). In the present study, we did not observe differences in the mean volume of the FG between the patients with autism and the controls. The same was observed by Pierce et al. (2001) in a structural neuroimaging study on the FG in autism, whereas Waiter et al. (2004) reported an increased FG volume in autism.

With respect to the neurobiological basis of the reduced activation of the FG during face processing tasks in autism, the main finding of the present study was a significant reduction in mean total neuron numbers in both output layers III and V of the FG in the patients with autism compared to the controls. Notably, these alterations were not found in area 17 and the CGM. Cortical layer III is the principal source of corticocortical (association) connections, whereas layer V is the principal source of efferent fibers to subcortical regions (Jones, 1986).

Accordingly, our results suggest a disconnection of the FG or under-developed connections in face processing networks (shown in Fig. S6 in Supplementary data). Area 17 projects via the inferior occipital gyrus (IOG) to the FG. In addition, the IOG is also connected to the superior temporal gyrus (STG). Efferent fibers project from the FG to the amygdala (AMG) and to two regions in the frontal lobe, the inferior frontal gyrus (IFG) and the orbitofrontal cortex (OFC) (Fairhall and Ishai, 2007). Thus, there is evidence that the FG receives input from the visual cortex via the IOG and provides the major input into an extended system consisting of cortical regions (including IFG and OFC) and subcortical regions such as the AMG (Fairhall and Ishai, 2007).

Although individuals with autism do not show deficits in visual perception in complex object recognition tasks not involving faces, abnormalities in the visual system in autism could be a first sign of a failure to develop perceptual expertise for faces. Thus, there may be a cortical explanation for the deficits in face perception seen in patients with autism rather than an involvement of limbic structures (Schultz et al., 2000). However, the present study found no differential effect in area 17 in patients with autism. This is supported by a recent finding showing no differences in activation of the visual cortex (areas V1 to V5) in 8 patients diagnosed with autism spectrum disorder compared to 4 IQ-matched controls (Hadjikhani et al., 2004). Rather the IOG and

STG showed reduced activity in patients with autism (Pierce et al., 2001), indicating that the altered function of the FG in patients with autism cannot be explained by abnormal input from area 17.

As mentioned above, Casanova et al. (2006) investigated a subset of the postmortem brains investigated in the present study for possible alterations in the modular organization of cellular microdomains (minicolumns) in the prefrontal cortex, primary motor cortex, primary sensory cortex and primary visual cortex. Casanova et al. (2006) found an increased neuron density and a slightly reduced mean neuron size in area 17 in the brains from the patients with autism compared with the controls. Although not directly comparable (because of methodological differences), the findings by Casanova et al. (2006) are in line with the results of the present study (as shown in Figs. 5 and S4 in Supplementary data).

Our finding of an age-related increase in the mean perikaryal volume of neurons in layer V of the FG was unexpected. In a sample of human postmortem control brains with ages 4-4-7-14-23-25-48-52-59-65 (in years) as the one investigated here, one would not predict significant changes as a function of age, particularly if all cases were controlled for the absence of neurodegenerative diseases (as done in our sample). No design-based stereologic studies have been published addressing the question of age-related alterations in perikaryal size of neurons in the human cerebral cortex. However, an earlier study by Schulz and Hunziker (1980) found no significant difference in the mean perikaryal size of cortical neurons between a group of people aged 19 to 44 and another group aged 65 to 74. Unfortunately, our sample did not include such age groups making a direct comparison between our data and the results by Schulz and Hunziker (1980) impossible. Additional research is necessary to evaluate the possible neurobiological repercussion of an age-related increase of the mean perikaryal volume of neurons in layer V of the FG in the human brain, but this was beyond the focus of the present study.

The reduced mean total neuron numbers in layers III and V of the FG and the reduced mean perikaryal volume of neurons in layers V and VI of the FG in the patients with autism could originate from pathologic events primarily in the FG itself, or from loss of targets to which the FG projects. In this regard it is important to note that the AMG receives input from the FG and is involved in face processing (as shown in Fig. S6 in Supplementary data) (Schultz et al., 2000; Fairhall and Ishai, 2007). The AMG plays a role in the

interpretation of faces (threatening or fearful) (Morris et al., 1999), monitors eye gaze (Kawashima et al., 1999) and has been implicated in autism because of its role in social behavior and cognition (Adolphs et al., 2002). Structural imaging studies have reported increased (Howard et al., 2000; Sparks et al., 2002; Schumann et al., 2004), decreased (Aylward et al., 1999; Pierce et al., 2001; Nacewicz et al., 2006) or unchanged (Haznedar et al., 2000; Palmen et al., 2006) mean volumes of the AMG in autism (note that this discrepancy may be due to differences in the ages of the patients among the available studies; it was suggested by Schumann et al. (2004) that larger volumes are typically observed in young subjects, whereas no difference or smaller volumes are observed in older subjects. However, this question was beyond the focus of the present study). In an earlier neuropathologic study, neurons in the AMG were found to be abnormally small and densely packed in autism (Kemper and Bauman, 1993), whereas a recent design-based stereologic study found no changes in mean neuron size but a significantly reduced mean total neuron number in the AMG overall and in its lateral nucleus in autism (Schumann and Amaral, 2006). The latter result suggests target loss of the FG in autism, which could contribute to reductions in mean total neuron numbers and mean neuronal size in the FG in autism as reported in the present study. The FG receives reciprocal input from the corticomedial nucleus of the AMG, however, these connections play a minor role during face perception (Fairhall and Ishai, 2007). Although no reduction in the mean total neuron number was found in this part of the AMG in patients with autism (Schumann and Amaral, 2006) and our data do not show alterations in the main input layers II and IV of the FG in autism, the results might point to an intact input from the AMG to the FG. In addition, because no alterations were found in area 17, input to the FG from the visual cortex seems to remain intact.

Finally it should be noted that a reduced mean total neuron number in the lateral nucleus of the AMG is not specific for autism, as the same finding was recently reported for schizophrenia (Kreczmanski et al., 2007). In this regard it will be important to evaluate whether the FG also shows reduced mean total neuron numbers in schizophrenia (as in autism). The mean volume of the FG is however comparable in patients with schizophrenia and controls (McDonald et al., 2000). There is indeed evidence that face processing deficits are also present in schizophrenia (Pinkham et al., 2005), yet patients with schizophrenia do not show reduced hemodynamic responses in the FG during face perception tasks studied with fMRI (Yoon et al., 2006).

In summary, although based on a relatively small sample of postmortem brains, the present study provides novel insight into the neuropathology of autism. Specifically, reduced mean total neuron numbers and smaller neurons in the main output layers of the FG in patients with autism might be involved in impaired face processing in autism. Although the precise interpretation of the reported FG hypoactivity in fMRI studies in autism has not yet been clearly established, Pierce et al. (2001) suggested that face processing can also occur outside the FG and FFA. In this regard, both the IFG (semantic aspects) (Leveroni et al., 2000) and the OFC (facial attractiveness and sexual relevance) (O'Doherty et al., 2003; Kranz and Ishai, 2006) belong to the cortical networks mediating face processing (Fairhall and Ishai, 2007) and are related to autism. Interestingly, imaging studies found a reduced activation of the IFG (Just et al., 2004; Harris et al., 2006; Koshino et al., 2007) and a decreased volume of the OFC in autism (Hardan et al., 2006; Girgis et al., 2007). It will therefore be of interest to investigate total neuron numbers and neuron densities in the IFG and OFC in postmortem brains of patients with autism as well. Further studies are needed to test the hypothesis that there is a causal relationship between abnormal activation of the FG and related cortical areas in face processing in autism and the neuropathologic findings reported in the present study.

Supplementary data

Neurons in the fusiform gyrus are fewer and smaller in autism
This supplement provides additional results of our high-precision design-based stereologic analysis of the fusiform gyrus (FG) in 7 postmortem brains from patients with autism and 10 matched controls. Specifically, the use of the Nucleator to estimate mean perikaryal volumes on coronal sections is briefly discussed, as well as the reason not to consider the history of seizures in some of the patients with autism in the statistical analysis. Also, Table S1 summarizes the clinical history of all patients with autism included in this study. Table S2 provides the results of the statistical analysis (p values) with a generalized linear model multivariate analysis of variance (MANOVA) focusing on differences in mean volumes, neuron densities, total neuron numbers and mean perikaryal volumes between the patients with autism and the controls. Fig. S1 shows the delineation procedure of the entire FG, and Fig. S2 the difference between neurons, glial cells and endothelial cells in a representative high-power photomicrograph of a 200 µm-thick coronal section (stained with Gallocyanin) in layer V of the FG from a patient with autism. Figs. S3 and S4 report the results of the volumes and neuron densities of the entire hemisphere, cortical gray matter, area 17, all layers of the FG, and layers II, III, IV, V, and VI of the FG, respectively, in the 7 patients with autism and 10 controls. Fig. S5 summarizes the results of the post-hoc tests in the analyses of covariance. Finally, Fig. S6 depicts an overview of the network of cortical and subcortical brain regions involved in face processing.

Use of the Nucleator to estimate mean perikaryal volumes on coronal sections
Estimates of mean perikaryal volumes obtained with the Nucleator on coronal sections cannot be considered free of bias. Obtaining unbiased estimates with the Nucleator requires the use of either so-called isotropic uniform random sections or so-called vertical sections (details are provided in (Schmitz and Hof, 2005; Glaser et al., 2007)). In preparing both isotropic uniform random sections and vertical sections, however, one cannot select a certain plane of section that might be necessary to identify the region of interest (as in the present study). In general, unbiased estimates of mean perikaryal volumes could be obtained on coronal sections with the Optical Rotator (Tandrup et al., 1997). However, shrinkage of the sections in the

z-axis (as in the present study; details are provided in Table 2 in the main text) may result in biased estimates using the Optical Rotator (details are provided in Schmitz and Hof, 2005; Glaser et al., 2007). Accordingly, using the Nucleator to estimate mean perikaryal volumes in the present study can be considered as optimum trade-off between the requirements of design-based stereologic techniques and requirements in cutting human postmortem brains to identify certain regions of interest (see also Schmitz and Hof, 2005). In a strict sense, the estimates of mean perikaryal volumes in the present study are based on the hypothesis that all neuronal cell bodies were either round or showed no anisotropy in their shape relative to the plane of section. There is no evidence for or against this hypothesis. However, it should be considered that estimates of mean nuclear volumes of neurons in the mouse hippocampus and cerebellum obtained with the Nucleator on isotropic uniform random sections showed no differences compared to corresponding estimates obtained on coronal sections (Schmitz et al., 1999).

History of seizures in patients with autism

One of the oldest questions in epilepsy is whether seizures are a cause or a result of brain damage (Holmes, 2002). This is of importance for the present study because the patients A4 to A7 had a history of seizures (see also Table S1). The emerging perspective in the literature is that seizure-induced damage should be regarded not only as neuronal loss but also as having adverse long-term behavioral and cognitive consequences (Sutula et al., 2003). Indeed, the FG can be the location of seizures and an epileptic focus within the FG have been identified using ictal magnetoencephalography (Suzuki et al., 1992; Oishi et al., 2002). However, it should be considered that a recent postmortem stereologic analysis of 28 patients with poorly controlled seizures identified a subgroup with absence of significant hippocampal neuron loss despite decades of generalized seizures, including status epilepticus (Thom et al., 2005). Corresponding data on the FG have not been reported. Furthermore, animal data have provided insights into the relationship between seizures and subsequent brain damage. It is now recognized that seizures can, in certain conditions, cause brain damage. However, whether seizures result in brain damage depends on a number of variables, including age of the animal, seizure type and duration, etiology of the seizures, and genetic substrate on which the seizures occur (Holmes, 2002).

In conclusion, seizures do not invariably lead to neuron loss. Specifically, the immature brain seems relatively resistant to seizure-induced neuronal loss (Lado et al., 2000).

There were substantial differences among the patients with a history of seizures in the present study. Specifically, patient A4 had a history of tonic-clonic seizures since the age of four months (and died at the age of 11 years). Patient A5 had a first seizure at the age of 24 months and was briefly treated with Dilantin. However, this medication was discontinued shortly thereafter due to adverse side effects. Subsequently, this patient continued to experience severe seizures until he died at 13 years of age. Patient A6 had a total of four grand mal seizures during lifetime, and Patient A7 might have had one seizure prior to death. Furthermore, the clinical records did not provide any evidence as to whether the patients with a history of seizures suffered from focal epilepsy within the FG. We do not even know whether the FG was involved in seizure pathology in any of these patients.

In summary, there is no evidence for or against the hypothesis that the results obtained on the brains from the patients with a history of seizures (i.e., patients A4 to A6) could have been influenced by the specific history of seizures. We have therefore not considered the history of seizures of these patients with autism in the statistical analysis. However, we graphically compared the results obtained on the brains from the patients with a history of seizures with those without a history of seizures and found no difference between the two groups (Figs. 3 and 4 in the main text and Figs. S3 and S4 in the Supplementary data).

Table S1. Clinical history of all patients with autism included in this study.

No	T	Description
A1	C	Asthma/bronchitis
	S	No
	M	Daily medication (not specified) for asthma/bronchitis
A2	C	Ear infections
	S	No
	M	Antibiotics (ear infections)
A3	C	Syndactyly of the fingers and feet, colitis, hay fever, neutropenia, metastic alveolar rhabdomyosarcoma, large paravertebral mass extending from chest cavity to abdomen
	S	Unusual brain activity (EEG); not diagnosed with seizure disorder
	M	Depakote (one year after EEG), chemotherapy, Peridex, Nystatin, GCSF, Benadryl, Pheergan, Dexamethasone and Morphine
A4	C	Chronic ear infections, perineal yeast infection, mild intellectual deficiency, hyperlexia
	S	History of tonic-clonic seizures since the age of four months.
	M	Lamictal, Adderall, Topamax and Tegretol
A5	C	Severe hypotonia, seizures, ketogenic diet for 1.5 years
	S	First seizure at the age of 24 months (brief treatment with Dilantin; medication discontinued shortly thereafter due to negative side effects). Subsequently continuation of experiencing severe seizures until the time of death.
	M	Dilatin, Anticonvulsants, Trileptal and Trazadone
A6	C	ADHD, microcephaly, epilepsy, schizophrenia
	S	Three grand mal seizures (the first one at the age of 5 years).
	M	Variety of psychotropic medications throughout life, including Haldol, Ritalin and Congentin; at time of death DepoProvera, Mellaril and Zoloft
A7	C	Pneumonia, bronchitis, behavioral problems
	S	First seizure prior to death.
	M	Quetiapine, Propanolol and Thioridazine

A, patient with autism. T, topic; C, clinical history; S, history of seizures; M, medication history.

Table S2. Results of statistical analysis (p values) with generalized linear model multivariate analysis of variance (MANOVA).

Variable	Brain region	D	Age	G	H	PMI	BW	Fix
Volume	Hem	0.252	0.070	**0.004**	**0.007**	0.177	0.407	**0.016**
	CGM	0.129	**0.004**	**0.013**	**0.006**	0.112	0.517	**0.010**
	Area 17	0.272	0.334	0.438	0.543	0.344	0.846	0.113
	FG I-VI	0.326	0.627	0.272	0.673	0.318	0.141	0.911
	FG I	0.310	0.536	**0.044**	0.364	0.245	0.285	0.833
	FG II	0.868	0.305	0.135	0.756	0.168	0.344	0.553
	FG III	0.635	0.095	0.898	0.335	0.759	0.496	0.661
	FG IV	0.322	0.903	0.470	0.725	0.462	0.117	0.948
	FG V	0.157	0.311	0.147	0.193	0.082	0.051	0.823
	FG VI	0.162	0.910	0.531	0.517	0.306	0.252	0.871
Neuron density	CGM	0.365	0.232	0.679	0.769	0.382	0.444	0.156
	Area 17	0.902	0.168	0.634	0.804	0.110	0.878	0.173
	FG II	0.749	0.924	0.563	0.261	0.861	0.786	0.663
	FG III	**0.002**	0.105	0.099	0.695	0.762	0.469	0.081
	FG IV	0.671	0.463	0.357	0.892	0.585	0.374	0.899
	FG V	0.139	0.116	**0.031**	0.940	0.073	0.820	0.523
	FG VI	0.885	0.188	0.569	0.653	0.145	0.354	0.814

Table S2. Continued.

Variable	Brain region	D	Age	G	H	PMI	BW	Fix
	CGM	0.513	0.622	0.774	0.206	0.575	0.466	0.414
	Area 17	0.199	0.406	0.213	0.983	0.319	0.744	0.724
	FG II	0.708	0.462	0.382	0.663	0.198	0.585	0.865
Neuron number	FG III	**0.033**	0.763	0.548	0.409	0.728	0.942	0.238
	FG IV	0.145	0.384	0.703	0.629	0.144	0.250	0.853
	FG V	**0.032**	0.400	0.860	0.286	0.639	0.139	0.620
	FG VI	**0.043**	0.078	0.701	0.469	0.744	0.563	0.689
Mean perikaryal volume	Area 17	0.299	0.717	0.324	0.901	0.251	0.457	**0.045**
	FG II	0.191	0.874	0.838	0.627	0.512	0.880	0.875
	FG III	0.879	0.799	0.769	0.728	0.929	0.587	0.769
	FG IV	0.168	0.134	0.793	0.558	0.690	0.765	0.660
	FG V	**0.004**	**0.027**	0.412	0.825	0.915	0.783	**0.044**
	FG VI	**0.016**	0.232	0.817	**0.049**	0.338	0.789	0.785

D, diagnosis; G, gender; H, hemisphere; PMI, post-mortem interval (time between death and autopsy); BW, brain weight; Fix, fixation time. Hem, entire hemisphere; CGM, cortical gray matter; FG, fusiform gyrus; I, II, III, IV, V, and VI, cortex layers I-VI. P values smaller than 0.05 are shown in boldface.

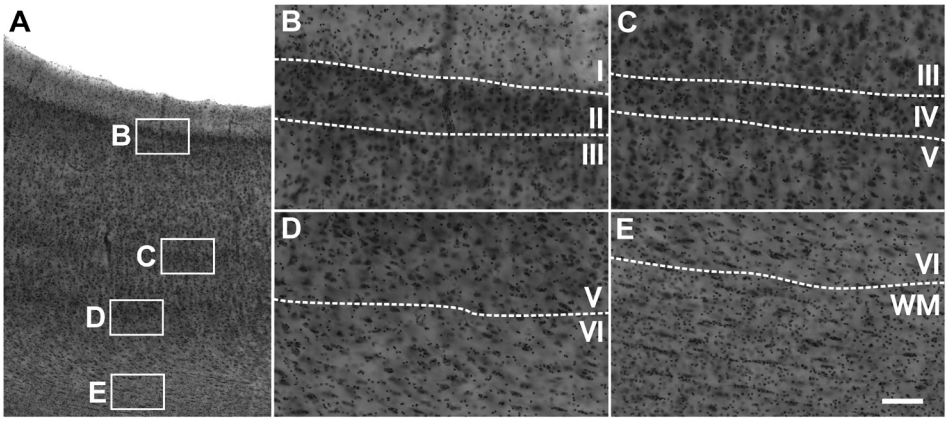

Figure S1. Representative photomicrographs of a 200 µm-thick coronal section throughout the fusiform gyrus (FG) in the postmortem brain from a patient with autism, showing the delineation procedure of the cortical layers. The small squares in A represent the high-power photomicrographs in B to E. Layer I, molecular layer (B); layer II, external granule cell layer (B); layer III, external pyramidal cell layer (B,C); layer IV, internal granule cell layer (C); layer V, internal pyramidal cell layer (C,D); layer VI, multiform layer (D,E); WM, white matter (E). It is important to note that photomicrographs of 200 µm thick sections stained with Gallocyanin can provide only a limited impression of the visualization of the boundaries between the cortical layers obtained at the microscope. Scale bar = 125 µm in A and 40 µm in B to E.

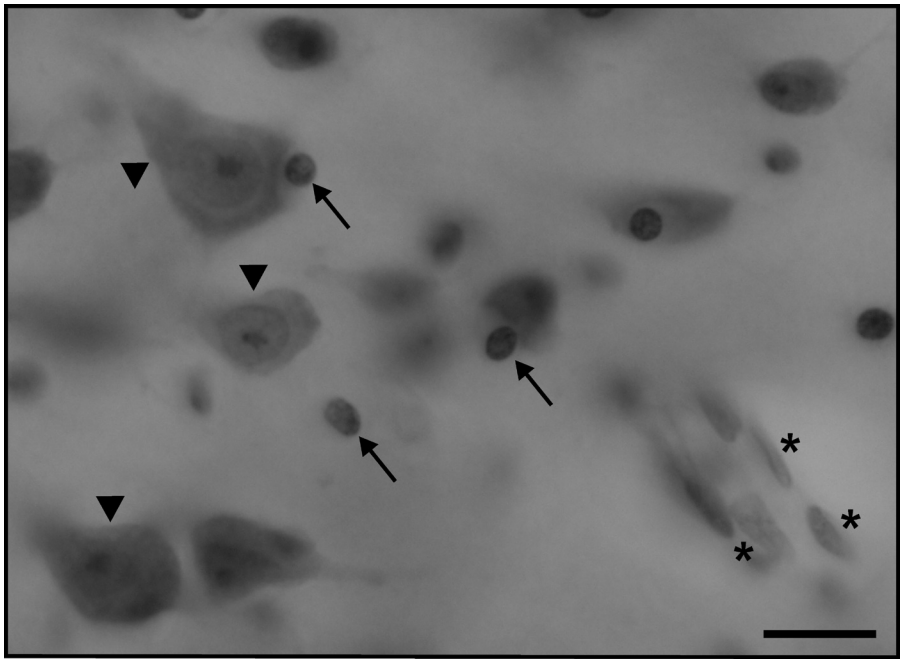

Figure S2. Representative high-power photomicrograph of a 200 µm-thick coronal section of layer V in the FG of a patient with autism. The section was stained with Gallocyanin and shows the difference between neurons (arrowheads), glial cells (arrows) and endothelial cells (asterisks). Neurons showed a large cytoplasm, and a prominent nucleolus within a pale nucleus. Glial cells were identified by the absence of cytoplasmic staining, intense staining of the nucleus with dispersed chromatin and lack of a nucleolus. Endothelial cells were identified by the characteristic, three-dimensional shape of their nucleus within the thick sections. Scale bar = 25 µm.

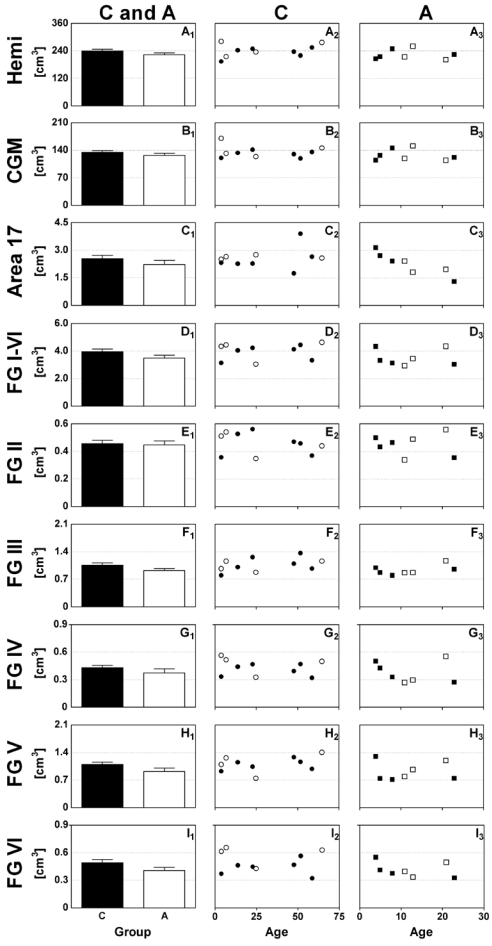

Figure S3. Volumes of the entire hemisphere (Hemi) (A_1, A_2, A_3), cortical gray matter (CGM) (B_1, B_2, B_3), area 17 (C_1, C_2, C_3), all layers of the fusiform gyrus (FG I-VI) (D_1, D_2, D_3), and layers II, III, IV, V and VI (E_1, E_2, E_3 to I_1, I_2, I_3, respectively) of the FG in postmortem brains from 7 patients with autism (A; open bars in A_1 to I_1, squares in A_3 to I_3) and 10 matched controls (C; black bars in A_1 to I_1, dots in A_2 to I_2). In A_1 to I_1, data from patients with autism and controls are shown as mean and standard error of the mean. In A_2 to I_2, individual data from controls are shown as a function of age. Black dots represent data obtained on brains cut at 200 µm and open dots data obtained on brains cut at 500 µm. In A_3 to I_3, individual data from patients with autism are shown as a function of the patients' age. Black squares represent data obtained on brains from patients without history of seizures, and open squares data obtained on brains from patients with a history of seizures.

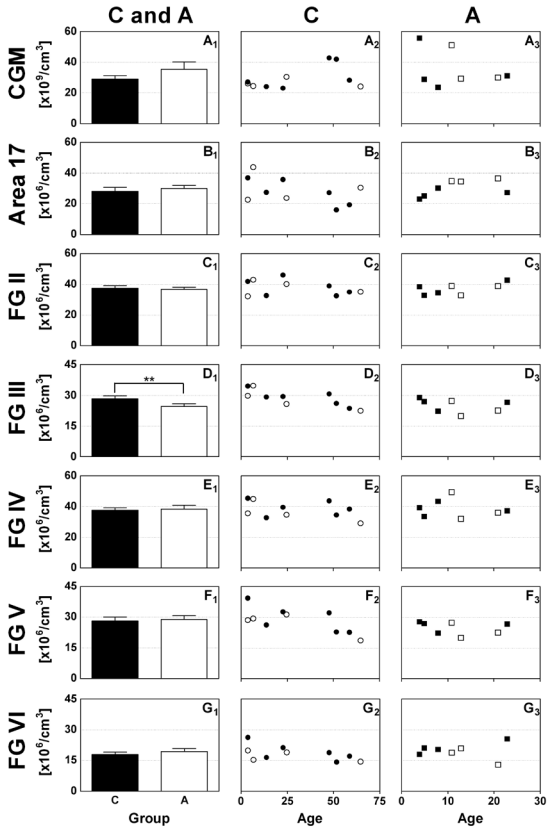

Figure S4. Neuron density in the cortical gray matter (CGM) (A_1, A_2, A_3), area17 (B_1, B_2, B_3), and layers II, III, IV, V and VI of the fusiform gyrus (FG) (C_1, C_2, C_3 to G_1, G_2, G_3, respectively) in postmortem brains from 7 autistic patients (A; open bars in A_1 to G_1, squares in A_3 to G_3) and 10 matched controls (C; black bars in A_1 to G_1, dots in A_2 to G_2). In A_1 to G_1, data from patients with autism and controls are shown as mean and standard error of the mean. In A_2 to G_2, individual data from controls are shown as a function of the patients' age. Black dots represent data obtained on brains cut at 200 µm and open dots data obtained on brains cut at 500 µm. In A_3 to G_3, individual data from patients with autism are shown as a function of the patients' age. Black squares represent data obtained on brains from patients without history of seizures, and open squares data obtained on brains from patients with a history of seizures. **, $p < 0.01$ for the fixed factor diagnosis in general linear model multivariate analysis of variance (MANOVA).

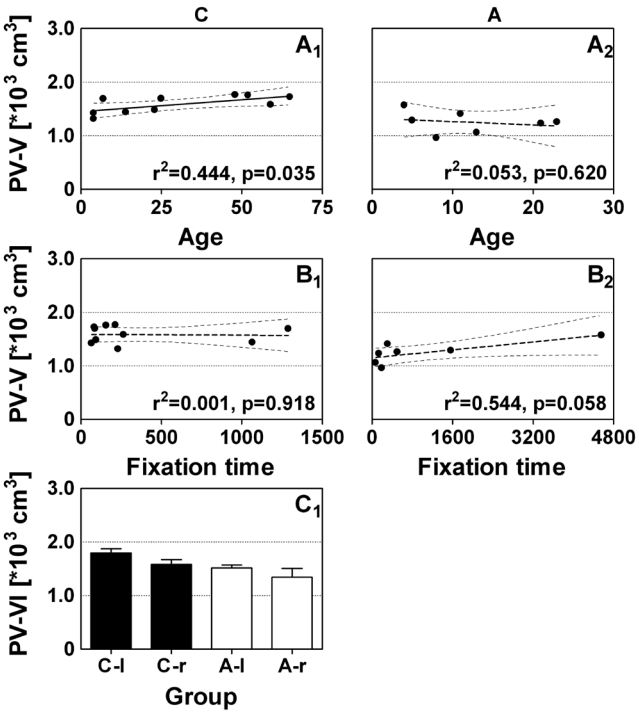

Figure S5. Mean perikaryal volume of neurons in layer V of the fusiform gyrus (FG; PV-V) as a function of the patients' age (A_1, A_2) and the fixation time (B_1, B_2) as well as mean perikaryal volume of neurons in layer VI of the FG (PV-VI) as a function of the hemisphere (C). Graphs A_1, A_2, B_1 and B_2 show individual values (dots) from controls (A_1, B_1) and patients with autism (A_2, B_2) as well as the results from linear regression analysis (regression lines with 95% confidence intervals, regression correlation coefficients [r^2 values] and p values). Solid regression lines indicate that the slope of the regression line was significantly different from zero ($p < 0.05$); otherwise regression lines are dotted. In C, data are shown as mean and standard error of the mean for the left (l) and right (r) hemispheres from controls (C-l and C-r, respectively) and patients with autism (A-l and A-r, respectively).

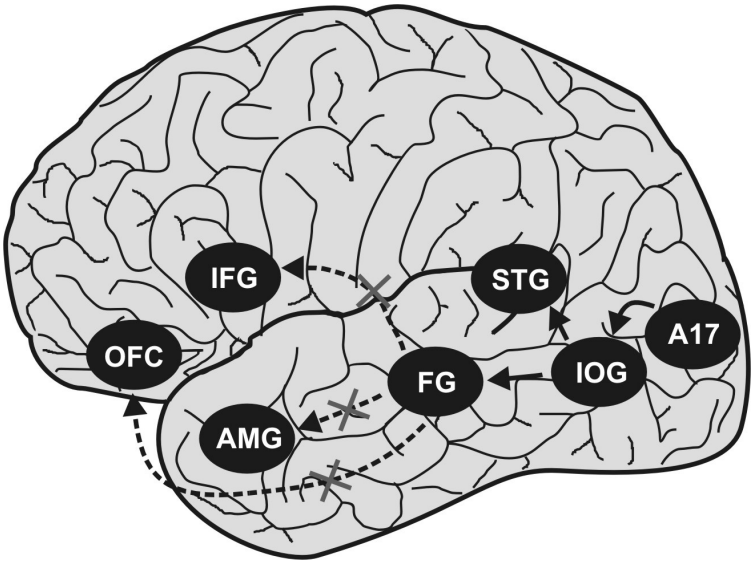

Figure S6. Network of cortical and subcortical brain regions involved in face processing (modified from Fairhall and Ishai (2007). Connections that may be disturbed in autism are indicated with arrows with broken lines. A17, area 17; IOG, inferior occipital gyrus; STG, superior temporal gyrus; FG, fusiform gyrus; AMG, amygdala; IFG, inferior frontal gyrus; OFC, orbitofrontal cortex.

Chapter 6

Alterations of Von Economo neurons in the anterior cingulate cortex and frontoinsular cortex in schizophrenia and autism

Van Kooten IAJ, Segal D, Rutten BPF, Kreczmanski P, Van Engeland H, Steinbusch HWM, Haroutunian V, Heinsen H, Allman JM, Schmitz C, Hof PR.

Submitted

Abstract

Von Economo neurons (VENs) are a specific cell type that is found exclusively in humans, great apes, and some whale species. In humans and great apes, these neurons are found solely in the anterior cingulate cortex (ACC) and frontoinsular cortex (FI). Both ACC and FI are involved in functions related to social cognition, and both have been proposed to be implicated in neuropsychiatric disorders, including schizophrenia and autism. It has been proposed that VENs in particular are abnormal in schizophrenia and autism, and that their dysfunction may lead to specific deficits noted in both psychiatric disorders. In the present study, we surveyed VEN morphology in the ACC and FI in 24 postmortem brains from patients with schizophrenia, 7 postmortem brains from patients with autism, and 34 postmortem brains from matched controls. We demonstrated that in both ACC and FI, patients with schizophrenia exhibited alterations of VEN morphology compared to controls. Specifically, VENs were irregularly shaped, shorter, showed only either the basal or the apical dendrite, and were usually curved. The same morphological abnormalities of VENs were also found in the ACC and FI in some patients with autism compared to matched controls. These findings suggest that specific alterations in morphology and perhaps function of VENs may significantly contribute to the neuropathology of schizophrenia and possibly autism.

Introduction

Von Economo neurons (VENs) are a particular type of neurons found exclusively in the anterior cingulate cortex (ACC) and the frontoinsular cortex (FI) that appears to be specific to humans, great apes, and certain cetacean species (Allman et al., 2005; Hof and Van der Gucht, 2007). VENs are large bipolar projection neurons, mostly located in layer V of both ACC and FI, although a few are also found in layer III (Nimchinsky et al., 1995; Allman et al., 2001, 2002). VENs have a radial orientation and show very sparsely branching dendritic trees with symmetric apical and basal projections and spine densities quite comparable to those of pyramidal neurons (Watson et al., 2006). They appear to be widely connected to several parts of the brain and may have a role in the coordination of distributed neuronal activity involving social cognition and emotion (Nimchinsky et al., 1995, 1999; Allman et al., 2001, 2002, 2005; Hof and Van der Gucht, 2007). Furthermore, VENs are immunopositive for the dopamine D3 receptor, which is involved in anticipation of reward under conditions of uncertainty (Allman et al., 2005). Both the ACC and FI show increased activity with the degree of uncertainty. VENs are also immunoreactive for the serotonin 2b receptor, which is in turn involved in peripheral reactions signalling impending danger or punishment ("gut feeling") (Allman et al., 2005). The ACC and FI also have an important role in interoception, the conscious awareness of visceral activity (Craig, 2002 ; Allman et al., 2005).

The existence of VENs exclusively in mammalian species with elaborate social structures suggests a possible role for these neurons in advanced social interactions (Sanders et al., 2002; Allman et al., 2005; Hof and Van der Gucht, 2007). The presence of VENs only in the ACC and FI, areas that have been linked to social functions such as intuition and reward expectation (Allman et al., 2005), supports this possibility. The ACC, which bridges limbic and prefrontal cortical areas (Allman et al., 2001), and FI have also been implicated in cognitive and social deficits seen in several neuropsychiatric disorders, including schizophrenia (Kopelman et al., 2005; Nagai et al., 2007) and autism (Allman et al., 2005; Kennedy et al., 2007). Therefore, it is reasonable to suggest that VENs may be specifically altered in the ACC and FI of patients with schizophrenia and autism, as both diseases are characterized by abnormal cognitive and social functions (Sanders et al., 2002; Allman et al., 2005; Kennedy et al., 2007). However,

Kennedy et al. (2007) found no reduction in the number of VENs in the FI in a small sample of patients with autism (n = 4) compared to controls (n = 5). On the other hand, Allman et al. (2001, 2005) speculated that VENs may be particularly vulnerable to certain neuropathological conditions, compared to other neuronal cell types, because they appear during development around the 35th week of gestation in humans (Allman et al., 2005). Their survival may be enhanced or reduced by environmental conditions such as enrichment or stress, thereby potentially influencing adult competence in emotional self-control and problem-solving capacity (Allman et al., 2001). A recent study by Seeley et al. (2006) found a dramatic and specific loss of VENs in the ACC of patients with frontotemporal dementia, a disease resulting in severe impairments of social behavior. These findings further strengthen the suggestion that VENs are involved in mediating or directing interpersonal interactions. VENs may thus contribute to dysfunction seen in schizophrenia (Sanders et al., 2002) and autism (Allman et al., 2001).

In the present study we hypothesized that the morphology of VENs is abnormal in the brains of patients with schizophrenia and autism, based on earlier reports in the literature (investigating ACC and FI function) that VENs play a key role in higher order cognitive functions. To address this hypothesis, we investigated the morphology of VENs in the ACC and FI in two independent samples of postmortem brains from patients with schizophrenia and autism and in corresponding matched controls.

Table 1. Overview of the investigated areas in patients with schizophrenia, patients with autism, and matched controls.

Group	Brain code	Investigated area
Schizophrenia/Controls	S1 - S13 / C_S1 – C_S13	ACC and FI
	S14 - S18 / C_S14 – C_S18	ACC
	S19 - S24 / C_S19 – C_S24	FI
Autism/Controls	A1 – A7 / C_A25 – C_A34	ACC and FI

S, patient with schizophrenia; A, patient with autism; C_S, control for the schizophrenia sample; C_A, control for the autism sample; ACC, anterior cingulate cortex; FI, frontoinsular cortex.

Materials and Methods

Brain specimens

Postmortem brains from 18 patients with schizophrenia (13 men, 5 women; mean age 59.7 ± 4.2 years; mean postmortem interval [i.e., the interval between death and autopsy] 22.9 ± 4.5 hours; data expressed as mean ± standard error of the mean [SEM]) and 18 age-matched controls (16 men, 2 women; mean age 58.9 ± 3.7 years; mean postmortem interval 20.3 ± 3.1 hours) were analyzed for the ACC (Table 1). The patients with schizophrenia did not differ from the controls with respect to mean age (Student's two-tailed t test; $t_{(34)} = 0.1392$ [34 degrees of freedom], $p = 0.890$), mean postmortem interval ($t_{(32)} = 0.4692$, $p = 0.642$), and mean fixation time ($t_{(34)} = 0.6022$, $p = 0.551$). For the FI, postmortem brains from 19 patients with schizophrenia (15 men, 4 women; mean age 59.8 ± 3.7 years; mean postmortem interval 21.1 ± 4.4 hours) and 19 age-matched controls (16 men, 3 women; mean age 56.9 ± 3.3 years; mean postmortem interval 17.8 ± 3.3 hours) were analyzed (Table 1). In this sample, as well, patients with schizophrenia did not differ from controls with respect to mean age (Student's two-tailed t test; $t_{(36)} = 0.5914$, $p = 0.558$), mean postmortem interval ($t_{(34)} = 0.6061$, $p = 0.549$), and mean fixation time ($t_{(36)} = 0.8060$, $p = 0.426$). For both samples, clinical diagnoses, gender, age, cause of death, age at disease onset, postmortem interval, and fixation time are summarized in Table 2. The patients with schizophrenia S1-S13 and the controls cases C_S1-C_S13 were the same cases that had been investigated in our previous studies for mean cell spacing abnormalities in the neocortex (Casanova et al., 2005, 2008); capillary length densities in the frontal cortex (Kreczmanski et al., 2005); and volume, neuron density, and total neuron number in five subcortical regions (Kreczmanski et al., 2007). In addition, the patients with schizophrenia S19-S24 and the controls cases C_S19-C_S24 were the same cases that had been investigated in our previous study of oligodendrocyte density and distribution (Segal et al., 2008).

The patients with schizophrenia S1-S13 had been hospitalized either in German university hospitals or in German state psychiatric hospitals (6 hospitals including one university hospital in which some of the control cases C_S1-C_S13 were also treated for nonpsychiatric or non-neurologic illnesses), and full clinical records were available. The control cases C_S1-C_S13 had been patients either in German university hospitals or in German local district hospitals (5 hospitals including one university hospital in which some of the patients with schizophrenia S1-S13 were also treated).

Table 2. Clinical characteristics and predominant type of von Economo neurons (VENs) in the anterior cingulate cortex and frontoinsular cortex of patients with schizophrenia and related controls investigated in the present study.

No	Age	S	H	Cause of death	PMI	Fix	Diagnosis		VEN	VEN
	[y]				[h]	[d]	DSM-IV	ICD-10	ACC	FI
S1	22	M	l	Suicide‡	88	130	295.30	F20.00	2	1
S2	36	M	l	Suicide‡	<72	115	295.30	F20.00	1	2
S3	46	M	l	Systemic hypothermia	<24	327	295.30	F20.01	2	1
S4	50	M	l	Peritonitis	<24	203	295.30	F20.00	2	2
S5	50	M	l	Suicide	18	170	295.30	F20.00	1	1
S6	51	M	l	Septicemia	33	127	295.60	F20.50	1	2
S7	54	M	l	Septicemia	27	250	295.60	F20.50	2	2
S8	55	M	l	Right-sided heart failure	25	84	295.30	F20.00	2	2
S9	57	M	l	Septicemia	76	163	295.30	F20.00	2	1
S10	60	M	l	Pulmonary embolism	<48	311	295.30	F20.01	2	2
S11	62	M	l	Aspiration	7	171	295.30	F20.00	2	2
S12	63	M	l	Acute myocardial infarct	15	338	295.60	F20.50	2	1
S13	64	M	l	Pulmonary embolism	6	817	295.60	F20.50	2	2
S14	59	F	l	Cardiopulmonary arrest	22	1856	295.70	F25.90	2	-
S15	79	F	l	Cardiopulmonary arrest	9	5347	295.32	F20.00	1	-
S16	86	F	l	Cardiopulmonary arrest	18	1856	295.32	F20.00	2	-
S17	90	F	l	Cardiopulmonary arrest / septic shock	8	1650	295.00	F20.90	2	-
S18	90	F	l	Cardiorespiratory failure	6	781	295.00	F20.60	2	-
S19	66	M	l	Cardiopulmonary arrest	8	2610	295.60	F20.50	-	2
S20	82	M	l	Respiratory failure	11	1530	295.70	F25.90	-	2
S21	74	F	l	Cardiopulmonary arrest	7	2010	295.92	†	-	2
S22	77	F	l	Cardiopulmonary arrest	10	1650	295.92	†	-	2
S23	79	F	l	Cardiac arrest	10	2340	295.70	F29.50	-	2
S24	89	F	l	Cardiopulmonary arrest	10	1950	295.90	F20.30	-	2

S, patient with schizophrenia; C_S, control for the schizophrenia sample. y, years. S, sex; M, male; F, female. H, hemisphere; l, left; r, right; PMI, postmortem interval (i.e., time between death and autopsy); h, hours. Fix, fixation time; d, days. VEN, predominant type of VENs in the anterior cingulate cortex (ACC) and frontoinsular cortex (FI). VEN 1, regularly shaped VENs (Type-1-VENs) predominating; VEN 2, irregularly shaped VENs (Type-2-VENs) predominating. A Fisher's exact test showed a significant difference between patients with schizophrenia and controls with respect

Table 2. Continued

No	Age [y]	S	H	Cause of death	PMI [h]	Fix [d]	Diagnosis DSM-IV	Diagnosis ICD-10	VEN ACC	VEN FI
C_S1	25	M	I	Cardiac tamponade	14	119	-	-	1	1
C_S2	36	M	I	Gunshot	24	143	-	-	1	1
C_S3	47	M	I	Acute myocardial infarct	<24	133	-	-	1	1
C_S4	50	M	I	Acute myocardial infarct	35	433	-	-	2	1
C_S5	50	M	I	Avalanche accident	23	498	-	-	1	1
C_S6	51	M	I	Septicemia	7	285	-	-	1	1
C_S7	54	M	I	Acute myocardial infarct	18	168	-	-	2	2
C_S8	56	M	I	Acute myocardial infarct	60	3570	-	-	2	1
C_S9	58	M	I	Acute myocardial infarct	28	126	-	-	1	1
C_S10	60	M	I	Gastrointestinal hemorrhage	18	101	-	-	1	1
C_S11	60	M	I	Gastrointestinal hemorrhage	27	302	-	-	1	1
C_S12	62	M	I	Acute myocardial infarct	<24	3696	-	-	1	1
C_S13	65	M	I	Bronchopneumonia	6	2289	-	-	1	2
C_S14	70	M	I	Cardiopulmonary arrest	21	1418	-	-	1	-
C_S15	73	M	I	Neoplasm	20	901	-	-	1	
C_S16	74	F	I	Cardiopulmonary arrest	5	1021	-	-	1	-
C_S17	76	F	I	Acute myocardial infection	8	2975	-	-	1	-
C_S18	93	M	I	Acute myocardial infection	4	1058	-	-	1	-
C_S19	65	M	I	Cardiac arrest	4	2100	-	-	-	1
C_S20	66	M	I	Cardiac arrest	8	1920	-	-	-	1
C_S21	75	M	I	Myocardial infarction	5	1050	-	-	-	1
C_S22	78	F	I	Cardiorespiratory arrest	4	810	-	-	-	1
C_S23	40	F	I	Aortic dissection	4	780	-	-	-	1
C_S24	83	F	I	Cardiopulmonary arrest	6	1920	-	-	-	1

to the predominant type of VENs in the anterior ACC ($p < 0.001$) and FI ($p < 0.001$). † no ICD-10 diagnosis available. ‡ These two patients had relatively long postmortem intervals. However, both had committed suicide (one by hanging, the other by jumping from a building), were found within one hour of death and were kept at 4°C until autopsy. Accordingly, the postmortem intervals between death and autopsy of these patients cannot be compared to the corresponding intervals of the other cases and were thus excluded from the calculation of the mean postmortem intervals.

The brains from the patients with schizophrenia S14-S24 were obtained from the Pilgrim Psychiatric Center (West Brentwood, NY, USA) and the Bronx VA Hospital (Bronx, NY, USA). Records from autopsy (including a summary of the medical history) were available for all patients with schizophrenia and all controls.

All patients with schizophrenia met the Diagnostic Statistical Manual, 4th revision (DSM-IV) and International Statistical Classification of Diseases and Related Health Problems, 10th revision (ICD-10) diagnostic criteria. The clinical records were assessed by experienced clinical psychiatrists to ensure that the controls were free from psychopathology and for clear evidence that the patients with schizophrenia conformed to DSM-IV criteria for schizophrenia. Exclusion criteria for both patients with schizophrenia and controls were neurological problems that required intervention or interfered with cognitive assessment (e.g., stroke with aphasia), history of recurrent seizure disorder, history of severe head injury with loss of consciousness, diabetes mellitus with free plasma glucose >200 mg/dl, and history of self-administered intoxication. Patients with schizophrenia and corresponding controls were similar in terms of the ethnic backgrounds. However, they were not fully matched for socio-economical status and education, which would have placed severe constraints on our samples. Moreover, all patients with schizophrenia were subjected to long-term treatment with typical neuroleptics (because of the fact that most of the patients were not hospitalized throughout the duration of their illness, and, therefore, the clinical records did not cover fully the entire medication histories, it was not possible to calculate lifetime medication exposures). In all of the cases, autopsy was performed after consent was obtained from a relative according to the laws of the Federal Republic of Germany and the USA. The use of these autopsy cases for scientific investigations as outlined here has been approved by the relevant Institutional Review Boards.

In addition, postmortem brains (one hemisphere per case) from 7 patients with autism (4 men, 3 women; mean age 12.1 ± 2.8 years; mean ± SEM) and 10 matched controls (8 men, 2 women; mean age 30.1 ± 7.5 years) were analyzed (Table 1). The relevant clinical data are shown in Table 3; more clinical data of these patients are provided elsewhere (Van Kooten et al., 2008). The patients with autism did not differ from the controls with respect to mean age (Student's two-tailed *t* test; $t_{(15)} = 1.917$, $p = 0.07$), mean postmortem interval ($t_{(15)} = 0.0423$, $p = 0.967$), and mean fixation time ($t_{(15)} = 1.296$, $p = 0.215$).

The patients with autism A1-A3 and A5-A7 and the control cases C_A25-C_A30 were the same cases that had been investigated in our previous studies for alterations in the modular organization of cellular microdomains (minicolumns) in the prefrontal, primary motor, primary sensory, and primary visual cortex (Casanova et al., 2006). Furthermore, the patients with autism A1-A7 and the control cases C_A25-C_A34 were the same cases that had been investigated in another study of neuronal alterations in the fusiform gyrus (Van Kooten et al., 2008). All patients with autism met the Diagnostic Statistical Manual, 4th revision (DSM-IV) (American Psychiatric Association, 1994) and Autism Diagnostic Interview (Lord et al., 1994) criteria of autism, and none of them exhibited any chromosomal abnormalities. In all cases, autopsy was performed after informed consent had been obtained from a relative. The use of these autopsy cases for scientific investigations was approved by the relevant Institutional Review Boards. Except for the tissue provided by the Morphologic Brain Research Unit, University of Wuerzburg (Wuerzburg, Germany; UWMBRU), allocation of tissue was officially approved by the Tissue Advisory Board (TAB) of the US-Autism Tissue Program (ATP). Clinical records were available for all cases.

Tissue processing

For the patients with schizophrenia S1-S13 and the control cases C_S1-C_S13, the brainstem with the cerebellum was cut at the level of the rostral pons, and the hemispheres were divided mediosagittally. Brains were then fixed by immersion in 10% formalin (1 part commercial 40% aqueous formaldehyde in 9 parts H2O) prior to histological processing (fixation and tissue processing was performed at UWMBRU). Both hemispheres were then cut into serial 440- to 500-µm-thick coronal sections as previously described (Kreczmanski et al., 2007). Briefly, the hemispheres were cryoprotected in a mixture of glycerol-dimethylsulfoxide-formalin after careful removing of the meninges and the pial vessels, embedded in gelatin, deeply frozen at -60°C, and serially sectioned using a cryomicrotome (Jung, Nussloch, Germany). One brain (control case CS7) was embedded in celloidin as described earlier (Heinsen et al., 2000) and was cut into serial 440 µm-thick coronal sections using a sliding microtome (Polycut, Cambridge Instruments, UK). Sections were stored in formalin for up to 10 years. From all brains of the patients with schizophrenia and all control cases older than 40 years, sections through the central portion of the entorhinal and transentorhinal cortex that were not stained with Gallocyanin were labeled with the Gallyas method to detect

Table 3. Clinical characteristics and predominant type of von Economo neurons (VENs) in the anterior cingulate cortex and frontoinsular cortex of the patients with autism and the related controls investigated in the present study.

No	ATP no.	Age [y]	S	H	Cause of death	PMI [h]	Fix [d]	VEN ACC	VEN FI
A1	425-02	4	M	l	Drowning	30	4560	2	1
A2	443-02	5	F	l	Car accident	13	1568	1	1
A3	M5-03	8	M	r	Sarcoma	22	196	1	1
A4	427-02	11	F	l	Seizure prior to drowning	13	311	1	2
A5	445-02	13	M	l	Seizures	8	75	2	1
A6	M1-03	21	F	r	Obstructive pulmonary disease	50	136	1	1
A7	93-01	23	M	r	Drowning	14	505	1	1
C_A25	--	4	M	l	Myocardial infarct	3	67	1	1
C_A26	426-02	4	F	r	Lymphocytic myocarditis	21	233	1	2
C_A27	--	7	F	r	Status asthmaticus	74	1290	1	1
C_A28	M9-03	14	M	r	Electrocution	20	1067	2	1
C_A29	444-02	23	M	r	Ruptured spleen	6	95	1	2
C_A30	--	25	M	r	Cardiac tamponade	14	89	1	1
C_A31	M10-03	48	M	l	Atherosclerotic heart disease	24	215	2	1
C_A32	M14-03	52	M	r	Atherosclerotic cardiovascular disease	13	158	1	1
C_A33	M11-03	59	M	l	Cardiac arrest	24	266	1	1
C_A34	--	65	M	l	Bronchpneumonia	19	85	2	1

A, patient with autism; C_A, control for the autism sample. ATP no., original brain bank numbers of the U.S. Autism Tissue Program (ATP) (the controls C_A25, C_A27, C_A30 and C_A34 were not provided by ATP). y, years. S, sex; M, male; F, female. H, hemisphere; l, left; r, right; PMI, postmortem interval (i.e., time between death and autopsy); h, hours. Fix, fixation time; d, days. VEN, predominant type of VENs in the anterior cingulate cortex (ACC) and frontoinsular cortex (FI). VEN 1, regularly shaped VENs (Type-1-VENs) predominating; VEN 2, irregularly shaped VENs (Type-2-VENs) predominating. A Fisher's exact test showed no significant difference between the patients with autism and the controls with respect to the predominant type of VENs in the ACC and FI.

neurofibrillary changes (Heinsen et al., 1989). Neurofibrillary tangles were very rarely detected in the transentorhinal and entorhinal cortex on Gallyas stained sections, compatible with Braaks stage I (Braak and Braak, 1995). Furthermore, each section was coded and controlled for the absence of tumors, infarcts, heterotopias, signs of autolysis, staining artifacts, and gliosis. For the patients with schizophrenia S14-S24 and the control cases C_S14-C_S24, the brain specimens obtained at autopsy were divided in half along the midsagittal plane. The left hemispheres were dissected fresh and subjected to snap-freezing and storage for use in biochemical, molecular and other studies requiring unfixed tissues. The right hemispheres were placed in freshly prepared chilled 4% paraformaldehyde in phosphate buffer (4°C, pH 7.4). Following 7-10 days in this fixative the hemibrain specimens were placed in phosphate buffer and blocked coronally at regular intervals using a multi-blade knife specially designed for a stereology-oriented brain bank as previously described (Perl et al., 2000; Hof et al., 2003). None of these cases showed significant accumulation of neurofibrillary tangles beyond Braak's stage I on paraffin sections stained with Bielchowsky and hematoxylin-eosin. Brains S14-S18 and C_S14-C_S18 were used for investigating the ACC, and brains S19-S24 and C_S19-C_S24 were used for investigating the FI. Different brains were used for ACC and FI studies due to availability and integrity of the materials. For morphologic analyses of the ACC, alternate blocks were serially sectioned at 50 µm thickness on a vibratome through the entire block, maintaining the order of the resultant sections (Hof et al., 2003). The FI samples were dissected out from the block directly posterior to the genu of the corpus callosum and cut at 50 µm on a cryostat. Several sections were mounted on gelatin-coated slides.

For the patients with autism A1-A7 and the control cases C_A25-C_A34, the brains were divided mediosagittally. Either the left or the right hemisphere was available for each case (see Table 3). After immersion-fixation in 10% formalin for at least 3 months, the selected hemispheres were embedded in celloidin and cut into complete series of 200 µm-thick coronal sections as previously described (Heinsen et al., 2000) (All steps were performed at the New York State Institute for Basic Research in Developmental Disabilities, Staten Island, NY, USA.) Every third section was shipped to UWMBRU. The hemispheres provided by UWMBRU were cut at a 500 µm thickness, and every other section was selected. These differences in section thickness did not influence the outcome of this study.

Histology

Sections of the brains from the patients with schizophrenia S1-S13, the patients with autism A1-A7, and the control cases C_S1-C_S13 and C_A25-C_A34, respectively, were stained with Gallocyanin, mounted, and coverslipped as described (Heinsen and Heinsen, 1991). Sections from the patients with schizophrenia S14-S18 and the control cases C_S14-C_S18 were dehydrated, permeabilized with chloroform, rehydrated, and stained with a mixture of 0.1% thionin and cresyl violet (2:1 vol/vol). After dehydration, the section were coverslipped using DPX (Fluka, Buchs, Switzerland). Sections from the patients with schizophrenia S19-S24 and the control cases C_S19-C_S24 were stained with cresyl violet according to the protocol described above, in which the mixture of thionin and cresyl violet was replaced by cresyl violet (0.1%, 6 min) only.

Microscopy

ACC and FI were identified on all sections showing these regions according to anatomical landmarks and cytoarchitectural criteria (Fig. 1). The ACC, lying immediately superior to and along the corpus callosum, consists of Brodmann's areas 24, 33, and 25, which can be further subdivided by functional, cytoarchitectural, and immunohistochemical criteria (Vogt et al., 1995; Nimchinsky et al., 1997; Gittins and Harrison, 2004, 2004b). Area 24 of the ACC can be differentiated from area 23 in the posterior cingulate cortex by the presence of a cortical layer IV in area 23. Area 24 can be further divided into areas 24a, 24b and 24c by Nissl staining patterns that reveal distinct cell types, including VENs. VENs exhibit a ventral-to-dorsal density gradient within the ACC, but have similar morphology across the three subdivisions of the ACC (Nimchinsky et al., 1995, 1997, 1999; Vogt et al., 1995). The FI is buried in the anterior-most portion of the lateral fissure and abuts the posterior aspect of the orbitofrontal plane laterally. It is the region known as the limen insulae which continues posteriorly into the anterior agranular insular cortex (Von Economo, 1929). Microscopically, the FI is an agranular cortex showing a sparse layer II creating an irregular appearance, and a complete absence of layer IV.

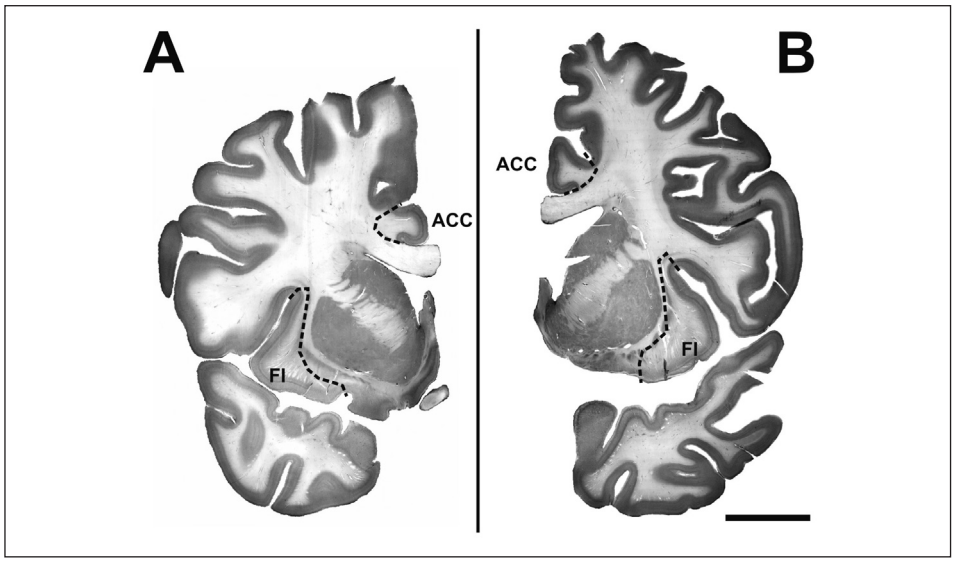

Figure 1. Representative photomicrographs of 500 µm-thick coronal sections from a control (A) and a patient with schizophrenia (B), showing the entire hemisphere, the anterior cingulate cortex (ACC), and the frontoinsular cortex (FI). Scale bar = 20 mm.

Regularly shaped VENs (henceforth referred to as Type-1-VENs) were easily distinguishable and morphologically different from pyramidal neurons based on their very elongate, gradually tapering, large size soma with single large apical and basal dendrites, and no radial arborization (Fig. 2 A-E) (Nimchinsky et al., 1995, 1999). Type-1-VENs have a radial orientation and show very sparsely branching dendritic trees with symmetric apical and basal projections. In addition, Type-1-VENs have a large apical dendrite extending toward the pial surface of the cortex and a single large basal dendrite extending toward the underlying white matter (Nimchinsky et al., 1995, 1999; Watson et al., 2006). Type-1-VENs in the ACC were usually found in layer V, although a small number of them occurred in deep layer III as well. In addition, layer VI exhibited many small spindle-shaped or fusiform vertical and horizontal neurons, which were morphologically different from Type-1-VENs. However, our region of interest included only layer Vb of the ACC and FI. The Type-1-VENs were symmetric about their horizontal and vertical axes. In addition, Type-1-VENs were frequently larger than the neighboring pyramidal cells located in layer V of both ACC and FI (Fig. 2 F-H), and much larger than the small fusiform neurons of layer VI.

Pyramidal cells in layer V of both ACC and FI showed a pyramid-shaped cell body and an apical dendrite emerging from its apex oriented perpendicular to the cortical surface (Fig. 2 F-H). In addition, pyramidal cells usually exhibit several basal dendrites (instead of one basal dendrite in case of the Type-1-VENs) that arise from the basal aspect of the cell body, running horizontally and parallel to the cortical surface.

We observed VENs in layer Vb of the ACC and FI that did not conform to the criteria above (henceforth referred to as Type-2-VENs). These Type-2-VENs were shorter, showed only their basal or apical dendrite and had usually a curved soma (Fig. 2 L-P). Type-2-VENs could easily be distinguished from Type-1-VENs, pyramidal cells, glial cells (Fig. 2 I), and endothelial cells (Fig. 2 K).

The differentiation between Type-1-VENs, Type-2-VENs, pyramidal cells, glial cells, and endothelial cells was performed by I.A.J.v.K and D.S. who were blind to the clinical diagnosis until all brains were analyzed, and was independently cross-evaluated by P.R.H., C.S. and H.H. We did not quantitatively investigate inter-rater and intra-rater reliabilities because in almost all cases the classification of a VEN as either Type-1-VEN or Type-2-VEN was unambiguous to all observers (as shown in Fig. 2). Ambiguous morphologies of single VENs were discussed jointly at a discussion microscope or on photomicrographs of the sections.

For each brain from the patients with schizophrenia S1-S24, the patients with autism A1-A7 and the control cases C_S1-C_S24 and C_A25–C_A34, respectively, the ACC and FI were divided into subseries containing 10 sections per each region. Furthermore, for each brain from the patients with schizophrenia, the patients with autism, and the controls, the morphology of 200 randomly selected VENs distributed throughout these 10 selected sections of the ACC and FI were investigated. These 200 VENs were sampled from the entire extent of the ACC and the FI. Each brain was classified as showing predominantly either Type-1-VENs or Type-2-VENS, respectively, when more than 80% of the 200 investigated VENs showed the corresponding morphology (this was the case in all investigated brains; Fig. 3). When repeating the analysis in the FI, tissue from the patients with schizophrenia S19-S24 and the controls C_S19-C_S24 were not in optimal condition for this kind of analysis. Instead, all identifiable VENs were classified as either Type-1-VENs or Type-2-VENs, respectively. The analysis was performed separately for the ACC and the FI. This analysis resulted in four groups for the schizophrenia sample (i.e., S-VEN1 [brain from a patient with schizophrenia with Type-1-VENs

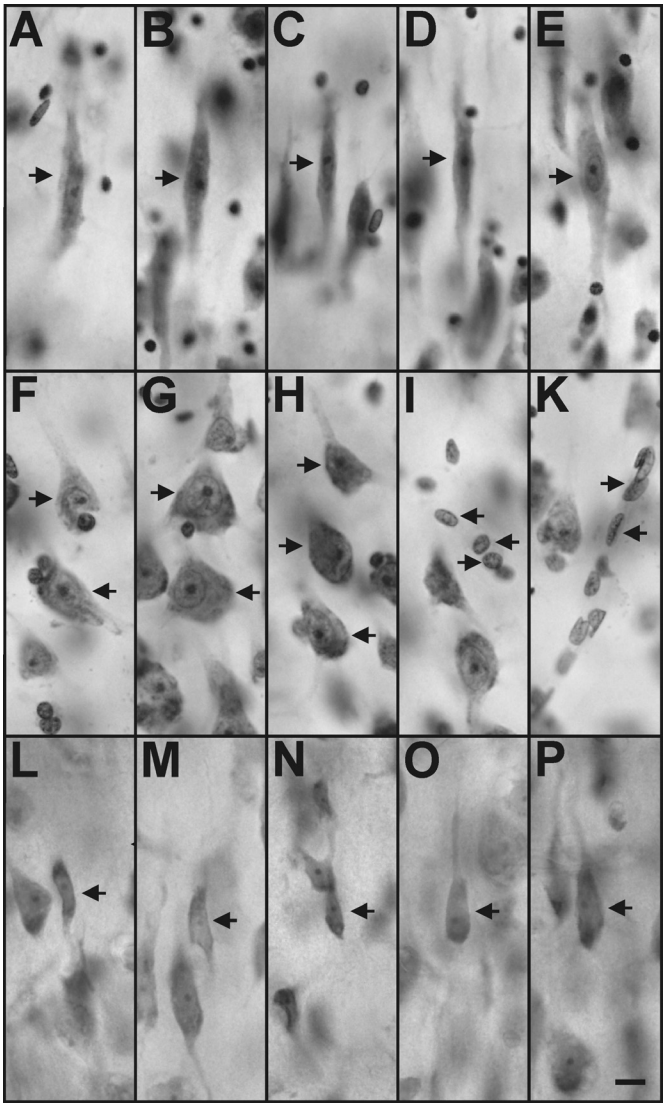

Figure 2. Representative high-power photomicrographs of 200 µm-thick coronal sections from different human brains. The arrows point to neurons (or to glial and endothelial cells in I and K, respectively) in layer Vb of the ACC. A to E, regularly shaped VENs (Type-1-VENs); F to H, pyramidal cells; I, glial cells; K, endothelial cells; L to P, irregularly shaped VENs (Type-2-VENs). Scale bar = 25 µm.

predominating], S-VEN2 [brain from a patient with schizophrenia with Type-2-VENs predominating], C_S-VEN1 [brain from a control in the schizophrenia sample with Type-1-VENs predominating] and C_S-VEN2 [brain from a control in the schizophrenia sample with Type-2-VENs predominating], respectively) as well as in four corresponding groups for the autism sample (i.e., A-VEN1, A-VEN2, C_A-VEN1 and C_A-VEN2, respectively).

Photography

Photomicrographs shown in Fig. 1 were produced by digital photography using a MBF Bioscience Stereo Investigator system (MBF Bioscience; Williston, VT), consisting of a modified Olympus BX51 microscope (Olympus, Tokyo, Japan) with Olympus UPlanSApo objective (4×, numerical aperture [N.A.] = 0.16), three-axis high-accuracy computer-controlled stepping motor specimen stage (4x4 Grid Encoded Stage; Ludl Electronic Products, Hawthorne, NY), linear z-axis position encoder (Ludl), CCD camera (MBF-CX9000; MBF Bioscience) and controlling software (MBF Bioscience). On average approximately 170 images were captured for the composite in each Fig. 1A and B. These images were made into one montage using the Virtual Slice module of the StereoInvestigator software (MBF Bioscience; Williston, VT). Photomicrographs depicted in Figs. 2 and 3 were captured with an Olympus DP 70 digital camera attached to an Olympus AX 70 microscope and cellP software (version 2.3; Soft Imaging System, Münster, Germany). The final figures were constructed using Corel Photo-Paint v.11 and Corel Draw v.11 (Corel, Ottawa, Canada). Only minor adjustments of contrast and brightness were made, without altering the appearance of the original materials.

Statistical analysis

For the patients with schizophrenia and the related controls as well as for the patients with autism and the related controls, mean and standard error of the mean of the patients' age, postmortem interval, and fixation time were calculated for each group, and differences between groups were tested with two-way ANOVA. Then, Fisher's exact test was used to test for a significant difference between either the patients with schizophrenia and the related controls or between the patients with autism and the related controls with respect to the predominant type of VENs in the ACC and FI (i.e., among the groups S-VEN1, S-VEN2, C_S-VEN1 and C_S-VEN2, and among the groups

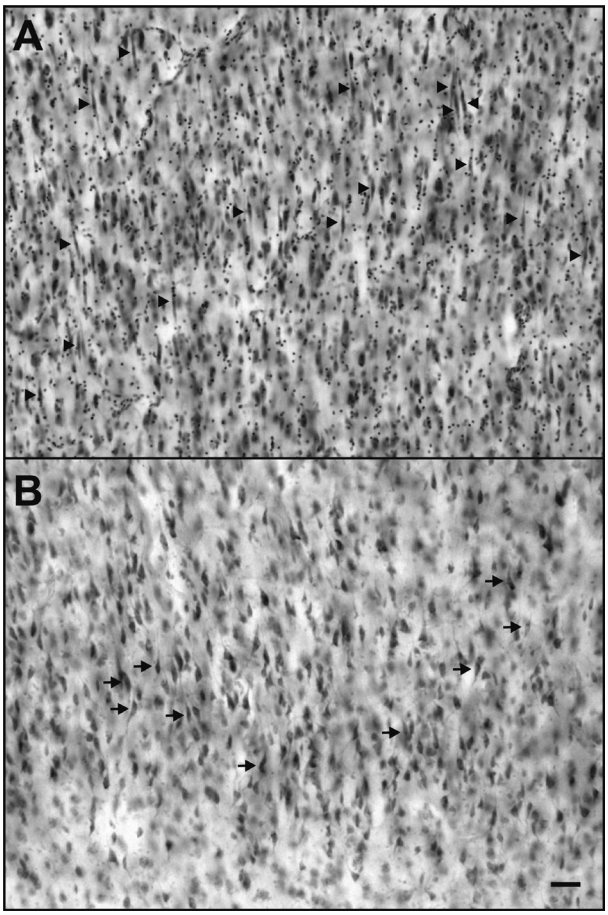

Figure 3. Representative medium-power photomicrographs of 200 μm-thick coronal sections showing layer V of the ACC. A, section from the patient with autism A2. Almost all VENs are Type-1-VENs (arrowheads). B, section from the patient with autism A1. Here, almost all VENs are Type-2-VENs (arrows). Scale bar = 25 μm

A-VEN1, A-VEN2, C_A-VEN1 and C_A-VEN2, respectively). In all analyses an effect was considered statistically significant if its associated P value was smaller than 0.05. All calculations were performed using GraphPad Prism version 4.00 for Windows (GraphPad Software, San Diego, CA, USA).

Results

VEN morphology

Compared to the controls, the patients with schizophrenia showed a significant difference with respect to the predominant type of VENs both in the ACC ($p < 0.001$) and in the FI ($p < 0.001$). In both the ACC and FI, the control cases in the schizophrenia sample mainly showed Type-1-VENs, whereas Type-2-VENs were present mainly in the brains from the patients with schizophrenia. However, patients with schizophrenia S2, S5, S6, and S15 showed predominantly Type-1-VENs in the ACC, whereas the controls C_S4, C_S7, and C_S8 exhibited predominantly Type-2-VENs (Table 2, Fig. 4). Furthermore, the patients with schizophrenia S1, S3, S5, S9, and S12 showed predominantly Type-1-VENs in the FI, whereas the controls C_S7 and C_S13 exhibited predominantly Type-2-VENs in the FI (Table 2, Fig. 4).

The patients with autism did not differ significantly from the related controls with respect to the predominant type of VENs in the ACC ($p = 1.000$) and the FI ($p = 1.000$). Rather, both the patients with autism and the related controls showed predominantly Type-1-VENs in the ACC and FI (Table 3). Furthermore, no significant differences were found with respect to the predominant type of VENs in the ACC and FI when the patients with autism were compared to all controls investigated in the present study (i.e., C_S1-C_S24 and C_A25-C_A34) ($p = 0.648$ in case of the ACC and $p = 1.000$ in case of the FI). Nevertheless, the patients with autism A1 and A5 as well as the control cases C_A28, C_A31 and C_A34 showed predominantly Type-2-VENs in the ACC, whereas patient A4 and the control cases C_A26 and C_A29 displayed predominantly Type-2-VENs in the FI (Table 2).

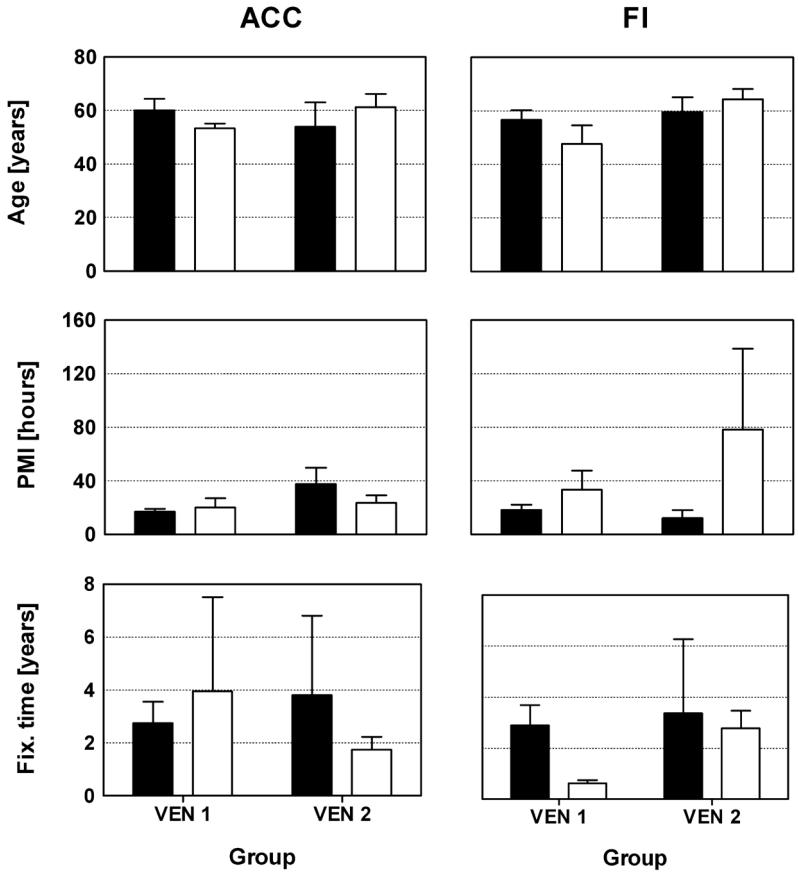

Figure 4. Predominant type of von Economo neurons (VENs) in the anterior cingulate cortex (ACC) (n=18) and frontoinsular cortex (FI) (n = 19) of patients with schizophrenia (open bars) and age-matched controls (ACC, n = 18 controls; FI, n = 19 controls) (closed bars) as a function of the patients' age (upper panel), the postmortem interval (medial panel), and the fixation time (lower panel). VEN1, brains with regularly shaped VENs (Type-1-VENs) predominating; VEN2, brains with irregularly shaped VENs (Type-2-VENs) predominating. Two-way ANOVA did not show significant differences between the groups.

Influence of age, postmortem interval and fixation time on VEN morphology
For the schizophrenia sample, two-way ANOVA showed that the four groups (i.e., S-VEN1, S-VEN2, C_S-VEN1, and C_S-VEN2) in both ACC and FI did not differ with respect to the mean age of the patients, mean postmortem interval, and mean fixation time ($p > 0.05$ for all investigated variables; Fig. 4). In contrast, the four groups of the autism sample (i.e., A-VEN1, A-VEN2, C_A-VEN1 and C_A-VEN2) showed a significant effect of the individuals' age on the VEN morphology ($F_{(1)} = 4.742$ [one degree of freedom]; $p = 0.049$). However, Bonferroni post hoc tests revealed that neither in the VEN1 groups (i.e., A-VEN1 and C_A-VEN1) nor the VEN2 groups (i.e., A-VEN2 and C_A-VEN2) was the mean age of the patients with autism significantly different compared to the mean age of the corresponding controls ($p > 0.05$). Accordingly, within the groups (i.e., VEN1 and VEN2) the patients with autism did not differ significantly with respect to age compared to the corresponding controls. Furthermore, no significant effect was found among the four groups (i.e., A-VEN1, A-VEN2, C_A-VEN1 and C_A-VEN2) in either ACC or FI with respect to the mean postmortem interval and the mean fixation time ($p > 0.05$ for all investigated variables; Fig. 5). Finally, it should be mentioned that the results obtained on the brains from the patients with autism with a history of seizures (A4 to A6) showed no systematic deviation from those without a history of seizures (see also Van Kooten et al. (2008) for the clinical data of these patients).

Discussion
In the present study, the morphology of VENs in the ACC and FI was compared between patients with schizophrenia and matched controls as well as between patients with autism and matched controls. We observed that the patients with schizophrenia showed a significant difference in the predominant morphologic type of VENs in both cortical regions compared to the corresponding controls. This significant difference was not found in the postmortem brains from the patients with autism compared to the corresponding controls. In addition, age, the postmortem interval, and the fixation time had no influence on the morphology of the VENs in either ACC or FI in the postmortem brains from the patients with schizophrenia and autism compared to the relevant controls. This suggests that Type-2-VENs represent a morphological variant of this neuron type, that can be observed in some normal brains as well as in some patients with autism, but that is far more prevalent in schizophrenia.

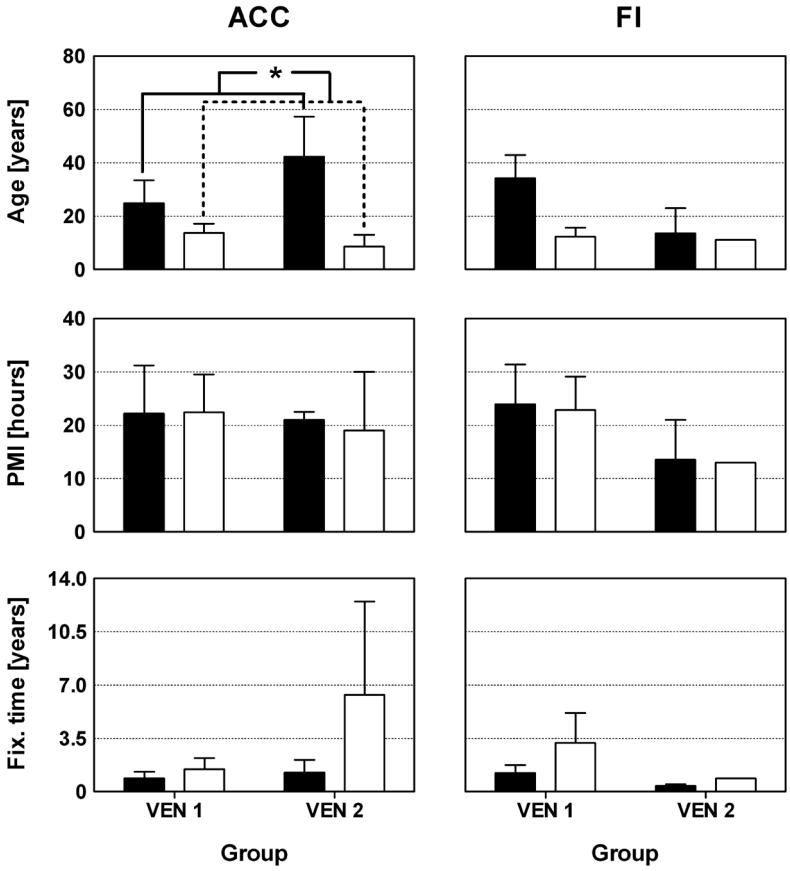

Figure 5. Predominant type of von Economo neurons (VENs) in the anterior cingulate cortex (ACC) and frontoinsular cortex (FI) of 7 patients with autism (open bars) and 10 matched controls (closed bars) as a function of the patients' age (upper panel), the postmortem interval (medial panel), and the fixation time (lower panel). VEN1, brains with regularly shaped VENs (Type-1-VENs) predominating; VEN2, brains with irregularly shaped VENs (Type-2-VENs) predominating. Two-way ANOVA showed only a significant effect for diagnosis when testing the effect of the persons' age on the type of VEN predominating in the ACC (upper left panel; *, $p = 0.049$). However, Bonferroni post-hoc tests revealed that neither in the VEN1 groups (i.e., A-VEN1 and C_A-VEN1) nor the VEN2 groups (i.e., A-VEN2 and C_A-VEN2) was mean age of the patients with autism significantly different compared to the mean age of the corresponding controls ($p > 0.05$).

Substantial evidence indicates that the ACC and FI are abnormal in schizophrenia and autism. Functional neuroimaging studies on patients with schizophrenia showed abnormalities in ACC activation during specific cognitive tasks (Carter et al., 1997, 2001; Artiges et al., 2000; Meyer-Lindenberg et al., 2001; Yucel et al., 2002) in addition to decreases in ACC dopamine activation (Dolan et al., 1995), glucose metabolism (Haznedar et al., 1997a), regional cerebral metabolism (Liddle et al., 1992), and cerebral blood flow (Tamminga et al., 1992). At the morphologic level, data are inconsistent with respect to overall and bilateral volume of the ACC as well as asymmetry of the ACC (Noga et al., 1995; Suzuki et al., 2002). However, cytoarchitectonic disturbances in layer II and a decreased density of non-pyramidal neurons in the ACC have been found in postmortem brains from patients with schizophrenia compared to controls (Benes et al., 2001). With respect to the FI, neuroimaging studies using voxel based morphometry demonstrated a reduced gray matter volume in either the left (Crespo-Facorro et al., 2000; Sigmundsson et al., 2001), right (Duggal et al., 2005), or bilateral FI (Hulshoff Pol et al., 2001; Makris et al., 2006). Furthermore, the FI of patients with schizophrenia failed to activate during a verbal memory test (Crespo-Facorro et al., 2000), a verbal fluency test (Curtis et al., 1998), and an experiment to modulate the subject's degree of movement control (Farrer et al., 2004). In the present study, the patients with schizophrenia mainly showed the irregularly shaped VENs (i.e., Type-2-VENs) in both the ACC and FI. This may cause dysfunction of the VENs in the ACC and FI which could in turn be related to cognitive deficits thought to be responsible for some of the clinical symptoms seen in schizophrenia (Sanders et al., 2002). In addition, the FI is connected to, among others, the caudate-putamen, amygdala, thalamus, and ACC, regions that have all been implicated to be abnormal in patients with schizophrenia (Kim et al., 2007; Kreczmanski et al., 2007; Wang et al., 2007)

VENs are suspected to be large-scale cortical integrators that coordinate widely distributed neural activity involving emotion and cognition (Allman et al., 2001). Normal VENs have apical dendrites similar to those of the neighbouring pyramidal cells, but their basal dendritic pattern is simpler (Allman et al., 2005). VENs are known to be projection neurons (Nimchinsky et al., 1995), and likely have large, rapidly conducting axons which may provide a rapid relay to other parts of the brain of a simple signal derived from information processed within the ACC and FI. Thus, VENs might play a

role in fast adjustment of behavior in quickly changing situations (Allman et al., 2005). ACC and FI are connected to prefrontal, orbitofrontal, insular, and anterior temporal cortices, the amygdala, hypothalamus, various thalamic nuclei and the periaqueductal grey (Allman et al., 2005). In the present study, we found predominantly irregularly shaped VENs in both the ACC and FI in patients with schizophrenia. It has been suggested that VENs may contribute to schizophrenic dysfunction and disorganization via aberrant structure or connectivity (Sanders et al., 2002). The frequently blunted and shorter apical or basal dendrites of VENs in both the ACC and FI in postmortem brains from patients with schizophrenia suggest that such alterations may result in significant functional abnormalities of these particular neurons. However, as a postmortem study cannot determine the functional consequences of abnormal neuronal morphology, the present data provide an excellent opportunity to design further quantitative analysis of the dendritic defects of VENs in schizophrenia. It must also be kept in mind that long-term exposure to neuroleptics may have influenced the morphology of VENs in the schizophrenic samples. Whereas this is a common confound in neuropathologic studies of schizophrenia, it is unlikely to have played a role in this study as Type-2-VENs were observed in some control brains and in some patients with autism who had never been exposed to neuroleptics, arguing in favor of the specificity of these observations.

Reduced volume, decreased metabolism and blood flow, and an abnormal lamination pattern have been found in the ACC of patients with autism (Kemper and Bauman, 1993; Haznedar et al., 1997b; Ohnishi et al., 2000). In addition, functional imaging studies demonstrated that the right FI was not activated when patients with autism were asked to discriminate the mental states of individuals depicted on photographs (Baron-Cohen et al., 1999). Additionally, measures of embarrassment and empathy, processes involving both the ACC and FI, are reduced in patients with autism (Capps et al., 1992; Yirmiya et al., 1992; Baron-Cohen and Wheelwright, 2004). It has also been suggested that VENs fail to develop normally in autism and that this failure might be partially responsible for the associated social disabilities that result from abnormal fast intuition in autism (Allman et al., 2005). In the present study, we did not find a predominant type of VENs in the ACC or the FI in the brains from patients with autism compared to matched controls. This is in line with a recent study by Kennedy et al. (2007) that found no alterations in the mean number of VENs in the FI of three patients with autism compared to

five controls. It is, nevertheless, worth noting that in the present study, three patients with autism did show predominantly the irregularly shaped VENs (Type-2-VENs) in either the ACC or the FI whereas the other patients with autism did not (Table 3). However, the irregularly shaped VENs in the brains from these three patients with autism were not linked to special features in the clinical records (such as history of seizures, etc.) or to the patients' age, the PMI or the fixation time. Despite the relatively small size of the autism sample, it should be mentioned that there were also no significant differences between the predominant type of VENs when the patients with autism were compared to all controls investigated in the present study (i.e., the controls from the schizophrenia sample and the autism sample).

An important question in schizophrenia and autism is what role VENs play during development. Hayashi et al. (2001) demonstrated VENs at embryonic day 224 in a fetal chimpanzee brain. In humans, Allman et al. (2005) found a few VENs in the 35th week of gestation. At birth only about 15% of the number of VENs found in the adult brain is present, the adult number being stabilized by the age of 4 years. This postnatal increase in the number of VENs suggests an increased differentiation from pre-existing cell types or migration from a potentially proliferative zone in the ventricles. In addition, some VENs in the brains from 4-8 month-old infants showed elongated, undulating leading and trailing processes that are specific characteristics of migrating neurons (O'Rourke et al., 1992; Lois and Alvarez-Buylla, 1994). VENs appear to migrate into the ACC several months after birth (Allman et al., 2002). Nevertheless, it is possible that VENs are present during earlier stages of development but are not yet detectable because they still need to acquire their final shape (Allman et al., 2002). It has been hypothesized that disturbance of the emergence of VENs during postnatal development may have dysfunctional consequences related to psychiatric diseases such as schizophrenia (Allman et al., 2005).

Several authors have proposed a neurodevelopmental origin for schizophrenia (Lewis and Levitt, 2002; Murray et al., 2004) and autism (Piven et al., 1990; Bailey et al., 1998; Gillberg, 1999). With respect to the timing of the neuropathological abnormalities, some authors have suggested a prenatal origin of schizophrenia, most likely during the second trimester of pregnancy (Adams et al., 1993; McGrath et al., 1994), whereas autism may either develop during the first trimester of pregnancy (Gillberg, 1999) or have a postnatal basis (Gillberg, 1999; Kern, 2003). This may imply that precursors

of VENs are selectively vulnerable during the second trimester of pregnancy and that the emergence of VENs can be disrupted causing dysfunctional consequences related to the development of schizophrenia and to autism in some patients. In this context, it will also be important to analyze, with rigorous stereologic methods, possible differences in the number of VENs in schizophrenia and autism, as well as their spatial distribution in ACC and FI. It would also be highly relevant to validate the hypothesis that the precursors of VENs, assuming they could be identified, are selectively vulnerable during the second trimester of pregnancy. However, as VENs seem to be specific to only a few mammalian species, such as humans, great apes, and cetaceans (Allman et al., 2005; Hof and Van der Gucht, 2007) it is not possible to test this hypothesis in rodent or nonhuman primate models of schizophrenia and autism.

In conclusion, VENs appear to represent a neuronal subclass with a restricted morphology showing vulnerability within the ACC and FI of patients with schizophrenia as well as in some patients with autism. As VENs are involved in emotion, social behaviors, and high-level cognitive functions, our findings suggest that a specific dysfunction and disorganization of VEN structure and connectivity may contribute to the symptoms of schizophrenia and, at least in some cases, autism.

Chapter 7

Consequences of maternal infection: cytoarchitectonic abnormalities in the offspring of mice exposed to influenza virus

Van Kooten IAJ, Shi L, Burks I, Sierksma ASR, Hof PR, Steinbusch HWM, Van Engeland H, Patterson PH, Schmitz C.

In preparation for submission

Abstract

Autism is a neurodevelopmental disorder conditioned by both genetic and several known environmental risk factors, such as maternal viral infection. In addition, its onset of etiology is likely to occur during prenatal development. We propose that subjecting pregnant mice to human influenza virus on embryonic day (E) 9.5 will result in morphological alterations in the offsprings' entire hemisphere (HEMI), cortical grey matter (CGM) and the whole amygdala (AMG), as well as the lateral (LN) and basolateral nucleus (BLN) of the AMG, resembling alterations found in brains from patients with autism. Using a high precision design-based stereologic approach we investigated the mean total volume of the AMG, CGM and HEMI as well as mean total neuron numbers and neuron densities in the LN and BLN of exposed, sham-exposed and control offspring at postnatal (P)0, P25 and 3 months of age (M3). Compared to controls, we found that exposing pregnant mice to human influenza virus on E9.5 resulted in a delayed growth of the brain between P25 and M3, which is reflected in a significantly decreased mean volume of the CGM at P25. However, no difference in mean total neuron number and mean neuron density were seen in the LN and BLN at birth or during postnatal development. In addition, no signs of astrogliosis were observed in the brains of the exposed offspring. Although brain growth is altered in this animal model, exposure of pregnant mice to human influenza virus at E9.5 does not reproduce the entire neuropathology of autism with respect to the amygdala. This should be considered in the use of this model as animal model of autism.

Introduction

Autism is a neurodevelopmental disorder with both genetic and several known environmental risk factors (Glasson et al., 2004; Veenstra-Vanderweele et al., 2004; Hyman et al., 2006), including maternal infection (Patterson, 2002; Van Kooten et al., 2005b; Jonakait, 2007). Infection during human pregnancy is common with more than 10% of women experiencing an influenza infection during the second or third trimester (Irving et al., 2000). In addition, maternal viral infection has been associated with autism (Desmond et al., 1967; Rutter and Bartak, 1971; Chess, 1977; Stubbs et al., 1984; Singh et al., 1997; Barak et al., 1998). Regarding the timing of the neuropathology in autism, several authors have suggested a prenatal origin, most likely during the first six months of gestation (Piven et al., 1990; Rorke, 1994; Rodier et al., 1996; Bauman et al., 1997; Courchesne, 1997; Bailey et al., 1998; Gillberg, 1999; see also Glasson et al., 2004). On the other hand, some children with autism do not show obvious behavioral symptoms until a substantial period after birth (Kern, 2003). Accordingly, it was suggested that some children might become autistic from postnatal neuronal cell death or brain damage as a result of injuries (Kern, 2003).

Compared to age-matched controls, the total brain volume of children who eventually develop autism is normal or even smaller at birth. However, these children subsequently display abnormal brain overgrowth, which is followed by a slowing of growth during early childhood, leading to brain size equivalent to typical adults (Courchesne et al., 2001, 2003, 2004; Courchesne, 2004). In addition, the gray matter in the frontal and temporal lobes and the amygdala (AMG) display peak overgrowth in 2-4 year old children with autism (Schumann et al., 2004; Courchesne et al., 2007). In postmortem brains from adults with autism, however, significantly fewer neurons have been found in the AMG overall and in its lateral nucleus (LN) (Schumann and Amaral, 2006). The molecular and cellular mechanisms underlying these morphologic abnormalities in the brains of patients with autism are unknown.

Several animal models of autism have been developed based on genetic, neurochemical, neurophysiological or behavioral manipulations (Van Kooten et al., 2005; Patterson, 2006; Moy and Nadler, 2008). Subjecting pregnant mice to human influenza virus on embryonic day (E) 9.5 and investigating the offspring of these mice for behavioral alterations and morphologic abnormalities in the brain is of particular interest in this regard (Patterson,

2002). These offspring display behaviors consistent with those found in patients with autism, including deficits in exploratory and social behavior, sensorimotor gating and pup-mother attachment (Shi et al., 2003; Patterson, 2005a). In terms of neuropathology, the finding that the offspring of infected dams display a regionally-restricted deficit in cerebellar Purkinje cells is the most relevant to autism (Shi et al., 2008). These offspring have also been reported to display macrocephaly, gliosis, increased pyramidal cell density and atrophy, decreased neurogenesis, reduced reelin immunoreactivity and reduced thickness of the neocortex (Fatemi et al., 1999, 2002a; Fatemi, 2005). However, the latter observations have not been confirmed applying rigorous, quantitative histologic techniques.

We have therefore examined the brains of mice born to dams infected with human influenza virus on E9.5 using a high-precision, design-based stereology approach. According to the known alterations in the brains of patients with autism (i.e., precocious enlargement followed by growth arrest of the entire brain and specifically the AMG) we focused our analysis on alterations of the mean volumes of the entire hemisphere (HEMI), the cortical gray matter (CGM), the entire AMG, the lateral (LN) and basolateral (BLN) of the AMG (shown in Fig. 1), as well as alterations in the mean total numbers and densities of neurons in the LN and the BLN. In addition, we searched for signs of astrogliosis in these brain regions by immunofluorescence detection of glial fibrillary acidic protein (GFAP). To cover the entire period of postnatal development we investigated offspring immediately after birth (postnatal day [P]0), at P25 and at 3 months of age (M3). The behavioral abnormality in prepulse inhibition that is related to autism was demonstrated in the M3 animals, as shown previously (Shi et al. 2003; Smith et al. 2007).

Materials and methods

Animals

C57/Bl6 mice were obtained from Jackson Laboratories (Bar Harbor, ME, USA) and bred in the California Institute of Technology animal facility for several generations before use. Pregnant mice were anesthetized intraperitoneally (i.p.) with 10 mg/kg xylazine and 50 mg/kg ketamine on E9.5 (plugged day is day 0) and inoculated intranasally with either 6000 plaque-forming units (PFU) of human influenza virus (Strain A/NWS/33CHINI virus collected from the supernatant of infected MDCK cells, titered, and stored at -80°C until use; the original strain was provided by Dr. R. Sidwell at the

Institute for Antiviral Research, Utah State University; Logan, UT, USA) in 90 µl phosphate buffered saline (PBS), or with PBS alone (sham-treatment), or received no treatment (control group). Five mice were included in each group. As the average litter-size in the infected group was about 4 per litter, offspring in sham and control groups were also reduced to 4 per litter. All offspring were separated from their dams 4 weeks after birth, and males and females were housed separately in groups of 2-4. All experiments were officially approved by the Office of Laboratory Animal Resources of the California Institute of Technology and followed the recommendations of the NIH guidelines for care and use of laboratory animals.

Immediately after birth (P0) one offspring per dam was randomly selected and killed by decapitation. On P25 and at M3, respectively, another offspring per group (P25: males only; M3: males or females) was killed by intracardial perfusion-fixation as described (Schmitz et al., 2004). General health conditions of the mice were controlled by daily inspection. Body weight was recorded at the day the animals were killed.

Prepulse inhibition

The M3 mice were tested at 8 weeks of age with the prepulse inhibition (PPI) assay to confirm that maternal infection had the expected effect in causing a behavioral abnormality in sensory gating that is related to autism (Shi et al., 2003; Smith et al., 2007). The PPI apparatus (San Diego Instruments, San Diego, CA, USA) consists of a sound-insulated chamber with a speaker mounted on the ceiling. The subject is restrained in a plexiglass cylinder inside the chamber, and a piezo-electric sensor is mounted beneath the restraining device to measure the startle response. After a 5 min acclimation period, the subject is presented with 6, 120 dB pulses of white noise. The subject is then presented with 14 blocks of four different trial types in a pseudo-random order. Trial types include P5P, where a pre-pulse of 5 dB above background (67 dB) precedes the startle stimulus by 100 ms, P15P in which the prepulse is 15 dB above background, startle stimulus alone, and no stimulus. Trials are averaged for each individual, and PPI is defined as PPI(X) = (Startle alone – PXP)/(Startle alone) where X = 5 or 15 dB above background.

Tissue processing

After opening the skull, the brains were removed, cut in the midsaggital line (P25 and M3 mice) and postfixed in 4% paraformaldehyde solution for

2 hrs at room temperature (RT) as described (Schmitz et al., 2004). Then, either the whole brain (P0 mice) or the left brain halves (P25 and M3 mice) were cryoprotected in sucrose solution (5%, 10%, 15% and 30% sucrose in 0.1M Tris-HCl buffer each; 24 hrs per solution at 4°C), quickly frozen with carbogen snow and stored at -80°C. Afterwards, the brains (or brain halves) were entirely cut into complete series of either 25 µm-thick (P0 mice) or 30 µm-thick (P25 and M3 mice) coronal sections on a cryostat (Leica CM 3050; Leica, Nussloch, Germany). The right brain halves of the P25 and M3 mice were stored for future analyses.

Stereological analysis

One series of every 4th (P0 mice), 5th (P25 mice) or 8th (M3 mice) section per animal was mounted on glass slides (Superfrost Plus, Menzel, Braunschweig, Germany), dried, defatted with Triton x-100 (0.025%; 20 min; Merck; Darmstadt, Germany) and stained with cresyl violet (0.01%, 13 min). Slides were mounted and coverslipped using DePeX (Serva, Heidelberg, Germany). Stereologic analyses were performed with a computerized stereology workstation, consisting of a modified light microscope (Olympus BX50 with PlanApo objective 1.25× [numerical aperture (N.A.) = 0.04] and UPlanApo objectives 10× [N.A. = 0.4] and 40× [oil; N.A. = 1.0]; Olympus, Tokyo, Japan), motorized specimen stage for automatic sampling (Ludl Electronics; Hawthorne, NY, USA), CCD color video camera (HV-C20AMP; Hitachi, Tokyo, Japan), and stereology software (StereoInvestigator; MBF Bioscience, Williston, VT, USA.

The following brain regions were identified on all sections showing these regions (Fig. 1): (i) the entire hemisphere (HEMI); (ii) the cortical gray matter (CGM); (iii) the whole amygdala (AMG); (iv) the of the amygdala (LN-AMG); and (v) the basolateral nucleus of the amygdala (BLN-AMG). The whole AMG, LN and BLN of the AMG were identified according to published anatomical landmarks and cytoarchitectonic criteria described in the literature (Pitkänen, 2000). Briefly, the lateral border was defined by the amygdalar capsule and the medial boundary by the external capsule. The divisions between the LN-AMG and BLN-AMG were made according to the standard atlas of the mouse brain by (Paxinos and

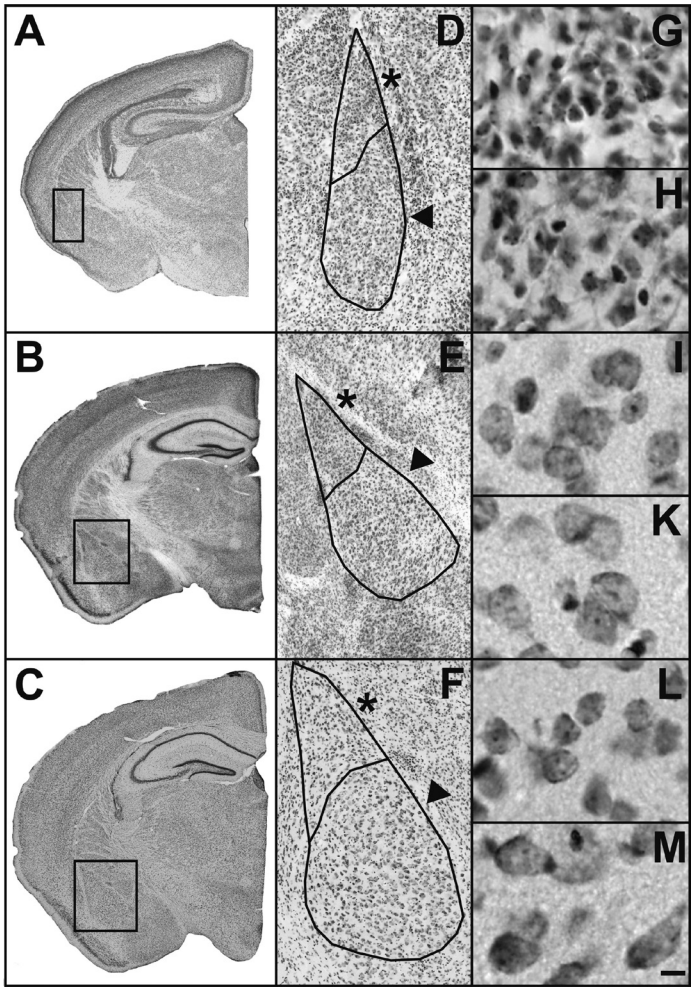

Figure 1. Representative photomicrographs of 25-µm thick (A,D,G,H) or 30-µm thick (B,C,E,F,I,K,L,M) coronal sections from control mouse brains stained with cresyl violet, showing the entire hemisphere (A-C), the lateral nucleus of the amygdala (LN) (asterisks in D-F), the basolateral nucleus of the amygdala (BLN) (arrowheads in D-F) as well as neurons within the LN (G,I,L) and the BLN (H,K,M). The pictures shown in A,D,G,H represent an animal that was killed at P0 (i.e. immediately after spontaneous delivery) whereas the pictures shown in B,E,I,K represent an animal that was killed at P25 and those shown in C,F,L,M an animal that was killed at M3. The small squares in A-C correspond to the positions of the high-power photomicrographs shown in D-F. The scale bar represents 500 µm in A-C, 175 µm in D-F and 25 µm in G-M.

Franklin, 2001). Identification and delineation of the boundaries of these regions was performed in a blind manner by I.A.J.v.K. and I.B. until all regions per animal were analyzed, and were independently cross-evaluated (and, if necessary, slightly modified) by C.S.

Volume measurements of all investigated brain regions were performed with Cavalieri's principle (Cavalieri, 1966; Schmitz and Hof, 2005) by (i) tracing their boundaries on all sections showing these regions imaged with the 10× objective on video images displayed on the monitor of the stereology workstation, (ii) determining the projection area of each region, (iii) summing up the data from all sections, and (iv) multiplying this value with the interval of selecting sections for staining with cresyl violet (as outlined above) and the average actual section thickness after tissue processing (determined with the stereology workstation).

Total neuron numbers in the LN and BLN were estimated with the Optical Fractionator (West et al., 1991; Schmitz and Hof, 2005). Briefly, all neurons whose nucleus came into focus within unbiased virtual counting spaces distributed in a systematic-random fashion throughout the delineated regions were counted. Neurons were differentiated from glial and endothelial cells by histologic criteria. Neurons showed a large cytoplasm and a prominent nucleolus within a pale nucleus. Glial cells were identified by the absence of cytoplasmic staining, intense staining of the nucleus with dispersed chromatin and lack of a nucleolus. Total neuron numbers were calculated from the numbers of counted neurons and the corresponding sampling probability. All details of the stereologic analysis procedures are summarized in Table 1.

Neuron densities were calculated as individual ratios of the total neuron number in a given brain region and the volume of this brain region.

Immunohistochemistry

Another series of every 4th (P0), 5th (P25) or 8th (M3) section per animal was collected for immunohistochemical detection of glial fibrillary acidic protein (GFAP). Briefly, the sections were mounted on glass slides (Superfrost Plus) and air-dried overnight. GFAP labeling was conducted by incubating the sections with primary antibody (rabbit anti-GFAP; 1:500; DAKO, Glostrup, Denmark) for 12 hrs after rinsing them with 0.01M Tris-buffered saline (TBS) and 0.01M TBS with 0.2% Triton X-100 (TBS-T). Following incubation and rinsing with 0.01M TBS and TBS-T the sections were incubated with a

Table 1. Details of the stereologic analysis procedures

			LN			BLN	
	Treatment group	P0	P25	M3	P0	P25	M3
Obj. 1	C, S and E	10x	10x	10x	10x	10x	10x
Obj. 2	C, S and E	100x	100x	100x	100x	100x	100x
sln-x, sln-y [µm]	C, S and E	45	70	90	45	90	100
a [µm^2]	C, S and E	18	30	65	20	45	65
h [µm]	C, S and E	18	30	45	20	45	45
d [µm]	C, S and E	6	6	6	6	6	6
∑UVCS	C	167	140	195	177	189	250
	S	173	160	184	236	197	204
	E	143	141	180	141	173	236
∑n	C	604	314	758	581	578	760
	S	534	353	645	503	576	674
	E	523	328	619	475	526	691
t [µm]	C	10.9	13.6	11.6	10.7	13.8	11.6
	S	10.9	12.7	13.9	11.0	12.8	14.0
	E	10.7	12.1	13.3	10.6	12.6	13.1
$CE_{pred.}$[n]	C	0.041	0,056	0.036	0.041	0.042	0.036
	S	0.043	0.053	0.039	0.045	0.042	0.039
	E	0.044	0.055	0.040	0.046	0.044	0.038

LN, lateral nucleus of the amygdala; BLN, basolateral nucleus of the amygdala. C, offspring of control dams; S, offspring of sham infected dams; E, offspring of dams exposed to human influenza virus A/NWS/33CHINI on embryonic day 9.5. P0, postnatal day 0; P25, postnatal day 25; M3, 3 months of age. Obj. 1, objective used for delineating the regions of interest; Obj. 2, objective used for counting neurons; sln-x and sln-y, distance between the unbiased virtual counting spaces used for counting neurons in mutually orthogonal directions x and y; a and h, base and height of the unbiased virtual counting spaces; d, depth within the section at which the unbiased virtual counting spaces were placed; ∑UVCS, average number of unbiased virtual counting spaces used per animal; ∑n, average number of neurons counted per animal; t, measured actual average section thickness after histological processing; $CE_{pred.}$[n], average predicted coefficient of error of the estimated total numbers of neurons using the prediction method described by Schmitz (1998) and Schmitz and Hof (2000).

fluorescent secondary IgG antibody (biotinylated donkey anti-rabbit IgG, 1:100; Jackson, West Grove, PA, USA) for 90 min. After rinsing with 0.01M TBS, the sections were stained with Hoechst (1:500, Sigma Chemical Co., St. Louis, MO, USA) for 30 min and mounted with 80% glycerol in TBS. All steps were carried out at 4ºC.

Statistical analysis

For each group of offspring from exposed, sham-exposed and control dams, mean and standard error of the mean (SEM) were calculated for all investigated variables. Volumes of brain regions were expressed as absolute values as well as relative values, i.e., related to the individual volume of the entire hemisphere. Comparisons between groups were perfomed with two-way ANOVA (with age and treatment as fixed factors) followed by Bonferroni post-hoc tests for pair-wise comparisons. Statistical significance was established at $p = 0.05$. Calculations were performed using SPSS (Version 15.0 for Windows; SPSS, Chicago, IL, USA) and GraphPad Prism (Version 4.0 for Windows, GraphPad software, San Diego, CA, USA).

Photography

Photomicrographs shown in Fig. 1A-F were produced by digital photography using the stereology workstation described above. On average approximately 115 images were captured for the composite in each Fig. 1A-C, and 60 images for the composite in each Fig. 1D-F. These images were made into one montage using the Virtual Slice module of the StereoInvestigator software. Photomicrographs shown in Fig. 1G-M were produced by digital photography using an Olympus DP 70 digital camera attached to an Olympus AX 70 microscope and cell^{P} software (version 2.3; Soft Imaging System, Münster, Germany). The final figures were constructed using Corel Photo-Paint v.11 and Corel Draw v.11 (Corel, Ottawa, Canada). Only minor adjustments of contrast and brightness were made, without altering the appearance of the original materials.

Results

Body weight

In all treatment groups, the mean body weight of the mice increased with age (Fig. 2). Two-way ANOVA showed a significant effect of the age of the animals ($p < 0.001$) but not of the treatment ($p = 0.089$) or the interaction between

age and treatment (p = 0.149). When testing for age-related differences within a given treatment group, Bonferroni post-hoc tests showed significant differences between P0 and P25, between P0 and M3 and between P25 and M3 for all treatment groups (p < 0.001 each). However, when testing for differences between the treatment groups at a given age, Bonferroni post-hoc tests showed a significant difference only at M3 between the offspring of the infected dams and the offspring of control dams (Controls [C]: 24.2 ± 2.0 g [mean ± SEM]; Exposed [E]: 28.5 ± 0.99 g; +15%; p < 0.05). Thus, exposing pregnant mice to human influenza virus on E9.5 resulted at M3 in a small increase in mean body weight of the offspring compared to offspring of control dams.

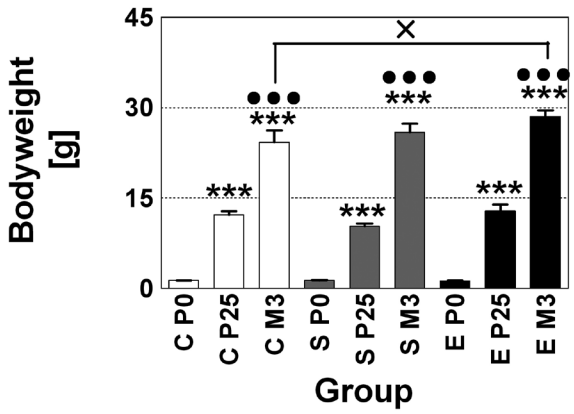

Figure 2. The body weights of the experimental groups are similar to controls. Mean and standard error of the mean of the bodyweight of offspring of dams exposed to human influenza virus on day E9.5 (Group E; closed bars), sham-exposed dams (Groups S; gray bars) or control dams (Group C; open bars) at postnatal day (P) 0, P25 and 3 months of age (M3). ***, p < 0.001 (compared to P0 within the same treatment group). •••, p < 0.001 (compared to P25 within the same treatment group). ×, p < 0.05 (between E and C at M3).

Prepulse inhibition

Although the dams given influenza virus displayed obvious sickness behavior (Shi et al., 2003), the M3 mice were tested at 8 weeks of age with the prepulse inhibition assay to confirm that maternal infection resulted in

the expected behavioral deficit. The values at 15 dB obtained for the control (sham infected plus naive controls) and maternal infection cohorts, were 59.18 ± 4.26 and 42.22 ± 2.55, respectively (n = 9 for each; p = 0.004 using Student's *t* test; details are provided in the results section of prepulse inhibition). These data confirm that exposure of dams to human influenza virus had the expected effect in causing a behavioral abnormality in sensory gating in the offspring that is related to autism (Shi et al., 2003; Smith et al., 2007).

Table 2. Results of statistical analysis (p values) with two-way ANOVA.

Variable	Brain region	P (Age)	P (Treatment)	P (Interaction)
Volume (absolute values)	HEMI	**< 0.001**	0.625	0.280
	CGM	**< 0.001**	0.067	0.068
	AMG	**< 0.001**	0.749	0.610
	LN	**< 0.001**	0.650	0.985
	BLN	**< 0.001**	0.702	0.296
Volume (relative values)	CGM	**< 0.001**	**0.041**	0.836
	AMG	**< 0.001**	0.951	0.360
	LN	**< 0.001**	0.832	0.392
	BLN	**< 0.001**	0.987	0.472
Neuron numbers	LN	**0.008**	0.505	0.999
	BLN	**< 0.001**	0.367	0.534
Neuron densities	LN	**< 0.001**	0.752	0.966
	BLN	**< 0.001**	0.568	0.645

HEMI, entire hemisphere; CGM, cortical gray matter; AMG; entire amygdala; LN, lateral nucleus of the amygdala; BLN, basolateral nucleus of the amygdala. P values smaller than 0.05 are shown in boldface.

Volume of brain regions

In all treatment groups, the mean volumes of all investigated brain regions increased with age (Fig. 3). Moreover, for both the absolute and relative volumes, two-way ANOVA showed for all brain regions significant effects of the age of the animals but no significant effects of the treatment (except for the relative volume of the CGM) and no significant effects of the interaction between age and treatment (P values are listed in Table 2). When testing for age-related differences within a given treatment group, Bonferroni post-hoc tests demonstrated significant differences between P0 and P25 as well as between P0 and M3 for all investigated brain regions (P values of the Bonferroni tests are provided in Fig. 3). In addition, significant differences were found between P25 and M3 in the absolute values obtained for all investigated brain regions in the offspring of infected dams, but this difference was not observed in HEMI, CGM, whole AMG and BLN of the sham and control offspring. Thus, in terms of absolute volumes, the HEMI, CGM, whole AMG and BLN developed slower in the offspring of infected dams.

In terms of volumes relative to total brain size (HEMI), however, all brain areas (except LN) reached mature size by P25 in all treatment groups. Accordingly, the difference between P25 and M3 in the absolute total brain volume seen in the offspring of infected dams was not observed in the sham and control groups. Importantly, compared to the offspring of the sham-exposed and control dams, the offspring of infected dams showed at P25 the smallest absolute values, and at M3, the highest absolute values (except for the LN). This indicates delayed growth of the brains of the offspring of infected dams. When testing for differences between the treatment groups at a given age, post-hoc Bonferroni tests showed a significant difference only for the mean absolute volume of the CGM at P25 between the offspring of infected dams and offspring of control dams (C: 19.7 ± 0.7 mm^3; E: 16.1 ± 1.1 mm^3; -18%; $p < 0.05$).

In summary, the offspring of infected dams displayed delayed brain growth between P25 and M3, as reflected by a significantly decreased mean absolute volume of the CGM at P25 compared to controls.

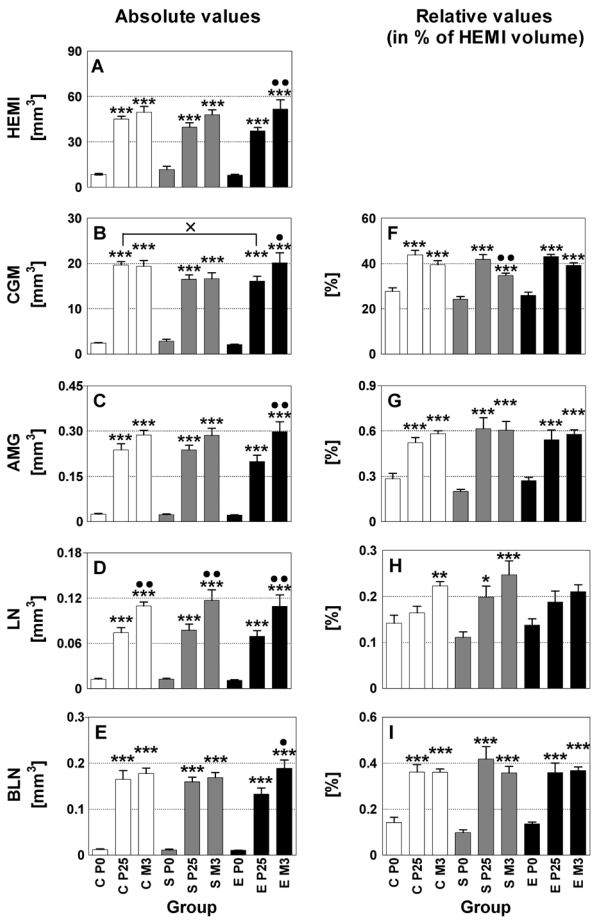

Figure 3. Development of brain region volumes. Mean and standard error of the mean of the volumes of the entire hemisphere (HEMI) (A), the cortical gray matter (CGM) (B,F), the entire amygdala (C,G), the lateral nucleus of the amygdala (LN) (D,H) and the basolateral nucleus of the amygdala (BLN) (E,I) within the brains of offspring of dams exposed to human influenza virus (Group E; closed bars), sham-exposed dams (Group S; gray bars) or control dams (Group C; open bars) at postnatal day P0, P25 and M3. The data are shown as absolute values (A-E) as well as relative values (i.e., related to the volume of the entire hemisphere of the same mouse) (F-I). *, ** and ***, $p < 0.05$, $p < 0.01$ and $p < 0.001$, respectively (compared to P0 within the same treatment group). • and ••, $p < 0.05$ and $p < 0.01$, respectively (compared to P25 within the same treatment group). ×, $p < 0.05$ (between E and C at P25).

Total neuron number

In all treatment groups, the mean total neuron number in the LN and BLN increased between P0 and P25 and between P0 and M3 (Fig. 4). Two-way ANOVA showed significant effects of age but not treatment or the interaction between age and treatment (see Table 2 for the corresponding P values). In contrast to the LN, Bonferroni post-hoc tests showed, when testing for age-related differences in the BLN within a given treatment group, significant increases in the mean total neuron numbers between P0 and P25 as well as between P0 and M3 for all treatment groups (Fig. 4).

In addition, a significant decrease in mean total neuron number in BLN was found for the offspring of control dams between P25 and M3. This effect was not observed for the offspring of the sham-exposed dams or infected dams. When testing for differences between the treatment groups at a given age, Bonferroni post-hoc tests showed no significant differences (Fig. 4). In summary, while total neuron numbers in these brain regions were lower in the offspring of infected dams than in sham and control groups, the differences did not reach significance.

Neuron density

In all treatment groups, the mean neuron density in the LN and BLN decreased with age (Fig. 4). Two-way ANOVA showed significant effects of age but not treatment or the interaction between age and treatment (P values are listed in Table 2). When testing for age-related differences within treatment groups, Bonferroni post-hoc tests showed for both the LN and the BLN significant differences between P0 and P25 as well as between P25 and M3 for all treatment groups (P values of the Bonferroni tests are provided in Fig. 4). However, when testing for differences between the treatment groups at a given age, Bonferroni post-hoc tests showed no significant differences. In summary, maternal infection did not affect mean neuron density in the LN and BLN in the offspring at birth or during postnatal development.

GFAP immunoreactivity

No qualitative increase in GFAP immunoreactivity was observed in the brains of the offspring of infected dams or in the sham-exposed dams from P0 to P25 or M3 (not shown). Thus, there was no evidence of astrogliosis in this sample. There is also no apparent GFAP difference in these brain areas between the offspring of infected dams and controls.

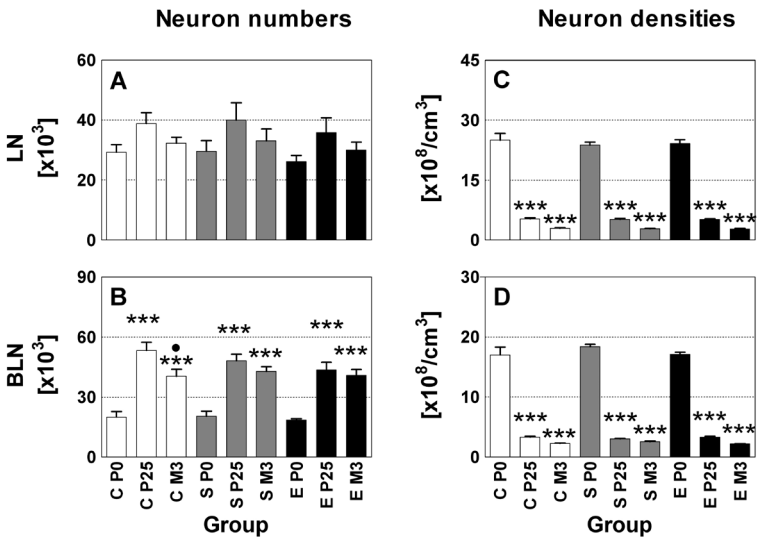

Figure 4. Development of neuron numbers and densities in the amygdala. Mean and standard error of the mean of both neuron numbers (A,B) and neuron densities (C,D) in the lateral nucleus of the amygdala (LN) (A,C) and the basolateral nucleus of the amygdala (BLN) (B,D) within the brain of offspring of dams exposed to human influenza virus on E9.5 (Group E; closed bars), sham- exposed dams (Group S; gray bars) or control dams (Group C; open bars) at postnatal day (P) 0, P25 and at three months of age (M3). ***, $p < 0.001$ (compared to P0 within the same treatment group). •, $p < 0.05$ (compared to P25 within the same treatment group).

Discussion

In the present study we demonstrate that maternal infection on E9.5 resulted in delayed growth of the brain between P25 and M3, as reflected in a significantly decreased mean volume of the CGM at P25 compared to controls. Although total neuron numbers in the LN and BLN were lower in the offspring of influenza-infected dams compared to the sham and control group, the differences did not reach significance. Furthermore, maternal infection did not affect mean neuron densities in the LN and BLN in their offspring at birth or during postnatal development. Compared to controls, exposed offspring showed a small increase in mean body weight at M3. No evidence of astrogliosis was found in this sample.

There is substantial evidence indicating that patients with autism have

enlarged brains (for review see Palmen and van Engeland, 2004). While some studies reported macroencephaly during childhood in autism (Courchesne et al., 2001; Aylward et al., 2002; Carper et al., 2002; Sparks et al., 2002; Palmen et al., 2004b), others did not (Rojas et al., 2002; Van Kooten et al., 2008). According to Courchesne et al. (2003, 2004) and Webb et al. (2007), brain growth takes place during the first year of life; patients with autism show a reduced or normal brain size at birth followed by brain overgrowth in the first year of life and then an abrupt cessation of growth by the age of 2-4 years (Redcay and Courchesne, 2005), leading to comparable adult brain size between patients with autism and typical subjects (Redcay and Courchesne, 2005; but see also Hardan et al., 2001; Piven et al., 1995; 1996). The ages of P0, P25 and M3 in the mouse correspond, respectively, to birth, childhood and early adulthood in humans. In the present study, offspring of infected damns had normal brain volumes at birth, a finding that is in agreement with the human data of Redcay and Courchesne (2005). However, we did not find brain overgrowth, but rather a delayed growth of the brain between P25 and M3, as reflected in a significantly decreased mean volume of the CGM at P25 compared to controls. Mean volumes of all investigated brain regions increased in all treatment groups with increasing age, and compared to sham-exposed and controls, we did not find enlarged brains in the adult offspring of infected dams. Although it does display an altered pattern of brain growth compared to contriols, the mouse model investigated in the present study does not appear to display the transient postnatal brain overgrowth described for autism, for which both the involvement of genetic (Bailey et al., 1995; Muhle et al., 2004) and environmental factors (Juul-Dam et al., 2001; Hultman et al., 2002) have been discussed.

The present findings contrast with those of Fatemi et al. (2002), who reported that the brain size and weight of adult offspring of infected dams were slightly larger than controls. This discrepancy could be due to a difference in the degree of sickness induced in the dams, and therefore the maternal immune influence on the embryos (Smith et al., 2007). Such differences can arise through the method and speed of virus delivery, the degree of stress to which the dam is subjected, or possibly subclinical infections in the animal quarters. The discrepancy in results could also arise from the methods used for analysis of brain size.

The AMG plays an important role in social behavior and cognition (for reviews see, Adolphs et al., 2002; Amaral et al., 2003, 2008). Structural imaging

studies found larger (Howard et al., 2000; Sparks et al., 2002; Schumann et al., 2004), smaller (Aylward et al., 1999; Pierce et al., 2001; Nacewicz et al., 2006), or unchanged (Haznedar et al., 2000; Palmen et al., 2006) volumes of the AMG in patients with autism. The latter observation is in agreement with the findings of the present study showing no significant differences in AMG volume between the exposed, sham-exposed and control offspring. In a recent study of postmortem brains from patients with autism, Schumann and Amaral (2006) also reported no difference in the mean overall volume of the AMG in patients with autism compared to controls.

Abnormal neuron number and neuron density in the AMG have been described in autism. Specifically, Kemper and Bauman (1993) reported in a qualitative study smaller and more densely packed neurons in the AMG. In a design-based stereologic study, Schumann and Amaral (2006) demonstrated a reduction in the mean total number of neurons (as well as in mean neuron density) in the entire AMG as well as in the LN. However, these authors could not confirm the smaller cells described by Kemper and Bauman (1993). Moreover, the offspring of influenza-infected mice displayed reduced social and exploratory behavior as well as marked signs of anxiety (Shi et al., 2003), suggesting the possible involvement of the AMG in this model. Although we did not address cell size, we did not find a significant difference in the mean total neuron number or neuron density in the LN and BLN between the different treatment groups over time.

With respect to the timing of the neuropathological alterations during brain development, autism may either develop during the first six months of gestation (Piven et al., 1990; Rorke, 1994; Rodier et al., 1996; Bauman et al., 1997; Courchesne, 1997; Bailey et al., 1998; Gillberg, 1999; see also Glasson et al., 2004) or has a postnatal basis (Gillberg, 1999; Kern, 2003). A substantial body of evidence supports the existence of several critical developmental periods in the mouse brain, during which neurogenesis, gliogenesis and neuronal migration peak (see Shimada et al. (1977) and Morgane et al. (1992). Critical periods for neurogenesis occur in E11.5-16 for the CGM (Fatemi, 2005) and at E12.5 for the AMG (Finlay and Darlington, 1995). The vulnerable period between E8-E10 in the mouse corresponds roughly to the late first trimester in humans (Fatemi, 2005). Accordingly, the observed lack of abnormal total neuron number and neuron density in the AMG of mice born to dams infected at E9.5 might be related to the timing of the influenza exposure.

Fatemi et al. (2002a) investigated the effect of maternal human influenza virus exposure on E9 of pregnancy on total brain size, pyramidal and non-pyramidal cell density and nuclear area of these cells in offspring at P0 and M3.5. They reported that offspring of dams prenatally exposed to human influenza virus have, despite the smaller brain size at birth, an increased brain size at adult age, increased pyramidal cell densities at birth and adulthood, a decreased non-pyramidal cell density at P0, which reached normal levels at M3, and pyramidal cell atrophy at birth persisting into adulthood. Although these authors used the same virus, mouse strain and time point of exposure as in the present study, their results differ from those presented here. Possible reasons for the discrepancies are cited above. It is relevant that Fatemi et al. (2002a) did not apply rigorous quantitative histological techniques, i.e., design-based stereology. In addition, the exposed mice investigated in the present study showed a behavioral abnormality in sensory gating (PPI) that is related to autism (Shi et al., 2003; Smith et al., 2007), whereas corresponding data were not reported by Fatemi et al. (2002a).

In summary, in contrast to some reports in literature, exposure of pregnant mice to human influenza virus at E9.5 does not reproduce the entire neuropathology of autism with respect to the AMG. Accordingly, this mouse model cannot be applied to understand the underlying molecular and cellular mechanisms causing these neuropathological alterations. This should be considered in the use of this model as animal model of autism.

7

Chapter 8

General discussion and future implications

In order to develop new therapeutic approaches for the prevention and treatment of autism, it is important to identify the neurobiological mechanisms underlying autism. The findings described in the present thesis have provided the following novel insights:

First, we replicated earlier reported findings of minicolumnar abnormalities in the brains of patients with autism in an independent sample. Specifically, patients with autism showed smaller minicolumns, increased neuron densities, decreased cell size and mean interneuronal distances within in the prefrontal, primary sensory, motor and visual cortex, and increased neuropil space in the frontopolar and anterior cingulate cortex.

Second, we found a significant reduction in the mean neuron density in layer III, a reduced mean total neuron number in layers III, V and VI, and a decreased mean perikaryal volume of neurons in layers V and VI in the fusiform gyrus (FG) in the brains of patients with autism compared to controls. Notably, these alterations were not found in area 17 and the cortical grey matter (CGM), reflecting local rather than general neuropathological alterations found in cortical regions in autism. These results might reflect a disconnected FG or underdeveloped connections within the network of brain regions mediating face processing.

Third, we could show that in both anterior cingulate cortex (ACC) and frontoinsular cortex (FI), patients with schizophrenia exhibited alterations in the morphology of the Von Economo neurons (VENs) compared to controls. Specifically, VENs were irregularly shaped, shorter, showed only either the basal or the apical dendrite, and were usually curved (we named them Type-2-VENs). Although not statistically significant, the same morphological abnormalities of VENs were also found in the ACC and FI of some of the patients with autism compared to matched controls. This suggests that Type-2-VENs represent a morphological variant of this neuron type that can be observed in some brains from patients with autism (as well as in a few brains from normal controls), but that is far more prevalent in schizophrenia.

Fourth, our findings on a mouse model for autism indicated that exposing pregnant mice to human influenza virus on embryonic (E) day 9.5 resulted in a delayed growth of the brain between postnatal day 25 (P25) and 3 months

of age (M3), reflected by a significantly decreased mean volume of the CGM at P25 compared to controls, while at birth or during postnatal development the mean neuron numbers and mean neuron densities in the lateral nucleus (LN) of the amygdala (AMG) and basolateral nucleus (BLN) of the AMG was not affected. This might implicate that exposure of pregnant mice to human influenza virus at E9.5 does not reproduce the entire neuropathology of autism with respect to the amygdala which should be considered in the further use of this model as animal model for autism.

Our observations of minicolumnar abnormalities in the prefrontal, primary sensory, motor and visual cortex and increased neuropil space in patients with autism shows that alterations in the minicolumnar structure in the cerebral cortex may be crucial in the understanding of the neurobiological deficit in autism (Casanova et al., 2003; Courchesne et al., 2004). On the basis of recent studies and the results presented here, it is tempting to hypothesize that patients with autism show increased numbers of neurons and a disorganized neuropil within the cerebral cortex. However, these minicolumnar alterations are restricted to specific brain regions, reflecting local rather than general neuropathological alterations found in cortical regions in autism. In line with this is the lack of evidence of increased neuron numbers within the cortical grey matter as a whole in patients with autism (see Chapter 5). The proposed disorganized neuropil space in patients with autism involves both axonal and dendritic components and is in line with the recent finding of generalized loss in the expression of MAP2, a major dendritic protein, in the frontal cortex of patients with autism compared to controls (Mukaetova-Ladinska et al., 2004). Detailed analysis of total neuron numbers as well as dendritic analysis of separate regions within the cerebral cortex in large samples of human postmortem brains of patients with autism will be necessary to determine the potential mechanism underlying the minicolumnar alterations in patients with autism.

GABAergic interneurons, located in the neuropil space, determine the minicolumnar response to thalamic input by modulating the activity of neighboring minicolumns. Smaller minicolumns, representing increased types of inhibitory interneurons, and reductions in the neuropil space in patients with autism, may lead to a decreased activity of the GABAergic system (Casanova, 2006). This might reduce the threshold for developing seizures, a frequent comorbidity in patients with autism (Rubenstein and

Merzenich, 2003). Furthermore, it turns out that GABA dysfunction may occur in conjunction with Reelin dysfunction in autism thereby affecting neuronal migration and the arrangement of cortical minicolumns. It will therefore be interesting to test these hypotheses in future studies by investigating the GABAergic system in combination with minicolumnar analyses in humans and animal models for autism. Nevertheless, skepticism exists about the origin and functional implications of the cell minicolumns (Jones, 2000; Buxhoeveden and Casanova, 2002b; Rockland and Ichinohe, 2004). Importantly, this uncertainty argues for further analysis of these minicolumnar structures by investigating the microdomains in 3D (instead of 2D) (Hutsler and Galuske, 2003; Rockland and Ichinohe, 2004). As a result, the analysis will become independent of the plane of section, staining intensity of the tissue and shape of the cells, all potentially sources of bias in analyzing minicolumns with optical density measurements by computerized imaging in 2D.

Autism is a complex disorder caused by perturbations in the development and functioning of cellular circuitry that governs human social interaction and cognition. Neuroimaging and neuropathology studies point to a set of increasingly well-defined areas in the human brain that are associated with circuits that are responsible for social interaction and cognition. Among these are the ACC, FI cortex and the FG. So far, more than 15 studies (involving over 150 autistic patients) have indicated a hypoactivation of the FG when patients with autism view faces compared to controls (Schultz, 2005). The observed cytoarchitectonic abnormalities in the output layers III and V of the FG provide evidence for a disconnected FG or underdeveloped connections in face processing networks in patients with autism. As the FG is a part of a complete network of brain regions mediating face processing, it is tempting to hypothesize that these specific brain regions show cytoarchitectonic alterations as well. Minicolumnar analysis of the FG and the regions mediating face processing will be necessary for testing the hypothesis whether the observed cytoarchitectonic abnormalities within the FG might originate primarily in the FG itself or whether they might derive from loss of targets to which the FG projects. In this regard, both the inferior frontal gyrus (IFG) (semantic aspects) (Leveroni et al., 2000) and the orbitofrontal cortex (OFC) (facial attractiveness and sexual relevance) (O'Doherty et al., 2003; Kranz and Ishai, 2006) are of particular interest and are related to autism. Interestingly, imaging studies found

a reduced activation of the IFG (Just et al., 2004; Harris et al., 2006; Koshino et al., 2007) and a decreased volume of the OFC in autism (Hardan et al., 2006; Girgis et al., 2007). The IFG and OFC are cortical areas located downstream of the FG. In Chapter 5 we proposed that the input to the FG remains intact, whereas the output from the FG to cortical and subcortical brain regions might be abnormal in autism. According to this hypothesis, both the IFG and OFC will receive, as a result, abnormal visual input from the FG. Therefore we expect that the IFG and OFC will show cytoarchitectonic abnormalities in the patients with autism compared to controls as well. Furthermore, significantly reduced activity in face perception tasks in autism was also reported for the inferior occipital gyrus (IOG) and the superior temporal gyrus (STG) (Pierce et al., 2001). The IOG is located in the occipital lobe upstream of the FG. This would imply, according to the hypothesis outlined above, that the IOG will not show cytoarchitectonic abnormalities in patients with autism compared to controls. As a result, the output projections from the IOG to the STG will stay intact as well. For these reasons it will be of interest to investigate total neuron numbers and neuron densities in the IFG, OFC, IOG and STG in postmortem brains of patients with autism.

Furthermore, it is important to note that the AMG receives reciprocal input from the FG and is involved in face processing as well (Schultz et al., 2000; Fairhall and Ishai, 2007). Inconsistent results were reported with respect to the volume of the AMG in patients with autism. However, in a classical neuropathology study, neurons in the AMG were found to be abnormally small and densely packed in autism (Kemper and Bauman, 1993), whereas a recent design-based stereologic study found no changes in mean neuron size but a significantly reduced mean total neuron number in the AMG overall and in its lateral nucleus in autism (Schumann and Amaral, 2006). More importantly, the latter finding has been replicated in the brains of the same sample of postmortem brains from patients with autism and controls that was investigated in the present study (Dr. J. Wegiel, NY State Institute for Basic Research in Developmental Disabilities, Staten Island, NY, USA; personal communication).

Particular candidate populations of cells, such as VENs in the ACC and FI, were related to social emotions and cognition. Although Allman et al. (2005) have proposed a role of VENs in the underlying pathology of the social deficits in patients with autism, their hypothesis has not been proven yet. Based on

our findings and a recently reported study of Kennedy et al. (2007), it cannot be decided whether the abnormal VEN morphology found in some, but not all, patients with autism can be related to any specific clinical symptom of the disorder. In fact, it seems that the VEN pathology is not specific for patients with autism. It might be that subtle differences in candidate cell populations such as VENs in patients with autism versus controls could reflect subtle differences in gene expression. Therefore, future studies should focus on molecular genetic differences between brains from patients with autism and normal controls in vulnerable cell populations, such as the VENs. Preliminary evidence suggests that VENs in the FI are strongly and selectively labeled with an antibody for the product of the MET gene (J. Allman, California Institute of Technology, Pasadena, CA, USA; personal communication). In addition, the ACC contains MET RNA as well (J. Allman, California Institute of Technology, Pasadena, CA, USA; personal communication). The MET gene encodes a multifunctional receptor tyrosine kinase, and recent human genetic data have shown that a specific MET allele is strongly linked to autism (Campbell et al., 2006). Large-scale analysis of gene expression of VENs might give more insight into the role of VENs in the etiology of autism.

It appears too early to conclude to which extent abnormal morphology of VENs in the brains from patients with schizophrenia and autism contribute - via abnormal VEN function - to clinical symptoms of these disorders. Accordingly, it is important to identify the projection areas of the VENs. Cell filling and Golgi staining of the dendritic architecture of the VENs in the ACC and FI will be relevant for elucidating the projection areas of the VENs. As VENs are found exclusively in humans, great apes and some whale species, it is not possible to investigate morphological and cytoarchitectonic alterations of VENs in an experimental manner in rodent models for autism.

Another related concern is the influence of the effects of possible co-morbidity with epilepsy, which can affect the neuronal populations and might therefore confound interpretation of what is attributable to autism and what are downstream effects in brain pathology. Therefore, alterations in VEN morphology and cytoarchitecture should be investigated using a carefully selected sample of human postmortem brains from patients with autism compared to age and sex matched controls.

With respect to the timing of the neuropathological abnormalities in patients with autism, it remains plausible that interindividual differences observed in

morphological and biochemical alterations are also related to interindividual differences in the (prenatal) onset of developmental disturbance. Several authors suggested a prenatal origin, most likely during the first six months of gestation (Piven et al., 1990; Rorke, 1994; Rodier et al., 1996; Bauman et al., 1997; Courchesne, 1997; Bailey et al., 1998; Gillberg, 1999). In this regard disorders such as fetal alcohol syndrome and fetal valproate syndrome were described in relation with autism (Aronson et al., 1997; Williams and Hersh, 1997). Some of these associations suggest that injury persistent during the first trimester of the developing brain could lead to autism in some cases (Gillberg, 1999). Conversely, the individual time point of developmental disturbance can also be in the very late prenatal period or (in a minority of cases) even in the early postnatal phase (up to the second year of postnatal life) (Gillberg, 1999). The observed increase in cortical modularity may originate during neurogenesis implying a disruption during earlier stages of gestation in patients with autism (Casanova et al., 2003). Furthermore, the spatiotemporal pattern of VEN emergence during brain development correlates with onset of symptoms in autism (Allman et al., 2005). On the other hand, some children with autism do not show any pathological symptoms until a substantial period after birth. Therefore, Kern (2003) suggested that it is possible that some children become autistic from neuronal cell death or brain damage occurring postnatally as a result of injuries. Thus, an evolving pathologic process is taking place in the brain of patients with autism which extends from the fetal period of brain development into adulthood. However, detailed analysis on appropriate animal models might explain the potential developmental origin of the described neuropathological alterations in autism. Despite the fact that the neuropathological results in patients with autism are revealing, animal models are essential for better understanding of the pathophysiology, cause and treatment of autism. However, the scarcity of consistent data concerning cellular and molecular pathological alterations underlying autism, in turn, impacts directly on attempts to generate and assess relevant animal models of the disease. The question remains whether the neuropathological and behavioral deficits in patients with autism can be detected in animal models of the disease. Although a variety of animal models for autism exist, resembling behavioral and neuropathological alterations found in patients with autism, we are still very early in studying the characteristics of autism in animal models. The generation of new animal models for autism should first of all focus on the possible different time points

of hit during development. In addition, as genetic factors contribute about 90% and environmental factors about 10% to autism (Garber, 2007), it would be very interesting to generate new animal models by combining transgenic approaches and developmental hits, ultimately in one and the same animal model. For instance, the R451C knock-in mouse (Arg451-->Cys451 (R451C) substitution in neuroligin-3) could be subjected to an environmental hit at a specific time point in the first or third trimester of pregnancy. This would be crucial in revealing the mechanisms of synaptic dysfunction during development in patients with autism.

In summary, many questions wait for elucidation, and further detailed neuropathological research is highly necessary to answer these questions.

In other words, autism really counts.

Summary

Autism is a neurodevelopmental disorder with a strong genetic component and several known environmental risk factors. Classical neuropathology studies have reported consistent findings in the limbic system, cerebellum and cerebral cortex of patients with autism. However, the neurobiological mechanism underlying these gross morphological alterations remain to be established and it is not known whether these alterations reflect different aspects of a unique neuropathologic defect or represent different morphological phenotypes of the disorder. In addition, it has not been possible to find functional interpretations of the gross morphological alterations reported in patients with autism. Furthermore, all studies had to contend with small sample sizes, biased quantification techniques and high percentages of patients suffering form comorbid mental retardation and epilepsy. In the present thesis we investigated cytoarchitectonic abnormalities in specific regions within the cerebral cortex related to social functioning in both postmortem brains from patients with autism and an animal model for autism, using high precision design-based stereology.

To overcome the aforementioned difficulties in autism research we generated a unique case series, consisting of 7 brains of patients with autism compared to 10 matched controls, developed in the framework of the Autism Brain Atlas Project supported by the U.S. Autism Tissue Program and Autism Speaks (New York, NY, USA). Showing the validity of the sample, we corroborated previous findings of minicolumnar abnormalities in an independent sample. Furthermore, a potential neurobiological correlate of alterations in the fusiform gyrus (FG) as described in clinical and imaging studies was found. Besides this, some patients with autism showed altered morphology of the Von Economo neurons (VENs) within the anterior cingulate cortex (ACC) and frontoinsular cortex (FI) (VENs play an important role in the coordination of distributed neuronal activity involving social functioning). Moreover, our analyses revealed that the maternal influenza infection mouse model cannot be applied to understand the underlying mechanisms of postnatal brain overgrowth in autism, and exposure of pregnant mice to human influenza virus at E9.5 does not reproduce the entire neuropathology of autism with respect to the amygdala.

Although studies on autism neuropathology are revealing, further research is necessary to clarify the influence of neuropathological alterations in the etiology of autism. The results of the present study argue for a neural systems approach in autism research, rather then investigating individual

brains regions. Thus, the present study may be seen as starting point to open new horizons in autism research. In order to get more insight into the functional interpretation of neuropathological findings, future studies should focus on the brain regions involved in the neuronal networks mediating face processing as well as on the projection areas and function of the VENs, using quantitative histology. In addition, detailed analyses on appropriate animal models (combining transgenic approaches with environmental hits during development) might explain the potential developmental origin of the described neuropathological alterations in autism.

S

Samenvatting

Autisme telt: het is een ernstige neurologische ontwikkelingsstoornis die enerzijds wordt gekenmerkt door een achterblijvende ontwikkeling op het gebied van sociale interacties, communicatie en taal en anderzijds door de aanwezigheid van rigide en stereotype gedragspatronen. Samen met bijvoorbeeld Aspergers en Rett syndroom, maakt autisme deel uit van de autisme spectrum stoornissen. Tegenwoordig hebben ongeveer 1 à 2 op de 1000 kinderen autisme. Het komt driemaal meer voor bij jongens dan bij meisjes. Ondanks dat vroeger werd gedacht dat autisme ontstond door een slechte opvoeding van de ouders, is er de afgelopen decennia veel onderzoek gedaan naar de onderliggende biologische mechanismen die mogelijk autisme kunnen veroorzaken. Inmiddels is uit onderzoek gebleken dat autisme een aandoening is van de hersenen, maar de exacte oorzaak is nog steeds niet bekend.

Uit de literatuurstudie beschreven in **Hoofdstuk 2** is gebleken dat een groot deel van de patiënten met autisme een vergroot brein heeft. Verder zijn er consistente neuropathologische afwijkingen gevonden in het limbisch systeem, het cerebellum en de cerebrale cortex van patiënten met autisme. De neuronen (zenuwcellen) in het limbisch systeem liggen dichter bij elkaar en zijn ook kleiner dan in controle breinen. Daarnaast is er zowel in de laterale kern van de amygdala als in de Purkinje cellaag van het cerebellum een verlies van neuronen gevonden. Meer dan de helft van het aantal tot nu toe onderzochte postmortem breinen van patiënten met autisme vertonen kenmerken van corticale dysgenese (abnormale ontwikkeling van de cortex), veranderingen in de migratie van neuronen (cellen liggen niet op de juiste plaats) en een abnormale structuur van de zogenaamde minicolumns in de cortex. Tenslotte zijn er aanwijzingen dat het gamma aminoboterzuur (GABA) neurotransmitter systeem niet optimaal functioneert. Echter, de cellulaire mechanismen die ten grondslag liggen aan deze algemene morfologische afwijkingen zijn niet bekend. Men weet ook niet in hoeverre de genoemde neuropathologische verschillen in de hersenen van patiënten met autisme, één groot neuropathologisch defect weerspiegelen, of dat ze mogelijk de heterogeniteit van dit ziektebeeld verklaren. Bovendien is het onduidelijk hoe deze afwijkingen gerelateerd zijn aan functionele verschillen die patiënten met autisme vertonen.

Overigens had de meerderheid van alle klassieke neuropathologische studies te maken met een kleine steekproef (per studie vaak slechts één of enkele patiënten) waarbij de onderzochte patiënten vaak epilepsie hadden

of mentaal geretardeerd waren. Een ander vaak voorkomend probleem was het gebrek aan degelijke kwantitatieve methoden, zoals design-based stereologie.

In dit proefschrift hebben we de morfologische afwijkingen onderzocht met behulp van design-based stereologie in verschillende hersengebieden die een rol spelen bij sociale interacties in zowel de hersenen van patiënten met autisme als in een muismodel voor autisme. Voorbeelden van onderzochte parameters zijn het volume van de neuronen, het aantal en de densiteit van neuronen en het volume van de betrokken hersengebieden.

Om de bovengenoemde tekortkomingen van andere studies te ondervangen, hebben we een unieke set van humane postmortem breinen gegenereerd in samenwerking met het Autism Brain Atlas Project gesteund door het Autism Tissue Program en Autism Speaks (New York, VS). Deze set omvat 7 breinen van patiënten met autisme en 10 corresponderende gezonde breinen. Omdat autisme een heterogene ziekte is, is het van belang om onze resultaten te valideren en te onderzoeken of bepaalde afwijkingen in specifieke hersengebieden ook worden gevonden door andere onafhankelijke onderzoeksgroepen met andere collecties van humane postmortem breinen. Daarom hebben we in de **Hoofdstukken 3 en 4** de zogenaamde minicolumn structuur onderzocht in verschillende hersengebieden die een rol spelen bij sociaal gedrag bij patiënten met autisme. Een minicolumn is een verticale structuur in de hersenschors die wordt gezien als het kleinste stukje grijze stof waarbinnen informatie tussen neuronen, maar ook tussen verschillende hersengebieden kan worden uitgewisseld. Onze bevindingen komen inderdaad overeen met de eerder gepubliceerde resultaten van een onafhankelijke onderzoeksgroep. In de prefrontale, primaire sensorische, motorische en visuele cortex vonden we namelijk smallere minicolumns, een vergrote dichtheid van neuronen, kleinere neuronen binnen één minicolumn en een kortere afstand tussen de neuronen in een minicolumn in een subset van 6 breinen van patiënten met autisme en 6 controle breinen. Verder was de extracellulaire ruimte van de frontopolaire en anterior cingulate cortex vergroot.

Er is bewijs dat de cognitieve veranderingen bij patiënten met autisme mogelijk gerelateerd zijn aan veranderingen op cellulair niveau. In **Hoofdstuk 5** hebben we de fusiform gyrus (FG) onderzocht op laagspecifieke afwijkingen in volume, neuron dichtheid, aantal neuronen en de grootte van neuronen. De FG is een hersengebied dat betrokken is bij het verwerken van gezichten

en is daardoor belangrijk voor sociale interactie. Om de specificiteit van de resultaten te kunnen bepalen hebben we ook de visuele cortex, de grijze stof en de totale hemisfeer geanalyseerd. Visuele informatie komt via de ogen binnen in de visuele cortex, wordt dan naar de FG verstuurd, die op zijn beurt weer informatie doorstuurt naar frontale en subcorticale gebieden. De resultaten van onze studie laten zien dat de FG significant minder neuronen heeft in de lagen III, V en VI, dat laag III een afname in de dichtheid van neuronen vertoont en dat de neuronen in laag V kleiner zijn in de hersenen van patiënten met autisme in vergelijking met controles. Deze uitkomsten zijn specifiek voor de FG omdat er geen significante verschillen zijn gevonden in de visuele cortex, de grijze stof en de totale hemisfeer. Hieruit kunnen we concluderen dat bij patiënten met autisme de FG wel de juiste informatie binnenkrijgt vanuit de visuele cortex, maar dat deze informatie mogelijk niet goed aankomt in de projectiegebieden van de FG. De mogelijkheid bestaat dan ook dat de FG is losgekoppeld van het netwerk van hersenregio's die betrokken zijn bij gezichtsverwerking, of dat de verbindingen hiermee onderontwikkeld zijn.

Bepaalde type zenuwcellen, de zogenaamde Von Economo neuronen (VENs), in de anterior cingulate cortex (ACC) en de frontoinsular cortex (FI) spelen een belangrijke rol in sociaal gedrag, waarbij ze betrokken zijn bij de coördinatie van neuronale activiteit. Om onderscheid te maken tussen verschillende psychiatrische aandoeningen hebben we in **Hoofdstuk 6** de VENs onderzocht in zowel patiënten met autisme als schizofrenie in vergelijking met controles. Uit deze studie is naar voren gekomen dat een aantal patiënten met autisme, maar niet alle, afwijkingen vertoonden in de morfologie van de VENs in de ACC en de FI. De VENs hadden een andere vorm, waren korter, verdraaid en mistten vaak een dendrite (uitloper). Opvallend was echter dat dit effect meer uitgesproken was in patiënten met schizofrenie. Desondanks is het nog te vroeg om iets te zeggen hoe en in welke mate deze abnormale VENs, mogelijk via een afwijkende functie, bijdragen aan de klinische symptomen van patiënten met autisme en schizofrenie.

Om de cellulaire mechanismen die ten grondslag liggen aan neuronale veranderingen in de hersenen van patiënten met autisme te onderzoeken, is de ontwikkeling van diermodellen voor autisme van groot belang. Het is bekend dat influenza infecties tijdens het eerste of tweede trimester van de zwangerschap gerelateerd zijn aan een verhoogd risico op het

krijgen van een kind met autisme. In **Hoofdstuk 7** hebben we zwangere moedermuizen blootgesteld aan het humane influenza virus op dag 9.5 van de zwangerschap. Vervolgens zijn de nakomelingen onderzocht op drie verschillende tijdstippen: postnatale dag (P)0, P25 en 3 maanden (M3). Deze tijdstippen bij de muis komen overeen met respectievelijk geboorte, kleuter en vroeg volwassen leeftijd bij de mens. De blootgestelde nakomelingen vertoonden een significant vertraagde groei van de grijze stof tussen P25 en M3. Echter, er was geen verschil in de densiteit en het totaal aantal neuronen in de twee kernen van de amygdala bij de geboorte of tijdens de postnatale ontwikkeling. De bevindingen in het muismodel weerspiegelen niet de gehele neuropathologie van patiënten met autisme. Daarom suggereren we dat het influenza muismodel waarschijnlijk niet bruikbaar is voor het bestuderen van de onderliggende mechanismen van de verhoogde postnatale hersengroei en amygdala afwijkingen bij patiënten met autisme.

Ondanks dat er tegenwoordig steeds meer neuropathologisch onderzoek wordt uitgevoerd naar de onderliggende cellulaire mechanismen van autisme, is nog altijd veel onbekend. Verder onderzoek moet dan ook bijdragen aan onze kennis over het ontstaan van autisme. De resultaten beschreven in dit proefschrift pleiten voor de zogenaamde 'neurale systemen' aanpak (waarbij meerdere hersenregio's worden bestudeerd), in plaats van het bestuderen van individuele hersenregio's. De studies beschreven in dit proefschrift kunnen dan ook worden gezien als het beginpunt van deze nieuwe aanpak. Om meer inzicht te krijgen in de functionele interpretatie van onze bevindingen zullen toekomstige studies zich vooral moeten richten op hersengebieden die betrokken zijn bij het verwerken van gezichten/visuele informatie. Ook is het van belang de functies en projectiegebieden van de VENs nader te bestuderen, met behulp van design-based stereologie. En tot slot is het belangrijk nieuwe diermodellen (bijvoorbeeld transgene modellen in combinatie met verschillende omgevingsveranderingen tijdens de ontwikkeling) te ontwikkelen om zo meer inzicht te krijgen in de mogelijke invloed van (prenatale) ontwikkeling op het ontstaan van autisme (**Hoofdstuk 8**).

Samengevat zijn er nog veel onbeantwoorde vragen over autisme en is gedetailleerd neuropathologisch onderzoek nodig om deze vragen te kunnen beantwoorden.

Met andere woorden: autisme telt.

S

Dankwoord

Mede dankzij de hulp van velen, zijn de afgelopen vier jaar zeer leuk, gezellig en leerzaam geweest. Ik wil daarom ook iedereen bedanken die op enige wijze heeft bijgedragen aan dit proefschrift.

Mijn Utrechtse promotor Prof. dr. H. van Engeland. Beste Herman, van je kennis op het gebied van autisme heb ik enorm veel geleerd. Je wist als geen ander mijn neuropathologische bevindingen in een breder perspectief te plaatsen. Verder maakte je altijd tijd vrij en stond je altijd voor me klaar wanneer ik weer eens naar Utrecht kwam om nieuwe resultaten te bespreken. Onze discussies, die vaak werden bijgewoond door mede-AiO's, heb ik als zeer waardevol beschouwd. Bedankt voor je grenzeloze enthousiasme, vertrouwen en goede begeleiding de afgelopen vier jaar.

Mijn Maastrichtse promotor Prof. dr. H.W.M. Steinbusch. Beste Harry, jij hebt de deuren van het AiO-schap voor me geopend. Vanaf het begin af aan heb je me in de gelegenheid gesteld om het onderzoek in alle vrijheid te verrichten. Bedankt voor de fijne samenwerking.

Mijn co-promotor Dr. C. Schmitz. Dear Christoph, I'm very grateful that you gave me the opportunity to develop myself in the area of science. Although we did not always have the same ideas of how to do research, you were there to support me by asking the right questions and indicating the right direction if necessary. This always accompanied with an espresso which you drank each time before every meeting. Thanks for your support the past four years.

Natuurlijk ben ik veel dank verschuldigd aan de mensen buiten het UMC Utrecht en de Universiteit Maastricht die hebben bijgedragen aan het tot stand komen van dit proefschrift. Prof. dr. M. Casanova, dear Manny, our cooperation finally resulted in two very nice publications. You were always willing to work together, no matter what. Thanks for the pleasant collaboration. Prof. dr. H. Heinsen, thanks for all your work regarding the preparation of the human postmortem tissue. The excellent quality of the human postmortem tissue made it much easier to analyze. Prof. dr. P.H. Patterson, your mouse model was of great importance for my research. Great thanks. Prof. dr. J. Allman, an important part of this thesis has been the result of a great collaboration. Thanks for teaching me the ins and outs

of the Von Economo neurons. Prof. dr. P.H. Hof, dear Patrick, thank you very much for your valuable scientific input. Dr. J. Pickett, dear Jane, thank you for your help and hard work in collecting the human postmortem sample. I will never forget your agenda point mentioning “keep Imke in science” at the IMFAR meeting in London.

Natuurlijk gaat ook veel dank uit naar mijn collega’s. Zonder jullie was promoveren een saaie bedoeling geweest! In het bijzonder wil ik de volgende personen bedanken. Annerieke, ik heb genoten van je enthousiasme, vrolijkheid en gezelligheid. Het was me een waar genoegen je kamergenootje te mogen zijn! Heel veel succes met je nieuwe PhD project! Evi, Kim, Rinske, Kathleen, Tibo, Anthony, Sonny, Eva, Olga, Jochen, Daniël, Kris, Jos, Gunther, Yasin Ronald, Anja, Nicole en ex-collega’s Bart en Pawel, bij jullie kon ik terecht voor het maken van een praatje of om iets te vragen. Bedankt voor alles! Helen en Marjanne, bedankt voor jullie hulp en gezelligheid in het lab maar ook daarbuiten. Akke, Mirèse, Sandra en Marie-Thérèse, bedankt voor de secretariële hulp. Mijn enige student Iris, bedankt voor al je inzet en harde werk tijdens je stage! Utrechtse collega’s, jullie hielden mij altijd op de hoogte van het reilen en zeilen op de afdeling Kinder- en Jeugd Psychiatrie. Bedankt voor de gezelligheid tijdens congressen, jullie hulp met het invullen van promotieformulieren en de interesse in mijn -in jullie ogen soms nogal vreemd- onderzoek. Ondanks dat ik er niet zoveel was, heb ik me altijd zeer welkom gevoeld! Saskia, bedankt voor alles.

Mijn paranimfen, Marijke en Eveline. Marijke, ik zal je reactie nooit vergeten toen ik je vroeg mijn paranimf te zijn. Bedankt voor je steun, hulp en eindeloze geduld! Nu ben jij de ‘grote’ AiO! Eveline, je kritische blik, probleem oplossend vermogen en sportiviteit waren onmisbaar de afgelopen tijd. Ik ben er trots op dat we de “wasmachine” uiteindelijk toch nog voor elkaar hebben gekregen! Meisjes, bedankt voor de gezelligheid, lach- en huilmomenten (en die huilmomenten waren vaak van het lachen). Ik vind het een eer dat jullie beiden op deze dag naast me staan!

Joyce, Juul en Nic, lieve vriendinnetjes, zonder jullie was het doen van promotieonderzoek nooit zo leuk geweest! Bij jullie vond ik altijd een luisterend oor, ook in moeilijkere tijden. Bedankt voor de altijd gezellige lunches, DE-breaks, etentjes, avondjes uit en weekendje weg. Dit gaan we

zeker voortzetten in de toekomst! Linda, beste vriendinnetje van “thuis”. Ondanks dat we het grootste deel van mijn AiO tijd ver uit elkaar woonden (gelukkig nu niet meer!) was jij altijd geïnteresseerd in mijn onderzoek en kon ik altijd bij je terecht. Super bedankt!

Jack en Connie, Sigrid en Tino, bedankt voor jullie hulp, steun en interesse voor mijn onderzoek. Tino, creatief brein, ik kan je niet genoeg bedanken voor het maken van de cover en lay-out van mijn proefschrift. Het is echt supermooi geworden!

Mam en Pap, Maud en Aswin, dankzij jullie ben ik gekomen waar ik nu ben. Bedankt voor jullie onvoorwaardelijke steun en liefde.

Sjoerd, lief, zonder jou was dit nooit gelukt. Jij maakt mijn leven compleet. Ik hou van je.

Curriculum vitae

Imke van Kooten werd geboren op 22 oktober 1981 te Tegelen. In 2000 behaalde ze haar VWO diploma aan het Valuascollege te Venlo. In datzelfde jaar startte ze haar studie Gezondheidswetenschappen aan de Universiteit Maastricht. Haar afstudeerstage liep zij op de Afdeling Psychiatrie en Neuropsychologie van de Universiteit Maastricht waarbij de effecten van een verhoging van een endogene antioxidant en van een beperking van calorieën in de voeding werd onderzocht in de hippocampus van volwassen muizen. In 2004 behaalde zij haar doctoraalgetuigschrift in de afstudeerrichting Biologische Gezondheidskunde, waarna ze een maand later startte als promovenda bij het Rudolph Magnus Instituut voor Neurowetenschappen, Afdeling Kinder- en Jeugd Psychiatrie van het Universitair Medisch Centrum (UMC) Utrecht in samenwerking met de European Graduate School of Neuroscience (EURON), School for Mental Health and Neurosciences (MHeNS), Afdeling Cellulaire Neurowetenschappen van de Universiteit Maastricht. De resultaten van haar onderzoek zijn beschreven in dit proefschrift.

Imke van Kooten was born on October 22nd 1981 in Tegelen, The Netherlands. In 2000 she graduated for secondary school, VWO, at the Valuascollege in Venlo. In that same year she started her master in Health Sciences at Maastricht University. During her final research internship at the Department of Psychiatry and Neuropsychology at Maastricht University she investigated the effects of an upregulation of an endogenous antioxidant and a reduction in dietary caloric intake on the hippocampus of adult mice. After receiving her masters degree in Biological Health Sciences in 2004, she started her PhD project at the Rudolph Magnus Institute of Neuroscience, Department of Child- and Adolescent Psychiatry at the University Medical Center (UMC) Utrecht in collaboration with the European Graduate School of Neuroscience (EURON), School for Mental Health and Neurosciences (MHeNS), Department of Cellular Neuroscience at Maastricht University. The results of her PhD research were described in this thesis.

Publications

Journal Articles

Van Kooten IAJ, Hof PR, Van Engeland H, Patterson PH, Steinbusch HWM, Schmitz C (2005). Autism: neuropathology, alterations of the GABAergic system, and animal models. Int Rev Neurobiol 71: 1-26

Casanova MF, Van Kooten IAJ, Switala AE, Van Engeland H, Heinsen H, Steinbusch HWM, Hof PR, Trippe J, Stone J, Schmitz C (2006). Minicolumnar abnormalities in autism. Acta neuropathol (Berl) 112(3): 287-303

Casanova MF, Van Kooten IAJ, Switala AE, Van Engeland H, Heinsen H, Steinbusch HWM, Hof PR, Schmitz C (2006). Abnormalities of cortical minicolumnar organization in the prefrontal lobes of autistic patients. Clin Neurosc Res 6: 127-133

Van Kooten IAJ, Palmen SJMC, Von Cappeln P, Steinbusch HWM, Korr H, Heinsen H, Hof PR, Van Engeland H, Schmitz C (2008). Neurons in the fusiform gyrus are fewer and smaller in autism. Brain 131(Pt 4): 987-99

Van Kooten IAJ, Segal D, Rutten BPF, Kreczmanski P, Van Engeland H, Steinbusch HWM, Haroutunian V, Heinsen H, Allman JM, Schmitz C, Hof PR (2008). Alterations of Von Economo neurons in the anterior cingulate cortex and frontoinsular cortex in schizophrenia and autism. S*ubmitted*

Van Kooten IAJ, Shi L, Burks I, Sierksma ASR, Hof PR, Steinbusch HWM, Van Engeland H, Patterson PH, Schmitz C (2008). Consequences of maternal infection: cytoarchitectonic abnormaltities in the offspring of mice exposed to influenza virus. *In preparation for submission*

Abstracts

Van Kooten IAJ, Schmitz C, Palmen SJMC, Van Engeland H, Heinsen H, Steinbusch HWM, Hof PR. Neuropathologic findings in Autism – an overview. National Alliance for Autism Research: Integrating the clinical and basic sciences of autism - a developmental biology workshop, 2004, Fort Lauderdale, USA

Van Kooten IAJ, Casanova MF, Switala AE, Van Engeland H, Heinsen H, Steinbusch HWM, Hof PR, Pickett J, Schmitz C. Neuronal size and number in the neocortex of autistic patients. Society for Neuroscience, 2005, Washington, USA

Van Kooten IAJ, Casanova MF, Van Engeland H, Heinsen H, Steinbusch HWM, Hof PR, Schmitz C. Minicolumnar abnormalities in autism. Federation of European Neuroscience Societies, 2006, Vienna, Austria

Van Kooten IAJ, Palmen SJMC, Von Cappeln P, Steinbusch HWM, Korr H, Heinsen H, Hof PR, Van Engeland H, Schmitz C. Fewer and smaller neurons in the fusiform gyrus in autism. International Meeting for Autism Research, 2007, Seattle, USA

Van Kooten IAJ, Casanova MF, Switala AE, Van Engeland H, Heinsen H, Steinbusch HWM, Hof PR, Schmitz C. Minicolumnar abnormalities in the neocortex of individuals with autism. Autism Research United Kingdom, 2007, Milton Keynes, England

Van Kooten IAJ, Palmen SJMC, Von Cappeln P, Steinbusch HWM, Korr H, Heinsen H, Hof PR, Van Engeland H, Schmitz C. Fewer and smaller neurons in the fusiform gyrus in autism. International Association of Child and Adolescent Psychiatry and Allied Professions, 2008, Istanbul, Turkey

Van Kooten IAJ, Shi L, Burks I, Steinbusch HWM, Van Engeland H, Patterson PH, Schmitz C. Cytoarchitectonic abnormalities in the amygdala of mice infected with maternal influenza, International Meeting for Autism Research, 2008, Seattle, USA

Presentations

Van Kooten IAJ, Casanova MF, Switala AE, Segal D, Rutten BPF, Kreczmanski P, Van Engeland H, Steinbusch HWM, Heinsen H, Allman JM, Schmitz C, Hof PR. Neuropathology in Autism: minicolumns and spindle cells. Korczak Foundation, 2005, Amsterdam, The Netherlands

Van Kooten IAJ, Steinbusch HWM, Korr H, Heinsen H, Hof PR, Van Engeland H, Schmitz C. Cytoarchitectonic abnormalities in the temporal fusiform gyrus in autistic patients. European Graduate School of Neuroscience PhD days, 2006, Maastricht, The Netherlands

Van Kooten IAJ, Casanova MF, Switala AE , Steinbusch HWM, Korr H, Heinsen H, Hof PR, Van Engeland H, Schmitz C. Brain Atlas Project: Neuropathology Update. Autism Tissue Program Meeting, 2006, Vienna, Austria

Van Kooten IAJ, Palmen SJMC, Von Cappeln P, Steinbusch HWM, Korr H, Heinsen H, Hof PR, Van Engeland H, Schmitz C. Face recognition and neuropathology of the temporal fusiform gyrus in autistic patients. PhD Annual Meeting Graduate School Neurosciences Amsterdam and Rudolph Magnus Graduate School of Neuroscience, 2007, Zeist, The Netherlands

Van Kooten IAJ, Palmen SJMC, Von Cappeln P, Steinbusch HWM, Korr H, Heinsen H, Hof PR, Van Engeland H, Schmitz C. A quantitative post-mortem neuropathology study of the fusiform gyrus in autism. International Association for Child and Adolescent Psychiatry and Allied Professions, 2008, Istanbul, Turkey

Van Kooten IAJ, Palmen SJMC, Von Cappeln P, Steinbusch HWM, Korr H, Heinsen H, Hof PR, Van Engeland H, Schmitz C. Face recognition and neuropathology of the fusiform gyrus in patients with autism. International Meeting for Autism Research, 2008, London, England

References

Aarkrog T (1968). Organic factors in infantile psychoses and borderline psychoses. A retrospective study of 46 cases subjected to pneumoencephalography. Dan Med Bull 15(9): 283-8.
Adams W, Kendell RE, Hare EH, Munk-Jorgensen P (1993). Epidemiological evidence that maternal influenza contributes to the aetiology of schizophrenia. An analysis of Scottish, English, and Danish data. Br J Psychiatry 163: 522-34.
Adolphs R, Damasio H, Tranel D (2002). Neural systems for recognition of emotional prosody: a 3-D lesion study. Emotion 2(1): 23-51.
Allman JM, Hakeem A, Erwin JM, Nimchinsky E, Hof P (2001). The anterior cingulate cortex. The evolution of an interface between emotion and cognition. Ann N Y Acad Sci 935: 107-17.
Allman JM, Hakeem A, Watson K (2002). Two phylogenetic specializations in the human brain. Neuroscientist 8(4): 335-46.
Allman JM, Watson KK, Tetreault NA, Hakeem AY (2005). Intuition and autism: a possible role for Von Economo neurons. Trends Cogn Sci 9(8): 367-73.
Amaral DG, Bauman MD, Schumann CM (2003). The amygdala and autism: implications from non-human primate studies. Genes Brain Behav 2(5): 295-302.
Amaral DG, Schumann CM, Nordahl CW (2008). Neuroanatomy of autism. Trends Neurosci.
American Psychiatric Association (1994). Diagnostic and Statistical Manual of Mental Disorders (DSMIV). Washington, DC, American Psychiatric Association.
Anderson GM, Gutknecht L, Cohen DJ, Brailly-Tabard S, Cohen JH, Ferrari P, et al. (2002). Serotonin transporter promoter variants in autism: functional effects and relationship to platelet hyperserotonemia. Mol Psychiatry 7(8): 831-6.
Anderson SA, Marin O, Horn C, Jennings K, Rubenstein JL (2001). Distinct cortical migrations from the medial and lateral ganglionic eminences. Development 128(3): 353-63.
Anderson SA, Qiu M, Bulfone A, Eisenstat DD, Meneses J, Pedersen R, et al. (1997). Mutations of the homeobox genes Dlx-1 and Dlx-2 disrupt the striatal subventricular zone and differentiation of late born striatal neurons. Neuron 19(1): 27-37.
Andres C (2002). Molecular genetics and animal models in autistic disorder. Brain Res Bull 57(1): 109-19.
Aronson M, Hagberg B, Gillberg C (1997). Attention deficits and autistic spectrum problems in children exposed to alcohol during gestation: a follow-up study. Dev Med Child Neurol 39(9): 583-7.
Artiges E, Salame P, Recasens C, Poline JB, Attar-Levy D, De La Raillere A, et al. (2000). Working memory control in patients with schizophrenia: a PET study during a random number generation task. Am J Psychiatry 157(9): 1517-9.
Aylward EH, Minshew NJ, Field K, Sparks BF, Singh N (2002). Effects of age on brain volume and head circumference in autism. Neurology 59(2): 175-83.
Aylward EH, Minshew NJ, Goldstein G, Honeycutt NA, Augustine AM, Yates KO, et al. (1999). MRI volumes of amygdala and hippocampus in non-mentally retarded autistic adolescents and adults. Neurology 53(9): 2145-50.
Bacci A, Huguenard JR (2006). Enhancement of spike-timing precision by autaptic transmission in neocortical inhibitory interneurons. Neuron 49(1): 119-30.
Bailey A, Le Couteur A, Gottesman I, Bolton P, Simonoff E, Yuzda E, et al. (1995). Autism as a strongly genetic disorder: evidence from a British twin study. Psychol Med 25(1): 63-77.
Bailey A, Luthert P, Bolton P, Le Couteur A, Rutter M, Harding B (1993). Autism and megalencephaly. Lancet 341(8854): 1225-6.
Bailey A, Luthert P, Dean A, Harding B, Janota I, Montgomery M, et al. (1998). A clinicopathological study of autism. Brain 121 (Pt 5): 889-905.
Bailey A, Phillips W, Rutter M (1996). Autism: towards an integration of clinical, genetic, neuropsychological, and neurobiological perspectives. J Child Psychol Psychiatry 37(1): 89-126.
Barak Y, Kimhi R, Stien D, Gutman J, Weizinan A (1998). Autistic subjects with comorbid epilepsy: A possible association with viral infections. Child Psych Human Dev 29: 245-251.
Barbin G, Pollard H, Gaiarsa JL, Ben-Ari Y (1993). Involvement of GABAA receptors in the outgrowth of cultured hippocampal neurons. Neurosci Lett 152(1-2): 150-4.
Barlow HB (1972). Single units and sensation: a neuron doctrine for perceptual psychology? Perception 1(4): 371-94.
Baron-Cohen S (2002). The extreme male brain theory of autism. Trends Cogn Sci 6(6): 248-254.
Baron-Cohen S (2004). The cognitive neuroscience of autism. J Neurol Neurosurg Psychiatry 75(7): 945-8.
Baron-Cohen S, Leslie AM, Frith U (1985). Does the autistic child have a “theory of mind”? Cognition 21(1): 37-46.
Baron-Cohen S, Ring H, Moriarty J, Schmitz B, Costa D, Ell P (1994). Recognition of mental state terms. Clinical findings in children with autism and a functional neuroimaging study of normal adults. Br J Psychiatry 165(5): 640-9.
Baron-Cohen S, Ring HA, Wheelwright S, Bullmore ET, Brammer MJ, Simmons A, et al. (1999). Social intelligence in the normal and autistic brain: an fMRI study. Eur J Neurosci 11(6): 1891-8.
Baron-Cohen S, Wheelwright S (2004). The empathy quotient: an investigation of adults with Asperger syndrome or high functioning autism, and normal sex differences. J Autism Dev Disord 34(2): 163-75.
Bass MP, Menold MM, Wolpert CM, Donnelly SL, Ravan SA, Hauser ER, et al. (2000). Genetic studies in autistic disorder and chromosome 15. Neurogenetics 2(4): 219-26.
Bauman M, Kemper TL (1985). Histoanatomic observations of the brain in early infantile autism. Neurology 35(6): 866-74.
Bauman ML (1991). Microscopic neuroanatomic abnormalities in autism. Pediatrics 87(5 Pt 2): 791-6.
Bauman ML, Filipek PA, Kemper TL (1997). Early infantile autism. Int Rev Neurobiol 41: 367-86.
Bauman ML, Kemper TL (1987). Limbic involvement in a second case of early infantile autism. Neurology 37: 147.
Bauman ML, Kemper TL (1990). Limbic and cerebellar abnormalities are also present in an autistic child of normal intelligence. Neurology 40: 359.
Bauman ML, Kemper TL (1994). Neuroanatomic observations of the brain in autism. The neurobiology of autism. Baltimore, Johns Hopkins University**:** 119-145.
Bauman ML, Kemper TL (2005). Structural brain anatomy in autism: what is the evidence?. The Neurobiology of Autism. Bauman ML and Kemper TL. Maryland, The Johns Hopkins University Press. 2**:** 121-135.
Beaulieu C (1993). Numerical data on neocortical neurons in adult rat, with special reference to the GABA population. Brain Research 609(1-2): 284.
Beaulieu C, Colonnier M (1989). Number and size of neurons and synapses in the motor cortex of cats raised in different environmental complexities. J Comp Neurol. 289(1): 178-181.
Behar TN, Li YX, Tran HT, Ma W, Dunlap V, Scott C, et al. (1996). GABA stimulates chemotaxis and chemokinesis of embryonic cortical neurons via calcium-dependent mechanisms. J Neurosci 16(5): 1808-18.

Behar TN, Schaffner AE, Scott CA, Greene CL, Barker JL (2000). GABA receptor antagonists modulate postmitotic cell migration in slice cultures of embryonic rat cortex. Cereb Cortex 10(9): 899-909.
Behar TN, Schaffner AE, Scott CA, O'Connell C, Barker JL (1998). Differential response of cortical plate and ventricular zone cells to GABA as a migration stimulus. J Neurosci 18(16): 6378-87.
Belmonte MK, Allen G, Beckel-Mitchener A, Boulanger LM, Carper RA, Webb SJ (2004). Autism and abnormal development of brain connectivity. J Neurosci 24(42): 9228-31.
Ben-Ari Y (2001). Developing networks play a similar melody. Trends Neurosci 24(6): 353-60.
Ben-Ari Y (2002). Excitatory actions of gaba during development: the nature of the nurture. Nat Rev Neurosci 3(9): 728-39.
Ben-Ari Y, Cherubini E, Corradetti R, Gaiarsa JL (1989). Giant synaptic potentials in immature rat CA3 hippocampal neurons. J Physiol 416: 303-25.
Ben-Ari Y, Khalilov I, Represa A, Gozlan H (2004). Interneurons set the tune of developing networks. Trends Neurosci 27(7): 422-7.
Ben-Yaakov G, Golan H (2003). Cell proliferation in response to GABA in postnatal hippocampal slice culture. Int J Dev Neurosci 21(3): 153-7.
Benes FM, Vincent SL, Todtenkopf M (2001). The density of pyramidal and nonpyramidal neurons in anterior cingulate cortex of schizophrenic and bipolar subjects. Biol Psychiatry 50(6): 395-406.
Benowitz LI, Bear DM, Rosenthal R, Mesulam MM, Zaidel E, Sperry RW (1983). Hemispheric specialization in nonverbal communication. Cortex 19(1): 5-11.
Bespalova IN, Buxbaum JD (2003). Disease susceptibility genes for autism. Ann Med 35(4): 274-81.
Blatt GJ, Fitzgerald CM, Guptill JT, Booker AB, Kemper TL, Bauman ML (2001). Density and distribution of hippocampal neurotransmitter receptors in autism: an autoradiographic study. J Autism Dev Disord 31(6): 537-43.
Boddaert N, Zilbovicius M (2002). Functional neuroimaging and childhood autism. Pediatr Radiol 32(1): 1-7.
Bodfish JW, Symons FJ, Parker DE, Lewis MH (2000). Varieties of repetitive behavior in autism: comparisons to mental retardation. J Autism Dev Disord 30(3): 237-43.
Bolte S, Hubl D, Feineis-Matthews S, Prvulovic D, Dierks T, Poustka F (2006). Facial affect recognition training in autism: can we animate the fusiform gyrus? Behav Neurosci 120(1): 211-6.
Bonora E, Beyer KS, Lamb JA, Parr JR, Klauck SM, Benner A, et al. (2003). Analysis of reelin as a candidate gene for autism. Mol Psychiatry 8(10): 885-92.
Braak H (1980). Architectonics of the Human Telencephalic cortex. Berlin, Springer-Verlag.
Braak H, Braak E (1995). Staging of Alzheimer's disease-related neurofibrillary changes. Neurobiol Aging 16(3): 271-8; discussion 278-84.
Braitenberg V, Schuz A (1998). Cortex : Statistics and Geometry of Neuronal Connectivity. Berlin, Springer-Verlag.
Brock J, Brown CC, Boucher J, Rippon G (2002). The temporal binding deficit hypothesis of autism. Dev Psychopathol 14(2): 209-24.
Brodmann K (1909). Vergleichende Lokalisationslehre der Grosshirnrinde. Leipzig, Barth.
Brown C (2005). EEG in autism: is there just too much going on in there? Neocortical modularity and the cell minicolumn. Casanova MF. New York, NOVA Science Publishers**:** 109-126.
Bulfone A, Puelles L, Porteus MH, Frohman MA, Martin GR, Rubenstein JL (1993). Spatially restricted expression of Dlx-1, Dlx-2 (Tes-1), Gbx-2, and Wnt-3 in the embryonic day 12.5 mouse forebrain defines potential transverse and longitudinal segmental boundaries. J Neurosci 13(7): 3155-72.
Buxbaum JD, Silverman JM, Smith CJ, Greenberg DA, Kilifarski M, Reichert J, et al. (2002). Association between a GABRB3 polymorphism and autism. Mol Psychiatry 7(3): 311-6.
Buxhoeveden D, Casanova MF (2004). Accelerated maturation in brains of patients with Down syndrome. J Intellect Disabil Res. 48(Pt 7): 704-5.
Buxhoeveden D, Fobbs A, Roy E, Casanova M (2002). Quantitative comparison of radial cell columns in children with Down's syndrome and controls. J Intellect Disabil Res 46(Pt 1): 76-81.
Buxhoeveden DP, Casanova MF (2000). Comparative lateralisation patterns in the language area of human, chimpanzee, and rhesus monkey brains. Laterality 5(4): 315-30.
Buxhoeveden DP, Casanova MF (2002a). The minicolumn and evolution of the brain. Brain Behav Evol. 60(3): 125-51.
Buxhoeveden DP, Casanova MF (2002b). The minicolumn hypothesis in neuroscience. Brain 125(Pt 5): 935-51.
Buxhoeveden DP, Casanova MF (2005). The cell column in comparative anatomy. New York, NY, Nova Science Publishers, Inc.
Canitano R (2007). Epilepsy in autism spectrum disorders. Eur Child Adolesc Psychiatry 16(1): 61-6.
Capps L, Yirmiya N, Sigman M (1992). Understanding of simple and complex emotions in non-retarded children with autism. J Child Psychol Psychiatry 33(7): 1169-82.
Carpenter M (1985). Core text of neuroanatomy. Baltimore, Williams and Wilkins.
Carper RA, Courchesne E (2005). Localized enlargement of the frontal cortex in early autism. Biol Psychiatry 57(2): 126-33.
Carper RA, Moses P, Tigue ZD, Courchesne E (2002). Cerebral Lobes in Autism: Early Hyperplasia and Abnormal Age Effects. NeuroImage 16(4): 1038.
Carter CS, MacDonald AW, 3rd, Ross LL, Stenger VA (2001). Anterior cingulate cortex activity and impaired self-monitoring of performance in patients with schizophrenia: an event-related fMRI study. Am J Psychiatry 158(9): 1423-8.
Carter CS, Mintun M, Nichols T, Cohen JD (1997). Anterior cingulate gyrus dysfunction and selective attention deficits in schizophrenia: [15O]H2O PET study during single-trial Stroop task performance. Am J Psychiatry 154(12): 1670-5.
Caruncho HJ, Dopeso-Reyes IG, Loza MI, Rodriguez MA (2004). A GABA, reelin, and the neurodevelopmental hypothesis of schizophrenia. Crit Rev Neurobiol 16(1-2): 25-32.
Casanova MF (2004). White matter volume increase and minicolumns in autism. Ann Neurol 56(3): 453; author reply 454.
Casanova MF (2006). Neuropathological and genetic findings in autism: the significance of a putative minicolumnopathy. Neuroscientist 12(5): 435-41.
Casanova MF, Buxhoeveden D, Gomez J (2003). Disruption in the inhibitory architecture of the cell minicolumn: implications for autism. Neuroscientist 9(6): 496-507.
Casanova MF, Buxhoeveden DP, Switala AE, Roy E (2002a). Minicolumnar pathology in autism. Neurology 58(3): 428-32.
Casanova MF, Buxhoeveden DP, Switala AE, Roy E (2002b). Neuronal density and architecture (Gray Level Index) in the brains of autistic patients. J Child Neurol 17(7): 515-21.

Casanova MF, de Zeeuw L, Switala A, Kreczmanski P, Korr H, Ulfig N, et al. (2005). Mean cell spacing abnormalities in the neocortex of patients with schizophrenia. Psychiatry Res 133(1): 1-12.
Casanova MF, Kreczmanski P, Trippe J, 2nd, Switala A, Heinsen H, Steinbusch HW, et al. (2008). Neuronal distribution in the neocortex of schizophrenic patients. Psychiatry Res 158(3): 267-77.
Casanova MF, Switala AE (2005). Minicolumnar Morphometry: Computerized Image Analysis. Neocortical Modularity and the Cell Minicolumns. Casanova MF. New York, NY, Nova Science Publishers**:** 161-180.
Casanova MF, van Kooten IA, Switala AE, van Engeland H, Heinsen H, Steinbusch HW, et al. (2006). Minicolumnar abnormalities in autism. Acta Neuropathol (Berl) 112(3): 287-303.
Casarosa S, Fode C, Guillemot F (1999). Mash1 regulates neurogenesis in the ventral telencephalon. Development 126(3): 525-34.
Castelli F, Frith C, Happe F, Frith U (2002). Autism, Asperger syndrome and brain mechanisms for the attribution of mental states to animated shapes. Brain 125(Pt 8): 1839-49.
Cavalieri B (1635 (reprinted in 1966 as Geometrica degli Indivisibili. Unione Tipografico-editrice Torinese, Torino). Geometrica Indivisibilibus continuorum Bonoiae, Typis Clementis Ferronij.
Changizi MA (2001). Principles underlying mammalian neocortical scaling. Biol Cybern 84(3): 207-15.
Chen G, Trombley PQ, van den Pol AN (1995). GABA receptors precede glutamate receptors in hypothalamic development; differential regulation by astrocytes. J Neurophysiol 74(4): 1473-84.
Chenn A, Walsh CA (2002). Regulation of Cerebral Cortical Size by Control of Cell Cycle Exit in Neural Precursors. Science 297(5580): 365-369.
Chess S (1977). Follow-up report on autism in congenital rubella. J Autism Child Schizophr 7(1): 69-81.
Chih B, Afridi SK, Clark L, Scheiffele P (2004). Disorder-associated mutations lead to functional inactivation of neuroligins. Hum Mol Genet 13(14): 1471-7.
Chklovskii DB, Koulakov AA (2004). Maps in the brain: What Can We Learn from Them? Annual Review of Neuroscience 27(1): 369-392.
Ciaranello AL, Ciaranello RD (1995). The neurobiology of infantile autism. Annu Rev Neurosci 18: 101-28.
Cohen BI (1999). Elevated levels of plasma and urine gamma-aminobutyric acid - a case study for an autistic child. Autism 3: 437-440.
Cohen BI (2000). Infantile autism and the liver - a possible connection. Autism 4: 441-442.
Cohen BI (2002). Use of a GABA-transaminase agonist for treatment of infantile autism. Med Hypotheses 59(1): 115-6.
Coleman PD, Romano J, Lapham L, Simon W (1985). Cell counts in cerebral cortex of an autistic patient. J Autism Dev Disord 15(3): 245-55.
Colon EJ (1972). Quantitative cytoarchitectonics of the human cerebral cortex in schizophrenic dementia. Acta Neuropathol 20: 1-10.
Comery TA, Harris JB, Willems PJ, Oostra BA, Irwin SA, Weiler IJ, et al. (1997). Abnormal dendritic spines in fragile X knockout mice: maturation and pruning deficits. Proc Natl Acad Sci U S A 94(10): 5401-4.
Comoletti D, De Jaco A, Jennings LL, Flynn RE, Gaietta G, Tsigelny I, et al. (2004). The Arg451Cys-neuroligin-3 mutation associated with autism reveals a defect in protein processing. J Neurosci 24(20): 4889-93.
Connell S, Karikari C, Hohmann CF (2004). Sex-specific development of cortical monoamine levels in mouse. Brain Res Dev Brain Res 151(1-2): 187-91.
Cook EH, Jr., Courchesne RY, Cox NJ, Lord C, Gonen D, Guter SJ, et al. (1998). Linkage-disequilibrium mapping of autistic disorder, with 15q11-13 markers. Am J Hum Genet 62(5): 1077-83.
Cook EH, Leventhal BL (1996). The serotonin system in autism. Curr Opin Pediatr 8(4): 348-54.
Costa LG, Aschner M, Vitalone A, Syversen T, Soldin OP (2004). Developmental neuropathology of environmental agents. Annu Rev Pharmacol Toxicol 44: 87-110.
Courchesne E (1997). Brainstem, cerebellar and limbic neuroanatomical abnormalities in autism. Curr Opin Neurobiol 7(2): 269-78.
Courchesne E (2004). Brain development in autism: Early overgrowth followed by premature arrest of growth. Ment Retard Dev Disabil Res Rev 10(2): 106-11.
Courchesne E, Carper R, Akshoomoff N (2003). Evidence of brain overgrowth in the first year of life in autism. Jama 290(3): 337-44.
Courchesne E, Karns CM, Davis HR, Ziccardi R, Carper RA, Tigue ZD, et al. (2001). Unusual brain growth patterns in early life in patients with autistic disorder: an MRI study. Neurology 57(2): 245-54.
Courchesne E, Muller RA, Saitoh O (1999). Brain weight in autism: normal in the majority of cases, megalencephalic in rare cases. Neurology 52(5): 1057-9.
Courchesne E, Pierce K (2005). Why the frontal cortex in autism might be talking only to itself: local over-connectivity but long-distance disconnection. Curr Opin Neurobiol 15(2): 225-30.
Courchesne E, Pierce K, Schumann CM, Redcay E, Buckwalter JA, Kennedy DP, et al. (2007). Mapping early brain development in autism. Neuron 56(2): 399-413.
Courchesne E, Redcay E, Kennedy DP (2004). The autistic brain: birth through adulthood. Curr Opin Neurol 17(4): 489-96.
Craig AD (2002). How do you feel? Interoception: the sense of the physiological condition of the body. Nat Rev Neurosci 3: 655-66.
Crespo-Facorro B, Kim J, Andreasen NC, O'Leary DS, Bockholt HJ, Magnotta V (2000). Insular cortex abnormalities in schizophrenia: a structural magnetic resonance imaging study of first-episode patients. Schizophr Res 46(1): 35-43.
Curran T, D'Arcangelo G (1998). Role of reelin in the control of brain development. Brain Res Brain Res Rev 26(2-3): 285-94.
Curtis VA, Bullmore ET, Brammer MJ, Wright IC, Williams SC, Morris RG, et al. (1998). Attenuated frontal activation during a verbal fluency task in patients with schizophrenia. Am J Psychiatry 155(8): 1056-63.
Dalton KM, Nacewicz BM, Johnstone T, Schaefer HS, Gernsbacher MA, Goldsmith HH, et al. (2005). Gaze fixation and the neural circuitry of face processing in autism. Nat Neurosci 8(4): 519-26.
Davidovitch M, Patterson B, Gartside P (1996). Head circumference measurements in children with autism. J Child Neurol 11(5): 389-93.
Deacon TW (1990). Rethinking mammalian brain evolution. Am Zool 30: 629-705.
DeFelipe J (1997). Types of neurons, synaptic connections and chemical characteristics of cells immunoreactive for calbindin-D28K, parvalbumin and calretinin in the neocortex. J Chem Neuroanat 14(1): 1-19.
Del Rio JA, Martinez A, Auladell C, Soriano E (2000). Developmental history of the subplate and developing white matter in the murine neocortex. Neuronal organization and relationship with the main afferent systems at embryonic and perinatal stages. Cereb Cortex 10(8): 784-801.

Desmond MM, Wilson GS, Melnick JL, Singer DB, Zion TE, Rudolph AJ, et al. (1967). Congenital rubella encephalitis. Course and early sequelae. J Pediatr 71(3): 311-31.
Dhossche D, Applegate H, Abraham A, Maertens P, Bland L, Bencsath A, et al. (2002). Elevated plasma gamma-aminobutyric acid (GABA) levels in autistic youngsters: stimulus for a GABA hypothesis of autism. Med Sci Monit 8(8): PR1-6.
DiCicco-Bloom E, Lord C, Zwaigenbaum L, Courchesne E, Dager SR, Schmitz C, et al. (2006). The developmental neurobiology of autism spectrum disorder. J Neurosci 26(26): 6897-906.
Dietz D, Vogel M, Rubin S, Moran T, Carbone K, Pletnikov M (2004). Developmental alterations in serotoninergic neurotransmission in Borna disease virus (BDV)-infected rats: a multidisciplinary analysis. J Neurovirol 10(5): 267-77.
Dolan RJ, Fletcher P, Frith CD, Friston KJ, Frackowiak RS, Grasby PM (1995). Dopaminergic modulation of impaired cognitive activation in the anterior cingulate cortex in schizophrenia. Nature 378(6553): 180-2.
Duffy JD, Campbell JJ (2001). Regional prefrontal syndromes: a theoretical and clinical overview. Washington, DC, American Psychiatruc Publishing company.
Duggal HS, Muddasani S, Keshavan MS (2005). Insular volumes in first-episode schizophrenia: gender effect. Schizophr Res 73(1): 113-20.
Dunbar RIM (1998). The social brain hypothesis. Evol Anthropol 6: 178-190.
Eisenstat DD, Liu JK, Mione M, Zhong W, Yu G, Anderson SA, et al. (1999). DLX-1, DLX-2, and DLX-5 expression define distinct stages of basal forebrain differentiation. J Comp Neurol 414(2): 217-37.
Eliason DA, Cohen SA, Baratta J, Yu J, Robertson RT (2002). Local proliferation of microglia cells in response to neocortical injury in vitro. Brain Res Dev Brain Res 137(1): 75-9.
Evans PD, Anderson JR, Vallender EJ, Gilbert SL, Malcom CM, Dorus S, et al. (2004). Adaptive evolution of ASPM, a major determinant of cerebral cortical size in humans. Hum Mol Genet 13(5): 489-94.
Fairhall SL, Ishai A (2007). Effective connectivity within the distributed cortical network for face perception. Cereb Cortex 17(10): 2400-6.
Farrer C, Franck N, Frith CD, Decety J, Georgieff N, d'Amato T, et al. (2004). Neural correlates of action attribution in schizophrenia. Psychiatry Res 131(1): 31-44.
Fatemi SH (2002). The role of Reelin in pathology of autism. Mol Psychiatry 7(9): 919-20.
Fatemi SH (2004). Reelin glycoprotein: structure, biology and roles in health and disease. Mol Psychiatry.
Fatemi SH (2005). Prenatal human influenza viral infection, brain development, and schizophrenia. Neuropsychiatric disorders and infection. Fatemi SH. United Kingdom, Taylor and Francis**:** 66-82.
Fatemi SH, Cuadra AE, El-Fakahany EE, Sidwell RW, Thuras P (2000a). Prenatal viral infection causes alterations in nNOS expression in developing mouse brains. Neuroreport 11(7): 1493-6.
Fatemi SH, Earle J, Kanodia R, Kist D, Emamian ES, Patterson PH, et al. (2002a). Prenatal viral infection leads to pyramidal cell atrophy and macrocephaly in adulthood: implications for genesis of autism and schizophrenia. Cell Mol Neurobiol 22(1): 25-33.
Fatemi SH, Earle JA, McMenomy T (2000b). Reduction in Reelin immunoreactivity in hippocampus of subjects with schizophrenia, bipolar disorder and major depression. Mol Psychiatry 5(6): 654-63, 571.
Fatemi SH, Emamian ES, Kist D, Sidwell RW, Nakajima K, Akhter P, et al. (1999). Defective corticogenesis and reduction in Reelin immunoreactivity in cortex and hippocampus of prenatally infected neonatal mice. Mol Psychiatry 4(2): 145-54.
Fatemi SH, Halt AR (2001). Altered levels of Bcl2 and p53 proteins in parietal cortex reflect deranged apoptotic regulation in autism. Synapse 42(4): 281-4.
Fatemi SH, Halt AR, Realmuto G, Earle J, Kist DA, Thuras P, et al. (2002b). Purkinje cell size is reduced in cerebellum of patients with autism. Cell Mol Neurobiol 22(2): 171-5.
Fatemi SH, Halt AR, Stary JM, Kanodia R, Schulz SC, Realmuto GR (2002c). Glutamic acid decarboxylase 65 and 67 kDa proteins are reduced in autistic parietal and cerebellar cortices. Biol Psychiatry 52(8): 805-10.
Fatemi SH, Halt AR, Stary JM, Realmuto GM, Jalali-Mousavi M (2001). Reduction in anti-apoptotic protein Bcl-2 in autistic cerebellum. Neuroreport 12(5): 929-33.
Fatemi SH, Pearce DA, Brooks AI, Sidwell RW (2005a). Prenatal viral infection in mouse causes differential expression of genes in brains of mouse progeny: A potential animal model for schizophrenia and autism. Synapse 57(2): 91-99.
Fatemi SH, Sidwell R, Kist D, Akhter P, Meltzer HY, Bailey K, et al. (1998). Differential expression of synaptosome-associated protein 25 kDa [SNAP-25] in hippocampi of neonatal mice following exposure to human influenza virus in utero. Brain Res 800(1): 1-9.
Fatemi SH, Snow AV, Stary JM, Araghi-Niknam M, Reutiman TJ, Lee S, et al. (2005b). Reelin signaling is impaired in autism. Biol Psychiatry 57(7): 777-87.
Feldman ML, Peters A (1974). A study of barrels and pyramidal dendritic clusters in the cerebral cortex. Brain Research 77(1): 55.
Field D (1994). What is the goal of sensory coding? Neural Comput. 6: 559-601.
Finlay BL, Darlington RB (1995). Linked regularities in the development and evolution of mammalian brains. Science 268(5217): 1578-84.
Fiszman ML, Borodinsky LN, Neale JH (1999). GABA induces proliferation of immature cerebellar granule cells grown in vitro. Brain Res Dev Brain Res 115(1): 1-8.
Fode C, Ma Q, Casarosa S, Ang SL, Anderson DJ, Guillemot F (2000). A role for neural determination genes in specifying the dorsoventral identity of telencephalic neurons. Genes Dev 14(1): 67-80.
Fombonne E (2000). Is a large head circumference a sign of autism? J Autism Dev Disord 30(4): 365.
Fombonne E (2006). Past and future perspectives on autism epidemiology. Understanding Autism. From Basic Neuroscience to Treatment. Moldin SO and Rubenstein JL. Boca Raton, Taylor & Francis
Frith C (2003). What do imaging studies tell us about the neural basis of autism? Novartis Found Symp 251: 149-66; discussion 166-76, 281-97.
Frith C (2004). Is autism a disconnection disorder? Lancet Neurol 3(10): 577.
Fritschy JM, Paysan J, Enna A, Mohler H (1994). Switch in the expression of rat GABAA-receptor subtypes during postnatal development: an immunohistochemical study. J Neurosci 14(9): 5302-24.
Fuster J (2003). Cortex and Mind: Unifying cognition. Oxford, Oxford University Press.
Galvez R, Gopal AR, Greenough WT (2003). Somatosensory cortical barrel dendritic abnormalities in a mouse model of the fragile X mental retardation syndrome. Brain Res 971(1): 83-9.
Garber K (2007). Neuroscience. Autism's cause may reside in abnormalities at the synapse. Science 317(5835): 190-1.

Garreau B, Herry D, Zilbovicius M, Samson Y, Guerin P, Lelord G (1993). Theoretical aspects of the study of benzodiazepine receptors in infantile autism. Acta Paedopsychiatr 56(2): 133-8.
Gaspar P, Cases O, Maroteaux L (2003). The developmental role of serotonin: news from mouse molecular genetics. Nat Rev Neurosci 4(12): 1002-12.
Geary DC (2005). The origin of mind: Evolution of brain, cognition, and general intelligence. Washington, DC, Americam Psychiatruc Association.
Gharani N, Benayed R, Mancuso V, Brzustowicz LM, Millonig JH (2004). Association of the homeobox transcription factor, ENGRAILED 2, 3, with autism spectrum disorder. Mol Psychiatry 9(5): 474-84.
Gillberg C (1999). Neurodevelopmental processes and psychological functioning in autism. Dev Psychopathol 11(3): 567-87.
Gingrich JA, Ansorge MS, Merker R, Weisstaub N, Zhou M (2003). New lessons from knockout mice: The role of serotonin during development and its possible contribution to the origins of neuropsychiatric disorders. CNS Spectr 8(8): 572-7.
Girgis RR, Minshew NJ, Melhem NM, Nutche JJ, Keshavan MS, Hardan AY (2007). Volumetric alterations of the orbitofrontal cortex in autism. Prog Neuropsychopharmacol Biol Psychiatry 31(1): 41-5.
Gittins R, Harrison PJ (2004a). Neuronal density, size and shape in the human anterior cingulate cortex: a comparison of Nissl and NeuN staining. Brain Res Bull 63(2): 155-60.
Gittins R, Harrison PJ (2004b). A quantitative morphometric study of the human anterior cingulate cortex. Brain Res 1013(2): 212-22.
Glaser J, Greene G, Hendricks S (2007). Stereology for Biological Research. Williston, MBF Press.
Glasson EJ, Bower C, Petterson B, de Klerk N, Chaney G, Hallmayer JF (2004). Perinatal factors and the development of autism: a population study. Arch Gen Psychiatry 61(6): 618-27.
Goddard AW, Mason GF, Almai A, Rothman DL, Behar KL, Petroff OA, et al. (2001). Reductions in occipital cortex GABA levels in panic disorder detected with 1h-magnetic resonance spectroscopy. Arch Gen Psychiatry 58(6): 556-61.
Goldman-Rakic PS (1988). Changing concepts of cortical connectivity: parallel distributed networks. Neurobiology of neocortex. Rakic P and Singer W. New York, NY, John Wiley**:** 177-202.
Goldman-Rakic PS (1993). Specification of higher cortical functions. J Head Trauma Rehabil 8: 15-23.
Goldman-Rakic PS, Selemon LD (1997). Functional and anatomical aspects of prefrontal pathology in schizophrenia. Schizophr Bull 23(3): 437-58.
Goldman RS, Emberger KM, Smet IC, Singh M, Keefe RSE (2004). Cognitive neuroscience an Neuropsychology. Psychiatry. Tasman A, Kay J and Lieberman JA. New York, NY, John Wiley**:** 363-402.
Gomez TM, Spitzer NC (1999). In vivo regulation of axon extension and pathfinding by growth-cone calcium transients. Nature 397(6717): 350-5.
Gonzalez JL, Russo CJ, Goldowitz D, Sweet HO, Davisson MT, Walsh CA (1997). Birthdate and cell marker analysis of scrambler: a novel mutation affecting cortical development with a reeler-like phenotype. J Neurosci 17(23): 9204-11.
Goodhill GJ (1997). Stimulating issues in cortical map development. Trends Neurosci 20(9): 375-6.
Grandin T (2005). A personal perspective of Autism. Handbook of Autism and Pervasive Developmental Disorders. Volkmar F, Paul R, Klin A and Cohen D. New Jersey, John Wiley and Sons. II**:** 1276-1286.
Grelotti DJ, Gauthier I, Schultz RT (2002). Social interest and the development of cortical face specialization: what autism teaches us about face processing. Dev Psychobiol 40(3): 213-25.
Gressens P, Evrard P (1993). The glial fascicle: an ontogenic and phylogenic unit guiding, supplying and distributing mammalian cortical neurons. Brain Res Dev Brain Res. 76(2): 272-277.
Guerin P, Lyon G, Barthelemy C, Sostak E, Chevrollier V, Garreau B, et al. (1996). Neuropathological study of a case of autistic syndrome with severe mental retardation. Dev Med Child Neurol 38(3): 203-11.
Guidotti A, Auta J, Davis JM, Di-Giorgi-Gerevini V, Dwivedi Y, Grayson DR, et al. (2000). Decrease in reelin and glutamic acid decarboxylase67 (GAD67) expression in schizophrenia and bipolar disorder: a postmortem brain study. Arch Gen Psychiatry 57(11): 1061-9.
Guillemot F, Joyner AL (1993). Dynamic expression of the murine Achaete-Scute homologue Mash-1 in the developing nervous system. Mech Dev 42(3): 171-85.
Gundersen HJ (1988). The nucleator. J Microsc 151(Pt 1): 3-21.
Gundersen HJ, Jensen EB (1987). The efficiency of systematic sampling in stereology and its prediction. J Microsc 147(Pt 3): 229-63.
Gupta A, Wang Y, Markram H (2000). Organizing principles for a diversity of GABAergic interneurons and synapses in the neocortex. Science 287(5451): 273-8.
Hadjikhani N, Joseph RM, Snyder J, Chabris CF, Clark J, Steele S, et al. (2004). Activation of the fusiform gyrus when individuals with autism spectrum disorder view faces. Neuroimage 22(3): 1141-50.
Hadjikhani N, Joseph RM, Snyder J, Tager-Flusberg H (2007). Abnormal activation of the social brain during face perception in autism. Hum Brain Mapp 28(5): 441-9.
Hahnloser RHR, Kozhevnikov AA, Fee MS (2002). An ultra-sparse code underliesthe generation of neural sequences in a songbird. Nature 419(6902): 65.
Hall GB, Szechtman H, Nahmias C (2003). Enhanced salience and emotion recognition in Autism: a PET study. Am J Psychiatry 160(8): 1439-41.
Hansen GH, Meier E, Abraham J, Schousboe A (1987). Trophic effects of GABA on cerebellar granule cells in culture. Neurology and neurobiology; Neurotrophic activity of GABA during development. Redbum DA and Schousboe A. New York, Liss. 32**:** 109-138.
Happe F (1999). Autism: cognitive deficit or cognitive style? Trends Cogn Sci 3(6): 216-222.
Hardan AY, Girgis RR, Lacerda AL, Yorbik O, Kilpatrick M, Keshavan MS, et al. (2006). Magnetic resonance imaging study of the orbitofrontal cortex in autism. J Child Neurol 21(10): 866-71.
Hardan AY, Minshew NJ, Mallikarjuhn M, Keshavan MS (2001). Brain volume in autism. J Child Neurol 16(6): 421-4.
Harris GJ, Chabris CF, Clark J, Urban T, Aharon I, Steele S, et al. (2006). Brain activation during semantic processing in autism spectrum disorders via functional magnetic resonance imaging. Brain Cogn 61(1): 54-68.
Hashimoto T, Tayama M, Murakawa K, Yoshimoto T, Miyazaki M, Harada M (1995). Development of the brainstem and cerebellum in autistic patients. J Autism Dev Disord 25: 1-18.
Hatten ME (1999). Central nervous system neuronal migration. Annu Rev Neurosci 22: 511-39.

Hawkins J (2004). On Intelligence. New York, Times Books.
Hayashi M, Ito M, Shimizu K (2001). The spindle neurons are present in the cingulate cortex of chimpanzee fetus. Neurosci Lett 309(2): 97-100.
Haydar TF, Wang F, Schwartz ML, Rakic P (2000). Differential modulation of proliferation in the neocortical ventricular and subventricular zones. J Neurosci 20(15): 5764-74.
Haznedar MM, Buchsbaum MS, Luu C, Hazlett EA, Siegel BV, Jr., Lohr J, et al. (1997a). Decreased anterior cingulate gyrus metabolic rate in schizophrenia. Am J Psychiatry 154(5): 682-4.
Haznedar MM, Buchsbaum MS, Metzger M, Solimando A, Spiegel-Cohen J, Hollander E (1997b). Anterior cingulate gyrus volume and glucose metabolism in autistic disorder. Am J Psychiatry 154(8): 1047-50.
Haznedar MM, Buchsbaum MS, Wei TC, Hof PR, Cartwright C, Bienstock CA, et al. (2000). Limbic circuitry in patients with autism spectrum disorders studied with positron emission tomography and magnetic resonance imaging. Am J Psychiatry 157(12): 1994-2001.
Heinsen H, Arzberger T, Schmitz C (2000). Celloidin mounting (embedding without infiltration) - a new, simple and reliable method for producing serial sections of high thickness through complete human brains and its application to stereological and immunohistochemical investigations. J Chem Neuroanat 20(1): 49-59.
Heinsen H, Beckmann H, Heinsen YL, Gallyas F, Haas S, Scharff G (1989). Laminar neuropathology in Alzheimer's disease by a modified Gallyas impregnation. Psychiatry Res 29(3): 463-5.
Heinsen H, Heinsen YL (1991). Serial thick, frozen, Gallocyanin stained sections of human central nervous system. J Histotechol 14: 167-173.
Heinsen H, Henn R, Eisenmenger W, Gotz M, Bohl J, Bethke B, et al. (1994). Quantitative investigations on the human entorhinal area: left-right asymmetry and age-related changes. Anat Embryol (Berl) 190(2): 181-94.
Herbert MR, Harris GJ, Adrien KT, Ziegler DA, Makris N, Kennedy DN, et al. (2002). Abnormal asymmetry in language association cortex in autism. Ann Neurol 52(5): 588-96.
Herbert MR, Ziegler DA, Makris N, Filipek PA, Kemper TL, Normandin JJ, et al. (2004). Localization of white matter volume increase in autism and developmental language disorder. Annals of Neurology 55(4): 530-540.
Herlenius E, Lagercrantz H (2001). Neurotransmitters and neuromodulators during early human development. Early Hum Dev 65(1): 21-37.
Herlenius E, Lagercrantz H (2004). Development of neurotransmitter systems during critical periods. Exp Neurol 190 Suppl 1: S8-21.
Hill EL, Frith U (2003). Understanding autism: insights from mind and brain. Philos Trans R Soc Lond B Biol Sci 358(1430): 281-9.
Hof PR, Haroutunian V, Friedrich VL, Jr., Byne W, Buitron C, Perl DP, et al. (2003). Loss and altered spatial distribution of oligodendrocytes in the superior frontal gyrus in schizophrenia. Biol Psychiatry 53(12): 1075-85.
Hof PR, Schmitz C (2000). Current trends in neurostereology - introduction to the special issue "Recent advances in neurostereology". J Chem Neuroanat 20(1): 3-5.
Hof PR, Van der Gucht E (2007). Structure of the cerebral cortex of the humpback whale, Megaptera novaeangliae (Cetacea, Mysticeti, Balaenopteridae). Anat Rec 290: 1-31.
Hofman MA (1985). Neuronal correlates of corticalization in mammals: a theory. J Theor Biol 112(1): 77-95.
Hofman MA (2001). Brain evolution in hominoids: are we at the end of the roof? Evolutionary anantomy of the rpimate cerebral cortex. Falk D and Gibson KR. Cambridge, UK, Cambridge University Press**:** 113-127.
Hohmann CF, Berger-Sweeney J (1998). Cholinergic regulation of cortical development and plasticity. New twists to an old story. Perspect Dev Neurobiol 5(4): 401-25.
Holloway RL, Jr. (1968). The evolution of the primate brain: some aspects of quantitative relations. Brain Res 7(2): 121-72.
Holmes GL (2002). Seizure-induced neuronal injury: animal data. Neurology 59(9 Suppl 5): S3-6.
Hornig M, Briese T, Lipkin WI (2003). Borna disease virus. J Neurovirol 9(2): 259-73.
Hornig M, Mervis R, Hoffman K, Lipkin WI (2002). Infectious and immune factors in neurodevelopmental damage. Mol Psychiatry 7 Suppl 2: S34-5.
Horwitz B, Rumsey JM, Grady CL, Rapoport SI (1988). The cerebral metabolic landscape in autism. Intercorrelations of regional glucose utilization. Arch Neurol 45(7): 749-55.
Howard MA, Cowell PE, Boucher J, Broks P, Mayes A, Farrant A, et al. (2000). Convergent neuroanatomical and behavioural evidence of an amygdala hypothesis of autism. Neuroreport 11(13): 2931-5.
Hubel DH, Wiesel TN (1962). Receptive fields, binocular interaction and functional architecture in the cat's visual cortex. J Physiol 160: 106-54.
Hubl D, Bolte S, Feineis-Matthews S, Lanfermann H, Federspiel A, Strik W, et al. (2003). Functional imbalance of visual pathways indicates alternative face processing strategies in autism. Neurology 61(9): 1232-7.
Hulshoff Pol HE, Schnack HG, Mandl RC, van Haren NE, Koning H, Collins DL, et al. (2001). Focal gray matter density changes in schizophrenia. Arch Gen Psychiatry 58(12): 1118-25.
Hultman CM, Sparen P, Cnattingius S (2002). Perinatal risk factors for infantile autism. Epidemiology 13(4): 417-23.
Huntley GW, Benson DL, Jones EG, Isackson PJ (1992). Developmental expression of brain derived neurotrophic factor mRNA by neurons of fetal and adult monkey prefrontal cortex. Brain Res Dev Brain Res 70(1): 53-63.
Hutsler J, Galuske RA (2003). Hemispheric asymmetries in cerebral cortical networks. Trends Neurosci 26(8): 429-35.
Hyman SL, Arndt T, Rodier PM (2006). Environmental Agents and Autism: Once and future associations. Int J Mental Retard Res Rev 30: 171-194.
Ingram JL, Peckham SM, Tisdale B, Rodier PM (2000). Prenatal exposure of rats to valproic acid reproduces the cerebellar anomalies associated with autism. Neurotoxicol Teratol 22(3): 319-24.
International Molecular Genetic Study of Autism Consortium (IMGSAC) (2001). A genomewide screen for autism: strong evidence for linkage to chromosomes 2q, 7q, and 16q. Am J Hum Genet 69: 570-81
Irving WL, James DK, Stephenson T, Laing P, Jameson C, Oxford JS, et al. (2000). Influenza virus infection in the second and third trimesters of pregnancy: a clinical and seroepidemiological study. Bjog 107(10): 1282-9.
Irwin SA, Patel B, Idupulapati M, Harris JB, Crisostomo RA, Larsen BP, et al. (2001). Abnormal dendritic spine characteristics in the temporal and visual cortices of patients with fragile-X syndrome: a quantitative examination. Am J Med Genet 98(2): 161-7.
Jacobsen M (1991). Developmental Neurobiology. New York, Plenum Press.
Jamain S, Quach H, Betancur C, Rastam M, Colineaux C, Gillberg IC, et al. (2003). Mutations of the X-linked genes encoding neuroligins NLGN3 and NLGN4 are associated with autism. Nat Genet 34(1): 27-9.

Jelitai M, Anderova M, Marko K, Kekesi K, Koncz P, Sykova E, et al. (2004). Role of gamma-aminobutyric acid in early neuronal development: studies with an embryonic neuroectodermal stem cell clone. J Neurosci Res 76(6): 801-11.
Jiang YH, Armstrong D, Albrecht U, Atkins CM, Noebels JL, Eichele G, et al. (1998). Mutation of the Angelman ubiquitin ligase in mice causes increased cytoplasmic p53 and deficits of contextual learning and long-term potentiation. Neuron 21(4): 799-811.
Jiang YH, Beaudet AL (2004). Human disorders of ubiquitination and proteasomal degradation. Curr Opin Pediatr 16(4): 419-26.
Jonakait GM (2007). The effects of maternal inflammation on neuronal development: possible mechanisms. Int J Dev Neurosci 25(7): 415-25.
Jones EG (1986). Connectivity of the primate sensory-motor cortex. Cerebral Cortex. Jones EG and Peters A. New York/London, Plenum**:** 113-183.
Jones EG (2000). Microcolumns in the cerebral cortex. Proc Natl Acad Sci U S A 97(10): 5019-21.
Joseph RM, Tanaka J (2003). Holistic and part-based face recognition in children with autism. J Child Psychol Psychiatry 44(4): 529-42.
Just MA, Cherkassky VL, Keller TA, Minshew NJ (2004). Cortical activation and synchronization during sentence comprehension in high-functioning autism: evidence of underconnectivity. Brain 127(Pt 8): 1811-21.
Juul-Dam N, Townsend J, Courchesne E (2001). Prenatal, perinatal, and neonatal factors in autism, pervasive developmental disorder-not otherwise specified, and the general population. Pediatrics 107(4): E63.
Kandel ER, Schwartz JH, Jessel TM (2000). Principles of Neural Science. Columbus, McGraw-Hill.
Kanner L (1943). Autistic disturbances of affective contact. Nervous Child 2: 217-250.
Kanwisher N, McDermott J, Chun MM (1997). The fusiform face area: a module in human extrastriate cortex specialized for face perception. J Neurosci 17(11): 4302-11.
Kanwisher N, Stanley D, Harris A (1999). The fusiform face area is selective for faces not animals. Neuroreport 10(1): 183-7.
Kawaguchi Y, Kubota Y (1997). GABAergic cell subtypes and their synaptic connections in rat frontal cortex. Cereb Cortex 7(6): 476-86.
Kawashima R, Sugiura M, Kato T, Nakamura A, Hatano K, Ito K, et al. (1999). The human amygdala plays an important role in gaze monitoring. A PET study. Brain 122 (Pt 4): 779-83.
Kemper TL, Bauman M (1998). Neuropathology of infantile autism. J Neuropathol Exp Neurol 57(7): 645-52.
Kemper TL, Bauman ML (1993). The contribution of neuropathologic studies to the understanding of autism. Neurol Clin 11(1): 175-87.
Kennedy DP, Semendeferi K, Courchesne E (2007). No reduction of spindle neuron number in frontoinsular cortex in autism. Brain Cogn 64(2): 124-9.
Kern JK (2003). Purkinje cell vulnerability and autism: a possible etiological connection. Brain Dev 25(6): 377-82.
Kim JJ, Kim DJ, Kim TG, Seok JH, Chun JW, Oh MK, et al. (2007). Volumetric abnormalities in connectivity-based subregions of the thalamus in patients with chronic schizophrenia. Schizophr Res 97(1-3): 226-35.
Koller H, Siebler M, Schmalenbach C, Muller HW (1990). GABA and glutamate receptor development of cultured neurons from rat hippocampus, septal region, and neocortex. Synapse 5(1): 59-64.
Kopelman A, Andreasen NC, Nopoulos P (2005). Morphology of the anterior cingulate gyrus in patients with schizophrenia: relationship to typical neuroleptic exposure. Am J Psychiatry 162(10): 1872-8.
Koshino H, Carpenter PA, Minshew NJ, Cherkassky VL, Keller TA, Just MA (2005). Functional connectivity in an fMRI working memory task in high-functioning autism. Neuroimage 24(3): 810-21.
Koshino H, Kana RK, Keller TA, Cherkassky VL, Minshew NJ, Just MA (2007). fMRI Investigation of Working Memory for Faces in Autism: Visual Coding and Underconnectivity with Frontal Areas. Cereb Cortex.
Kranz F, Ishai A (2006). Face perception is modulated by sexual preference. Curr Biol 16(1): 63-8.
Krebs MO, Betancur C, Leroy S, Bourdel MC, Gillberg C, Leboyer M (2002). Absence of association between a polymorphic GGC repeat in the 5' untranslated region of the reelin gene and autism. Mol Psychiatry 7(7): 801-4.
Kreczmanski P, Heinsen H, Mantua V, Woltersdorf F, Masson T, Ulfig N, et al. (2007). Volume, neuron density and total neuron number in five subcortical regions in schizophrenia. Brain 130(Pt 3): 678-92.
Kreczmanski P, Schmidt-Kastner R, Heinsen H, Steinbusch HW, Hof PR, Schmitz C (2005). Stereological studies of capillary length density in the frontal cortex of schizophrenics. Acta Neuropathol 109(5): 510-8.
Kriegstein AR, Owens DF (2001). GABA may act as a self-limiting trophic factor at developing synapses. Sci STKE 2001(95): PE1.
Krmpotic-Nemanic J, Kostovic I, Nemanic D (1984). Prenatal and perinatal development of radial cell columns in the human auditory cortex. Acta Otolaryngol 97(5-6): 489-95.
Kuemerle B, Zanjani H, Joyner A, Herrup K (1997). Pattern deformities and cell loss in Engrailed-2 mutant mice suggest two separate patterning events during cerebellar development. J Neurosci 17(20): 7881-9.
Lado FA, Sankar R, Lowenstein D, Moshe SL (2000). Age-dependent consequences of seizures: relationship to seizure frequency, brain damage, and circuitry reorganization. Ment Retard Dev Disabil Res Rev 6(4): 242-52.
Lainhart JE, Lazar M, Bigler ED, Alexander A (2005). The brain during life in autism: advances in neuroimaging research. Neicortical modularity and the cell minicolumn. Casanova MF. New York, NY, NOVA Science Publishers**:** 57-108.
Lau HC, Rogers RD, Haggard P, Passingham RE (2004). Attention to intention. Science 303(5661): 1208-10.
Laughlin SB (2004). The implications of metabolic energy requirements for the representation of information in neurons. The cognitive neurosciences. Gazzaniga MS. Cambridge, UK, MIT Press**:** 187-196.
Laughlin SB, Sejnowski TJ (2003). Communication in Neuronal Networks. Science 301(5641): 1870-1874.
Laumonnier F, Bonnet-Brilhault F, Gomot M, Blanc R, David A, Moizard MP, et al. (2004). X-linked mental retardation and autism are associated with a mutation in the NLGN4 gene, a member of the neuroligin family. Am J Hum Genet 74(3): 552-7.
Laurie DJ, Wisden W, Seeburg PH (1992). The distribution of thirteen GABAA receptor subunit mRNAs in the rat brain. III. Embryonic and postnatal development. J Neurosci 12(11): 4151-72.
Lee M, Martin-Ruiz C, Graham A, Court J, Jaros E, Perry R, et al. (2002). Nicotinic receptor abnormalities in the cerebellar cortex in autism. Brain 125(Pt 7): 1483-95.
Lega E, Scholl H, Alimi J-M, Bijaoui A, Bury P (1995). A parallel algorithm for structure detection based on wavelet and segmentation analysis. . Parallel Computing 21(2): 265-285.
Lepage M, Ghaffar O, Nyberg L, Tulving E (2000). Prefrontal cortex and episodic memory retrieval mode. Proc Natl Acad Sci U S A 97(1): 506-11.

Letinic K, Zoncu R, Rakic P (2002). Origin of GABAergic neurons in the human neocortex. Nature 417(6889): 645-9.
Leveroni CL, Seidenberg M, Mayer AR, Mead LA, Binder JR, Rao SM (2000). Neural systems underlying the recognition of familiar and newly learned faces. J Neurosci 20(2): 878-86.
Levitt JG, O'Neill J, Blanton RE, Smalley S, Fadale D, McCracken JT, et al. (2003). Proton magnetic resonance spectroscopic imaging of the brain in childhood autism. Biol Psychiatry 54(12): 1355-66.
Levitt P, Eagleson KL, Powell EM (2004). Regulation of neocortical interneuron development and the implications for neurodevelopmental disorders. Trends Neurosci 27(7): 400-6.
Levy WB, Baxter RA (1996). Energy efficient neural codes. Neural Comput 8(3): 531-43.
Lewis DA, Levitt P (2002). Schizophrenia as a disorder of neurodevelopment. Annu Rev Neurosci 25: 409-32.
Liddle PF, Friston KJ, Frith CD, Frackowiak RS (1992). Cerebral blood flow and mental processes in schizophrenia. J R Soc Med 85(4): 224-7.
Liu A, Joyner AL (2001). Early anterior/posterior patterning of the midbrain and cerebellum. Annu Rev Neurosci 24: 869-96.
Livesey FJ, Hunt SP (1997). Netrin and netrin receptor expression in the embryonic mammalian nervous system suggests roles in retinal, striatal, nigral, and cerebellar development. Mol Cell Neurosci 8(6): 417-29.
Lohr JB, Jeste DV (1986). Cerebellar pathology in schizophrenia? A neuronometric study. Biol Psychiatry 21(10): 865-75.
Lois C, Alvarez-Buylla A (1994). Long-distance neuronal migration in the adult mammalian brain. Science 264(5162): 1145-8.
Lopez-Bendito G, Lujan R, Shigemoto R, Ganter P, Paulsen O, Molnar Z (2003). Blockade of GABA(B) receptors alters the tangential migration of cortical neurons. Cereb Cortex 13(9): 932-42.
Lord C, Rutter M, Le Couteur A (1994). Autism Diagnostic Interview-Revised: a revised version of a diagnostic interview for caregivers of individuals with possible pervasive developmental disorders. J Autism Dev Disord 24(5): 659-85.
LoTurco JJ, Owens DF, Heath MJ, Davis MB, Kriegstein AR (1995). GABA and glutamate depolarize cortical progenitor cells and inhibit DNA synthesis. Neuron 15(6): 1287-98.
Lujan R, Shigemoto R, Lopez-Bendito G (2005). Glutamate and GABA receptor signalling in the developing brain. Neuroscience 130(3): 567-80.
Luk KC, Sadikot AF (2001). GABA promotes survival but not proliferation of parvalbumin-immunoreactive interneurons in rodent neostriatum: an in vivo study with stereology. Neuroscience 104(1): 93-103.
Luria AR (1973). The working brain. New York, Basic Books.
Maestrini E, Lai C, Marlow A, Matthews N, Wallace S, Bailey A, et al. (1999). Serotonin transporter (5-HTT) and gamma-aminobutyric acid receptor subunit beta3 (GABRB3) gene polymorphisms are not associated with autism in the IMGSA families. The International Molecular Genetic Study of Autism Consortium. Am J Med Genet 88(5): 492-6.
Makris N, Goldstein JM, Kennedy D, Hodge SM, Caviness VS, Faraone SV, et al. (2006). Decreased volume of left and total anterior insular lobule in schizophrenia. Schizophr Res 83(2-3): 155-71.
Mann DM (1982). Nerve cell protein metabolism and degenerative disease. Neuropathol Appl Neurobiol 8(3): 161-76.
Mann DM, Sinclair KG (1978). The quantitative assessment of lipofuscin pigment, cytoplasmic RNA and nucleolar volume in senile dementia. Neuropathol Appl Neurobiol 4(2): 129-35.
Mann DM, Yates PO, Barton CM (1977). Cytophotometric mapping of neuronal changes in senile dementia. J Neurol Neurosurg Psychiatry 40(3): 299-302.
Manning-Courtney P, Brown J, Molloy CA, Reinhold J, Murray D, Sorensen-Burnworth R, et al. (2003). Diagnosis and treatment of autism spectrum disorders. Curr Probl Pediatr Adolesc Health Care 33(9): 283-304.
Maric D, Liu QY, Maric I, Chaudry S, Chang YH, Smith SV, et al. (2001). GABA expression dominates neuronal lineage progression in the embryonic rat neocortex and facilitates neurite outgrowth via GABA(A) autoreceptor/Cl- channels. J Neurosci 21(7): 2343-60.
Marin O, Anderson SA, Rubenstein JL (2000). Origin and molecular specification of striatal interneurons. J Neurosci 20(16): 6063-76.
Marin O, Rubenstein JL (2001). A long, remarkable journey: tangential migration in the telencephalon. Nat Rev Neurosci 2(11): 780-90.
Martin ER, Menold MM, Wolpert CM, Bass MP, Donnelly SL, Ravan SA, et al. (2000). Analysis of linkage disequilibrium in gamma-aminobutyric acid receptor subunit genes in autistic disorder. Am J Med Genet 96(1): 43-8.
McClelland JL (2000). The basis of hyperspecificity in autism: a preliminary suggestion based on properties of neural nets. J Autism Dev Disord 30(5): 497-502.
McDonald B, Highley JR, Walker MA, Herron BM, Cooper SJ, Esiri MM, et al. (2000). Anomalous asymmetry of fusiform and parahippocampal gyrus gray matter in schizophrenia: A postmortem study. Am J Psychiatry 157(1): 40-7.
McGrath JJ, Pemberton MR, Welham JL, Murray RM (1994). Schizophrenia and the influenza epidemics of 1954, 1957 and 1959: a southern hemisphere study. Schizophr Res 14(1): 1-8.
Menold MM, Shao Y, Wolpert CM, Donnelly SL, Raiford KL, Martin ER, et al. (2001). Association analysis of chromosome 15 gabaa receptor subunit genes in autistic disorder. J Neurogenet 15(3-4): 245-59.
Mesulam MM (1990). Large-scale neurocognitive networks and distributed processing for attention, language, and memory. Ann Neurol 28(5): 597-613.
Mesulam MM (1998). From sensation to cognition. Brain 121 (Pt 6): 1013-52.
Mesulam MM (2000). Behavioral neuroanatomy: large-scale networks, association cortex, frontal syndromes, the limbic system, and hemispheric specializations. Principles of Behavioral and Cognitive Neurology. Mesulam MM. Oxford, Oxford University Press. **:** 1-120.
Mesulam MM (2002). The human frontal lobes: transcending the default mode through contigent encoding. Principles of forntal lobe function. Stuss T and Knight RT. Oxford, Oxford University Press**:** 8-30.
Meyer-Lindenberg A, Poline JB, Kohn PD, Holt JL, Egan MF, Weinberger DR, et al. (2001). Evidence for abnormal cortical functional connectivity during working memory in schizophrenia. Am J Psychiatry 158(11): 1809-17.
Mienville JM, Pesold C (1999). Low resting potential and postnatal upregulation of NMDA receptors may cause Cajal-Retzius cell death. J Neurosci 19(5): 1636-46.
Miles R (1999). Neurobiology. A homeostatic switch. Nature 397(6716): 215-6.
Miller KD (1994). A model for the development of simple cell receptive fields and the ordered arrangement of orientation columns through activity-dependent competition between ON- and OFF-center inputs. J Neurosci 14(1): 409-41.

Minshew N, Goldstein G, Maurer RG, Bauman ML, Goldman-Rakic PS (1989). The neurobiology of autism: an integrated theory of the clinical and anatomical defecits. J Clin Exp Neuropsychol 11: 38.
Minshew NJ, Goldstein G, Siegel DJ (1997). Neuropsychologic functioning in autism: profile of a complex information processing disorder. J Int Neuropsychol Soc 3(4): 303-16.
Moretti P, Zoghbi HY (2006). MeCP2 dysfunction in Rett syndrome and related disorders. Curr Opin Genet Dev 16(3): 276-81.
Morgane PJ, Austin-LaFrance RJ, Bronzino JD (1992). Malnutrition and the developing central nervous system. The Vulnerable Brain and Environmental Risks, Volume 1: Malnutrition and Hazard Assessment. Isaacson RL and Jensen RF. New York, Plenum Press: 3-44.
Morris JS, Ohman A, Dolan RJ (1999). A subcortical pathway to the right amygdala mediating "unseen" fear. Proc Natl Acad Sci U S A 96(4): 1680-5.
Mosier HD, Jr., Grossman HJ, Dingman HF (1965). Physical growth in mental defectives. A study in an institutionalized population. Pediatrics 36(3): Suppl:465-519.
Mountcastle VB (1997). The columnar organization of the neocortex. Brain 120 (Pt 4): 701-22.
Mountcastle VB (2003). Introduction. Computation in cortical columns. Cereb. Cortex 13(1): 2-4.
Moy SS, Nadler JJ (2008). Advances in behavioral genetics: mouse models of autism. Mol Psychiatry 13(1): 4-26.
Muhle R, Trentacoste SV, Rapin I (2004). The genetics of autism. Pediatrics 113(5): e472-86.
Mukaetova-Ladinska EB, Arnold H, Jaros E, Perry R, Perry E (2004). Depletion of MAP2 expression and laminar cytoarchitectonic changes in dorsolateral prefrontal cortex in adult autistic individuals. Neuropathol Appl Neurobiol 30(6): 615-23.
Mundy P (2003). Annotation: the neural basis of social impairments in autism: the role of the dorsal medial-frontal cortex and anterior cingulate system. J Child Psychol Psychiatry 44(6): 793-809.
Mundy P, Burnett C (2005). Joint attention and neurodevelopmental models of autism. Handbook of autism and pervasive developmental disorders. Volkmar FR, Paul R, Klin A and Cohen D. New York, Wiley: 650-681.
Mundy P, Neal AR (2001). Neuroal plasticity, joint attention, and a transactional social-orienting model of autism. Int Rev Res Ment Retard 23: 139-168.
Murakami JW, Courchesne E, Press GA, Yeung-Courchesne R, Hesselink JR (1989). Reduced cerebellar hemisphere size and its relationship to vermal hypoplasia in autism. Arch Neurol 46(6): 689-94.
Murray RM, Sham P, Van Os J, Zanelli J, Cannon M, McDonald C (2004). A developmental model for similarities and dissimilarities between schizophrenia and bipolar disorder. Schizophr Res 71(2-3): 405-16.
Nacewicz BM, Dalton KM, Johnstone T, Long MT, McAuliff EM, Oakes TR, et al. (2006). Amygdala volume and nonverbal social impairment in adolescent and adult males with autism. Arch Gen Psychiatry 63(12): 1417-28.
Nagai M, Kishi K, Kato S (2007). Insular cortex and neuropsychiatric disorders: a review of recent literature. Eur Psychiatry 22(6): 387-94.
Narita N, Kato M, Tazoe M, Miyazaki K, Narita M, Okado N (2002). Increased monoamine concentration in the brain and blood of fetal thalidomide- and valproic acid-exposed rat: putative animal models for autism. Pediatr Res 52(4): 576-9.
Nelson KB, Grether JK, Croen LA, Dambrosia JM, Dickens BF, Jelliffe LL, et al. (2001). Neuropeptides and neurotrophins in neonatal blood of children with autism or mental retardation. Ann Neurol 49(5): 597-606.
Nguyen L, Rigo JM, Rocher V, Belachew S, Malgrange B, Rogister B, et al. (2001). Neurotransmitters as early signals for central nervous system development. Cell Tissue Res 305(2): 187-202.
Nimchinsky EA, Gilissen E, Allman JM, Perl DP, Erwin JM, Hof PR (1999). A neuronal morphologic type unique to humans and great apes. Proc Natl Acad Sci U S A 96(9): 5268-73.
Nimchinsky EA, Oberlander AM, Svoboda K (2001). Abnormal development of dendritic spines in FMR1 knock-out mice. J Neurosci 21(14): 5139-46.
Nimchinsky EA, Vogt BA, Morrison JH, Hof PR (1995). Spindle neurons of the human anterior cingulate cortex. J Comp Neurol 355(1): 27-37.
Nimchinsky EA, Vogt BA, Morrison JH, Hof PR (1997). Neurofilament and calcium-binding proteins in the human cingulate cortex. J Comp Neurol 384(4): 597-620.
Nishikawa S, Goto S, Hamasaki T, Yamada K, Ushio Y (2002). Involvement of reelin and Cajal-Retzius cells in the developmental formation of vertical columnar structures in the cerebral cortex: evidence from the study of mouse presubicular cortex. Cereb Cortex 12(10): 1024-30.
Noga JT, Aylward E, Barta PE, Pearlson GD (1995). Cingulate gyrus in schizophrenic patients and normal volunteers. Psychiatry Res 61(4): 201-8.
Nowell MA, Hackney DB, Muraki AS, Coleman M (1990). Varied MR appearance of autism: fifty-three pediatric patients having the full autistic syndrome. Magn Reson Imaging 8(6): 811-6.
O'Doherty J, Winston J, Critchley H, Perrett D, Burt DM, Dolan RJ (2003). Beauty in a smile: the role of medial orbitofrontal cortex in facial attractiveness. Neuropsychologia 41(2): 147-55.
O'Rourke NA, Chenn A, McConnell SK (1997). Postmitotic neurons migrate tangentially in the cortical ventricular zone. Development 124(5): 997-1005.
O'Rourke NA, Dailey ME, Smith SJ, McConnell SK (1992). Diverse migratory pathways in the developing cerebral cortex. Science 258(5080): 299-302.
Ohnishi T, Matsuda H, Hashimoto T, Kunihiro T, Nishikawa M, Uema T, et al. (2000). Abnormal regional cerebral blood flow in childhood autism. Brain 123 (Pt 9): 1838-44.
Oishi M, Kameyama S, Morota N, Tomikawa M, Wachi M, Kakita A, et al. (2002). Fusiform gyrus epilepsy: the use of ictal magnetoencephalography. Case report. J Neurosurg 97(1): 200-4.
Otsu N (1979). A treshold selection method from grey-level histograms. IEEE Trans Syst Man Cybern 9: 377-393.
Owens DF, Boyce LH, Davis MB, Kriegstein AR (1996). Excitatory GABA responses in embryonic and neonatal cortical slices demonstrated by gramicidin perforated-patch recordings and calcium imaging. J Neurosci 16(20): 6414-23.
Owens DF, Liu X, Kriegstein AR (1999). Changing properties of GABA(A) receptor-mediated signaling during early neocortical development. J Neurophysiol 82(2): 570-83.
Ozonoff S, Pennington BF, Rogers SJ (1991). Executive function deficits in high-functioning autistic individuals: relationship to theory of mind. J Child Psychol Psychiatry 32(7): 1081-105.
Palmen SJ, Durston S, Nederveen H, H VANE (2006). No evidence for preferential involvement of medial temporal lobe structures in high-functioning autism. Psychol Med: 1-8.

Palmen SJ, Hulshoff Pol HE, Kemner C, Schnack HG, Janssen J, Kahn RS, et al. (2004b). Larger brains in medication naive high-functioning subjects with pervasive developmental disorder. J Autism Dev Disord 34(6): 603-13.
Palmen SJ, van Engeland H (2004). Review on structural neuroimaging findings in autism. J Neural Transm 111(7): 903-29.
Palmen SJ, Van Engeland H, Hof PR, Schmitz C (2004). Neuropathological findings in autism. Brain.
Parnavelas JG (2000). The origin and migration of cortical neurones: new vistas. Trends Neurosci 23(3): 126-31.
Patterson PH (2002). Maternal infection: window on neuroimmune interactions in fetal brain development and mental illness. Curr Opin Neurobiol 12(1): 115-8.
Patterson PH (2005a). Maternal infection causes abnormal behavior in the offspring. Neuropsychiatric disorders and infection. Fatemi SH. United Kingdom, Taylor and Francis**:** 83-90.
Patterson PH (2005b). Modeling features of autism in animals. Neurobiology of Autism in the Post-Genomic Era. Moldin SO and Rubenstein JL. Boca Raton, Taylor & Francis.
Patterson PH (2006). Modeling features of autism in animals. Understanding Autism: From Basic Neuroscience to Treatment. Moldin SO and Rubenstein JL. Boca Raton, Taylor & Francis**:** 277-302.
Paxinos G, Franklin KB (2001). The mouse brain in stereotaxic coordinates. San Diego, Academic Press.
Paxinos G, Mai K (2004). The Human Nervous System. San Diego, Elsevier Academic Press.
Pearce BD (2003). Modeling the role of infections in the etiology of mental illness. Clin. Neurosci. Res. 3: 271.
Perl DP, Good PF, Bussiere T, Morrison JH, Erwin JM, Hof PR (2000). Practical approaches to stereology in the setting of aging- and disease-related brain banks. J Chem Neuroanat 20(1): 7-19.
Perry EK, Lee ML, Martin-Ruiz CM, Court JA, Volsen SG, Merrit J, et al. (2001). Cholinergic activity in autism: abnormalities in the cerebral cortex and basal forebrain. Am J Psychiatry 158(7): 1058-66.
Persico AM, D'Agruma L, Maiorano N, Totaro A, Militerni R, Bravaccio C, et al. (2001). Reelin gene alleles and haplotypes as a factor predisposing to autistic disorder. Mol Psychiatry 6(2): 150-9.
Peters A, Kara DA (1987). The neuronal composition of area 17 of rat visual cortex. IV. The organization of pyramidal cells. J Comp Neurol 260(4): 573-90.
Peters A, Sethares C (1991). Organization of pyramidal neurons in area 17 of monkey visual cortex. J Comp Neurol 306(1): 1-23.
Peters A, Sethares C (1996). Myelinated axons and the pyramidal cell modules in monkey primary visual cortex. J Comp Neurol. 365(2): 232-55.
Peters A, Sethares C (1997). The organization of double bouquet cells in monkey striate cortex. Journal of Neurocytology 26(12): 779.
Peters A, Walsh TM (1972). A study of the organization of apical dendrites in the somatic sensory cortex of the rat. J Comp Neurol 144(3): 253-68.
Peters A, Yilmaz E (1993). Neuronal organization in area 17 of cat visual cortex. Cereb Cortex 3(1): 49-68.
Petrides M, Pandya DN (2002). Comparative cytoarchitectonic analysis of the human and the macaque ventrolateral prefrontal cortex and corticocortical connection patterns in the monkey. Eur J Neurosci 16(2): 291-310.
Petrides M, Pandya DN (2004). The prefrontal cortex. The human nervous system. Paxinos G and Mai JK. Amsterdam, Elsevier Academic Press**:** 950-972.
Piao X, Hill RS, Bodell A, Chang BS, Basel-Vanagaite L, Straussberg R, et al. (2004). G protein-coupled receptor-dependent development of human frontal cortex. Science 303(5666): 2033-6.
Pickett J (2003). Mapping the neuropathology of autism. NAARRATIVE 12: 4-5.
Pierce K, Haist F, Sedaghat F, Courchesne E (2004). The brain response to personally familiar faces in autism: findings of fusiform activity and beyond. Brain 127(Pt 12): 2703-16.
Pierce K, Muller RA, Ambrose J, Allen G, Courchesne E (2001). Face processing occurs outside the fusiform 'face area' in autism: evidence from functional MRI. Brain 124(Pt 10): 2059-73.
Piggot J, Kwon H, Mobbs D, Blasey C, Lotspeich L, Menon V, et al. (2004). Emotional attribution in high-functioning individuals with autistic spectrum disorder: a functional imaging study. J Am Acad Child Adolesc Psychiatry 43(4): 473-80.
Pinkham A, Penn D, Wangelin B, Perkins D, Gerig G, Gu H, et al. (2005). Facial emotion perception and fusiform gyrus volume in first episode schizophrenia. Schizophr Res 79(2-3): 341-3.
Pitkänen A (2000). Connectivity of the rat amygdaloid complex. The amygdala. Aggleton JP. New York, Oxford University Press Inc.
Piven J (1997). The biological basis of autism. Curr Opin Neurobiol 7(5): 708-12.
Piven J, Arndt S, Bailey J, Andreasen N (1996). Regional brain enlargement in autism: a magnetic resonance imaging study. J Am Acad Child Adolesc Psychiatry 35(4): 530-6.
Piven J, Bailey J, Ranson BJ, Arndt S (1998). No difference in hippocampus volume detected on magnetic resonance imaging in autistic individuals. J Autism Dev Disord 28(2): 105-10.
Piven J, Berthier ML, Starkstein SE, Nehme E, Pearlson G, Folstein S (1990). Magnetic resonance imaging evidence for a defect of cerebral cortical development in autism. Am J Psychiatry 147(6): 734-9.
Piven J, Saliba K, Bailey J, Arndt S (1995). An MRI study of autism: the cerebellum revisited. Neurology 49(2): 546-51.
Piven J, Saliba K, Bailey J, Arndt S (1997). An MRI study of autism: the cerebellum revisited. Neurology 49(2): 546-51.
Pletnikov MV, Rubin SA, Vogel MW, Moran TH, Carbone KM (2002). Effects of genetic background on neonatal Borna disease virus infection-induced neurodevelopmental damage. II. Neurochemical alterations and responses to pharmacological treatments. Brain Res 944(1-2): 108-23.
Porteus MH, Bulfone A, Liu JK, Puelles L, Lo LC, Rubenstein JL (1994). DLX-2, MASH-1, and MAP-2 expression and bromodeoxyuridine incorporation define molecularly distinct cell populations in the embryonic mouse forebrain. J Neurosci 14(11 Pt 1): 6370-83.
Powell EM, Mars WM, Levitt P (2001). Hepatocyte growth factor/scatter factor is a motogen for interneurons migrating from the ventral to dorsal telencephalon. Neuron 30(1): 79-89.
Preuss TM (1995). Do rats have prefrontal cortex ? J Cognitive Neurosci 7: 1-24.
Rajkowska G, Goldman-Rakic PS (1995a). Cytoarchitectonic definition of prefrontal areas in the normal human cortex: I. Remapping of areas 9 and 46 using quantitative criteria. Cereb Cortex. 5(4): 307-22.
Rajkowska G, Goldman-Rakic PS (1995b). Cytoarchitectonic definition of prefrontal areas in the normal human cortex: II. Variability in locations of areas 9 and 46 and relationship to the Talairach Coordinate System. Cereb Cortex. 5(4): 323-37.
Rakic P (1974). Neurons in rhesus monkey visual cortex: systematic relation between time of origin and eventual disposition. Science 183(123): 425-7.

Rakic P (1975). Local circuit neurons. Neurosci Res Program Bull 13(3): 295-416.
Rakic P (1985). Limits of neurogenesis in primates. Science 227(4690): 1054-6.
Rakic P (1995a). Radial versus tangential migration of neuronal clones in the developing cerebral cortex. Proc Natl Acad Sci U S A 92(25): 11323-7.
Rakic P (1995b). A small step for the cell, a giant leap for mankind: a hypothesis of neocortical expansion during evolution. Trends in Neurosciences 18(9): 383.
Rakic P, Kornack D (2001). Neocortical expansion and elaboration during primate evolution: A view from neurobiology. Evolutionary Anatomy of the Primate Cerebral Cortex. Falk D and Gibson K. Cambridge, UK, Cambridge University Press**:** 30-56.
Rapp PR, Bachevalier J (1993). Fundamental Neuroscience. Squire LR, Bloom FE, McConnell SK, Roberts JL, Spitzer NC and Zigmond MJ. San Diego, California, Academic Press**:** 179-411.
Raymond GV, Bauman ML, Kemper TL (1996). Hippocampus in autism: a Golgi analysis. Acta Neuropathol (Berl) 91(1): 117-9.
Redcay E, Courchesne E (2005). When is the Brain Enlarged in Autism? A Meta-Analysis of All Brain Size Reports. Biol Psychiatry.
Ritvo ER, Freeman BJ, Scheibel AB, Duong T, Robinson H, Guthrie D, et al. (1986). Lower Purkinje cell counts in the cerebella of four autistic subjects: initial findings of the UCLA-NSAC Autopsy Research Report. Am J Psychiatry 143(7): 862-6.
Rivara CB, Sherwood CC, Bouras C, Hof PR (2003). Stereologic characterization and spatial distribution patterns of Betz cells in the human primary motor cortex. Anat Rec A Discov Mol Cell Evol Biol 270(2): 137-51.
Rivera C, Voipio J, Payne JA, Ruusuvuori E, Lahtinen H, Lamsa K, et al. (1999). The K+/Cl- co-transporter KCC2 renders GABA hyperpolarizing during neuronal maturation. Nature 397(6716): 251-5.
Rockel AJ, Hiorns RW, Powell TP (1980). The basic uniformity in structure of the neocortex. Brain 103(2): 221-44.
Rockland KS, Ichinohe N (2004). Some thoughts on cortical minicolumns. Exp Brain Res 158(3): 265-77.
Rodier PM, Ingram JL, Tisdale B, Nelson S, Romano J (1996). Embryological origin for autism: developmental anomalies of the cranial nerve motor nuclei. J Comp Neurol 370(2): 247-61.
Rojas DC, Bawn SD, Benkers TL, Reite ML, Rogers SJ (2002). Smaller left hemisphere planum temporale in adults with autistic disorder. Neurosci Lett 328(3): 237-40.
Rolf LH, Haarmann FY, Grotemeyer KH, Kehrer H (1993). Serotonin and amino acid content in platelets of autistic children. Acta Psychiatr Scand 87(5): 312-6.
Rorke LB (1994). A perspective: the role of disordered genetic control of neurogenesis in the pathogenesis of migration disorders. J Neuropathol Exp Neurol 53(2): 105-17.
Rubenstein JL, Merzenich MM (2003). Model of autism: increased ratio of excitation/inhibition in key neural systems. Genes Brain Behav 2(5): 255-67.
Rutter M, Bartak L (1971). Causes of infantile autism: some considerations from recent research. J Autism Child Schizophr 1(1): 20-32.
Sanacora G, Mason GF, Rothman DL, Behar KL, Hyder F, Petroff OA, et al. (1999). Reduced cortical gamma-aminobutyric acid levels in depressed patients determined by proton magnetic resonance spectroscopy. Arch Gen Psychiatry 56(11): 1043-7.
Sanders GS, Gallup GG, Heinsen H, Hof PR, Schmitz C (2002). Cognitive deficits, schizophrenia, and the anterior cingulate cortex. Trends Cogn Sci 6(5): 190-192.
Sarna JR, Hawkes R (2003). Patterned Purkinje cell death in the cerebellum. Prog Neurobiol 70(6): 473-507.
Sasson NJ (2006). The development of face processing in autism. J Autism Dev Disord 36(3): 381-94.
Schleicher A, Palomero-Gallagher N, Morosan P, Eickhoff SB, Kowalski T, de Vos K, et al. (2005). Quantitative architectural analysis: a new approach to cortical mapping. Anat Embryol (Berl) 210(5-6): 373-86.
Schleicher A, Zilles K (1990). A quantitative approach to cytoarchitectonics: analysis of structural inhomogeneities in nervous tissue using an image analyser. J Microsc. 157(Pt 3): 367-81.
Schmitz C (1998). Variation of fractionator estimates and its prediction. Anat Embryol (Berl) 198(5): 371-97.
Schmitz C, Hof PR (2000). Recommendations for straightforward and rigorous methods of counting neurons based on a computer simulation approach. J Chem Neuroanat 20(1): 93-114.
Schmitz C, Hof PR (2005). Design-based stereology in neuroscience. Neuroscience 130(4): 813-31.
Schmitz C, Rezaie P (2008). The neuropathology of autism: where do we stand? Neuropathol Appl Neurobiol 34(1): 4-11.
Schmitz C, Rutten BP, Pielen A, Schafer S, Wirths O, Tremp G, et al. (2004). Hippocampal neuron loss exceeds amyloid plaque load in a transgenic mouse model of Alzheimer's disease. Am J Pathol 164(4): 1495-502.
Schmitz C, Schuster D, Niessen P, Korr H (1999). No difference between estimated mean nuclear volumes of various types of neurons in the mouse brain obtained on either isotropic uniform random sections or conventional frontal or sagittal sections. J Neurosci Methods 88(1): 71-82.
Schroer RJ, Phelan MC, Michaelis RC, Crawford EC, Skinner SA, Cuccaro M, et al. (1998). Autism and maternally derived aberrations of chromosome 15q. Am J Med Genet 76(4): 327-36.
Schultz RT (2005). Developmental deficits in social perception in autism: the role of the amygdala and fusiform face area. Int J Dev Neurosci 23(2-3): 125-41.
Schultz RT, Gauthier I, Klin A, Fulbright RK, Anderson AW, Volkmar F, et al. (2000). Abnormal ventral temporal cortical activity during face discrimination among individuals with autism and Asperger syndrome. Arch Gen Psychiatry 57(4): 331-40.
Schultz RT, Grelotti DJ, Klin A, Kleinman J, Van der Gaag C, Marois R, et al. (2003). The role of the fusiform face area in social cognition: implications for the pathobiology of autism. Philos Trans R Soc Lond B Biol Sci 358(1430): 415-27.
Schulz U, Hunziker O (1980). Comparative studies of neuronal perikaryon size and shape in the aging cerebral cortex. J Gerontol 35(4): 483-91.
Schumann CM, Amaral DG (2005). Stereological estimation of the number of neurons in the human amygdaloid complex. J Comp Neurol 491(4): 320-9.
Schumann CM, Amaral DG (2006). Stereological analysis of amygdala neuron number in autism. J Neurosci 26(29): 7674-9.
Schumann CM, Hamstra J, Goodlin-Jones BL, Lotspeich LJ, Kwon H, Buonocore MH, et al. (2004). The amygdala is enlarged in children but not adolescents with autism; the hippocampus is enlarged at all ages. J Neurosci 24(28): 6392-401.
Schwartz EL (1980). Computational anatomy and functional architecture of striate cortex: a spatial mapping approach to perceptual coding. Vision Res 20(8): 645-69.
Seeley WW, Carlin DA, Allman JM, Macedo MN, Bush C, Miller BL, et al. (2006). Early frontotemporal dementia targets neurons unique to apes and humans. Ann Neurol 60(6): 660-7.

Segal D, Schmitz C, Hof PR (2008). Spatial distribution and density of oligodendrocytes in the cingulum bundle are unaltered in schizophrenia. Acta Neuropathol.
Seldon H (1981a). Structure of human auditory cortex. I. Cytoarchitectonics and dendritic distributions. Brain Res. 229(2): 277-94.
Seldon HL (1981b). Structure of human auditory cortex. II. Axon distributions and morphological correlates of speech perception. Brain Research 229(2): 295.
Seldon HL (1982). Structure of human auditory cortex. III. Statistical analysis of dendritic trees. Brain Res 249(2): 211-21.
Seldon HL (1985). The anatomy of speech perception: human auditory cortex. Association and auditory cortices. Jones EG and Peters A. New York, NY, Plenum**:** 273-327.
Semendeferi K, Armstrong E, Schleicher A, Zilles K, Van Hoesen GW (2001). Prefrontal cortex in humans and apes: a comparative study of area 10. Am J Phys Anthropol 114(3): 224-41.
Semendeferi K, Damasio H (2000). The brain and its main anatomical subdivisions in living hominoids using magnetic resonance imaging. J Hum Evol 38(2): 317-32.
Shakow D (1946). The nature of deterioration in schizophrenic conditions. New York, NY, Cooligde Foundation.
Shi L, Fatemi SH, Sidwell RW, Patterson PH (2003). Maternal influenza infection causes marked behavioral and pharmacological changes in the offspring. J Neurosci 23(1): 297-302.
Shi L, Smith SEP, Malkova N, Tse D, Patterson PH (2008 in press). Activation of the maternal immune response alters cerebellar development in the offspring. Brain Behav Immun.
Shi L, Smith SEP, Malkova N, Tse D, Patterson PH (*in press*). Activation of the maternal immune response alters cerebellar development in the offspring. Brain Behav Immun.
Shimada M, Yamano T, Nakamura T, Morikawa Y, Kusunoki T (1977). Effect of maternal malnutrition on matrix cell proliferation in the cerebrum of mouse embryo: an autoradiographic study. Pediatr Res 11: 728-732.
Sigmundsson T, Suckling J, Maier M, Williams S, Bullmore E, Greenwood K, et al. (2001). Structural abnormalities in frontal, temporal, and limbic regions and interconnecting white matter tracts in schizophrenic patients with prominent negative symptoms. Am J Psychiatry 158(2): 234-43.
Silva AE, Vayego-Lourenco SA, Fett-Conte AC, Goloni-Bertollo EM, Varella-Garcia M (2002). Tetrasomy 15q11-q13 identified by fluorescence in situ hybridization in a patient with autistic disorder. Arq Neuropsiquiatr 60(2-A): 290-4.
Singh VK, Warren R, Averett R, Ghaziuddin M (1997). Circulating autoantibodies to neuronal and glial filament proteins in autism. Pediatr Neurol 17(1): 88-90.
Skaliora I, Singer W, Betz H, Puschel AW (1998). Differential patterns of semaphorin expression in the developing rat brain. Eur J Neurosci 10(4): 1215-29.
Smith SE, Li J, Garbett K, Mirnics K, Patterson PH (2007). Maternal immune activation alters fetal brain development through interleukin-6. J Neurosci 27(40): 10695-702.
Somogyi R, Wen X, Ma W, Barker JL (1995). Developmental kinetics of GAD family mRNAs parallel neurogenesis in the rat spinal cord. J Neurosci 15(4): 2575-91.
Sparks BF, Friedman SD, Shaw DW, Aylward EH, Echelard D, Artru AA, et al. (2002). Brain structural abnormalities in young children with autism spectrum disorder. Neurology 59(2): 184-92.
Stein V, Hermans-Borgmeyer I, Jentsch TJ, Hubner CA (2004). Expression of the KCl cotransporter KCC2 parallels neuronal maturation and the emergence of low intracellular chloride. J Comp Neurol 468(1): 57-64.
Steyaert JG, De La Marche W (2008). What's new in autism? Eur J Pediatr.
Stoyan D, Kendall W, Mecke J (1995). Stochastic Geometry and its applications. Winchester, John Wiley and Sons.
Striedter GF (2005). Principles of brain evolution. Sunderland, Massachusetts, Sinauer.
Stromland K, Nordin V, Miller M, Akerstrom B, Gillberg C (1994). Autism in thalidomide embryopathy: a population study. Dev Med Child Neurol 36(4): 351-6.
Stubbs EG, Ash E, Williams CP (1984). Autism and congenital cytomegalovirus. J Autism Dev Disord 14(2): 183-9.
Stuhmer T, Anderson SA, Ekker M, Rubenstein JL (2002). Ectopic expression of the Dlx genes induces glutamic acid decarboxylase and Dlx expression. Development 129(1): 245-52.
Sutula TP, Hagen J, Pitkanen A (2003). Do epileptic seizures damage the brain? Curr Opin Neurol 16(2): 189-95.
Suzuki I, Shimizu H, Ishijima B, Tani K, Sugishita M, Adachi N (1992). Aphasic seizure caused by focal epilepsy in the left fusiform gyrus. Neurology 42(11): 2207-10.
Suzuki M, Nohara S, Hagino H, Kurokawa K, Yotsutsuji T, Kawasaki Y, et al. (2002). Regional changes in brain gray and white matter in patients with schizophrenia demonstrated with voxel-based analysis of MRI. Schizophr Res 55(1-2): 41-54.
Tamminga CA, Thaker GK, Buchanan R, Kirkpatrick B, Alphs LD, Chase TN, et al. (1992). Limbic system abnormalities identified in schizophrenia using positron emission tomography with fluorodeoxyglucose and neocortical alterations with deficit syndrome. Arch Gen Psychiatry 49(7): 522-30.
Tanaka JW, Guauthier I (1997). Expertise in object and face recognition. Psychology of Learning and Motivation. Goldstone RL, Schyns PG and Medin DL. San Diego, academic Press**:** 83-125.
Tandrup T, Gundersen HJ, Jensen EB (1997). The optical rotator. J Microsc 186(Pt 2): 108-20.
Theodore WH, DeCarli C, Gaillard WD (2003). Total cerebral volume is reduced in patients with localization-related epilepsy and a history of complex febrile seizures. Arch Neurol 60(2): 250-2.
Thom M, Zhou J, Martinian L, Sisodiya S (2005). Quantitative post-mortem study of the hippocampus in chronic epilepsy: seizures do not inevitably cause neuronal loss. Brain 128(Pt 6): 1344-57.
Tillakaratne NJ, Medina-Kauwe L, Gibson KM (1995). gamma-Aminobutyric acid (GABA) metabolism in mammalian neural and nonneural tissues. Comp Biochem Physiol A Physiol 112(2): 247-63.
Tueting P, Costa E, Dwivedi Y, Guidotti A, Impagnatiello F, Manev R, et al. (1999). The phenotypic characteristics of heterozygous reeler mouse. Neuroreport 10(6): 1329-34.
Tyzio R, Represa A, Jorquera I, Ben-Ari Y, Gozlan H, Aniksztejn L (1999). The establishment of GABAergic and glutamatergic synapses on CA1 pyramidal neurons is sequential and correlates with the development of the apical dendrite. J Neurosci 19(23): 10372-82.
van Karnebeek CD, van Gelderen I, Nijhof GJ, Abeling NG, Vreken P, Redeker EJ, et al. (2002). An aetiological study of 25 mentally retarded adults with autism. J Med Genet 39(3): 205-13.

Van Kooten IA, Casanova MF, Switala AE, Van Engeland H, Heinsen H, Steinbusch HW, et al. (2005a). Neuronal size and number in the neocortex of autistic patients. Society for Neuroscience, Washington, DC.
Van Kooten IA, Hof PR, Van Engeland H, Steinbusch HW, Patterson PH, Schmitz C (2005b). Autism: neuropathology, alterations of the GABAergic system, and animal models. Int Rev Neurobiol 71: 1-26.
Van Kooten IA, Palmen SJ, Von Cappeln P, Steinbusch HW, Korr H, Heinsen H, et al. (2008). Neurons in the fusiform gyrus are fewer and smaller in autism. Brain 131: 987-999
Van Praag H, Zhao X, Gage FH (2004). Neurogenesis in the adult mammalian brain. The Cognitive Neurosciences iii. Gazzaniga MS. Cambridge, UK, MIT Press**:** 127-137.
Veenstra-Vanderweele J, Christian SL, Cook EH, Jr. (2004). Autism as a paradigmatic complex genetic disorder. Annu Rev Genomics Hum Genet 5: 379-405.
Vinje WE, Gallant JL (2000). Sparse Coding and Decorrelation in Primary Visual Cortex During Natural Vision. Science 287(5456): 1273-1276.
Vogt BA, Nimchinsky EA, Vogt LJ, Hof PR (1995). Human cingulate cortex: surface features, flat maps, and cytoarchitecture. J Comp Neurol 359(3): 490-506.
Vogt C, Vogt O (1919). Allgemeinere Ergebnisse unserer Hirnforschung, dritte Mitteilung: die architektonische Rindenfelderung im Lichte unserere neuesten Forschungen. Journal fur Psychologie und Neurologie 25(1): 361-376.
Volkmar FR, Pauls D (2003). Autism. Lancet 362(9390): 1133-41.
Von Bonin G, Mehler WR (1971). On columnar arrangement of nerve cell in the cerebral cortex. Brain Res 27: 1-10.
Von Economo C (1929). The cytoarchitectonics of the human cerebral cortex. Oxford, UK, Oxford University Press.
Waiter GD, Williams JH, Murray AD, Gilchrist A, Perrett DI, Whiten A (2004). A voxel-based investigation of brain structure in male adolescents with autistic spectrum disorder. Neuroimage 22(2): 619-25.
Walton MK, Schaffner AE, Barker JL (1993). Sodium channels, GABAA receptors, and glutamate receptors develop sequentially on embryonic rat spinal cord cells. J Neurosci 13(5): 2068-84.
Wang L, Hosakere M, Trein JC, Miller A, Ratnanather JT, Barch DM, et al. (2007). Abnormalities of cingulate gyrus neuroanatomy in schizophrenia. Schizophr Res 93(1-3): 66-78.
Wassink TH, Piven J, Patil SR (2001). Chromosomal abnormalities in a clinic sample of individuals with autistic disorder. Psychiatr Genet 11(2): 57-63.
Watson KK, Jones TK, Allman JM (2006). Dendritic architecture of the von Economo neurons. Neuroscience 141(3): 1107-12.
Webb SJ, Nalty T, Munson J, Brock C, Abbott R, Dawson G (2007). Rate of head circumference growth as a function of autism diagnosis and history of autistic regression. J Child Neurol 22(10): 1182-90.
Weliky M, Fiser J, Hunt RH, Wagner DN (2003). Coding of Natural Scenes in Primary Visual Cortex. Neuron 37(4): 703.
West MJ, Slomianka L, Gundersen HJ (1991). Unbiased stereological estimation of the total number of neurons in thesubdivisions of the rat hippocampus using the optical fractionator. Anat Rec 231(4): 482-97.
Whitaker-Azmitia PM (2001). Serotonin and brain development: role in human developmental diseases. Brain Res Bull 56(5): 479-85.
White EL, Peters A (1993). Cortical modules in the posteromedial barrel subfield (Sml) of the mouse. J Comp Neurol. 334(1): 86-96.
Wichterle H, Turnbull DH, Nery S, Fishell G, Alvarez-Buylla A (2001). In utero fate mapping reveals distinct migratory pathways and fates of neurons born in the mammalian basal forebrain. Development 128(19): 3759-71.
Williams PG, Hersh JH (1997). A male with fetal valproate syndrome and autism. Dev Med Child Neurol 39(9): 632-4.
Williams RS, Hauser SL, Purpura DP, DeLong GR, Swisher CN (1980). Autism and mental retardation: neuropathologic studies performed in four retarded persons with autistic behavior. Arch Neurol 37(12): 749-53.
Yamashita Y, Fujimoto C, Nakajima E, Isagai T, Matsuishi T (2003). Possible association between congenital cytomegalovirus infection and autistic disorder. J Autism Dev Disord 33(4): 455-9.
Yirmiya N, Sigman MD, Kasari C, Mundy P (1992). Empathy and cognition in high-functioning children with autism. Child Dev 63(1): 150-60.
Yoon JH, D'Esposito M, Carter CS (2006). Preserved function of the fusiform face area in schizophrenia as revealed by fMRI. Psychiatry Res 148(2-3): 205-16.
Yuan W, Zhou L, Chen JH, Wu JY, Rao Y, Ornitz DM (1999). The mouse SLIT family: secreted ligands for ROBO expressed in patterns that suggest a role in morphogenesis and axon guidance. Dev Biol 212(2): 290-306.
Yucel M, Pantelis C, Stuart GW, Wood SJ, Maruff P, Velakoulis D, et al. (2002). Anterior cingulate activation during Stroop task performance: a PET to MRI coregistration study of individual patients with schizophrenia. Am J Psychiatry 159(2): 251-4.
Zhang J (2003). Evolution of the human ASPM gene, a major determinant of brain size. Genetics 165(4): 2063-70.
Zilbovicius M, Garreau B, Samson Y, Remy P, Barthelemy C, Syrota A, et al. (1995). Delayed maturation of the frontal cortex in childhood autism. Am J Psychiatry 152(2): 248-52.
Zilles K (2004). Architecture of the Human Cerebral Cortex: regional and laminar organization. The Human Nervous System. Paxinos G and Mai JK. San Diego, Elsevier Academic Press**:** 997-1055.
Zilles K, Armstrong E, Moser KH, Schleicher A, Stephan H (1989). Gyrification in the cerebral cortex of primates. Brain Behav Evol 34(3): 143-50.